EARLY TRANSITION METAL ALKYL, ALKYLIDENE, AND ALKYLIDYNE CHEMISTRY

by

ZACHARY JOHN TONZETICH

B. S. (*summa cum laude*) in Chemistry
University of Rochester, Rochester, NY
(2002)

Submitted to the Department of Chemistry
in Partial Fulfillment of the Requirements
for the Degree of

DOCTOR OF PHILOSOPHY

at the
MASSACHUSETTS INSTITUTE OF TECHNOLOGY
May 2007

Signature of Author

Department of Chemistry
May 1, 2007

Certified by

Richard R. Schrock
Frederick G. Keyes Professor of Chemistry
Thesis Supervisor

Accepted by

Robert W. Field
Professor of Chemistry
Chairman, Departmental Committee on Graduate Students

This doctoral thesis has been examined by a Committee of the Department of Chemistry as follows:

Professor Christopher C. Cummins

Chairman

Professor Richard R. Schrock

Thesis Supervisor

Professor Stephen J. Lippard

EARLY TRANSITION METAL ALKYL, ALKYLIDENE, AND ALKYLIDYNE CHEMISTRY

by

ZACHARY JOHN TONZETICH

Submitted to the Department of Chemistry
in Partial Fulfillment of the Requirements
for the Degree of Doctor of Philosophy in Chemistry

ABSTRACT

CHAPTER 1

Zirconium and hafnium complexes of several new unsymmetric diamide ligands have been prepared and their proficiency in olefin polymerization reactions evaluated. The first set of supporting ligands examined are diamido-donor ligands that contain ethylene/*o*-phenylene "arms" and a phenyl-substituted amine donor in the central position. These ligands are derived from the triamines, [MesitylNH-*o*-C_6H_4N(Ph)CH_2CH_2NHMesityl] (H_2[MesNNPhMes]) and [*t*-Bu_{d6}-NH-*o*-C_6H_4N(Ph)CH_2CH_2NHMesityl] (H_2[*t*-BuNNPhNMes]). The Zr and Hf complexes that can be isolated include [MesNNPhNMes]MX_2 (M = Zr or Hf, X = NMe_2, Cl, or Me) and [*t*-BuNNPhNMes]MX_2 (M = Zr or Hf, X = NMe_2, Cl, Me). The structures of [MesNNPhNMes]$ZrMe_2$, [*t*-BuNNPhNMes]$ZrMe_2$, and a dimeric species with the formula [MesitylN-*o*-$C_6H_4NCH_2CH_2$NMesityl]$Zr_2(NMe_2)_5$ are reported. Abstraction of a methyl group in [MesNNPhNMes]MMe_2 (M = Zr or Hf) with $[Ph_3C][B(C_6F_5)_4]$ gives rise to cationic complexes which are active initiators for the polymerization of 1-hexene. Similar activation of [*t*-BuNNPhNMes]MMe_2 (M = Zr or Hf) gives rise to dimeric monocations that eventually break-up and react further to yield cationic monomethyl species. In all cases the poly[1-hexene] produced in the presence of the monometallic cations was found to be atactic. The second ligand explored is a diamido-didonor ligand based on the diamine, *rac*-H_2[MepyN] (*rac*-N,N′-di-(6-methylpyridin-2-yl)-2,2′-diaminobinaphthalene), which can be prepared through reductive amination of *rac*-2,2'-diaminobinaphthalene with 6-methylpyridinecarboxaldehyde. The deprotonated amine $[MepyN]^{2-}$ supports of variety of zirconium and hafnium complexes including [MepyN]MX_2 (M = Zr, X = NMe_2, Cl, OSO_2CF_3, CH_2CHMe_2, CH_2Ph; M = Hf, X = NMe_2, OSO_2CF_3, *i*-Bu). The solid state structures of [MepyN]$Zr(CH_2Ph)_2$, [MepyN]$Zr(NMe_2)Cl$, [MepyN]$Hf(CH_2CHMe_2)_2$, and [MepyN]$Hf(OSO_2CF_3)_2$ are reported. Activation of [MepyN]$Zr(CH_2Ph)_2$ and [MepyN]$Hf(i\text{-}Bu)_2$ with various Lewis acids leads to observable cationic alkyls that are not active towards 1-hexene polymerization. The third ligand examined is a diamide ligand based on the diamine *rac*-H_2[$HIPTN_2$] ($HIPTN_2$ = (N-hexaisopropyl-3,5-terphenyl)diaminobinaphthalene), which can be prepared through palladium-catalyzed *N*-aryl coupling of diaminobinaphthalene and 3,5-*bis*-(2,4,6-triisopropylphenyl)bromobenzene. The reaction between H_2[$HIPTN_2$] and $M(NMe_2)_4$ (M = Ti, Zr, and Hf) yields [$HIPTN_2$]$M(NMe_2)_2$ complexes. Other complexes of $[HIPTN_2]^{2-}$ that can be prepared include [$HIPTN_2$]$ZrCl_2$, [$HIPTN_2$]$ZrMe_2$, [$HIPTN_2$]$Zr(CH_2\text{-}t\text{-}Bu)_2$, [$HIPTN_2$]$HfCl_2$, [$HIPTN_2$]$HfMe_2$, and [$HIPTN_2$]$Hf(CH_2CHMe_2)_2$. Activation of [$HIPTN_2$]$ZrMe_2$ with a variety of Lewis acids gives rise to different species depending on the nature of the activator employed.

For example, $[HIPTN_2]ZrMe_2$ reacts with $[Ph_3C][B(C_6F_5)_4]$ to give a cationic complex that is active toward oligomerization of 1-hexene, while activation with $B(C_6F_5)_3$ leads to formation of $[HIPTN_2]Zr(C_6F_5)_2$. No polymerization of 1-hexene by activated complexes of the $[HIPTN_2]^{2-}$ ligand is observed.

CHAPTER 2

Imido alkylidene initiators for the controlled polymerization of diethyl dipropargylmalonate (DEDPM) have been prepared. A vinyl alkylidene complex, **2a**, containing a five-membered ring as part of a trienylidene unit can be obtained by treating $Mo(NAr)(CHCMe_2R)(O\text{-}t\text{-}Bu_{F6})_2$ (Ar = 2,6-diisopropylphenyl; R = Me, Ph; $t\text{-}Bu_{F6} = C(CF_3)_2Me$) with diethyl 3-(2-methylprop-1-enyl)-4-vinylcyclopent-3-ene-1,1-dicarboxylate in pentane. A related complex, **4b**, containing a six-membered ring alkylidene ligand can be prepared by a reaction between $Mo(NAr)(CH\text{-}t\text{-}Bu)(O\text{-}t\text{-}Bu_{F6})_2$ and 1-methylidene-5,5-bis(carboxyethyl)cyclohex-1-ene. Treatment of **2a** or **4b** with LiO-*t*-Bu yields the analogous *tert*-butoxide species (**2c** and **4c**). An X-ray structure of a sample of **4c** that retained two equivalents of $LiO\text{-}t\text{-}Bu_{F6}$ shows it to be a dimeric species in which two Mo complexes were joined through a Li_4O_4 heterocubane-type structure binding to one ester in each complex. Reactions between DEDPM and **4c** demonstrate smooth initiation with a k_p/k_i value of less than one. The carboxylate species, $Mo(NR)(CHCMe_2R')(O_2CCPh_3)_2$ (R = various aryl groups or 1-adamantyl; R′ = Ph or Me) can be prepared by salt metathesis reactions between $Mo(NR)(CHCMe_2R')(OTf)_2(DME)$ (OTf = trifluoromethanesulfonate; DME = 1,2-dimethoxyethane) and sodium triphenylacetate. Trimethylphosphine adducts of selected triphenylacetate complexes can also be synthesized, and the X-ray structure of $Mo(NAr'')(CH\text{-}t\text{-}Bu)(O_2CCPh_3)_2(PMe_3)$ (Ar″ = 2-*tert*-butylphenyl) is reported. Several of the triphenylacetate complexes are active initiators for the regioselective polymerization of DEPDM. Several of the alkylidene initiators serve as precursors to oligomeric fragments of poly[DEDPM], which represent structural models of the polymer chain.

CHAPTER 3

Reaction of $Mo(NR)(CHCMe_2R')(OTf)_2(DME)$ (R = 2,6-diisopropylphenyl, 2,6-dichlorophenyl, or 2-*tert*-butylphenyl; R′ = Me or Ph) with the lithium salt of various β-diketonate and β-diketiminates leads to complexes of the type $Mo(NR)(CHCMe_2R')(L)(OTf)$ (L = β-diketonate or β-diketiminate). Treatment of $Mo(NR)(CHCMe_2R')(L)(OTf)$ with $NaBAr_{f4}$ (Ar_f = 3,5-$(CF_3)_2C_6H_3$) in the presence of THF affords the cationic species $\{Mo(NR)(CHCMe_2R')(L)(THF)\}\{BAr_{f4}\}$. The reactivity of the cationic β-diketonate (acac) and β-diketiminate (nacnac) complexes towards olefins has been examined, as has the thermal decomposition modes of the neutral and cationic nacnac complexes. Results demonstrate that the cationic species have short catalyst lifetimes, and that decomposition modes dominate the chemistry of several of the nacnac complexes. The X-ray crystal structures of several neutral and cationic complexes are reported.

CHAPTER 4

Reaction of $WCl_3(OAr)_3$ (Ar = 2,6-diisopropylphenyl) with 4 equivalents of $t\text{-}BuCH_2MgCl$ in diethyl ether produces yellow crystalline $W(C\text{-}t\text{-}Bu)(CH_2\text{-}t\text{-}Bu)(OAr)_2$ in 40 – 50% isolated yield. The alkyl alkylidyne species reacts with 2-butyne and 3-hexyne in a metathetical fashion to generate the symmetric metallacyclobutadiene species, $W(C_3R_3)(CH_2\text{-}t\text{-}Bu)(OAr)_2$ (R = Me and Et, respectively). Replacement of the OAr ligands with $LiNPh_2$ generates $W(C\text{-}t\text{-}Bu)(CH_2\text{-}t\text{-}$

Bu)(NPh_2)$_2$ which serves as an *in situ* precursor to other dialkoxide species as demonstrated by alcoholysis with 1-adamantanol. The reaction between W(C-*t*-Bu)(CH_2-*t*-Bu)(OAr)$_2$ and benzonitrile generates the dimeric nitride species, [W(N)(CH_2-*t*-Bu)(OAr)$_2$]$_2$. The nitride reacts with trimethylsilyl trifluoromethanesulfonate to afford the imido complex, W(NTMS)(CH_2-*t*-Bu)(OAr)$_2$(OTf), The X-ray crystal structure of W(C-*t*-Bu)(CH_2-*t*-Bu)(OAr)$_2$, [W(N)(CH_2-*t*-Bu)(OAr)$_2$]$_2$, and W(NTMS)(CH_2-*t*-Bu)(OAr)$_2$(OTf) are reported as are studies concerning the catalytic efficiency of both W(C-*t*-Bu)(CH_2-*t*-Bu)(OAr)$_2$ and W(C-*t*-Bu)(CH_2-*t*-Bu)(O-1-adamantyl)$_2$.

APPENDIX A

The reaction of $Ph_3P{=}CH_2$ with Mo(NAr)(CH-*t*-Bu)(O-*t*-Bu_{F6})$_2$ (Ar = 2,6-*i*-$Pr_2C_6H_3$; O-*t*-Bu_{F6} = $OC(CF_3)_2Me$) produces the anionic alkylidyne complex {Ph_3PMe}{Mo(NAr)(C-*t*-Bu)(O-*t*-Bu_{F6})$_2$}. An X-ray structure determination of the complex reveals a bent Mo-N-C angle for the imido group, as expected when a metal-carbon triple bond is present. The reactivity of the anion towards electrophiles has been examined and shown to occur predominantly at the imido nitrogen.

Thesis: Supervisor: Richard R. Schrock

Title: Frederick G. Keyes Professor of Chemistry

TABLE OF CONTENTS

LIST OF FIGURES

LIST OF SCHEMES

CHAPTER 4

APPENDIX

LIST OF TABLES

LIST OF ABBREVIATIONS

anti	alkylidene rotational isomer with hydrogen substitutent directed toward the imide
acac	β-diketonate
Ad	1-adamantyl
Anal. calcd	analysis calculated
Ar	2,6-diisopropylphenyl
Ar′	2,6-dimethylphenyl
Ar′′	2-*tert*-butylphenyl
Ar^*	3,5-dimethylphenyl
Ar^{Cl}	2,6-dichlorophenyl
Ar^F	2,6-difluorophenyl
Ar_f	3,5-bis(trifluoromethyl)phenyl
Bn	benzyl
BenzBitet	3,3′-bis(benzhydryl)-5,5′,6,6′,7,7′,8,8′-octahydro-1,1′-binaphthyl-2,2′-diol
n-Bu	butyl
i-Bu	*iso*-butyl (2-methylpropyl)
t-Bu	*tert*-butyl (2-methyl-2-propyl)
H_2[*t*-BuNNPhNMes]	*t*-Bu_{d6}-NH-*o*-$C_6H_4N(Ph)CH_2CH_2NH$Mesityl
t-Bu_{d6}	hexadeutero-*tert*-butyl ($C(CD_3)_2Me$)
t-Bu_{F6}	hexafluoro-*tert*-butyl (1,1,1,3,3,3-hexafluoro-2-methyl-2-propyl; $C(CF_3)_2Me$)
DEDPM	diethyl dipropargylmalonate (diethyl 2,2-di(prop-2-ynyl)malonate
DME	1,2-dimethoxyethane
EI	electron impact ionization
ESI	electrospray ionization
Et	ethyl
ether	diethyl ether
$\Delta H^{\ddagger}$	activation enthalpy
HIPT	2′,2′′,4′,4′′,6′,6′′-hexaisopropyl-3,5-terphenyl
H_2[$HIPTN_2N$]	*N*,*N*′-bis-(hexaisopropyl-3,5-terphenyl)diaminobinaphthalene
HFAC	1,1,1,5,5,5-hexafluoropentane-2,4-dianato
HMQC	heteronuclear multiple quantum correlation
HRMS	high-resolution mass spectrometry
HSQC	heteronuclear single quantum correlation
ipso-	ipso position of phenyl ring
IR	infrared
J_{AB}	coupling constant between two nuclei, A and B
k	kinetic rate constant
k_i	kinetic rate constant of initiation
k_p	kinetic rate constant of propagation
lut	2,4-lutidine (2,4-dimethylpyridine)
m-	meta position of phenyl ring

M_n	number averaged molecular weight
M_w	weight averaged molecular weight
Me	methyl
H_2[MepyN]	*N*,*N*′-bis-(6-methylpyridin-2-yl)-1,1′-binaphthyl-2,2′-diamine
Mes	mesityl (2,4,6-trimethylphenyl)
H_2[MesNNPhNMes]	MesitylNH-*o*-$C_6H_4N(Ph)CH_2CH_2NH$Mesityl
nacnac	β-diketiminate
neopentyl	2,2-dimethylpropyl (CH_2-*t*-Bu)
neophyl	2-methyl-2-phenylpropyl (CH_2CMe_2Ph)
NMR	nuclear magnetic resonance
o-	ortho position of phenyl ring
OTf	trifluoromethanesulfonato (triflate; O_2SOCF_3)
p-	para position of phenyl ring
PDI	polydispersity index (M_w/M_n)
Ph	phenyl
ppm	parts per million
i-Pr	isopropyl (2-propyl)
quin	quinuclidine
RCMP	ring-closing metathesis polymerization
ROMP	ring-opening metathesis polymerization
$\Delta S^{\ddagger}$	activation entropy
syn	alkylidene rotational isomer with hydrogen substituent directed away from the imide
THF	tetrahydrofuran
TMHD	2,2,6,6-tetramethylheptane-3,5-dianato
TMS	trimethylsilyl
Trip	2,4,6-triisopropylphenyl
UV-vis	ultraviolet-visible

LIST OF COMPOUND NUMBERS

Compound Name or Formula

CHAPTER 1

1a	2-(2-Nitro-phenylamino)-ethyl-ammonium chloride
1b	2-(2-Amino-phenylamino)-ethyl-ammonium chloride
1c	*N*-(2,4,6-Trimethyl-phenyl)-*N*'-[2-(2,4,6-trimethyl-phenylamino)-ethyl]-benzene-1,2-diamine
1d	κ^3-μ^1-[MesNNNMes]Zr_2-μ^1-$(NMe_2)_5$
2a	*N*'-(2,4,6-Trimethyl-phenyl)-ethane-1,2-diamine
2b	*N*-(2-Nitro-phenyl)-*N*'-(2,4,6-trimethyl-phenyl)-ethane-1,2-diamine
2c	*N*-[2-(2,4,6-Trimethyl-phenylamino)-ethyl]-benzene-1,2-diamine
2d	*N*-Isopropylidene-d_6-*N*'-[2-(2,4,6-trimethyl-phenylamino)-ethyl]-benzene-1,2-diamine
2e	*N*-*tert*-Butyl-d_6-*N*'-[2-(2,4,6-trimethyl-phenylamino)-ethyl]-benzene-1,2-diamine
3a	[MesNNPhNMes]$Zr(NMe_2)_2$
3b	[MesNNPhNMes]$ZrCl_2$
3c	[MesNNPhNMes]$ZrMe_2$
3d	{[MesNNPhNMes]ZrMe}{$B(C_6F_5)_4$}
4a	[MesNNPhNMes]$Hf(NMe_2)_2$
4b	[MesNNPhNMes]$HfCl_2$
4c	[MesNNPhNMes]$HfMe_2$
4d	{[MesNNPhNMes]HfMe}{$B(C_6F_5)_4$}
5a	[*t*-BuNNPhNMes]$Zr(NMe_2)_2$
5b	[*t*-BuNNPhNMes]$ZrCl_2$
5c	[*t*-BuNNPhNMes]$ZrMe_2$
5d	{[*t*-BuNNPhNMes]ZrMe}{$B(C_6F_5)_4$}
5e	{([*t*-BuNNPhNMes]$Zr)_2$-μ^1-Me_3}{$B(C_6F_5)_4$}
6a	[*t*-BuNNPhNMes]$Hf(NMe_2)_2$
6b	[*t*-BuNNPhNMes]$HfCl_2$
6c	[*t*-BuNNPhNMes]$HfMe_2$
6d	{[*t*-BuNNPhNMes]HfMe}{$B(C_6F_5)_4$}
6e	{([*t*-BuNNPhNMes]$Hf)_2$-μ^1-Me_3}{$B(C_6F_5)_4$}
7a	[MepyN]$Zr(NMe_2)_2$
7a′	[MepyN]$Zr(NMe_2)Cl$
7b	[MepyN]$ZrCl_2$
7t	[MepyN]$Zr(OTf)_2$
7d	[MepyN]$Zr(i\text{-}Bu)_2$
7e	[MepyN]$Zr(Bn)_2$
7e′	{[MepyNH]$Zr(Bn)_2$}{$B(C_6F_5)_4$}
8a	[MepyN]$Hf(NMe_2)_2$
8t	[MepyN]$Hf(OTf)_2$
8d	[MepyN]$Hf(i\text{-}Bu)_2$

9a	$[HIPTN_2]Ti(NMe_2)_2$
10a	$[HIPTN_2]Zr(NMe_2)_2$
10b	$[HIPTN_2]ZrCl_2(Et_2O)_2$
10c	$[HIPTN_2]ZrMe_2$
10f	$[HIPTN_2]Zr(CH_2\text{-}t\text{-}Bu)_2$
10g	$[HIPTN_2]Zr(C_6F_5)_2$
11a	$[HIPTN_2]Hf(NMe_2)_2$
11b	$[HIPTN_2]HfCl_2$
11c	$[HIPTN_2]HfMe_2$
11d	$[HIPTN_2]Hf(i\text{-}Bu)_2$

CHAPTER 2

1a	Diethyl 2-(4-hydroxy-4-methylpent-2-ynyl)-2-(prop-2-ynyl)malonate
1b	Diethyl 3-formyl-4-(2-methylprop-1-enyl)cyclopent-3-ene-1,1-dicarboxylate
1c	Diethyl 3-(2-methylprop-1-enyl)-4-vinylcyclopent-3-ene-1,1-dicarboxylate
2a	$Mo(NAr)(CH[5])(O\text{-}t\text{-}Bu_{F6})_2$
2c	$Mo(NAr)(CH[5])(O\text{-}t\text{-}Bu)_2$
3a	Diethyl 5-methylene-3-vinylcyclohex-3-ene-1,1-dicarboxylate
3b	Diethyl 3-vinylcyclohex-3-ene-1,1-dicarboxylate
4a	$Mo(NAr)(CH[6]{=}CH_2)(O\text{-}t\text{-}Bu_{F6})_2$
4b	$Mo(NAr)(CH[6])(O\text{-}t\text{-}Bu_{F6})_2$
4c	$Mo(NAr)(CH[6])(O\text{-}t\text{-}Bu)_2$
4d	$\{Mo(NAr'')(O\text{-}t\text{-}Bu_{F6})_2\}_2\text{-}\mu\text{-}(CH[6])$
5a	$Mo(NAr)(CHCMe_2Ph)(O_2CCPh_3)_2$
5b	$Mo(NAr')(CHCMe_2Ph)(O_2CCPh_3)_2$
5c	$Mo(NAd)(CHCMe_2Ph)(O_2CCPh_3)_2$
5d	$Mo(NAr'')(CH\text{-}t\text{-}Bu)(O_2CCPh_3)_2$
5e	$Mo(NAr^{Cl})(CH\text{-}t\text{-}Bu)(O_2CCPh_3)_2$
5b·PMe$_3$	$Mo(NAr')(CHCMe_2Ph)(O_2CCPh_3)_2(PMe_3)$
5c·PMe$_3$	$Mo(NAd)(CHCMe_2Ph)(O_2CCPh_3)_2(PMe_3)$
5d·PMe$_3$	$Mo(NAr'')(CH\text{-}t\text{-}Bu)(O_2CCPh_3)_2(PMe_3)$
5e·PMe$_3$	$Mo(NAr^{Cl})(CH\text{-}t\text{-}Bu)(O_2CCPh_3)_2(PMe_3)$
5e′·PMe$_3$	$Mo(NHAr^{Cl})(C\text{-}t\text{-}Bu)(O_2CCPh_3)_2(PMe_3)$
6c	$\{Na\}\{Mo(NAd)(CHCMe_2Ph)(O_2CAr')_3\}$
6c·PMe$_3$	$Mo(NAd)(CHCMe_2Ph)(O_2CAr')_2(PMe_3)$
7a	$Mo(NAdr)(CHCMe_2Ph)(O_2CCMePh_2)_2$
8a	(E)-di-1,2-[1-(2-methyl-propenyl)-4,4-diethyl-carboxy-cyclopent-1-enyl]-ethene
8b	Diethyl 5-((4,4-di(ethoxycarbonyl)-2-(2-methylprop-1-enyl)cyclopent-1-enyl)methylene)-3-((1E)-2-(4,4-di(ethoxycarbonyl)-2-(2-methylprop-1-enyl)cyclopent-1-enyl)vinyl)cyclohex-3-ene-1,1-dicarboxylate

CHAPTER 3

1a	Mo(NAr)(CHCMe$_2$Ph)(TMHD)(OTf)(THF)
1b	Mo(NAr)(CHCMe$_2$Ph)(TMHD)(OTf)(quin)
1c	Mo(NAr)(CHCMe$_2$Ph)(TMHD)(OTf)(lut)
1d	Mo(NAr)(CHCMe$_2$Ph)(TMHD)(OTf)
1e	{Mo(NAr)(CHCMe$_2$Ph)(TMHD)(PMe$_3$)$_2$}{OTf}
2a	Mo(NAr)(CHCMe$_2$Ph)(HFAC)(OTf)(THF)
3a	{Mo(NAr)(CHCMe$_2$Ph)(TMHD)(THF)}{BAr$_{f4}$}
4a	{Mo(NAr)(CHCMe$_2$Ph)(HFAC)(OTf)}{BAr$_{f4}$}
5a	Mo(NAr)(CHCMe$_2$Ph)(Ar′-nacnac)(OTf)
5b	Mo(NAr^{Cl})(CH-*t*-Bu)(Ar′-nacnac)(OTf)
5c	Mo(NAr′′)(CH-*t*-Bu)(Ar′-nacnac)(OTf)
6a	Mo(NAr)(κ^1-κ^1-η^2-[Ar^x/Ar′-NC(Me)]$_2$CHCMe$_2$Ph)(OTf)
6b	Mo(NAr^{Cl})(κ^1-κ^1-η^2-[Ar^x/Ar′-NC(Me)]$_2$CH-*t*-Bu)(OTf)
6c	Mo(NAr′′)(κ^1-κ^1-η^2-[Ar^x/Ar′-NC(Me)]$_2$CH-*t*-Bu)(OTf)
7a	Mo(NAr)(CHCMe$_2$Ph)(Ar^F-Nacnac)(OTf)
8a	Mo(NAr)(CHCMe$_2$Ph)(Ar*-Nacnac)(OTf)
9a	{Mo(NAr)(CHCMe$_2$Ph)(Ar′-nacnac)(THF)}{BAr$_{f4}$}
9b	{Mo(NAr^{Cl})(CH-*t*-Bu)(Ar′-nacnac)(THF)}{BAr$_{f4}$}
9c	{Mo(NAr′′)(CH-*t*-Bu)(Ar′-nacnac)(THF)}{BAr$_{f4}$}
11a	{Mo(NAr)(κ^2-[Ar′-NC(Me)CHC(Me)NC$_6$H$_3$(Me)CH=](THF)}{BAr$_{f4}$}
11c	{Mo(NAr′′)(κ^2-[Ar′-NC(Me)CHC(Me)NC$_6$H$_3$(Me)CH=](THF)}{BAr$_{f4}$}
12a	{Mo(NAr)(κ^1-κ^1-η^2-[Ar^x/Ar′-NC(Me)]$_2$CHCMe$_2$Ph)(THF)}{B(C$_6$F$_5$)$_4$}
13a	{Mo(NAr)(CHCMe$_2$Ph)(Ar^F-nacnac)(THF)}{BAr$_{f4}$}
14a	{Mo(Nr)(CHCMe$_2$Ph)(Ar*-nacnac)(THF)}{B(C$_6$F$_5$)$_4$}
15a	{Mo(NAr)(CH$_2$CH$_2$)(Ar′-nacnac)(THF)}{BAr$_{f4}$}
15b	{Mo(NAr^{Cl})(CH$_2$CH$_2$)(Ar′-nacnac)(THF)}{BAr$_{f4}$}

CHAPTER 1

Synthesis, Activation, and Polymerization Behavior of Zirconium and Hafnium Complexes that Contain Unsymmetric Diamide Ligands

Portions of this chapter have appeared in print:

Tonzetich, Z. J.; Lu, C. C.; Schrock, R. R.; Hock, A. S.; Bonitatebus, P. J., Jr. "Synthesis, Characterization, and Polymerization Behavior of Zirconium and Hafnium Complexes that Contain Asymmetric Diamido-N-Donor Ligands" *Organometallics* **2004**, *23*, 4362-4372.

Tonzetich, Z. J.; Schrock, R. R.; Hock, A. S.; Müller, P. " Synthesis, Characterization, and Activation of Zirconium and Hafnium Dialkyl Complexes that Contain a C_2-Symmetric Diaminobinaphthyl Dipyridine Ligand" *Organometallics* **2005**, *24*, 3335-3342.

Tonzetich, Z. J.; Schrock, R. R. "Potential Group IV Olefin Polymerization Catalysts that Contain a Diamido Ligand Substituted with Hexaisopropylterphenyl Groups" *Polyhedron* **2006**, *25*, 469-476.

INTRODUCTION

The development of homogeneous Ziegler-Natta catalysts supported by cyclopentadienyl and modified cyclopentadienyl ligands (metallocene) has resulted in unprecedented levels of control over polymer microstructure and allowed for the realization of new polyolefin motifs.[1,2,3,4,5,6] Metallocene catalysts are not without their limitations, and a substantial body of recent work in the area of terminal olefin polymerization has focused on the design and implementation of Group IV *non*-metallocene catalysts.[7,8] Such systems have been targeted because of their potential in creating well-behaved catalytic species that avoid the unfavorable attributes associated with traditional metallocene catalysts (i.e. chain transfer, β-hydride elimination, and regio-misinsertions).[1] In this vein, a host of different ligands have been developed that support catalysts for the polymerization of simple olefins and show characteristics consistent with a living process.[9,10] Yet despite this success, there remain relatively few non-metallocene catalysts capable of promoting the stereospecific polymerization of olefins with the high degree of control displayed by metallocene catalysts. Furthermore, there exist only a few examples of catalysts capable of promoting both the living *and* stereospecific polymerization of simple olefins.[11,12,13,14] In each of these systems the stereochemistry and living characteristics are specific to the olefin employed, and no consistent mechanistic picture has arisen that complements the better-understood features of monomer binding and enchainment with Group IV metallocene catalysts.[1,15,16,17,18,19]

Catalysts capable of promoting stereospecific living polymerizations are highly valuable from a practical standpoint because of their potential in realizing new polymer microstructures including tactic diblock and triblock copolymers.[20,21,22] Interest in our laboratory in the area of olefin polymerization has focused on the development of amide-based ligands capable of supporting Zr and Hf catalysts for the living polymerization of simple olefins.[23,24,25,26,27,28,29] Many of the most successful examples of non-metallocene catalysts contain nitrogen-donor ligands, and examples throughout the transition series are abundant.[8] Amide ligands in particular have

found a great deal of use in early metal polymerization.[30] These ligands offer the advantage of both steric protection and electronic saturation of low-coordinate, electrophilic metal centers.[31] One particular subset of amide ligands that has found great utility among the Group IV metals are the diamido-donor ligands (donor = N, O, S). Examples of diamido-donor ligands from this laboratory incorporate a single donor moiety within a chelating diamide framework (Scheme 1.1).[32,33,34] Many of the Zr and Hf complexes supported by these ligands were found to be well-behaved initiators for the living polymerization of 1-hexene. Success with this type of

Scheme 1.1. Examples of diamido-donor ligand frameworks.

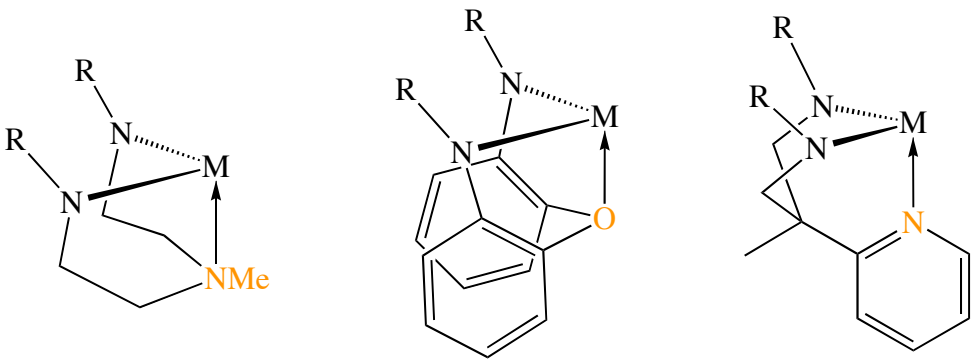

Diamido-donor Ligands

ligand architecture prompted an investigation of unsymmetric variations to this ligand class. Early modifications (Scheme 1.2) yielded catalysts that produced atactic polymer suggesting that the asymmetry in the ligand was inefficient in directing the stereochemistry of olefin binding and insertion.[35,36] Note that in two of the three asymmetric complexes depicted in Scheme 1.2, the chiral element arises from coordination of a prochiral ligand. Along these lines, a larger degree of asymmetry within the diamido-donor framework was sought after leading to the development of the ligands, $[MesNNPhNMes]^{2-}$ and $[t\text{-}BuNNPhNMes]^{2-}$, discussed in the first part of this chapter (Scheme 1.3).

Scheme 1.2. Previously synthesized Group IV complexes of unsymmetric diamido-donor ligands.

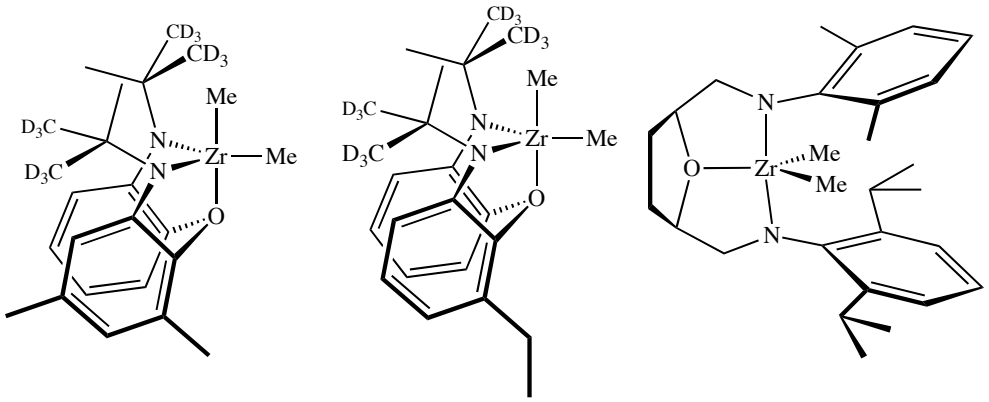

To complement the work with diamido-donor ligands, an asymmetric diamido ligand that contained a relatively rigid *and* chiral backbone, namely a C_2-symmetric (*rac*) binaphthyl backbone, was examined. The rigid biaryl backbone of binaphthalene provides a *fixed* stereochemical element capable of transmitting chiral information close to the metal through the amide linkages. The second ligand discussed in this chapter incorporates two pyridine donors into the binaphthalene diamide platform ($[MepyN]^{2-}$, Scheme 1.3). In this sense, $[MepyN]^{2-}$ may be viewed as a diamido-didonor.

The third ligand discussed in this chapter, $[HIPTN_2]^{2-}$ (Scheme 1.3), is a C_2-symmetric amide that lacks any pendant donor moiety. This ligand contains the bulky hexaisopropylterphenyl (HIPT) group. The HIPT group has found success recently in supporting molybdenum complexes for the catalytic reduction of dinitrogen.[37] In particular, the sterically demanding group inhibits bimolecular (bimetallic) reactivity while still allowing small molecules access to the coordination sphere.

This chapter details the synthesis, characterization, activation, and polymerization behavior of several asymmetric Group IV complexes supported by amide based ligands. Of the three ligand types mentioned (diamido-donor, diamido-didonor, and diamido) above, only the diamido-donor ligands were capable of supporting catalysts for the polymerization of 1-hexene.

In no case was tactic polymer produced. The ability of these complexes to serve as olefin polymerization catalysts is discussed, as well as the factors contributing to the lack of activity and/or stereoselectivity in all three ligand systems.

Scheme 1.3. Unsymmetric diamide ligands.

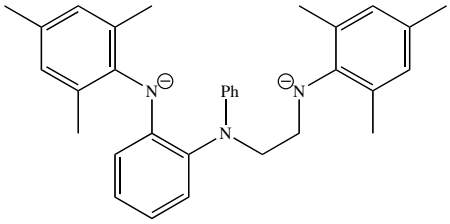

[MesNNPhNMes]$^{2-}$

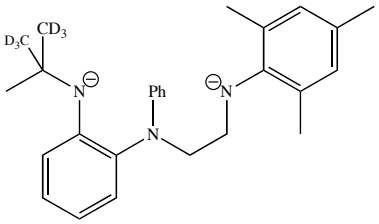

[t-BuNNPhNMes]$^{2-}$

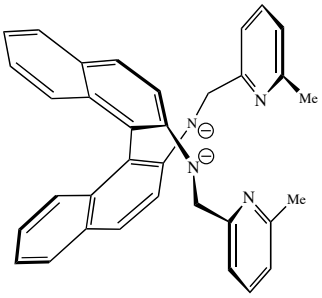

[MepyN]$^{2-}$

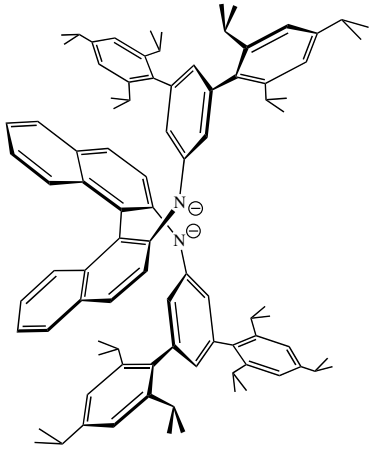

[HIPTN$_2$]$^{2-}$

RESULTS

1.1 Zr and Hf complexes possessing the [MesNNPhNMes]$^{2-}$ and [*t*-BuNNPhNMes]$^{2-}$ ligands

1.1.1 Ligand syntheses

The first set of ligands examined were initially prepared in this laboratory by Connie Lu.[38] These compounds are diamido/donor ligands in which one of the two "arms" contains a phenylene ring while the other contains an ethylene linkage. The amido substituents can be identical (H_2[MesNNPhNMes], Scheme 1.4) or different (H_2[*t*-BuNNPhNMes], Scheme 1.5). The synthesis of H_2[MesNNPhNMes] begins with addition of ethylenediamine to *o*-

chloronitrobenzene to generate the previously reported[39] hydrochloride salt **1a** in 60% yield after recrystallization. This reaction can be scaled up to 100 g without difficulty. Reduction of the nitro group in **1a** with Pd/C under 35 psi of H_2 affords the hydrochloride salt **1b** in satisfactory yield (70%, 20 g scale) after recrystallization from methanol. Addition of mesityl groups to the primary nitrogen atoms of compound **1b** is accomplished by a palladium/phosphine catalyzed *N*-aryl coupling using conditions reported by Buchwald.[40,41] The resulting dimesityl substituted triamine (**1c**) can be isolated in 65% yield after purification by column chromatography and crystallization from hexanes. Substitution of the central nitrogen donor of **1c** with a methyl group was attempted, although no suitable method could be found. For example, complex mixtures of products formed when MeI was employed in acetonitrile in the presence of potassium carbonate, presumably as a consequence of competing methylation at any of the three amine nitrogen atoms.

Scheme 1.4. Synthesis of H_2[MesNNPhNMes].

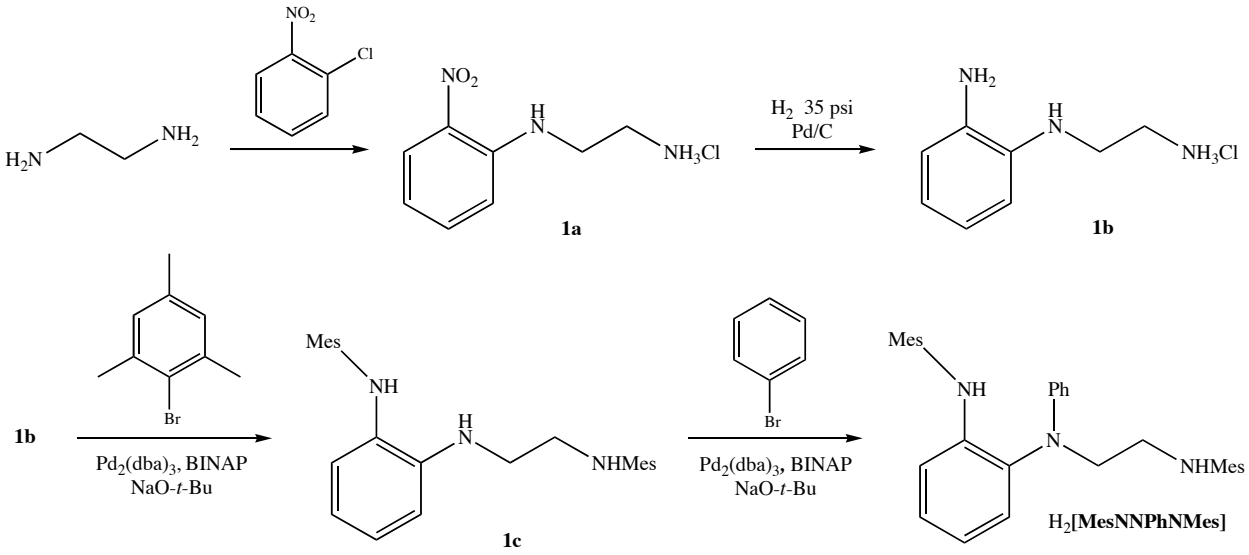

One potential way to substitute the central nitrogen atom is to prepare a *bis*-dimethylamide complex of zirconium employing **1c**, remove the proton with a lithium reagent,

and then add methyl iodide. Such a method was successful for preparing a complex that contained the $[(MesitylNCH_2CH_2)_2NMe]^{2-}$ ligand.[42] However, **1c** reacted with $Zr(NMe_2)_4$ to give **1d** (equation 1.1), as elucidated in an X-ray study (Figure 3.1, see caption for bond metrics); effectively **1c** is triply deprotonated and bound to two zirconium centers through two bridging amido nitrogen atoms. The $Zr\text{-}N_{amido}$ bond lengths are normal[28] (all close to 2.05 Å), whereas the $Zr\text{-}N_{bridging}$ distances are much longer, characteristic of Zr-N single bonds (2.275(2) to 2.453(2) Å; see caption to Figure 3.1). The longest $Zr\text{-}N_{bridging}$ bonds (2.333(2) and 2.453(2) Å) are to the central nitrogen in the ligand, presumably as a consequence of steric constraints.

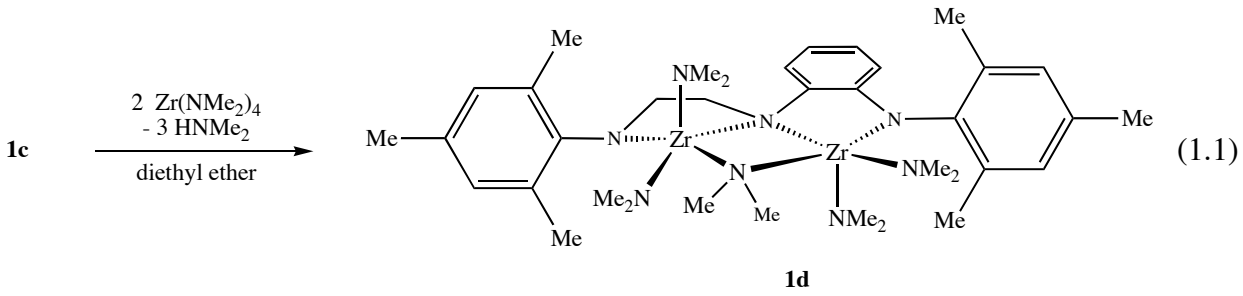

(1.1)

In the complex ^1H NMR spectrum of **1d**, two of the five dimethylamido groups display free rotation about the Zr-N bond on the NMR time scale at 20 ºC, while the remaining three (including the bridging dimethylamido group) appear as a set of broadened resonances. (See Experimental section.) A variable temperature spectrum in benzene-d_6 between 5 °C and 75 °C did not clarify the nature of the fluxional process or processes in the molecule.

Substitution of the central nitrogen in **1c** with a phenyl group can be achieved through a palladium/phosphine catalyzed *N*-aryl coupling reaction with bromobenzene.[40] Selective addition of the phenyl group to the central nitrogen proceeds in high yield to give the protonated form of the ligand, H_2[MesNNPhNMes]. The triamine is purified by column chromatography and isolated in 55% yield as a yellow-brown resin. Difficulties with chromatographic separation limited the scale at which the reaction can be performed. The highest isolated yields were realized when the phenylation was conducted on a four to five gram scale of **1c**.

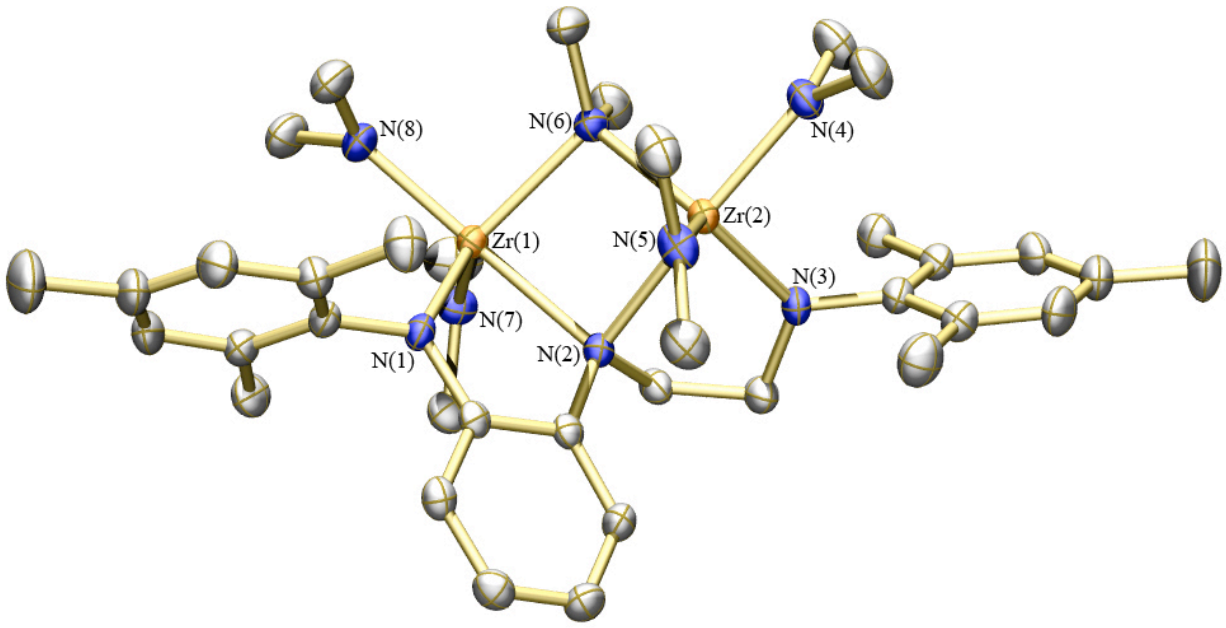

Figure 1.1. Thermal ellipsoid drawing (35%) of compound **1d**. Hydrogen atoms and cocrystallized benzene omitted for clarity. Selected bond lengths (Å) and angles (°): Zr(1)–N(1) = 2.112(2); Zr(1)–N(2) = 2.333(2); Zr(1)–N(6) = 2.295(2); Zr(1)–N(7) = 2.030(2); Zr(1)–N(8) = 2.064(2); Zr(2)–N(3) = 2.082(2); Zr(2)–N(2) = 2.453(2); Zr(2)–N(4) = 2.068(2); Zr(2)–N(5) = 2.039(2); Zr(2)–N(6) = 2.275(2); Zr(1)–N(2)–Zr(2) = 95.59(6); Zr(1)–N(6)–Zr(2) = 101.75(7); N(2)–Zr(1)–N(6) = 79.89(6); N(2)–Zr(2)–N(6) = 77.78(6); N(1)–Zr(1)–N(6) = 120.43(6); N(3)–Zr(2)–N(6) = 117.75(7).

The synthesis of the second diamido-donor ligand, H_2[*t*-BuNNPhNMes], begins with arylation of ethylenediamine to give compound **2a** (Scheme 1.5). To prevent over-arylation, a large excess of ethylenediamine was employed in the synthesis of **2a**, allowing for isolation on a large scale (>20 g) in good yield (65%) after vacuum distillation. Nucleophilic aromatic substitution of *o*-fluoronitrobenzene with diamine **2a** generates **2b**, which is subsequently reduced with Pd/C under 35 psi of H_2 to afford **2c**. Compound **2c** undergoes imine condensation with acetone-d_6 to give **2d**, which upon treatment with MeLi affords the triamine **2e**. Synthesis of precursors **2b** – **2e** all proceed without the need of chromatographic purification in good yields (≥70%) on scales of roughly 20 grams. Unlike H_2[MesNNPhNMes], the final phenylation

of **2e** with bromobenzene was found to give only 50% conversion (by ^{1}H NMR) using the traditional *rac*-BINAP (racemic-2,2′-*bis*-(diphenylphosphino)-1,1′-binaphthyl) cocatalyst. Use of the XPHOS (dicyclohexyl-(2′,4′,6′-triisopropyl-biphenyl-2-yl)-phosphine) ligand[43] resulted in a near quantitative conversion of **2e** to H_2[*t*-BuNNPhNMes] according to ^{1}H NMR spectroscopy. The final triamine can be purified by column chromatography and isolated in 50% yield as a yellow-brown resin.

Scheme 1.5. Synthesis of H_2[*t*-BuNNPhNMes].

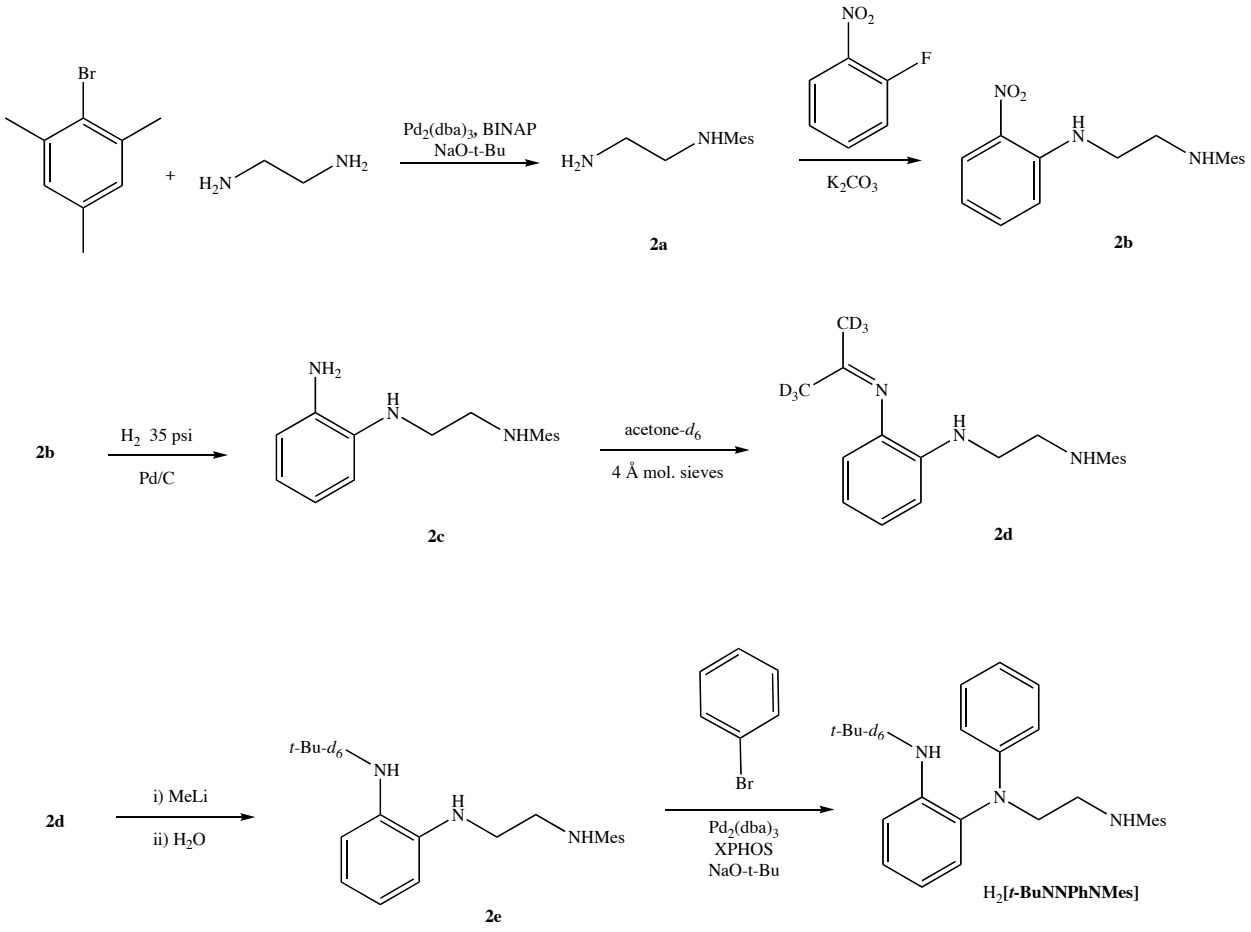

1.1.2 Synthesis of Zr and Hf complexes

Bis-dimethylamido zirconium and hafnium complexes were prepared as white or off-white, air- and moisture-sensitive crystalline solids through reaction of both H_2[MesNNPhNMes] and H_2[*t*-BuNNPhNMes] with $Zr(NMe_2)_4$ and $Hf(NMe_2)_4$ (Scheme 1.6).[44] ^{1}H NMR spectra of the resulting *bis*-dimethylamido species are complicated as a result of the unsymmetric nature of the supporting ligands. In general, NMR spectra of all analogous zirconium and hafnium complexes were identical except for some minor differences in chemical shift. In the compounds that contain $[MesNNPhNMes]^{2-}$ (**3a** and **4a**), it is evident that the mesityl rings do not rotate readily on the NMR timescale, although not all six mesityl methyl resonances are visible due to overlap with dimethylamido methyl resonances. Ortho and meta proton resonances for the central phenyl ring can be discerned (e.g. in **3a** at 7.07 ppm for *ortho* and 7.00 ppm *meta*), consistent with a readily rotating phenyl ring on the central nitrogen donor. The four backbone protons of the ethylene arm are clearly resolved as distinct multiplets (e.g. in **3a** at 4.30, 3.70, 3.62, and 3.02 ppm). Two sharp singlet resonances are observable for the methyl groups of the NMe_2 groups, characteristic of dimethylamido ligands that rotate readily about the Zr-N bond and that *do not* interconvert readily on the NMR time scale. Therefore, the central nitrogen donor must not dissociate from the metal, invert at nitrogen, and reassociate on the NMR time scale (~1-100 s^{-1}), as the two dimethylamido ligands would likely exchange in such a process.

In all compounds that contain the $[t$-BuNNPhNMes$]^{2-}$ ligand, the *t*-Bu-d_6 proton resonance contains a small upfield shoulder as a consequence of some pentadeutero *tert*-butyl group (primarily) being formed during the synthesis of H_2[*t*-BuNNPhNMes], a fact that contributes to a total integral for the *t*-Bu-d_6 group of between 3.1 and 3.2 protons. In **5a** and **6a** some slowing down of rotation of one of the two dimethylamido groups is apparent in the form of broadening of one of the dimethylamido resonances at room temperature. Replacement of the mesityl group on nitrogen with *t*-Bu-d_6 most likely renders complexes of $[t$-BuNNPhNMes$]^{2-}$ more crowded than those that contain $[MesNNPhNMes]^{2-}$. This increase in steric congestion is in turn responsible for hindered rotation of one of the dimethylamido groups.

Treatment of the *bis*-dimethylamido complexes with two equivalents of TMSCl yielded the dichloride derivatives, **3b - 6b** (Scheme 1.6). In these species, distinct mesityl methyl resonances are clearly discernable (see Experimental section), along with others characteristic of asymmetric species and a rotating central phenyl ring. The dichloride complexes are not soluble in pentane or diethyl ether, which raises the possibility that they are dimeric in the solid state. Dimeric structures have been observed for other dichloride compounds in this general family of diamido/donor complexes for which the structure has been determined.[42]

Scheme 1.6. Synthesis of Zr and Hf complexes of $[MesNNPhNMes]^{2-}$ and $[t\text{-BuNNPhNMes}]^{2-}$.

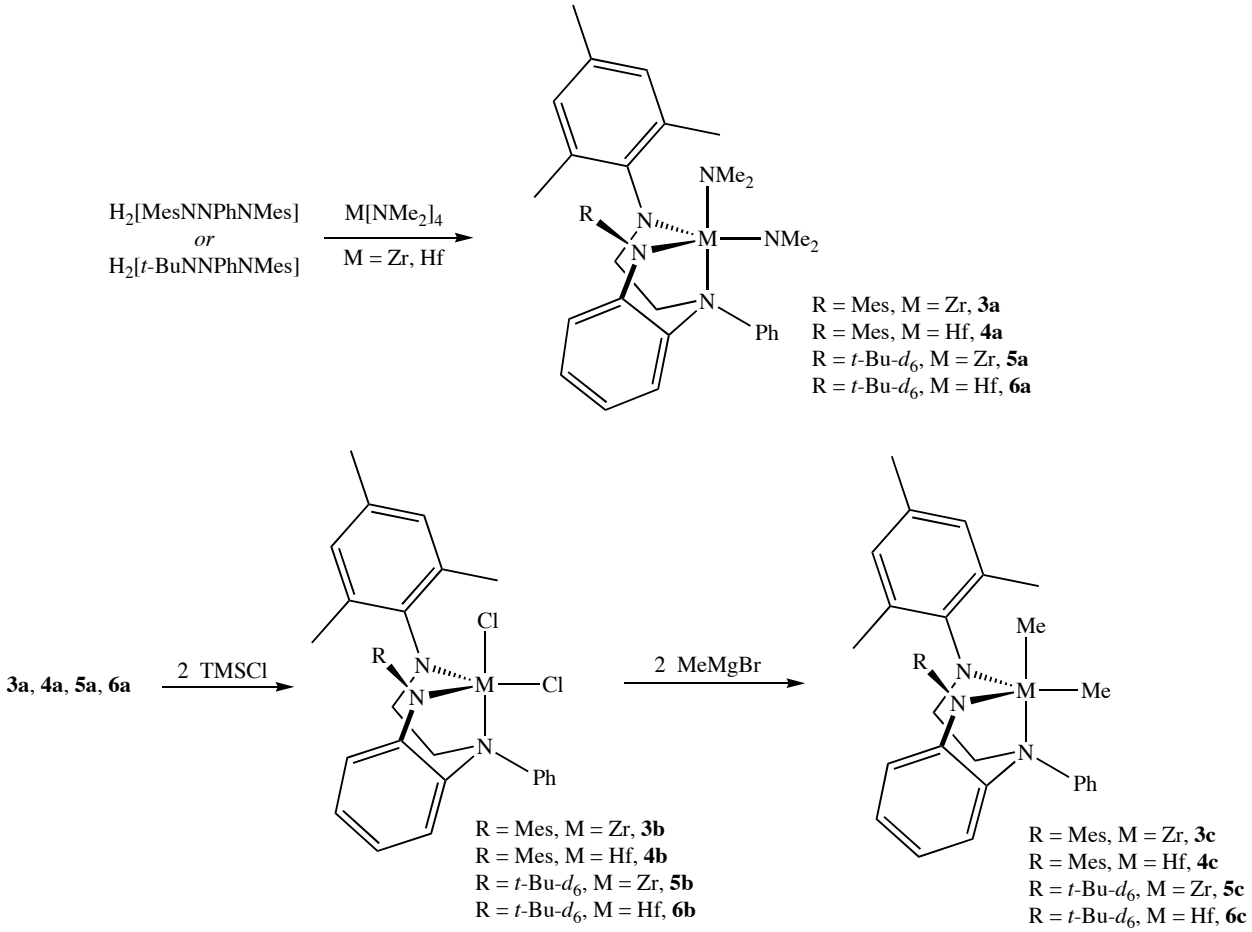

Alkylation of the dichloride complexes with two equivalents of MeMgBr yielded the dimethyl derivatives, **3c**-**6c** (Scheme 1.6). The most distinguishing feature of the dimethyl complexes are sharp singlet resonances for two inequivalent methyl groups bound to the metal near 0 ppm (e.g., at 0.22 and 0.11 in **4c**). Compound **6c** was also prepared using $^{13}CH_3MgI$ in ether. The carbon atoms of the methyl group in **6c** resonate at 58.9 ppm (J_{CH} = 111 Hz, J_{CC} = 2.9 Hz) and 57.2 ppm (J_{CH} = 112 Hz, J_{CC} = 2.9 Hz) in bromobenzene-d_5.

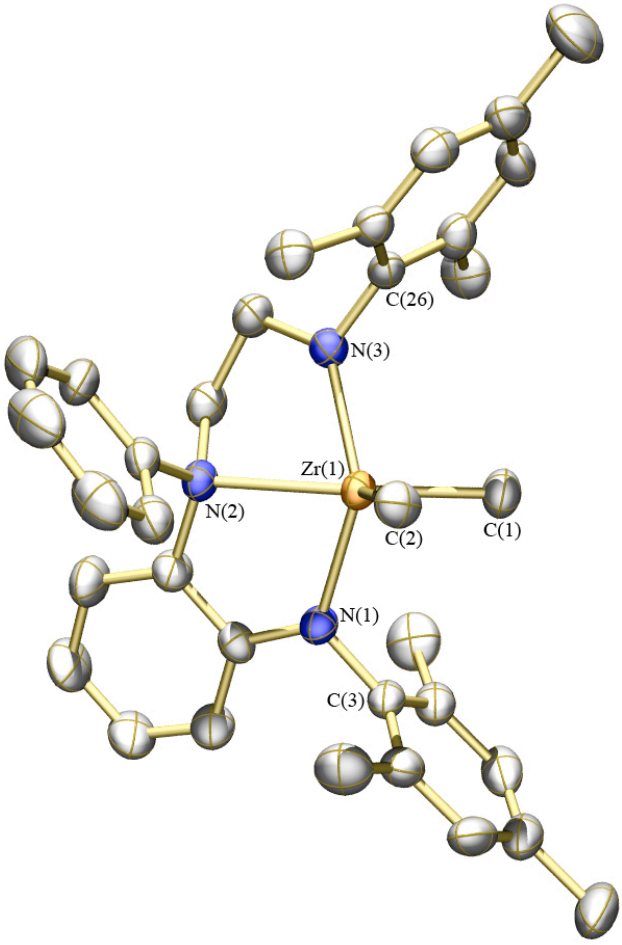

Figure 1.2. Thermal ellipsoid (35%) rendering of **3c**. Hydrogen atoms and cocrystallized molecule of diethyl ether omitted for clarity. Selected bond distances (Å) and angles (°): Zr(1)–N(1) = 2.123(4); Zr(1)–N(2) = 2.463(4); Zr(1)–N(3) = 2.061(4); Zr(1)–C(1) = 2.238(5); Zr(1)–C(2) = 2.257(5); N(1)–Zr(1)–N(3) = 134.17(15); C(1)–Zr(1)–C(2) = 95.8(2).

Crystals of **3c** suitable for X-ray diffraction were grown by Connie Lu. The solid state structure is displayed in Figure 1.2 and relevant metric parameters can be found in the caption. The geometry of **3c** is best viewed as a distorted square pyramid or distorted trigonal bipyramid with N(2)-Zr(1)-C(1) = 141.69(17)° and N(2)-Zr(1)-C(2) = 122.49(17)°. The sum of the angles around N(1) and N(3) is close to 360º (359.5 and 360.0º, respectively), as expected for π-donating disubstituted diamido ligands bound to Zr. The amide and carbon bond lengths around Zr in **3c** are within the range commonly encountered for complexes of this type,[32] although the Zr-N(1) bond is slightly longer (0.06 Å) than the Zr-N(3) bond. This difference is likely to be the consequence of weaker π-donation to Zr by the less basic diaryl amido nitrogen N(1). The Zr-N(2) bond length of 2.463(4) Å is one of the longest metal-donor bonds reported for alkyl complexes of Zr containing diamido/donor ligands of this general type.[32,33,34,36,45] This longer bond is consistent with the weaker donor ability of the diaryl/alkyl amine donor (as compared to donors shown in Scheme 1.1) and perhaps also the greater steric requirements of the phenylated central amine.

Compound **5c** crystallized in the triclinic space group $P\bar{1}$ with two independent molecules in the asymmetric unit, only one of which is shown in Figure 1.3 (see caption for metric parameters). Both molecules displayed disordered phenyl groups bound to the central nitrogen atom. The disorder was modeled satisfactorily, though several of the thermal ellipsoids in Figure 1.3 still appear elongated. The geometry of **5c** more closely approaches that of a TPB structure with C(1) and N(2) in axial positions. For example, the C(1)-Zr-N(2) angle (165.32(19)º) is much closer to 180º than the C(1)-Zr-N(2) angle in **3c**, and the N(1)-Zr-N(3) angle is 116.18(17)º (vs. 134.17(15)° in **3c**). The Zr-N_{amido} and Zr-C bond lengths are similar to those found for **3c**. As expected, there is no significant difference in the Zr-N_{amido} bond lengths in **5c** because both N(1) and N(3) are alkyl/aryl-substituted amides. The Zr-N(2) bond length (2.510(4) Å) is even longer than that in **3c**, possibly as a consequence of the larger steric demands of the *tert*-butyl substituent on N(1).

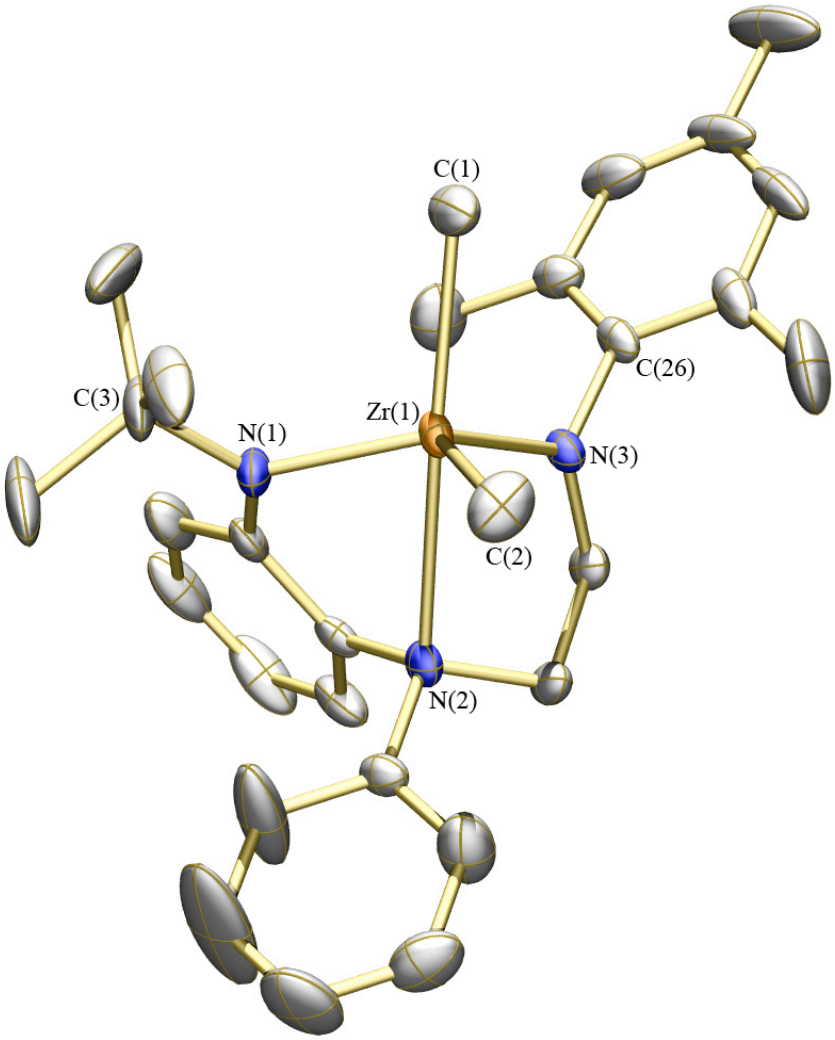

Figure 1.3. Thermal ellipsoid drawing (35%) of one of the two independent molecules of [*t*-BuNNPhNMes]ZrMe$_2$ (**5c**) in the asymmetric unit. Hydrogen atoms and disordered atoms omitted for clarity. Selected bond distances (Å) and angles (º): Zr(1)–N(1) = 2.070(4); Zr(1)–N(2) = 2.510(4); Zr(1)–N(3) = 2.062(4); Zr(1)–C(1) = 2.238(6); Zr(1)–C(2) = 2.239(6); C(1)–Zr(1)–C(2) = 100.1(3); C(1)–Zr(1)–N(2) = 165.32(19); N(1)–Zr(1)–N(3) = 116.18(17).

1.1.3 Activation of dimethyl species and formation of cations

Activation of the dimethyl complexes, **3c** and **4c**, in bromobenzene at 0 ºC or –10 ºC with one equivalent of {Ph_3C}{$B(C_6F_5)_4$} led to formation of Ph_3CCH_3 and generation of the methyl cations, **3d** and **4d** (equation 1.2). No four-coordinate cation (as a $[B(C_6F_5)_4]^-$ salt) in the general

category of diamido/donor complexes has ever been isolated. Therefore these cations, like others, were explored through NMR spectroscopic studies. In each case, the methyl resonance is found near 0 ppm, at -0.05 ppm in **3d** and -0.14 ppm in **4d**. One of the mesityl rings is beginning to rotate about the N-C_{ipso} bond on the NMR time scale, as judged by broadening of the *o*-methyl

$$\textbf{3c, 4c} + \{Ph_3C\}\{B(C_6F_5)_4\} \xrightarrow[C_6H_5Br \textit{ or } C_6D_5Br]{-\ Ph_3CCH_3} \{[MesNNPhNMes]M(Me)\}\{B(C_6F_5)_4\} \quad M = Zr\ (\textbf{3d})\ \text{or}\ Hf\ (\textbf{4d}) \tag{1.2}$$

and *m*-aryl proton resonances. It should be noted that these spectra were recorded at -10 °C (**3d**) and 0 °C (**4d**), where ring rotations would be slower relative to the rate at room temperature. The greater ease of rotation of the mesityl rings in these cations is attributed to their more open, pseudo tetrahedral nature, whereas all neutral compounds discussed so far have been five-coordinate. No information concerning the degree of association of the anion or bromobenzene with the cation, i.e., the degree of "solvation" of the ion pair was gathered from NMR spectroscopic studies.

In contrast to activation of **3c** and **4c**, activation of **5c** and **6c** in bromobenzene at 0 ºC or –10 ºC with one equivalent of $\{Ph_3C\}\{B(C_6F_5)_4\}$ first led to formation of Ph_3CCH_3 and generation of the dimeric monocations, **5e** and **6e** (equation 1.3). These dimeric cations are

$$\textbf{5c, 6c} + 0.5\ \{Ph_3C\}\{B(C_6F_5)_4\} \xrightarrow[C_6D_5Br]{-\ 0.5\ Ph_3CCH_3} \{[t\text{-}BuNNPhNMes]_2M_2Me_3\}\{B(C_6F_5)_4\} \quad M = Zr\ (\textbf{5e})\ \text{or}\ Hf\ (\textbf{6e}) \tag{1.3}$$

relatively long-lived when only 0.5 equivalents of $\{Ph_3C\}\{B(C_6F_5)_4\}$ are employed. However, they react further with $\{Ph_3C\}\{B(C_6F_5)_4\}$ as described below. In **5e** and **6e**, only two types of methyl groups are observed (at 0.27 (area 6) and 0.01 ppm (area 3) in **5e** and 0.13 (area 3) and 0.06 ppm (area 6) in **6e**). Dimeric monocations that contain diamido/donor ligands have been observed in other systems, and one has been crystallographically characterized that contains one

bridging methyl group and two terminal methyl groups.[42] In another system it has been proposed that the bimetallic monocation contains three bridging methyl groups.[34] In ^{13}C-labeled **6e**, the labeled methyl resonances are found at 64.8 ppm (for two methyl groups) and 50.2 ppm with J_{CH} values of 114 Hz and 133 Hz, respectively. Therefore, the structure of the bimetallic monocations is one that contains two terminal methyl groups (with resonances at 64. 8 ppm) and one bridging methyl group (with a resonance at 50.2 ppm). One possible structure that is attractive for steric reasons is the heterochiral species **C** (Scheme 1.7) in which the two terminal methyl groups are related by a center of symmetry. In a homochiral version the two terminal methyl groups would be related by a C_2 axis.

Scheme 1.7. Possible structure of dimeric monocations, **5e** and **6e**.

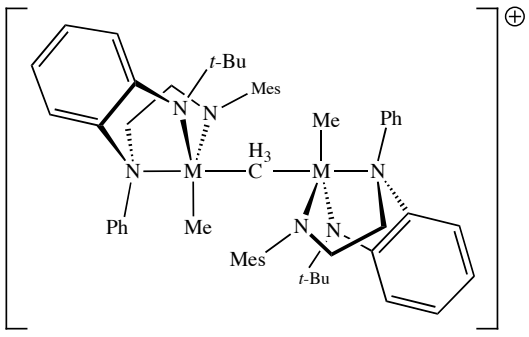

C

In the presence of $\{Ph_3C\}\{B(C_6F_5)_4\}$, the dimeric monocations **5e** and **6e** slowly react further to yield the monomeric cations shown in equation 1.4. Compound **5e** appeared to react in fewer than 5 minutes at 0 ºC, while **6e** required close to 45 minutes at 0 ºC at the concentrations employed (~0.1 M). On the basis of studies involving previous diamido-donor ligands, the dimeric monocations are believed to be in equilibrium with the monomethyl-monocation and the neutral dimethyl species.[34,35,42] The neutral dimethyl species then reacts further with $\{Ph_3C\}\{B(C_6F_5)_4\}$ to yield monomethyl-monocations (equation 1.4). In ^{13}C-labeled **6d** the methyl resonance is found at 66.3 ppm with J_{CH} = 114 Hz.

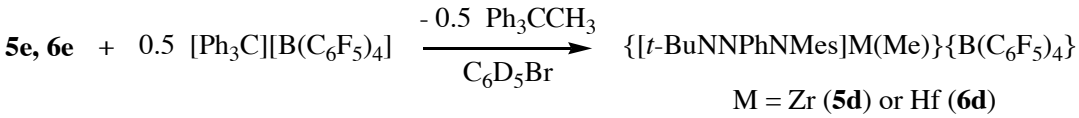

(1.4)

Attempts to observe bimetallic cations through reaction of **3c** or **4c** with 0.5 equivalents of $\{Ph_3C\}\{B(C_6F_5)_4\}$ were not successful; the activator was consumed but an unidentifiable mixture of products was produced, which did not evolve to a single product over a period of several days, according to ^{1}H NMR spectra.

1.1.4 Polymerization of 1-hexene

Complexes **3d** and **4d** proved to be effective initiators for the polymerization of 1-hexene. Polymerization of 100 equivalents of 1-hexene by **3d** was complete in less than 5 minutes at 0 ºC according to ^{1}H NMR studies. Results from a series of bulk polymerization experiments are summarized in Table 1.1. The poly[1-hexene] produced in each case was atactic, according to ^{13}C NMR spectra.[46,47] In all runs, the poly[1-hexene] formed had modest polydispersity indices and molecular weight distributions that tended to become bimodal with increasing molecular weight (monomer added). The bimodal nature of these molecular weight distributions for higher monomer equivalents suggests that some chain termination occurs during polymerization. Decomposition of the active catalyst by β-H elimination from 1,2 or 2,1 insertion products did not appear to be taking place with initiators **3d** and **4d**, i.e., no olefinic resonances were observed in the ^{1}H NMR spectra of the poly[1-hexene]. Carrying out the polymerization experiments at –25 ºC instead of 0 ºC did not significantly alter the molecular weights and polydispersities of the poly[1-hexene], nor did any tacticity become evident. These results are analogous to those obtained for poly[1-hexene] prepared with zirconium cations that contain the $[(MesitylNCH_2CH_2)_2NMe]^{2-}$ ligand system, where it was determined that CH activation in a mesityl methyl group led to catalyst deactivation.[48,49]

Table 1.1. Selected data for the polymerization of 1-hexene by **3d** or **4d** in C_6H_5Br.

Entry	[Cat] (mM)	1-Hex (equiv)	T (°C)	10^3M_n (theory)	10^3M_n (found)	PDI (M_w/M_n)
1 **3d**	10	100	0	8.4	10.0	1.68
2 **3d**	10	200	0	16.8	16.9	2.20
3 **3d**	10	300	0	25.2	26.6	2.43
4 **3d**	10	400	0	33.6	35.2	2.33
5 **3d**	5.0	290	-25	24.4	40.8	4.04
6 **4d**	10	200	0	16.8	14.4	2.54
7 **4d**	9.9	300	0	25.2	16.8	4.01
8 **4d**	9.9	200	-25	16.8	19.2	2.69

Polymerization of 1-hexene with **5d** was much slower than polymerization with either **3d** or **4d**. Consumption of 100 equivalents of 1-hexene at 0ºC required 6 hours as judged by ^{1}H NMR. The slower rate of monomer consumption by **5d** allowed the polymerization to be followed by ^{1}H NMR spectroscopy. The consumption of 90 equivalents of 1-hexene at 0 ºC is shown in Figure 1.4 in the form of a plot of the natural log of relative concentration versus time. The plot should be linear for a living polymerization in which the catalyst concentration remains constant. The curved plot suggest that the active catalyst derived from **5d** is decomposing during polymerization. The results from a series of bulk polymerization experiments are summarized in Table 1.2. The M_n values obtained for the poly[1-hexene] in these experiments are much lower than those found for polymers produced by **3d** and **4d**, which suggests that some form of more substantial catalyst decomposition is taking place. Lowering the reaction temperature to –25 ºC increased the M_n values of the poly[1-hexene], possibly as a result of a slowing of decomposition pathways relative to the rate of polymerization. Analysis of the poly[1-hexene] by ^{13}C NMR and ^{1}H NMR showed them to be atactic and olefinic resonances indicative of β-H elimination from a 1,2 insertion product were present as broad multiplets between 5.34 and 5.43 ppm.[50] Catalyst

decomposition after β hydride elimination would account for the observations shown in Figure 1.4. Results with initiator **5d** and the slow activation of precatalyst **6c** prompted us to discontinue further examination of initiator **6d**. It is clear from the polymerization results that polymerization of 1-hexene with **3d**-**5d** is not living and furthermore the process is not stereoselective to any significant degree.

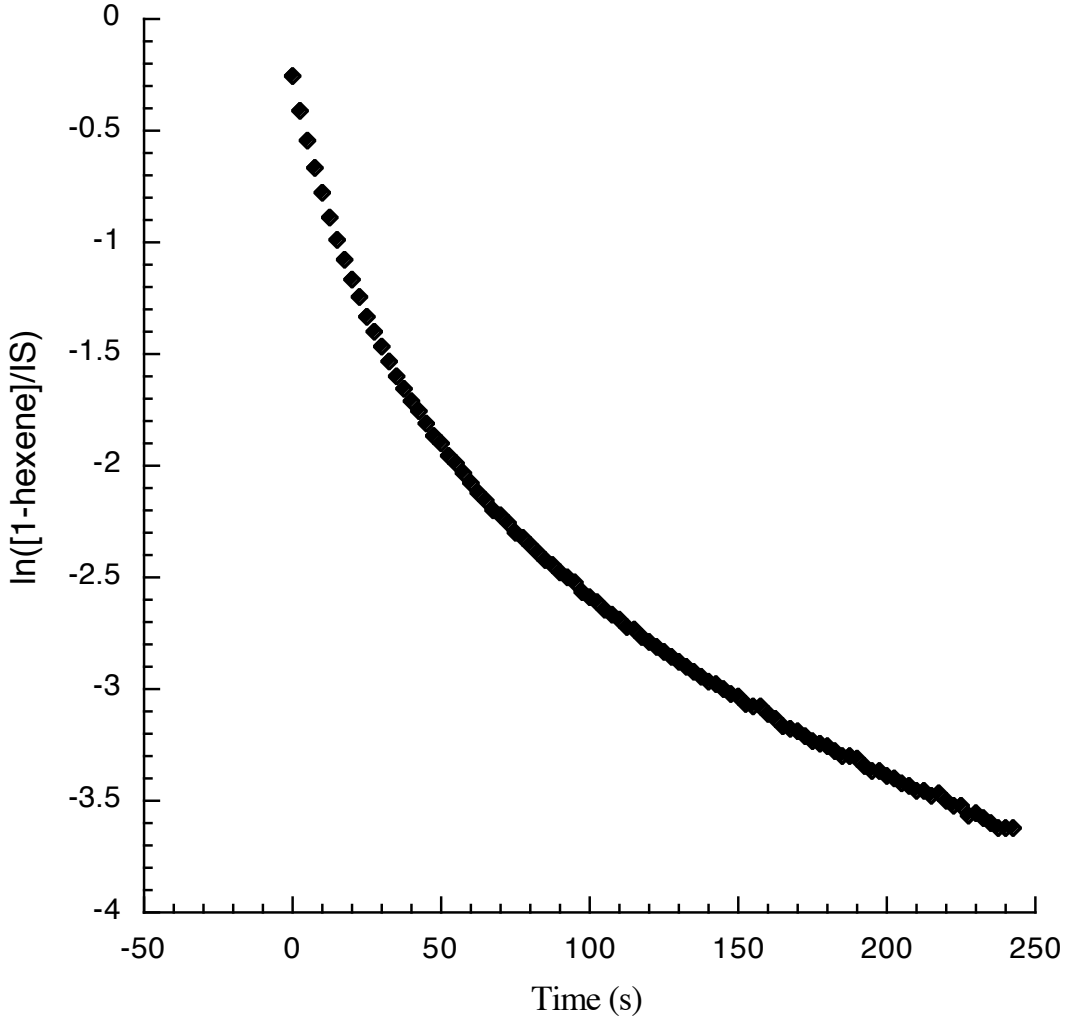

Figure 1.4. Consumption of 90 equiv of 1-hexene by {[*t*-BuNNPhNMes]ZrMe}{B(C_6F_5)$_4$} (**5d**, 20.0 mM) in C_6D_5Br (internal standard = diphenylmethane).

Table 1.2. Selected data for the polymerization of 1-hexene by **5d** in C_6H_5Br or C_6D_5Br.

Entry	[Cat] (mM)	1-Hex (equiv)	T (°C)	10^3M_n (theory)	10^3M_n (found)	PDI (M_w/M_n)
1	4.7	100	0	8.4	4.9	1.60
2	4.4	200	0	16.8	5.3	2.24
3	4.0	300	0	25.2	6.6	2.43
4	4.2	450	0	37.8	8.1	2.21
5	8.8	100	-25	8.4	8.7	1.29
6	8.2	200	-25	16.8	12.3	1.60

1.2 Zr and Hf complexes possessing the [MepyN] ligand

1.2.1 Synthesis of *rac*-H_2[MepyN] and its complexes with Zr and Hf

The next supporting ligand examined was chosen so that it contained a fixed chiral center. The binaphthyl group was chosen because of its ease in preparation and documented success in asymmetric catalysis.[51] The diamine *rac*-H_2[MepyN] is prepared from *rac*-2,2′-diamino-1,1′-binaphthalene as shown in equation 1.5. Condensation of *rac*-2,2′-diamino-1,1'-binaphthalene with 6-methyl-2-pyridinecarboxaldehyde[52] followed by reduction with $NaBH_4$ produces the racemic diamine in 80% yield after recrystallization on a scale of 5 – 10 grams. H_2[MepyN] is a white crystalline solid that is soluble in aromatic and chlorinated solvents, but is relatively insoluble in alkanes or diethyl ether. The ^{1}H NMR spectrum is consistent with a species possessing C_2 symmetry; nine aryl resonances can be observed, while the methylene protons appear as a complex multiplet at 4.15 ppm and the methyl group as a singlet at 2.27 ppm in benzene-d_6.

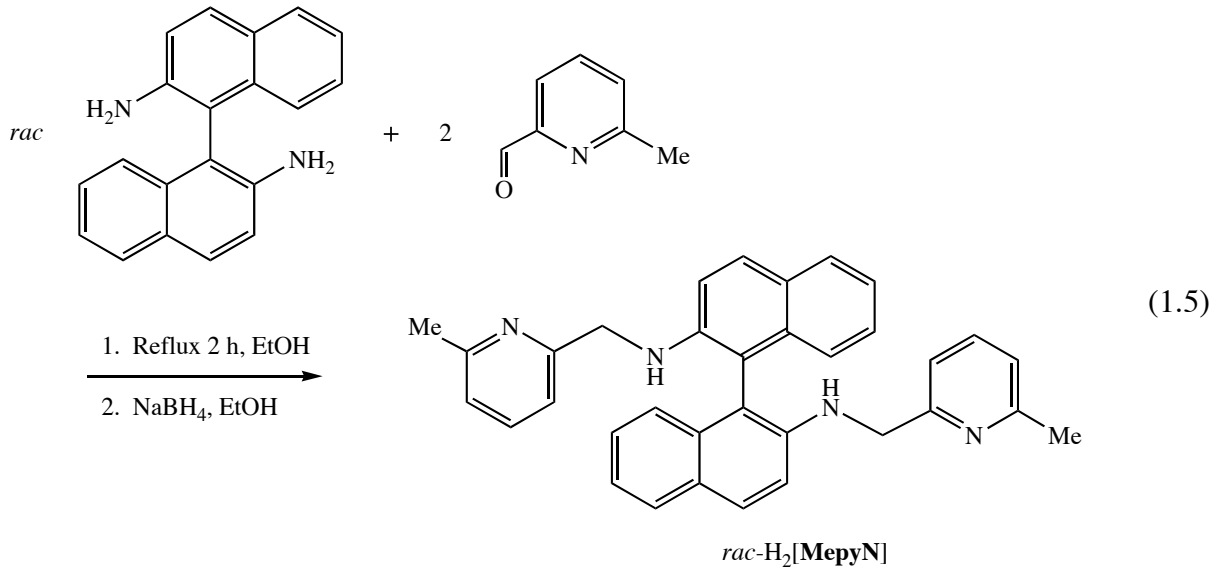

rac-H_2[**MepyN**] (1.5)

The reaction between H_2[MepyN] and $M(NMe_2)_4$ (M = Zr or Hf) proceeds readily to give [MepyN]$M(NMe_2)_2$ complexes in good yields (equation 1.6). ^{1}H NMR spectra of compounds **7a** and **8a** are consistent with C_2-symmetric structures in solution. Nine aryl resonances can be observed, whereas the methylene protons give rise to an AB doublet centered

$$H_2[\text{MepyN}] \xrightarrow[\text{- 2 HNMe}_2]{\text{M(NMe}_2)_4} \underset{\text{toluene}}{} [\text{MepyN}]\text{M(NMe}_2)_2 \quad \begin{matrix}\text{M = Zr, } \mathbf{7a} \\ \text{M = Hf, } \mathbf{8a}\end{matrix} \tag{1.6}$$

around 5.15 ppm in benzene-d_6. The methyl groups of the dimethylamido ligands and the pyridine moieties appear as sharp singlets in a 2:1 ratio, as expected. Two of the three possible modes of coordination of the diamido ligand in a [MepyN]MX_2 complex (Scheme 1.8) contain a C_2 axis (C_2-*cis* and C_2-*trans*). Structural characterization of zirconium complexes that contain a related ligand suggest that both C_2-*cis* and C_2-*trans* coordination are adopted by the ligand.[53] No information concerning the geometry of the [MepyN]$M(NMe_2)_2$ species was obtained. However, the C_2-*cis* structure depicted in Scheme 1.8 is favored based on the solid state structures of other C_2-symmetric complexes supported by this ligand (*vida infra*).

Scheme 1.8. Possible coordination modes of $[MepyN]^{2-}$.

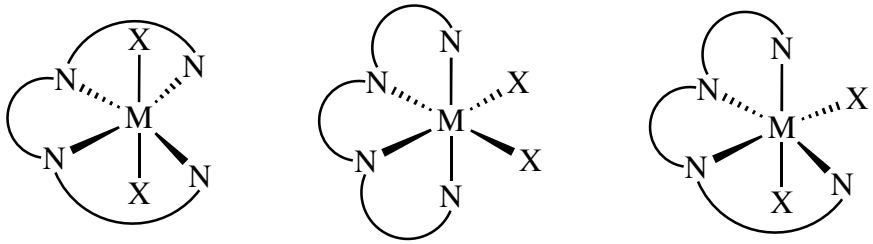

C_2-*cis* C_2-*trans* C_1

Initial attempts to synthesize $[MepyN]Zr(NMe_2)_2$ led to an unexpected result. Upon addition of $H_2[MepyN]$ to $Zr(NMe_2)_4$, a yellow crystalline material was obtained, the ^1H NMR spectrum of which showed it to have C_1 symmetry and a broad peak assignable to only 6 dimethylamide protons. Four doublets arise for each of the inequivalent methylene protons of the ligand instead of the AB patterns encountered in C_2 symmetric species, whereas 18 aryl resonances are observed for each proton in the binaphthyl and pyridine residues. A crystal structure of the complex revealed it to be $[MepyN]Zr(NMe_2)Cl$ (**7a′**, Figure 1.8).

Scheme 1.9. Synthetic routes to **7a′**.

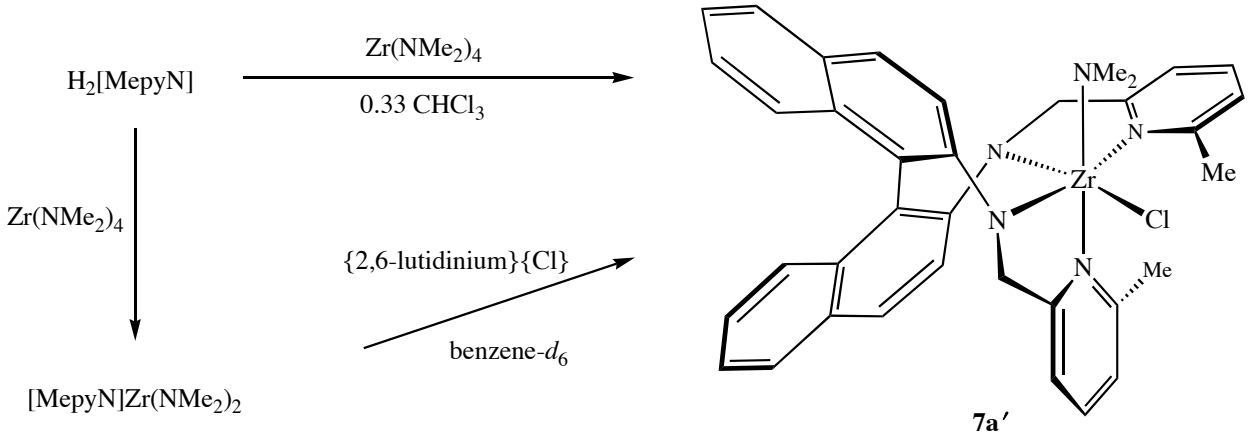

A rational synthesis of [MepyN]Zr(NMe_2)Cl consists of a reaction between [MepyN]Zr(NMe_2)$_2$ and lutidinium chloride in benzene-d_6. Recrystallization of H_2[MepyN] from non-chlorinated solvents produced samples that yielded exclusively the desired *bis*-dimethylamide complex. Therefore it is likely that [MepyN]Zr(NMe_2)Cl arises through reaction of [MepyN]Zr(NMe_2)$_2$ (generated *in situ*) with chloroform that had been retained in the sample of H_2[MepyN] that was first employed in the reaction (Scheme 1.9).

The solid state structure of [MepyN]Zr(NMe_2)Cl is best described as a distorted octahedron, with the ligand adopting the C_1 geometry depicted in Scheme 1.8 (Figure 1.5 and caption). In the observed diastereomer, the dimethylamide ligand resides *trans* to one of the pyridine donors, while the chloride is bound *trans* to an amide. The Zr(1)-N(5) bond length of 2.048(1) Å is within the expected range for a π-donating amide, as are the Zr(1)-N(2) and Zr(1)-N(3) distances of 2.091(1) and 2.130(1) Å, respectively. The pyridine-zirconium lengths differ to a significant degree (2.413(1) vs. 2.490(1) Å), as might be expected from the asymmetric binding mode of the ligand. The angles around Zr are consistent with a distorted octahedral geometry, with the most acute angle arising from the five-membered chelate ring formed from N(1) and N(2). The broadened dimethylamido resonance is probably the consequence of hindered rotation about the Zr-N(5) bond.

The [MepyN]Zr(NMe_2)Cl compound is noteworthy for two reasons. First, the structure illustrates that the [MepyN]$^{2-}$ ligand can adopt a geometry that does not contain *trans*-disposed pyridyl ligands, one of three possible coordination geometries (Scheme 1.8). Second, the complex exists as only one diastereomer in solution and in the solid state.

Conversion of [MepyN]Zr(NMe_2)$_2$ to [MepyN]$ZrCl_2$ (**7b**) was accomplished by heating compound **7a** in toluene or benzene in the presence of two equivalents of TMSCl at 80 ºC for 16 hours. Unfortunately the resulting dichloride species is relatively insoluble in common organic solvents, dissolving only sparingly in dichloromethane. ^{1}H NMR spectra of the dichloride

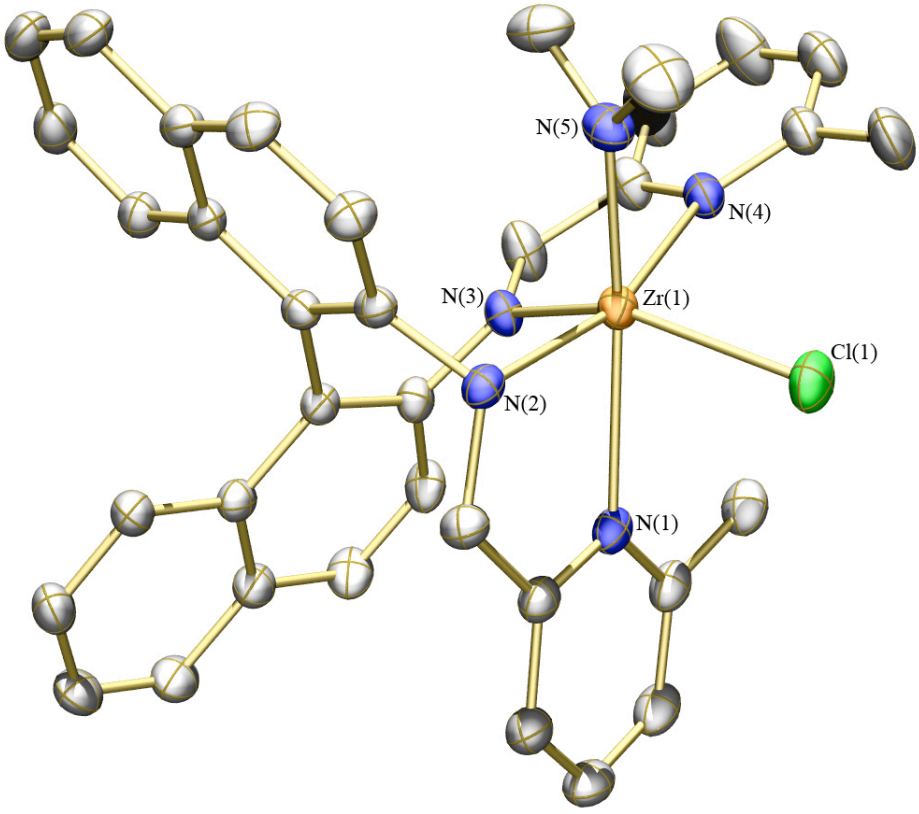

Figure 1.5. Thermal ellipsoid rendering (35%) of compound **7a′**. Hydrogen atoms and cocrystallized benzene molecule omitted for clarity. Selected bond distances (Å) and angles (°): Zr(1)–N(1) = 2.413(1); Zr(1)–N(2) = 2.091(1); Zr(1)–N(3) = 2.130(1); Zr(1)–N(4) = 2.490(1); Zr(1)–N(5) – 2.048(1); Zr(1)–Cl(1) = 2.517(1); N(1)–Zr(1)–N(4) = 112.81(5); N(1)–Zr(1)–N(5) = 164.09(6); N(1)–Zr(1)–N(2) = 71.91(5).

complex in methylene chloride-d_2 are consistent with the structure being C_2-symmetric in solution, and are overall similar to spectra of **7a**. Insolubility of the [MepyN]$ZrCl_2$ species hampered efforts to convert it to dialkyl complexes by reaction with Grignard reagents. For example, the reaction between **7b** and *i*-BuMgBr was only successful when conducted in dichloromethane. However, the yield was poor and not reproducible, most likely as a consequence of side reactions involving dichloromethane.

To circumvent problems ascribable to insolubility of the dichloride complex, *bis*-triflate complexes were prepared. Treatment of [MepyN]M$(NMe_2)_2$ (M = Zr, Hf) with two equivalents

of trimethylsilyl triflate in benzene proceeded in less than 10 minutes at room temperature to yield white crystalline [MepyN]M(OSO_2CF_3)$_2$ species after crystallization (**7t** and **8t**; equation 1.7). The *bis*-triflate complexes are soluble in benzene and toluene at elevated temperatures, and they dissolve readily in THF and methylene chloride. ^{1}H NMR spectra of compounds **7t** and **8t** are highly solvent dependent, but in each case the spectra are consistent with a C_2-symmetric

$$[\text{MepyN}]\text{M}(\text{NMe}_2)_2 \xrightarrow[\text{benzene}]{\begin{array}{c}2\ \text{TMSOSO}_2\text{CF}_3 \\ -\ 2\ \text{TMSNMe}_2\end{array}} [\text{MepyN}]\text{M}(\text{OSO}_2\text{CF}_3)_2 \quad \begin{array}{l}\text{M = Zr, } \mathbf{7t} \\ \text{M = Hf, } \mathbf{8t}\end{array} \qquad (1.7)$$

structure in solution. Upon changing from benzene-d_6 to methylene chloride-d_2 or THF-d_8, resonances for the methylene protons of the ligand (between the amide and pyridine donor) broaden significantly. The reason is not known, though partial ionization of one of the triflates as the polarity/donating ability of the solvent is increased is one possibility. The solution IR spectrum[54] of **7t** in methylene chloride was examined, but proved inconclusive. In all solvents resonances for the hafnium complex broaden to a greater degree than those for the zirconium species.

The solid state structure of [MepyN]Hf(OSO_2CF_3)$_2$ was determined by X-ray diffraction (Figure 1.6). Crystals of the triflate complex were grown by vapor diffusion of pentane into a bromobenzene solution containing approximately one equivalent of benzene per hafnium. Due to partial decomposition of **8t** in bromobenzene, ~5% of the compound contained a bromide in place of one of the triflate oxygen atoms. This disorder was modeled successfully. The geometry about Hf is a highly distorted octahedron, with the ligand adopting a binding mode that is approximately C_2-*cis* (Scheme 1.8). The triflates are bound in an κ^1 fashion, but the O(1)-Hf(1)-O(2) angle is only 132.54(14)°. The Hf-N_{amide} and Hf-$N_{pyridyl}$ bond lengths are similar to those in **7a′**. The highly distorted geometry of compound **8t** likely results from steric restraints imposed by the ligand, and is similar to distortions found in structures of C_2-symmetric dialkyl species discussed below.

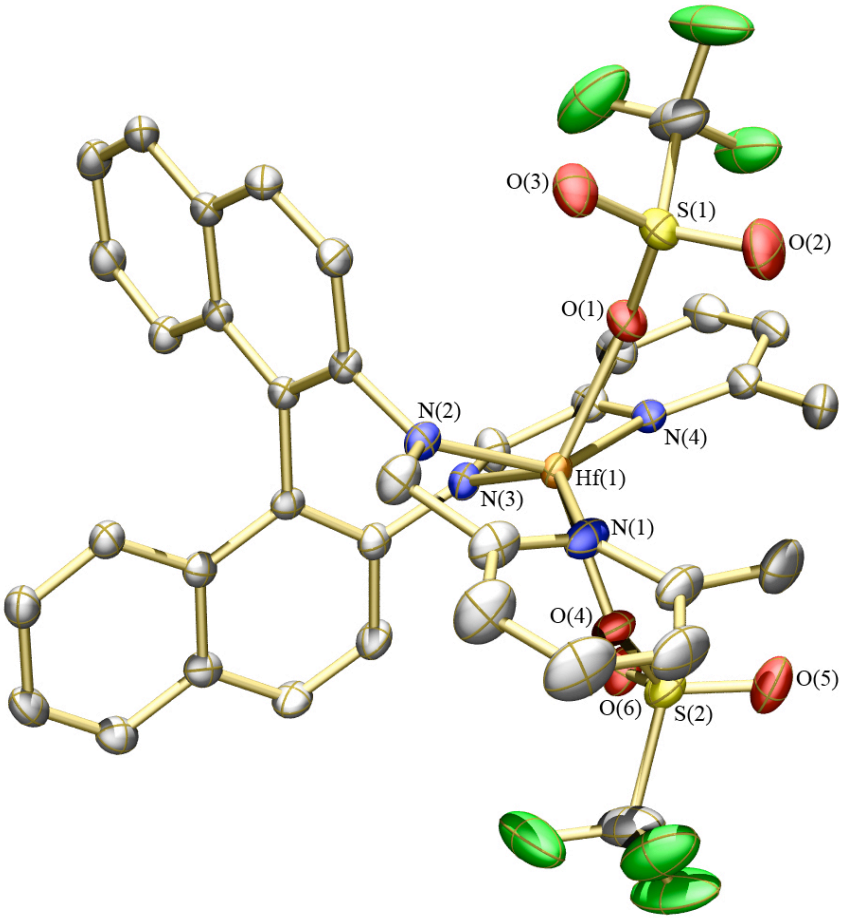

Figure 1.6. Thermal ellipsoid (35%) rendering of compound **8d**. Hydrogen atoms, cocrystallized bromobenzene molecule, and minor components of disordered atoms omitted for clarity. Selected bond distances (Å) and angles (°): Hf(1)–N(1) = 2.389(4); Hf(1)–N(2) = 2.047(4); Hf(1)–N(3) = 2.048(4); Hf(1)–N(4) = 2.418(4); Hf(1)–O(1) = 2.087(3); Hf(1)–O(4) = 2.093(4); N(1)–Hf(1)–N(4) = 139.76(14); O(1)–Hf(1)–O(4) = 132.54(14); N(1)–Hf(1)–N(2) = 72.44(14).

Attempts to prepare [MepyN]MMe_2 by treating either [MepyN]MCl_2 or [MepyN]$M(OSO_2CF_3)_2$ with a variety of methylating agents ($AlMe_3$, MeLi, and Me_2Mg) under different conditions in different solvents met with no success. Aggressive methyl nucleophiles may deprotonate the benzyl position of the ligand backbone leading to decomposition. By

contrast, alkylation was successful with *i*-BuMgBr to give [MepyN]M(*i*-Bu)$_2$ (M = Zr, **7d**; M = Hf, **8d**) species. These reactions proceed best in THF using the [MepyN]M(OSO$_2$CF$_3$)$_2$ precursors. ^{1}H NMR spectra of the zirconium and hafnium isobutyl complexes are almost identical, displaying resonances consistent with C_2 symmetry. The isobutyl methine proton appears as a multiplet, while the methyl groups appear as doublets and the methylene protons as doublet of doublets (see Experimental section). The [MepyN]M(*i*-Bu)$_2$ complexes are readily soluble in aromatic solvents and THF but insoluble in pentane and diethyl ether.

The structure of compound **8d** was determined in an X-ray diffraction study (Figure 1.7). The compound crystallizes with two crystallographically independent but chemically equivalent molecules in the asymmetric unit, only one of which is shown in Figure 1.7. Like compound **8t**, [MepyN]Hf(*i*-Bu)$_2$ is a highly distorted octahedron with the ligand again adopting the C_2-*cis* orientation shown in Scheme 1.8. The bond lengths and angles for the [MepyN]$^{2-}$ ligand are very similar to those of the triflate species. The isobutyl ligands are approximately *trans* to one another (C(1B)-Hf(1)-C(5B) = 145.31(12)°) with relatively long Hf-C bond lengths (Hf(1)-C(1B) = 2.308(3) Å; Hf(1)-C(5B) = 2.319(3) Å), as expected in a relatively crowded six-coordinate complex.

An alternative preparation of dialkyl complexes consists of addition of H$_2$[MepyN] to tetraalkyl complexes of Zr or Hf. Reaction of H$_2$[MepyN] with Zr(CH$_2$-*t*-Bu)$_4$ did not lead to any observable [MepyN]Zr(CH$_2$-*t*-Bu)$_2$ even upon heating to 60 ºC. At this temperature, decomposition of the tetraalkyl was apparent as judged by ^{1}H NMR. However, a reaction between H$_2$[MepyN] and Zr(CH$_2$Ph)$_4$ produced [MepyN]Zr(CH$_2$Ph)$_2$ (**7e**) in good yield as a yellow-orange crystalline solid. The benzyl complex is considerably less soluble than the isobutyl species discussed earlier, although it dissolves readily in dichloromethane. The spectral features of **7e** are similar to those for the [MepyN]M(*i*-Bu)$_2$ species, with the benzyl

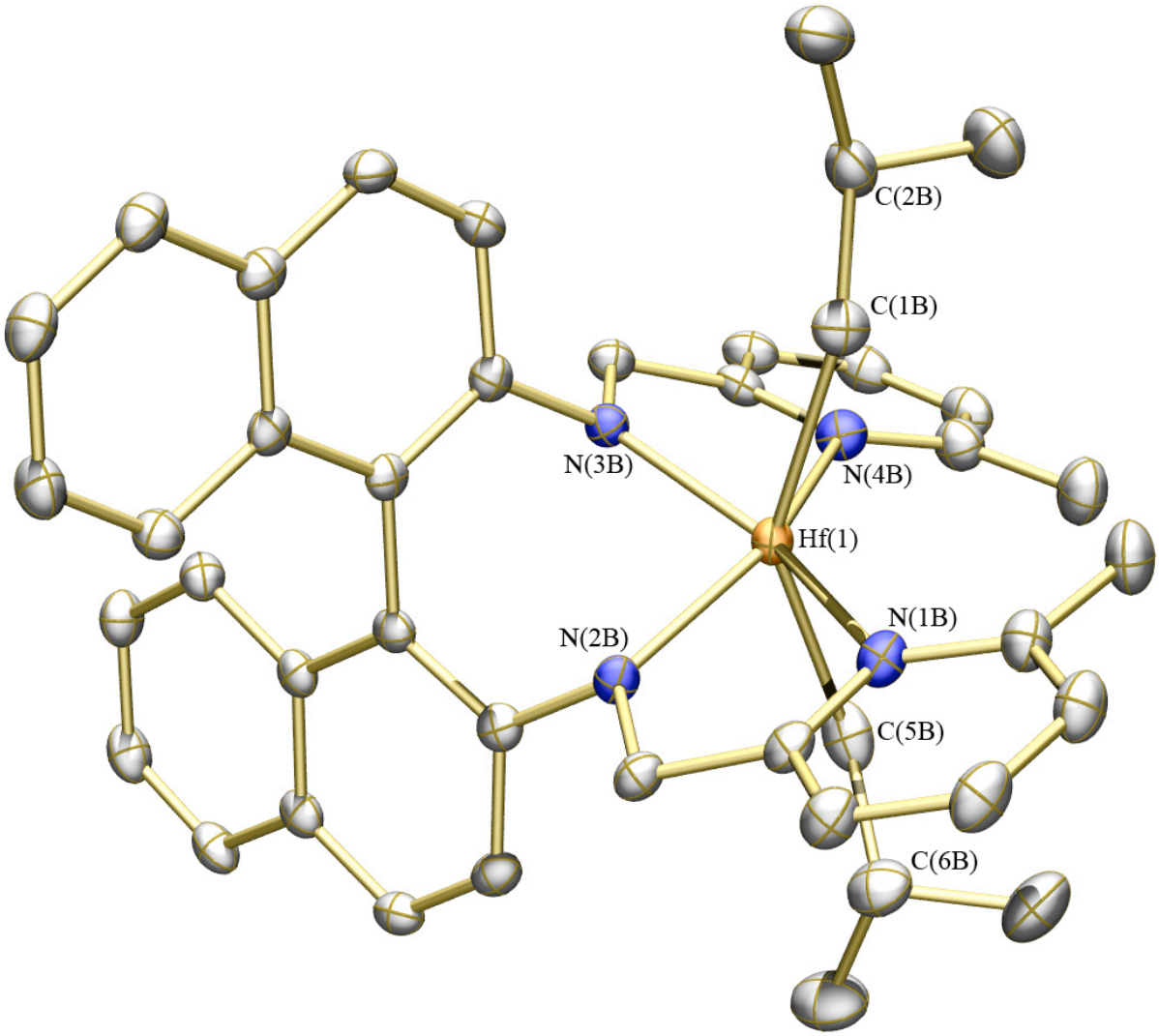

Figure 1.7. Thermal ellipsoid (35%) rendering of one of the two independent molecules of **8d** in the asymmetric unit. Hydrogen atoms and cocrystallized benzene molecules omitted for clarity. Selected bond distances (Å) and angles (°): Hf(1)–N(1B) = 2.391(2); Hf(1)–N(2B) = 2.111(2); Hf(1)–N(3B) = 2.093(2); Hf(1)–N(4B) = 2.435(3); Hf(1)–C(1B) = 2.308(3); Hf(1)–C(5B) = 2.319(3); C(1B)–Hf(1)–C(5B) = 145.31(12); Hf(1)–C(1B)–C(2B) = 125.4(2).

methylene resonances appearing as a set of doublets at 2.26 and 1.89 ppm in methylene chloride-d_2. The aryl protons of the benzyl group resonate at relatively low field, with the *ortho* proton resonance appearing at 5.63 ppm. The solid state structure of compound **7e** (Figure 1.8) shows it

to be similar to the isobutyl and *bis*-triflate structures discussed earlier. The ligand once again adopts the C_2-*cis* structure shown Scheme 1.8. The Zr-C bond lengths and Zr-C-C angles (caption to Figure 1.8) are not consistent with any tendency of a benzyl group to bond in an η^2 fashion.

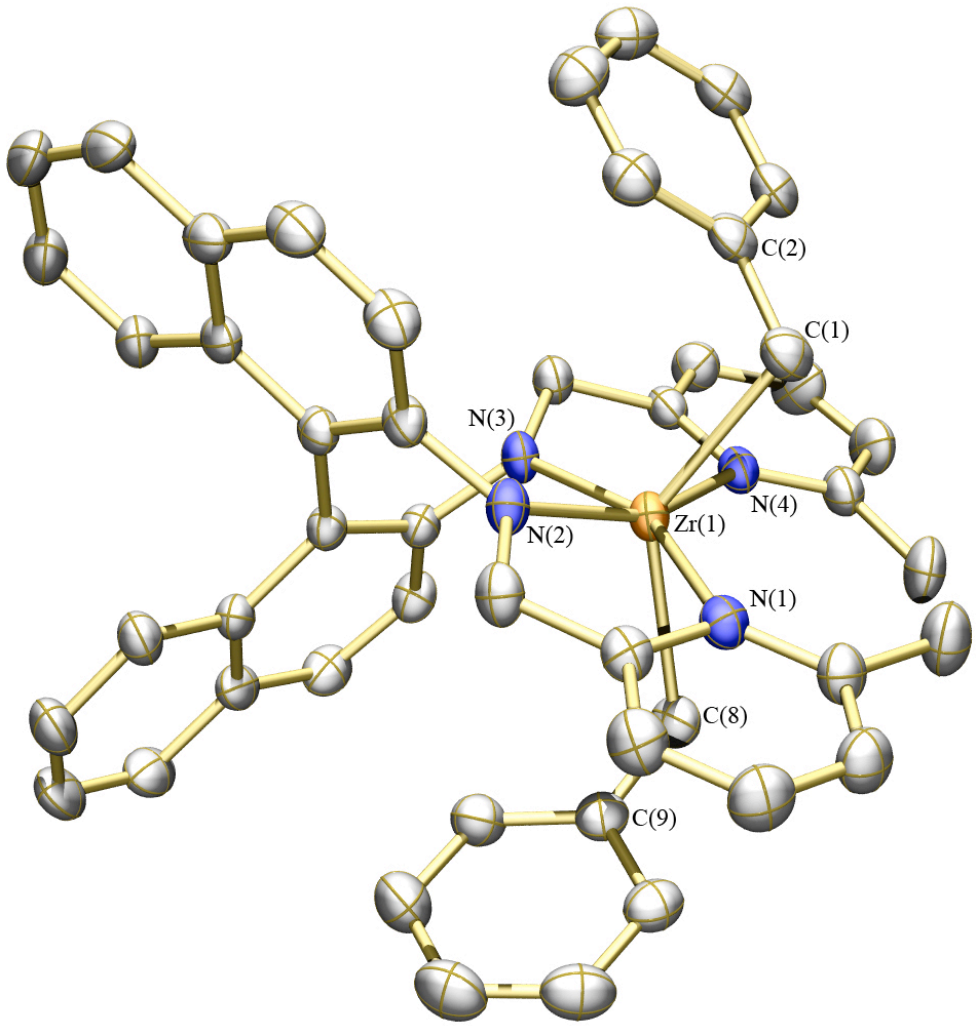

Figure 1.8. Thermal ellipsoid (35%) rendering of **7f**. Hydrogen atoms and cocrystallized benzene molecule omitted for clarity. Selected bond distances (Å) and angles (°): Zr(1)–N(1) = 2.518(2); Zr(1)–N(2) = 2.104(2); Zr(1)–N(3) = 2.111(2); Zr(1)–N(4) = 2.540(2); Zr(1)–C(1) = 2.337(3); Zr(1)–C(8) = 2.311(3); C(1)–Zr(1)–C(8) = 132.07(11); Zr(1)–C(1)–C(2) = 104.97(18).

1.2.2 Activation of dialkyl complexes

Activation of [MepyN]M(*i*-Bu)$_2$ at 23 ºC with B(C_6F_5)$_3$, {$HNMe_2Ph$}{B(C_6F_5)$_4$}, or {Ph_3C}{B(C_6F_5)$_4$} in toluene, benzene, or bromobenzene gave rise in each case to a monoisobutyl cation with concomitant formation of the expected byproducts (equations 1.8 - 1.10). NMR spectra of the cation show the expected asymmetry, with individual resonances visible for each of the protons of the ligand. The resonances for the isobutyl ligand are shifted upfield with one of the methylene protons of [MepyN]Hf(*i*-Bu)}{$HB(C_6F_5)_3$}

$$[\text{MepyN}]\text{M}(CH_2CHMe_2)_2 \xrightarrow[\text{bromobenzene-}d_5]{\text{B}(C_6F_5)_3 \text{ - } Me_2C{=}CH_2} \{[\text{MepyN}]\text{M}(CH_2CHMe_2)\}\{\text{B}(C_6F_5)_4\} \quad (1.8)$$

$$[\text{MepyN}]\text{M}(CH_2CHMe_2)_2 \xrightarrow[\text{bromobenzene-}d_5]{\{Ph_3C\}\{\text{B}(C_6F_5)_4\} \text{ - } Ph_3CH,\ Me_2C{=}CH_2} \{[\text{MepyN}]\text{M}(CH_2CHMe_2)\}\{\text{B}(C_6F_5)_4\} \quad (1.9)$$

$$[\text{MepyN}]\text{M}(CH_2CHMe_2)_2 \xrightarrow[\text{bromobenzene-}d_5]{\{HNMe_2Ph\}\{\text{B}(C_6F_5)_4\} \text{ - } Me_2NPh,\ Me_3CH} \{[\text{MepyN}]\text{M}(CH_2CHMe_2)\}\{\text{B}(C_6F_5)_4\} \quad (1.10)$$

appearing at –1.23 ppm in bromobenzene-d_5. An α-agostic interaction is unlikely, however, because the methylene resonances remain sharp in bromobenzene-d_5 with splitting patterns similar to those in the neutral dialkyl. Treatment of any of these species with an excess of 1-hexene yielded no detectable poly[1-hexene] at either room temperature or 60 ºC. Solutions were unchanged for several days at room temperature, although at elevated temperature decompositions to yield some isobutene and unidentifiable metal-containing product(s) were observed after several hours.

A reaction between **7e** and {$HNMe_2Ph$}{B(C_6F_5)$_4$} in methylene chloride-d_2 at –30 ºC or room temperature occurs quantitatively in seconds along with formation of free Me_2NPh. The ^{1}H

NMR spectrum of the activated species (**7e′**) shows a large number of peaks, consistent with formation of a C_1-symmetric species. However, no toluene is formed, although resonances attributable to two benzyl ligands are observed. The proton resonances of the ligand backbone resemble those of the isobutyl cation except for the resonances due to the methylene groups between the amido nitrogen atoms and the pyridine moiety. Unlike the isobutyl cation, only *three* doublets are apparent in the range 3–4 ppm, instead of the expected four. Additionally, a doublet of doublets appears at 2.79 ppm; this type of resonance is not observed in any species discussed so far. The gCOSY spectrum shows a cross peak between the resonance at 2.79 ppm and a doublet resonance at 5.63 ppm, with an H-H coupling constant of 7.5 Hz, consistent with a three bond separation. This feature, along with the presence of two benzyl groups points towards formulation of the species as an amido-amine dibenzyl cation such as that shown in Scheme 1.10. As expected, this cationic species is not a catalyst for polymerization of 1-hexene.

Scheme 1.10. Possible structure of **7e′**.

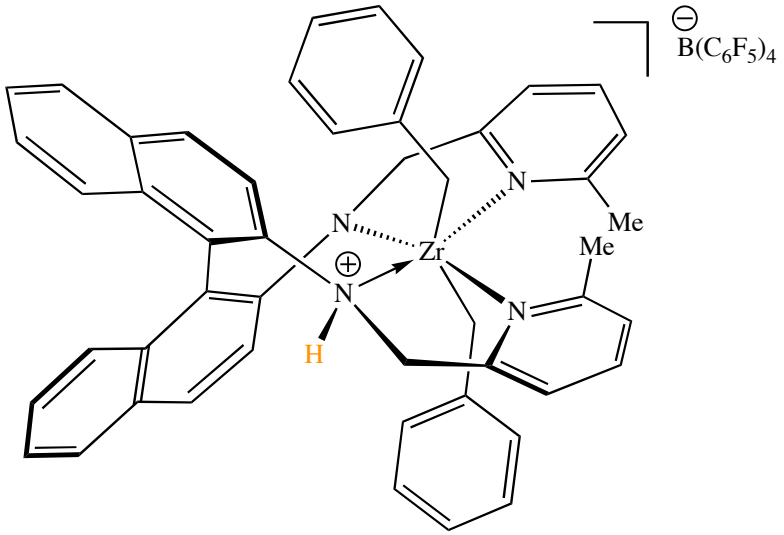

In a similar experiment, **7e** was allowed to react with {$HNMe_2Ph$}{Cl} in methylene chloride-d_2. Formation of free dimethylaniline, a mixture of [MepyN]$Zr(CH_2Ph)_2$,

[MepyN]$ZrCl_2$, and [MepyN]$Zr(CH_2Ph)Cl$, and one equivalent of toluene was observed by ^1H NMR spectroscopy. Prior protonation of the amide followed by proton transfer to benzyl cannot be ruled out. However, the anilinium chloride is not consumed immediately, and monitoring of the reaction mixture by NMR does not reveal any intermediate species similar to the one discussed in the preceding paragraph. Solutions of **7e** activated with $\{HNMe_2Ph\}\{B(C_6F_5)_4\}$ do not yield any monobenzyl cation over a period of days, even at elevated temperatures. This result is somewhat surprising considering the observed tendency for anilinium chloride to selectively protonate the benzyl ligand, and also the presence of free (uncoordinated) dimethylaniline that could serve as proton shuttle between different parts of the complex. This observation may also be relevant to the dibenzyl species reported by Brintzinger, which was inactive toward propene polymerization when activated with anilinium borate.[53]

In contrast to protonation, treatment of **7e** with strong Lewis acids does lead to a mono-benzyl cation. Reaction with $B(C_6F_5)_3$ or trityl in methylene chloride-d_2 proceeds to the monobenzyl cation which has been observed spectroscopically (equations 1.11 – 1.12).

$$[\text{MepyN}]Zr(CH_2Ph)_2 \xrightarrow[CD_2Cl_2]{B(C_6F_5)_3} \{[\text{MepyN}]Zr(CH_2Ph)\}\{PhCH_2B(C_6F_5)_3\} \qquad (1.12)$$

$$[\text{MepyN}]Zr(CH_2Ph)_2 \xrightarrow[CD_2Cl_2]{\{Ph_3C\}\{B(C_6F_5)_4\} \\ -\ PhCH_2CPh_3} \{[\text{MepyN}]Zr(CH_2Ph)\}\{B(C_6F_5)_4\} \qquad (1.13)$$

The ^1H NMR spectrum of the benzyl cation at 20 ºC displays broadened resonances for all protons of the $[MepyN]^{2-}$ ligand. The time-averaged symmetry remains C_2-symmetric, as judged by the presence of a broadened singlet for the pyridine methyl resonances. Resonances for the methylene protons of the benzyl ligand appear at 1.53 ppm (sharp doublet) and 0.02 ppm (broad doublet). The aryl protons of the benzyl ligand also remain sharp as do the peaks corresponding to the $PhCH_2B(C_6F_5)_3$ anion in the case of activation with $B(C_6F_5)_3$. To further elucidate the

nature of the benzyl cation, the ^{1}H NMR spectrum was recorded at temperatures down to –70 ºC. Upon decreasing in temperature, the resonances of the ligand environment sharpen consistently until at –70 ºC they appear very similar to those of the isobutyl cation. At this temperature, two singlets of area three are observed for the pyridine methyl groups, as are four doublets of area one for each of the methylene protons of the ligand. The resonances for the methylene protons of the benzyl group broaden upon decreasing in temperature then sharpen at –70 ºC and appear as a set of doublets of area one with a $^2J_{HH}$ of 12.5 Hz. One of the methylene protons is significantly shifted to lower field (-0.54 ppm), while the other shifts slightly to 1.44 ppm (methylene chloride-d_2).

Addition of dimethylaniline to solutions of the benzyl cation at room temperature did not reveal any tendency for the cation to form base adducts. Zirconium and hafnium alkyl cations that show activity toward 1-hexene polymerization typically demonstrate at least weak adduct formation with Me_2NPh.[48] Reaction of the benzyl cation with 1-hexene failed to give any detectable amount of poly[1-hexene] even at elevated temperatures.

1.3 Group IV complexes of the $[HIPTN_2]^{2-}$ ligand

1.3.1 Synthesis of $H_2[HIPTN_2]$ and its complexes with Ti, Zr, and Hf

The third ligand examined contained the binaphthyl diamine core substituted with the bulky hexaisopropylterphenyl (HIPT) groups. The parent diamine, *rac*-$H_2[HIPTN_2]$, was prepared through a palladium catalyzed *N*-aryl coupling between *rac*-diaminobinaphthalene and 3,5-*bis*(2,4,6-triisopropylphenyl)bromobenzene (HIPTBr). Using the XPHOS[43] cocatalyst, the reaction is complete in less than 4 hours, and can be scaled up to 15 grams with yields of >80% after purification by column chromatography (equation 1.13). White, crystalline

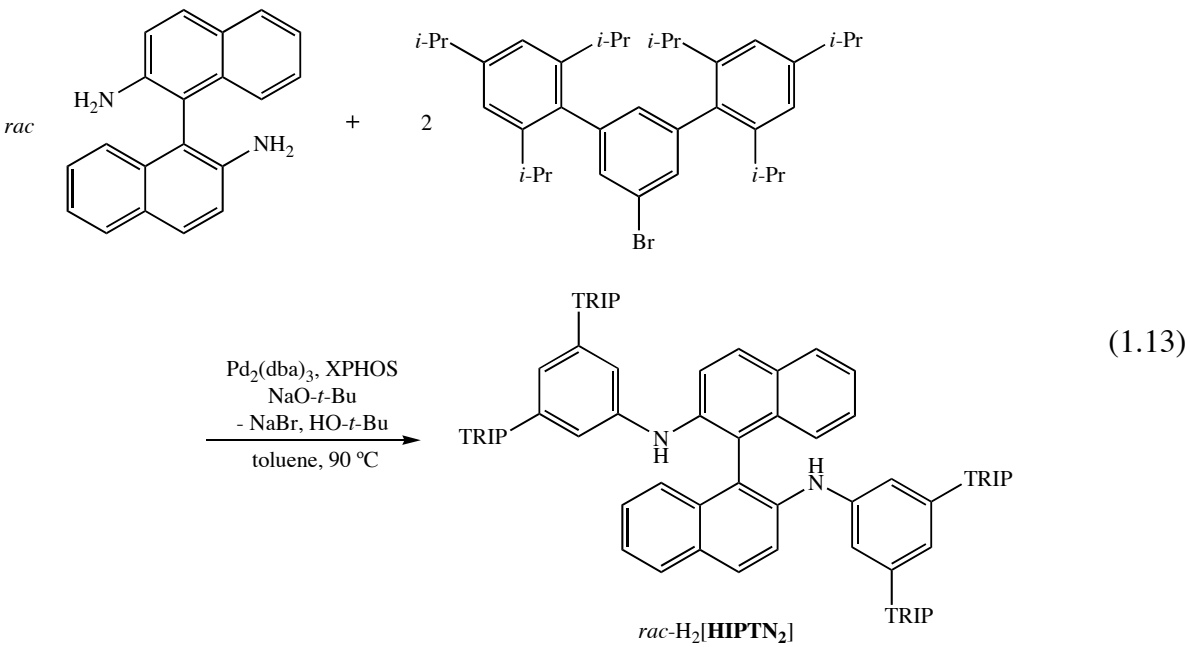

rac-H_2[**HIPTN$_2$**]

(1.13)

H_2[HIPTN$_2$] is readily soluble in all organic solvents including pentane and diethyl ether. The NMR spectrum contains three septets of area 4 for each of the methine protons of the triisopropylphenyl ring, indicating that rotation about the aryl-aryl bond of the terphenyl groups is not possible, but rotation about the *N*-aryl bond is facile. Other features of the ^{1}H NMR spectrum are consistent with a C_2-symmetry and no rotation about the aryl-aryl bond.

Metallation of the ligand with Ti, Zr, or Hf occurs readily upon reaction with M(NMe$_2$)$_4$ (equation 1.14). In the case of hafnium and zirconium, the parent diamine reacts with M(NMe$_2$)$_4$ in pentane at 23 ºC to yield the [HIPTN$_2$]M(NMe$_2$)$_2$ species as yellow microcrystals after 24 hours. The titanium congener, **9a**, is somewhat more difficult to prepare, requiring elevated temperatures and significantly longer reaction time to go to completion. Heating H_2[HIPTN$_2$] and Ti(NMe$_2$)$_4$ in toluene at 110 ºC for 6 days affords **9a** as an orange amorphous solid. ^{1}H NMR spectra of **9a**-**11a** are similar, and all show the expected C_2-symmetry. A large singlet of area 12 near 2.7 ppm is assigned to the NMe$_2$ protons. The sharp resonances suggest that rotation about the metal-nitrogen bond is fast on the NMR time scale at room temperature, as is typically observed for early metal dimethylamido complexes.[44]

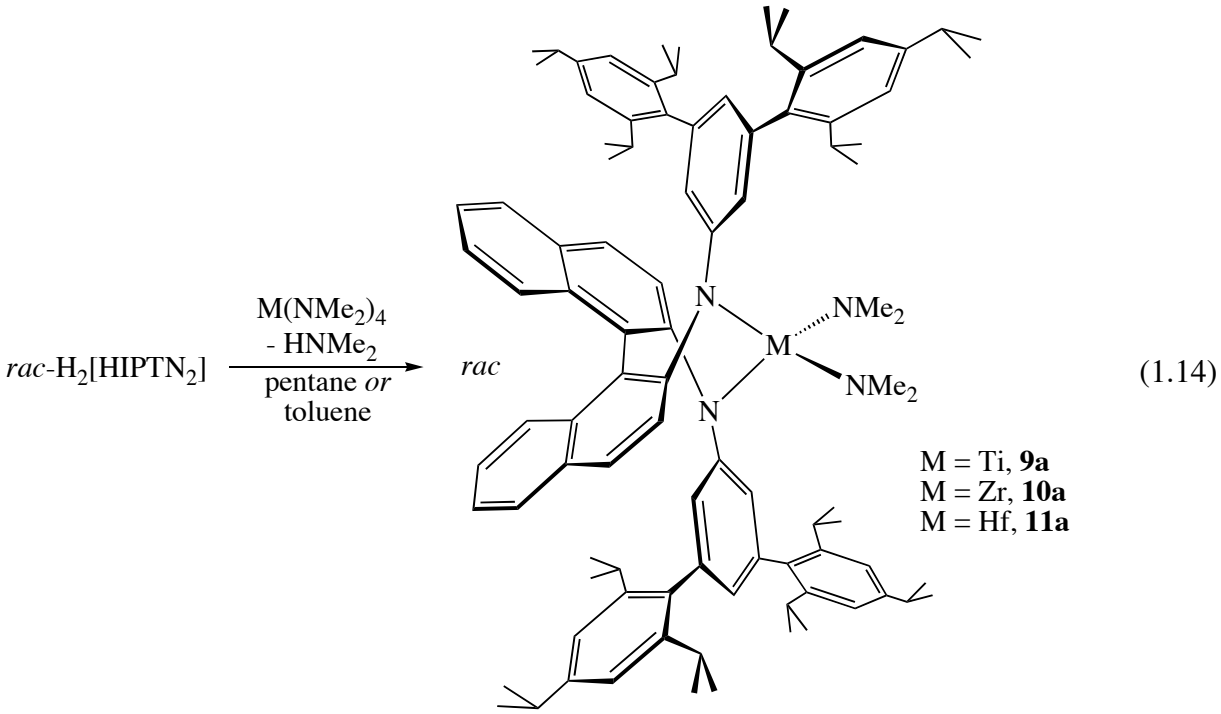

(1.14)

Treatment of compounds **10a** and **11a** with two equivalents of TMSCl in benzene at 60 ºC affords $[HIPTN_2]MCl_2$ (M = Zr, **10b**; M = Hf, **11b**). ^{1}H NMR spectra of the yellow hafnium species show the expected sharp features of the ligand in a C_2-symmetric environment. However, proton spectra of the zirconium species reveal relatively broad resonances. The zirconium dichloride complex is deep red, but yields orange-yellow solutions in diethyl ether. ^{1}H NMR spectra of samples recrystallized from diethyl ether show a broad peak for two equivalents of diethyl ether near 3.70 ppm. Combustion analyses of the Zr compound were also consistent with the presence of two molecules of diethyl ether. The fact that neither the Zr nor the Hf complex dissolve readily in pentane suggests that the compounds may be dimers in the absence of a coordinating solvent. Apparently the dimer does not dissociate readily when the metal is hafnium, while a dynamic mixture of monomer and dimer exists in the zirconium case at room temperature, giving rise to the broadened spectrum.

Attempts to prepare $[HIPTN_2]TiCl_2$ were unsuccessful. Heating solutions of $[HIPTN_2]Ti(NMe_2)_2$ with excess TMSCl for several days resulted only in formation of

[$HIPTN_2$]Ti(NMe_2)Cl, according to ^{1}H NMR spectra. A reaction between [$HIPTN_2$]Ti(NMe_2)$_2$ and Me_3SiOTf also resulted in formation of only [$HIPTN_2$]Ti(NMe_2)(OTf), according to NMR spectra. These results are similar to those found in the titanium chemistry of a related diamido-donor ligand.[32]

Alkylation of compounds **10b** and **11b** yielded [$HIPTN_2$]MR_2 (R = Me, CH_2-*t*-Bu, *i*-Bu; Scheme 1.11). The dialkyl species are all yellow solids that are readily soluble in all organic solvents, including pentane. ^{1}H NMR spectra are consistent with monomeric C_2-symmetric species with resonances for the alkyl ligands appearing in a range typically encountered for d^0 alkyl complexes of hafnium and zirconium (Table 1.3).[45] Attempts to grow X-ray quality crystals of dialkyl complexes were unsuccessful, leading in each case to small needles or amorphous solids.

Scheme 1.11. Zr and Hf alkyl complexes of [$HIPTN_2$]$^{2-}$.

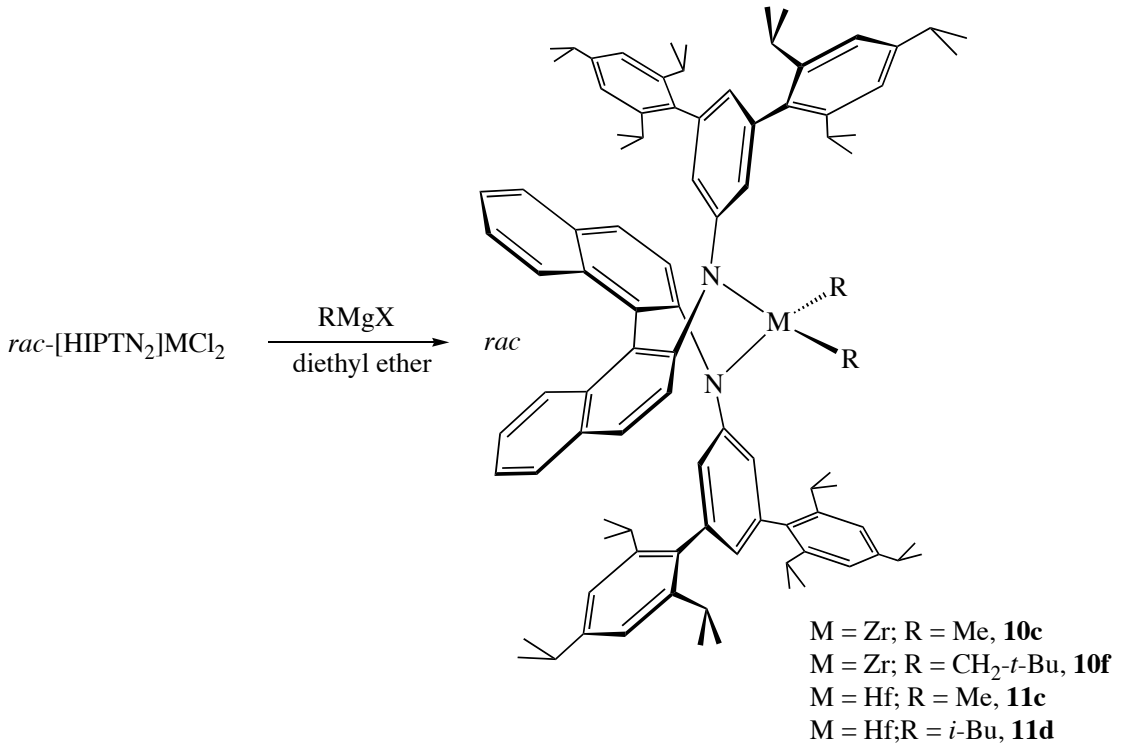

1.3.2 Activation of dialkyl species

Activation of **10c** was attempted with $B(C_6F_5)_3$, $\{Ph_3C\}\{B(C_6F_5)_4\}$, and $\{HNMe_2Ph\}\{B(C_6F_5)_4\}$ with the aim of preparing a cationic monomethyl species. Reaction of **10c** with $B(C_6F_5)_3$ in C_6D_6 yielded a deep red solution. ^1H NMR spectra of the red solution demonstrated it to contain a C_2-symmetric species, although no resonance could be found assignable to a methyl group. Examination of the ^{19}F NMR spectrum of the product showed that the expected $\{MeB(C_6F_5)_3\}^-$ anion was not present, although one major species appeared. Activation of the ^{13}C labeled derivative gave identical ^1H and ^{19}F NMR spectra to those obtained upon activation of the unlabeled compound. The ^{13}C NMR spectrum was more enlightening, showing only a very broad resonance at 17 ppm in bromobenzene-d_5 assignable to the $^{13}CH_3$ groups. The appearance and chemical shift of these methyl resonances points to a species with both methyl groups bound to boron. Decomposition of the $\{MeB(C_6F_5)_3\}^-$ anion by C_6F_5 transfer to the metal is now a well-documented reaction pathway for Group IV methyl cations.[55] Decomposition by this pathway could account for the presence of a C_2-symmetric species, namely, a complex with two pentafluorophenyl ligand, $[HIPTN_2]Zr(C_6F_5)_2$ (**10g**). A plausible reaction accounting for the formation of **10g** is shown in equation 1.15. One equivalent of $Me_2B(C_6F_5)$ is produced per molecule of **10g**, consistent with the observed broad resonance for the methyl groups by ^{13}C NMR spectroscopy. A double exchange of methyl for pentafluorophenyl is somewhat more rare and may be due to the highly electron deficient nature of the metal center and its relatively open architecture. This reaction can be used

$$[HIPTN_2]ZrMe_2 \xrightarrow[\text{bromobenzene-}d_5]{\begin{array}{c}B(C_6F_5)_3\\ -\ Me_2B(C_6F_5)\end{array}} [HIPTN_2]Zr(C_6F_5)_2 \qquad (1.15)$$

on larger scales to prepare $[HIPTN_2]Zr(C_6F_5)_2$ in good yield after recrystallization from hexanes. ^1H, ^{13}C, and ^{19}F NMR spectra, as well as combustion analysis of the recrystallized material, are

all consistent with the product being $[HIPTN_2]Zr(C_6F_5)_2$; NMR spectra are also all identical to those obtained in NMR scale activation experiments. Attempts to polymerize 1-hexene by a cationic species that may be formed transiently upon activation of **10c** with $B(C_6F_5)_3$ were unsuccessful, even when the reaction was conducted in neat 1-hexene, and at -30 ºC. These results differ from those obtained by McConville for a titanium diamido catalyst where decomposition of the $MeB(C_6F_5)_3$ anion was avoided by conducting polymerization experiments in neat 1-hexene.[56,57]

The reaction between **10c** and $\{HNMe_2Ph\}\{B(C_6F_5)_4\}$ in bromobenzene proceeded as anticipated with elimination of methane and formation of a dimethylaniline adduct of the monomethyl cation, as shown in equation 1.16. The activation required several hours at

$$[HIPTN_2]ZrMe_2 \xrightarrow[\text{bromobenzene-}d_5]{\{HNMe_2Ph\}\{B(C_6F_5)_4\}\ -\ CH_4} \{[HIPTN_2]Zr(Me)(NMe_2Ph)\}\{B(C_6F_5)_4\} \qquad (1.16)$$

room temperature to go to completion, perhaps as a consequence of the limited solubility of $\{HNMe_2Ph\}\{B(C_6F_5)_4\}$ in bromobenzene. ^1H and ^{13}C NMR spectra are both consistent with the product being asymmetric and containing one methyl group. Two singlet resonances are found for the Me groups of dimethylaniline in the ^1H NMR spectrum, consistent with a tightly bound dimethylaniline. The low coordination number of the formally three-coordinate and sterically accessible metal in the cation allows for tight binding of the dimethylaniline. Only one diastereomer is observed. Addition of 1-hexene to $\{[HIPTN_2]Zr(Me)(NMe_2Ph)\}\{B(C_6F_5)_4\}$ yielded no polymer, even at elevated temperatures (60 ºC). The lack of catalytic activity for this complex might be ascribed to the tight binding of dimethylaniline. Irreversible coordination of bases to other low coordinate Group IV cations has been observed in other systems to shut down catalytic activity.[58]

Reaction of **10c** with $\{Ph_3C\}\{B(C_6F_5)_4\}$ in bromobenzene-d_5 at –10 ºC over a period of 20-30 minutes yielded a dark red solution. ^1H and ^{13}C NMR spectra were consistent with formation of an asymmetric monomethyl cation. When a full equivalent of trityl was employed, two similar species were formed in a roughly 1:1 ratio. The two compounds have nearly identical NMR spectra, which suggests that they may be diastereomers (Table 1.3). The two species do not appear to form at the same rate; one is formed before all $[HIPTN_2]ZrMe_2$ is consumed, while the other grows in as $[HIPTN_2]ZrMe_2$ reacts with the remaining trityl. The dimethyl species therefore may play a role in conversion of one diastereomer to the other.

Activation of dimethyl species with trityl has been shown to produce monocationic dimers through capture of the monomethyl cation by unreacted dimethyl species (see section 1.1.3). To test the likelihood of dimer formation with **10c**, the activation experiment was conducted with 0.5 equivalents of trityl. ^1H NMR spectra from this reaction show a 1:1 ratio of starting material to one of the diastereomers observed above, indicating that monocationic dimeric species are not present. The J_{CH} coupling constants of 120 Hz for the methyl groups in each diastereomer also argue in favor of monomeric species. Therefore, it seems likely that the relatively strong ion pairing gives rise to the two different species being observable by NMR.

Solutions of **10c** activated with trityl react instantly and exothermically with several equivalents of 1-hexene at –30 ºC. Examination of these reactions by ^1H and ^{13}C NMR spectroscopy revealed that the 1-hexene was oligomerized. This result is similar to that found with the $[(MesN\text{-}o\text{-}C_6H_4)_2O]^{2-}$ ligand system and suggests that chain termination by β-H elimination (from either the 1,2 or especially a 2,1 insertion product is facile).[32] The relatively open environment at the metal may not allow effective discrimination between 1,2 and 2,1 olefin insertion, thereby leading to an enhanced proclivity towards β-H elimination.[50]

Activation of the hafnium dimethyl species, **11c**, with the three activators discussed above yielded results that are essentially identical to those observed with zirconium (see Experimental section). Interestingly, $[HIPTN_2]Hf(C_6F_5)_2$, **11g**, formed by reaction with $B(C_6F_5)_3$ is the first such compound of hafnium to be formed by aryl transfer from boron. The diisobutyl

species, **11d**, showed similar behavior to the dimethyl species when activated with $\{Ph_3C\}\{B(C_6F_5)_4\}$ and $\{HNMe_2Ph\}\{B(C_6F_5)_4\}$. Unlike the methyl species, the isobutyl complex did not undergo exchange with $B(C_6F_5)_3$, but rather reacted slowly to give an asymmetric Hf species and isobutene as judged by ^{1}H NMR. This asymmetric species could not be identified positively as the isobutyl cation, but the fact that it did not react with 1-hexene at room temperature to yield polymer or oligomer argues against its formulation as a mono-isobutyl cation.

The dineopentyl zirconium species, **11f**, was also examined as an initiator. The complex did not react readily with $B(C_6F_5)_3$, and it reacted only very slowly with the other two activators to give products which could not be identified by NMR.

Table 1.3. Selected NMR data for alkyl complexes of $[HIPTN_2]^{2-}$.

Compound	^{1}H NMR	^{13}C NMR
$[HIPTN_2]ZrMe_2$	0.60*	53.17†
$\{[HIPTN_2]Zr(Me)(NMe_2Ph)\}^+$	0.73§	51.95§
$\{[HIPTN_2]Zr(Me)\}^+$	0.42§ (major); 0.64 (minor)	47.51§ (major); 49.76 (minor)
$[HIPTN_2]Zr(C_6F_5)_2$	N/A	148.52† (*o*); 146.11 (*ipso*); 142.71 (*p*); 136.48 (*m*)
$[HIPTN_2]Zr(CH_2CMe_3)_2$	1.60*, 1.11 (C*H*$_2$); 0.91 (*Me*)	99.91† (*C*H$_2$); 37.24 (*C*Me$_3$); 34.76 (*Me*)
$[HIPTN_2]HfMe_2$	0.46*	63.16†
$\{[HIPTN_2]Hf(Me)(NMe_2Ph)\}^+$	0.49§	-
$\{[HIPTN_2]Hf(Me)\}^+$	0.66§	-
$[HIPTN_2]Hf(CH_2CHMe_2)_2$	2.25* (C*H*); 0.97, 0.85 (C*H*$_2$); 0.81, 0.63 (*Me*)	98.11† (*C*H$_2$)

Measured in $^*C_6D_6$, $^\S C_6D_5Br$, $^\dagger CD_2Cl_2$.

DISCUSSION

Cationic zirconium and hafnium complexes supported by the unsymmetric diamido-N-donor ligands, $[MesNNPhNMes]^{2-}$ and $[t\text{-}BuNNPhNMes]^{2-}$, are initiators for the polymerization of 1-hexene at or below 0 ºC in bromobenzene. However, the polymerizations are not living and the resulting poly[1-hexene] is atactic. Since chirality at the metal is established only if the central, diphenylalkylamine-like donor remains bound *throughout* a polymerization reaction (i.e., for seconds to minutes, or longer), the central donor most likely dissociates too readily during polymerization, thereby interconverting chirality at the metal center and dramatically reducing the possibility of stereocontrol (Scheme 1.12). It is still possible that the donor remains firmly bound, but the asymmetric induction afforded by the diamido-donor ligand is simply insufficient in controlling the stereochemistry of 1-hexene enchainment.

Scheme 1.12. Possible mode of racemization in monoalkyl cations of $[RNNPhNMes]^{2-}$.

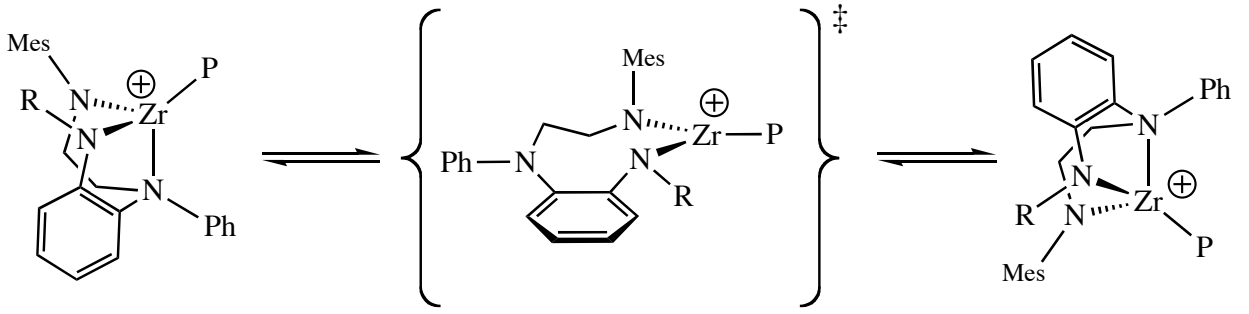

P = growing polymer chain
R = Mes or *t*-Bu

The $[MepyN]^{2-}$ was next examined because it possesses a fixed chiral element. Interconversion of enantiomeric metal complexes is not possible in the temperature range examined, nor is coordination to the metal is necessary to produce the desired asymmetry. Furthermore, the C_2-symmetric nature of the ligand was deemed advantageous owing to the

documented success of the *ansa*-metallocenes.[1] The tetradentate $[MepyN]^{2-}$ ligand affords the opportunity to exam the reactivity of coordinatively more saturated species with well defined activators such as boranes, carbocations, and proton sources. The variety of alkyl complexes that can be prepared with $[MepyN]^{2-}$ is somewhat more limited than with the other ligand types. Synthetic difficulties are most likely a consequence of the reactivity of the benzylic protons within the backbone of the $[MepyN]^{2-}$ ligand. Recent work by Gibson with a diimino-pyridine ligand has demonstrated the propensity for secondary reactions about the ligand periphery in the presence of alkylating agents.[59] Nevertheless, activation of dialkyl species of $[MepyN]^{2-}$, especially $[MepyN]M(i\text{-}Bu)_2$, gives rise to asymmetric, cationic, monoalkyl complexes that are readily observable by NMR spectroscopy. None of these cationic species serve as initiators for the polymerization of 1-hexene. The absence of catalytic activity with these complexes can be ascribed both to their high coordination number and to the presence of a sterically encumbering diamido-dipyridine ligand, which serves to decrease the Lewis acidity at the metal and hinder olefin approach and binding. The geometry of all the symmetric complexes of $[MepyN]^{2-}$ examined here also suggests a preference for coplanar binding of the ligand (c.f. structures of **8t**, **8d**, and **7e**). If this preference is maintained in cationic species, the alkyl ligand will be situated *trans* to the open coordination site, preventing enchainment of incoming olefin.

In an attempt to remedy several of the problems encountered with the $[MepyN]^{2-}$ ligand, the simpler diamido ligand, $[HIPTN_2]^{2-}$, was examined. Lacking any coordinative saturation, complexes of $[HIPTN_2]^{2-}$ proved to be more reactive toward Lewis acids such as $B(C_6F_5)_3$. As a result, only activation of $[HIPTN_2]MMe_2$ by trityl gave rise to cationic monoalkyl complexes. In contrast to $\{[MepyN]MR\}^+$, cationic complexes of $[HIPTN_2]^{2-}$ did demonstrate reactivity toward olefins but yielded oligomeric products. Chain termination events such as β-H elimination are likely both frequent *and* irreversible in these highly-reactive three-coordinate monoalkyl cations.

CONCLUSIONS

All three ligand types described in this chapter support asymmetric dialkyl complexes of Zr and Hf. Many of these complexes can be successfully activated with appropriate Lewis acids giving rise to cationic monoalkyl species. The alkyl cations derived from the two binaphthyl-based ligands were not successful initiators for the polymerization of 1-hexene. The diamido-donor ligands did support active initiators for 1-hexene polymerization, but the resulting polymer was found to be atactic. It is concluded that the facial coordination of diamido-donor ligands is necessary to support catalytically active four-coordinate monoalkyl cations, but that the nature of the diamido-donor framework is ill-suited to effect the stereospecific polymerization of terminal olefins.

EXPERIMENTAL

General comments. All manipulations of air- and moisture-sensitive materials were performed in oven-dried (200 ºC) glassware under an atmosphere of nitrogen on a dual-manifold Schlenk line or in a Vacuum Atmospheres glovebox. NMR measurements were carried out in Teflon-valve sealed J-Young type NMR tubes. HPLC grade organic solvents were sparged with nitrogen and dried by passage through activated alumina (for diethyl ether, toluene, pentane, THF, and methylene chloride) followed by passage through Q-5 supported copper catalyst (for benzene) prior to use, then stored over 4 Å Linde-type molecular sieves. Benzene-d_6, toluene-d_8, and THF-d_8 were dried over sodium/benzophenone ketyl and vacuum-distilled. Methylene chloride-d_2 and bromobenzene-d_5 were dried over CaH_2, vacuum distilled and stored over 4 Å Linde-type molecular sieves. NMR spectra were recorded on a Varian 500 or Varian 300 spectrometer. Chemical shifts for ^1H and ^{13}C spectra were referenced to the residual $^1H/^{13}C$ resonances of the deuterated solvent (^1H: C_6D_6, δ 7.16; $C_6D_5CD_3$, δ 2.15; CD_2Cl_2, δ 5.32; C_6D_5Br, δ 7.29; ^{13}C: C_6D_6, δ 128.39; CD_2Cl_2, δ 54.00; C_6D_5Br δ 125.45) and are reported as parts per

million relative to tetramethylsilane. ^{19}F NMR spectra were referenced externally to fluorobenzene (δ -113.15 ppm upfield of $CFCl_3$). High resolution mass spectrometry measurements were performed at the MIT Department of Chemistry Instrument Facility, and elemental analyses were performed by H. Kolbe Microanalytics Laboratory, Mülheim an der Ruhr, Germany.

GPC analyses were carried out on a system equipped with two Jordi-Gel DVB mixed bed columns (250 mm length × 10 mm inner diameter) in series. HPLC grade THF was supplied at a flow rate of 1.0 mL/min with a Knauer 64 HPLC pump. A Wyatt Technology mini Dawn light-scattering detector coupled with a Knauer differential refractometer was employed. Data analysis was carried out using Astrette 1.2 software (Wyatt technology). M_n and M_w values for poly[1-hexene] were obtained using d*n*/d*c* = 0.076 mL/g (Wyatt Technology), and the auxiliary constant of the apparatus (5.9×10^{-4}) was calibrated using a polystyrene standard ($M_n = 2.2 \times 10^5$).

Materials. $M(NMe_2)_4$ (M = Ti, Zr, or Hf),[44] 2,2′-diamino-1,1′-binaphthalene,[60] 3,5-*bis*-(2,4,6-triisopropylphenyl)bromobenzene (HIPTBr),[61] $Zr(CH_2C_6H_5)_4$,[62] anilinium tetrakis(pentafluorophenyl)borate ($\{HNMe_2Ph\}\{B(C_6F_5)_4\}$),[63] and *t*-$BuCH_2MgCl$[64] were prepared according to published procedures, or slightly modified versions thereof. 6-Methyl-2-pyridinecarboxaldehyde, Me_3SiCl, *i*-BuMgBr, and MeMgBr were purchased from Aldrich Chemical Co. and used as received. Tris(pentafluorophenyl)borane, trimethylsilyl trifluoromethanesulfonate (Me_3SiOTf), $Pd_2(dba)_3$, BINAP and XPHOS were purchased from Strem Chemical Co. and used as received. Trityl tetrakis(pentafluorophenyl)borate, $\{Ph_3C\}\{B(C_6F_5)_4\}$, was obtained as a gift from the Exxon Mobil Corp. and used as received.

Crystallography. Mounting of crystals and refinement of X-ray diffraction data was performed by Adam Hock, Dr. William Davis, or Dr. Peter Müller of the Department of Chemistry Diffraction Facility. Low temperature diffraction data were collected on a Siemens Platform three-circle diffractometer coupled to a Bruker-AXS Smart 1K CCD detector (for the structures of **1d**, **3c**, **5c**, **7a′**, and **7e**) or a Bruker-AXS Apex CCD detector (for the structures of

8d and **8t**) with graphite-monochromated Mo Kα radiation (λ = 0.71073 Å), performing φ- and *ω*-scans. All structures were solved by direct methods using SHELXS[65] and refined against F^2 on all data by full-matrix least squares with SHELXL-97[66] (Sheldrick, G. M. SHELXL 97, Universität Göttingen, Göttingen, Germany, 1997). All non-hydrogen atoms were refined anisotropically. All hydrogen atoms were included into the model at geometrically calculated positions and refined using a riding model. The isotropic displacement parameters of the hydrogen atoms were fixed to 1.2 times the *U* value of the atoms they are linked to (1.5 times for methyl groups).

2-(2-Nitro-phenylamino)-ethyl-ammonium chloride, 1a. *o*-Chloronitrobenzene (100 g, 0.63 mol) was refluxed with excess ethylenediamine (340 mL, 5.1 mol) and water (184 mL, 10.2 mol) at 120 °C for 2 h. The unreacted ethylenediamine was removed in vacuo and the resulting residue was dissolved in hot, dilute HCl (pH = 3-4). The solution was filtered and cooled to –20 °C to give 85.87 g (60%) of brilliant orange needle-shaped crystals in two crops: ^{1}H NMR (300 MHz, C_2D_6SO) δ 8.17 (br t, N*H*), 8.07 (d, 1, *m*-aryl), 8.01 (br s, 3, NH_3), 7.55 (t, 1, *p*-aryl), 7.15 (d, 1, *o*-aryl), 6.73 (t, 1, *m*-aryl), 3.67 (m, 2, CH_2), 3.00 (t, 2, CH_2).

2-(2-Amino-phenylamino)-ethyl-ammonium chloride, 1b. A Fischer-Porter bottle was charged with 22.3 g (0.10 mol) of **1a** and 1 L of methanol. The bottle was sealed with a septum and the orange mixture was sparged with nitrogen for 15 minutes. To the mixture was added 1.1 g of Pd/C (3% Pd). The reaction vessel was flushed with hydrogen before being pressurized to 35 psi (hydrogen). The mixture was then stirred for 12 h at 60 °C. The warm mixture was filtered through Celite and the pale brown filtrate concentrated to half its volume in vacuo. Storage of the solution at –20 °C afforded 14.0 g (73%) pale pink needles in two crops over the course of 1-2 days: ^{1}H NMR (300 MHz, C_2D_6SO) δ 8.20 (br s, 3, NH_3), 6.50 (m, 4, aryl), 4.69 (br s, 2, NH_2), 3.24 (t, 2, CH_2), 3.04 (t, 2, CH_2).

***N*-(2,4,6-Trimethyl-phenyl)-*N*'-[2-(2,4,6-trimethyl-phenylamino)-ethyl]-benzene-1,2-diamine, 1c.** Under an atmosphere of nitrogen, 0.748 g (1.5 mol%) of $Pd_2(dba)_3$ and 1.520 g (4.5 mol%) of BINAP were dissolved in toluene and stirred for 20 minutes while heating gently with a heat gun. The mixture was filtered through Celite into a flask containing 10.17 g (54.2 mmol) of **1b** and 20.5 g (210 mmol) of NaO-*t*-Bu. To the mixture was added 300 mL of toluene and 17.5 mL (114 mmol) of 2-bromomesitylene. The reaction vessel was sealed with a septum and the red-brown mixture allowed to stir at 100 °C for 65 h. After cooling to room temperature, the reaction mixture was extracted into 300 mL of diethyl ether and washed three times with 250 mL of water followed by two times with 250 mL of a saturated NaCl solution. The organic layer was separated, dried over $MgSO_4$, and filtered through Celite to give a dark red-brown solution. The volatiles were removed in vacuo, and the resulting dark brown oil was purified by flash chromatography on SiO_2, eluting with a 1:1 mixture of diethyl ether to hexanes. The pooled fractions were concentrated to ~20 mL and stored at –20 °C for 24 h. Compound **1c** precipitated as 12.06 g (57%) of a pale yellow crystalline powder: ^{1}H NMR (300 MHz, $CDCl_3$) δ 6.94 (s, 2, *m*-Mes), 6.84 (s, 2, *m*-Mes), 6.79 (m, 2, *m*/*p*-aryl), 6.65 (t, 1, *m*-aryl), 6.27 (d, *o*-aryl), 4.72 (s, 1, N*H*), 4.09 (br t, 1, N*H*), 3.41 (t, 2, CH_2), 3.32 (t, 2, CH_2), 3.25 (br s, 1, N*H*), 2.32 (s, 3, *p*-Me), 2.31 (s, 6, *o*-Me), 2.22 (s, 3, *p*-Mes), 2.12 (s, 6, *o*-Me); ^{13}C NMR (75 MHz, $CDCl_3$): δ 142.8, 137.9, 137.0, 134.4, 133.7, 133.1, 131.8, 129.9, 129.6, 129.3, 120.6, 118.9, 114.5, 111.5, 48.1, 44.9, 21.1, 20.8, 18.7, 18.3. HRMS calcd for $C_{26}H_{33}N_3$ $[M+H]^+$: 388.2747. Found $[M+H]^+$: 388.2747.

Complex 1d. A reaction vessel was charged with 1.00 g (2.58 mmol) of **1c** and 1.424 g (5.33 mmol) of $Zr(NMe_2)_4$ and made homogeneous through addition of 100 mL of diethyl ether. The amber solution was allowed to stir for 16 hours at room temperature during which time compound **1d** precipitated from solution as 1.49 g (70%) of a pale yellow powder. Crystals suitable for X-ray diffraction were grown by vapor diffusion of pentane into benzene: ^{1}H NMR (500 MHz, C_6D_6) δ 7.71 (d, 1, aryl), 7.04 (s, 1, *m*-Mes), 7.01 (s, 1, *m*-Mes), 6.97 (s, 1, *m*-Mes),

6.96 (s, 1, *m*-Mes), 6.90 (t, 1, aryl), 6.79 (t, 1, aryl), 6.13 (d, 1, aryl), 4.56 (td, 1, CH_2), 4.40 (td, 1, CH_2), 4.01 (dd, 1, CH_2), 3.21 (dd, 1, CH_2), 2.85 (br, 9, NMe_2), 2.63 (v br, 15, NMe_2), 2.55 (s, 3, Mes-*Me*), 2.51 (s, 3, Mes-*Me*), 2.31 (s, 3, Mes-*Me*), 2.27 (s, 3, Mes-*Me*), 2.26 (s, 3, Mes-*Me*), 2.21 (s, 3, Mes-*Me*). Anal. Calcd for $C_{36}H_{60}N_8Zr_2$: C, 54.92; H, 7.68; N, 14.23. Found: C, 55.11; H, 7.59; N, 14.28.

***N*-Phenyl-*N*'-(2,4,6-trimethyl-phenyl)-*N*-[2-(2,4,6-trimethyl-phenylamino)-ethyl]-benzene-1,2-diamine, H_2[MesNNPhNMes].** H_2[MesNNPhNMes] was prepared in a manner analogous to **1c** through a $Pd_2(dba)_3$/BINAP catalyzed N-Aryl coupling that employed 3.998 g (0.0103 mol) of **1c** and 1.4 mL (0.013 mol) of bromobenzene. After the aqueous workup, the crude product was purified by flash chromatography (SiO_2, 5% EtOAc in hexanes) to give 2.69 g (56%) of H_2[MesNNPhNMes] as an extremely viscous brown-yellow oil that was used without further purification: ^{1}H NMR (500 MHz, $CDCl_3$) δ 7.20 (t, 2, *m*-Ph), 7.12 (d, 2, *o*-Ph), 7.03 (t, 1, *p*-Ph), 6.90 (s, 2, *m*-Mes), 6.80 (s, 2, *m*-Mes), 6.74 (m, 3, aryl), 6.23 (d, 1, aryl), 5.76 (s, 1, N*H*), 3.88 (t, 2, CH_2), 3.34 (t, 2, CH_2), 3.11 (br s, 1, N*H*), 2.30 (s, 3, *p*-Me), 2.23 (s, 3, *p*-Me), 2.19 (s, 6, *o*-Me), 2.07 (s, 6, *o*-Me); ^{13}C NMR (125 MHz, $CDCl_3$) δ 148.3, 143.7, 143.1, 136.3, 135.6, 135.0, 132.2, 131.7, 129.9, 129.7, 129.6, 129.4, 129.3, 127.9, 118.3, 118.0, 114.4, 112.3, 51.5, 46.4, 21.1, 20.7, 18.4, 18.4. HRMS Calcd $[M+H]^+$: 464.3060, Found $[M+H]^+$: 464.3040.

***N*'-(2,4,6-Trimethyl-phenyl)-ethane-1,2-diamine, 2a.** Compound **2a** was prepared by a $Pd_2(dba)_3$/BINAP (1.5 mol%/4.5 mol%) catalyzed *N*-aryl coupling between 23 mL (0.15 mol) of bromomesitylene and 40 mL (0.59 mol) of ethylenediamine in the same manner as compounds **1c** and H_2**1**. After aqueous workup, crude **2a** was purified by vacuum distillation (85˚C, 10 mTorr) yielding 17.46 g (65%) of a colorless oil: ^{1}H NMR (500 MHz, $CDCl_3$) δ 6.86 (s, 2, *m*-Mes), 3.00 (t, 2, CH_2), 2.92 (t, 2, CH_2), 2.31 (s, 6, *o*-Me), 2.27 (s, 3, *p*-Me), 2.01 (br s, 2, NH_2); ^{13}C NMR (125 MHz, $CDCl_3$) δ 143.6, 131.3, 129.8, 129.5, 51.3, 42.7, 20.6, 18.5. HRMS calcd for $C_{11}H_{18}N_2$ $[M]^+$: 178.1465. Found $[M]^+$: 178.1468.

***N*-(2-Nitro-phenyl)-*N*'-(2,4,6-trimethyl-phenyl)-ethane-1,2-diamine, 2b.** A reaction vessel was charged with 12.36 g (0.0693 mol) of **2a**, 7.7 mL (0.073 mol) of 2-nitrofluorobenzene, 19.7 g (0.143 mol) of K_2CO_3 and 250 mL of acetonitrile. The reaction mixture was degassed with nitrogen for 10 minutes and then heated to 80 ºC for 18 h. During this time the mixture changed from yellow to bright orange. The acetonitrile was removed in vacuo and the residue extracted into 300 mL of diethyl ether. The ether extract was washed once with 200 mL of water and twice with 200 mL of a saturated NaCl solution. The organic layer was dried over $MgSO_4$ and filtered through Celite. The ether was removed in vacuo to give 18.50 g (89%) of **2b** as bright orange crystals: ^{1}H NMR (300 MHz, $CDCl_3$) δ 8.35 (br t, 1, N*H*), 8.21 (d, 1, *m*-aryl), 7.45 (t, 1, *m*-aryl), 6.88 (d, 1, *o*-aryl), 6.85 (s, 2, *m*-Mes), 6.68 (t, 1, *p*-aryl), 3.52 (m, 2, CH_2), 3.29 (t, 2, CH_2), 3.04 (br s, 1, N*H*), 2.29 (s, 6, *o*-Me), 2.25 (s, 3, *p*-Me); ^{13}C NMR (75 MHz, $CDCl_3$): δ 145.4, 142.2, 136.3, 132.2, 132.1, 130.5, 129.6, 126.9, 115.5, 113.8, 47.2, 43.5, 20.8, 18.4. HRMS calcd for $C_{17}H_{21}N_3O_2$ $[M+H]^+$: 300.1707. Found $[M+H]^+$: 300.1705.

***N*-[2-(2,4,6-Trimethyl-phenylamino)-ethyl]-benzene-1,2-diamine, 2c.** A Fischer-Porter bottle was charged with 18.50 g (62.8 mmol) of **2b** and 500 mL of methyl alcohol. The orange solution was degassed with nitrogen for 15 minutes before 1.74 g of Pd/C (3% Pd) was added. The system was flushed with hydrogen, pressurized to 35 psi (hydrogen), and then stirred at 60 ºC for 3.5 h. The warm reaction mixture was filtered through Celite and the volatiles removed in vacuo to give 16 g (~95%) of **2c** as a crude dark red oil that was used without further purification: ^{1}H NMR (500 MHz, $CDCl_3$) δ 6.86 (s, 2, *m*-Mes), 6.84 (t, 1, *m*-aryl), 6.73 (m, 3, aryl), 3.66 (br s, 2, NH_2), 3.37 (t, 2, CH_2), 3.28 (t, 2, CH_2), 2.31 (s, 6, *o*-Me), 2.26 (s, 3, *p*-Me); ^{13}C NMR (125 MHz, $CDCl_3$) δ 142.5, 137.5, 134.8, 132.3, 130.3, 129.8, 120.7, 119.2, 116.6, 112.0, 48.2, 44.6, 20.8, 18.5. HRMS calcd for $C_{17}H_{23}N_3$ $[M+H]^+$: 270.1970. Found $[M+H]^+$: 270.1963.

***N*-Isopropylidene-d_6-*N*'-[2-(2,4,6-trimethyl-phenylamino)-ethyl]-benzene-1,2-diamine, 2d.** Crude **2c** (16g) was dissolved in 50 g of acetone-d_6 and 30 g of 4 Å molecular sieves were added. The reaction vessel was sealed with a septum and flushed with nitrogen. The reaction was allowed to stand at room temperature for 5 days. The dark red solution was filtered through Celite and the volatiles were removed in vacuo to give 16.7 g (86% for **2b**) of compound **2d** as a yellow-red oil that was immediately carried on to the next step in the synthesis: ^{1}H NMR (300 MHz, acetone-d_6) δ 6.79 (s, 2, *m*-Mes), 6.53 (t, 1, *m*-aryl), 6.46 (t, 1, *p*-aryl), 6.40 (d, 1, *m*-aryl), 6.31 (d, 1, *o*-aryl), 4.81 (br s, 1, N*H*), 3.54 (v br s, 1, N*H*), 3.30 (t, 2, CH_2), 3.15 (t, 2, CH_2), 2.26 (s, 6, *o*-Me), 2.21 (s, 3, *p*-Me).

***N-tert*-Butyl-d_6-*N*'-[2-(2,4,6-trimethyl-phenylamino)-ethyl]-benzene-1,2-diamine, 2e.** Methyl lithium (200 mL, 320 mmol) was transferred under nitrogen to a Schlenk flask equipped with a pressure-equalizing addition funnel. The funnel was capped with a septum, and charged with a solution of 16.68 g (52.7 mmol) of **2d** in 125 mL of diethyl ether. The solution of methyl lithium in the base of the flask was chilled to –78 ºC, and the solution of **2d** added dropwise over 24 h. The reaction was then heated at 35 ºC for 2 days during which time any precipitate dissolved. The reaction was allowed to cool to room temperature and the contents were poured over 150 mL of ice. The organic layer was separated and washed three times with 250 mL of distilled water. The solution was then dried over $MgSO_4$ and purified by flash chromatography on SiO_2 eluting with 10% EtOAc in hexanes (by volume) to give 13.37 g (76%) of a viscous pale yellow oil: ^{1}H NMR (300 MHz, $CDCl_3$) δ 6.93 (m, 2, *m*/*p*-aryl), 6.85 (s, 2, *m*-Mes), 6.70 (m, 2, *m*/*o*-aryl), 4.60 (br s, 1, N*H*), 3.31 (m, 2, CH_2), 3.21 (m, 2, CH_2), 2.97 (br s, 2, N*H*), 2.29 (s, 6, *o*-Me), 2.25 (s, 3, *p*-Me), 1.28 (s, 3, C(CD_3)$_2$*Me*); ^{13}C NMR (125 MHz, $CDCl_3$) δ 143.5, 143.4, 133.4, 131.9, 130.4, 129.7, 122.9, 122.9, 117.7, 111.6, 52.3, 48.2, 45.1, 29.9, 20.8, 15.5. HRMS calcd for $C_{21}H_{25}D_6N_3$ $[M+H]^+$: 332.2967. Found $[M+H]^+$: 332.2970.

***N*-*tert*-butyl-d_6-*N*'-(2-(mesitylamino)ethyl)-*N*'-phenylbenzene-1,2-diamine, H_2[*t*-BuNNPhNMes].** H_2[*t*-BuNNPhNMes] was prepared through a $Pd_2(dba)_3$/XPHOS (XPHOS = Dicyclohexyl-(2',4',6'-triisopropylbiphen-2-yl)phosphine) (1.1 mol%/4.2 mol%) catalyzed *N*-aryl coupling between 4.253 g (0.0128 mol) of **2e** and 1.62 mL (0.0154 mol) of bromobenzene in the same manner as compounds **1c**, H_2[MesNNPhNMes], and **2a**. After aqueous workup, the crude compound was purified by column chromatography on silica gel eluting with 5% ethyl acetate in hexanes (by volume). The purified product was dried in vacuo at 70 °C for several hours to afford 2.582 g (50%) of an amber oil: ^{1}H NMR (500 MHz, C_6D_6) δ 7.09 (m, 4, aryl), 6.98 (m, 2, aryl), 6.76 (s, 2, *m*-Mes) 6.74 (m, 2, aryl), 6.69 (t, 1, aryl), 4.68 (s, 1, N*H*), 3.56 (t, 2, CH_2), 3.11 (m, 2, CH_2), 2.92 (br t, 1, N*H*), 2.15 (s, 3, *p*-Me), 2.11 (s, 6, *o*-Me), 1.11 (s, 3, C$(CD_3)_2$*Me*); ^{13}C NMR (125 MHz, $CDCl_3$): δ 148.5, 145.0, 143.3, 133.4, 131.6, 129.9, 129.6, 129.3, 129.3, 127.5, 118.2, 117.1, 114.4, 114.4, 51.8, 50.5, 46.2, 23.0, 20.7, 18.5. HRMS calcd for $C_{27}H_{29}D_6N_3$ $[M+H]^+$: 408.3282. Found $[M+H]^+$: 408.3264.

[MesNNPhNMes]Zr$(NMe_2)_2$, 3a. To a cold solution (-25 ºC) of 1.386 g (2.98 mmol) of H_2[MesNNPhNMes] in 8 mL of pentane was added dropwise a cold solution of 0.810 g of $Zr(NMe_2)_4$ in 8 mL of pentane. A slight darkening of the solution occurred upon addition of the $Zr(NMe_2)_4$. The reaction was stirred for 15 minutes then allowed to stand at 23 ºC for 24 hours. The reaction solution was concentrated until a precipitate formed. The precipitate was collected by filtration and washed with pentane yielding 1.440 g (76%) of **3a** as an off-white crystalline solid: ^{1}H NMR (500 MHz, C_6D_6) δ 7.07 (m, 3, aryl), 7.00 (m, 3, aryl), 6.94 (s, 1, *m*-Mes), 6.90 (s, 1, *m*-Mes), 6.85 (m, 2, aryl), 6.54 (d, 1, aryl), 6.44 (t, 1, aryl), 6.20 (d, 1, aryl), 4.30 (t, 1, CH_2), 3.70 (td, 1, CH_2), 3.62 (app d, 1, CH_2), 3.02 (dd, 1, CH_2), 2.48 (s, 9, NMe_2 + Mes-*Me*), 2.38 (s, 3, Mes-*Me*), 2.37 (s, 3, Mes-*Me*), 2.34 (s, 3, *Mes*-Me), 2.24 (s, 9, NMe_2 + Mes-*Me*), 2.17 (s, 3, Mes-*Me*). Anal. Calcd for $C_{36}H_{47}N_5Zr$: C, 67.45; H, 7.39; N, 10.93. Found: C, 67.32; H, 7.28; N, 11.06.

[MesNNPhNMes]ZrCl$_2$, 3b. TMSCl (0.22 mL, 1.73 mmol) was added dropwise to a cold (-25 ºC) solution of 0.552 g (0.861 mmol) of **3a** in 10 mL of toluene. The reaction was allowed to stir at 23 ºC for 24 hours. All volatiles were removed in vacuo leaving 0.400 g (75%) of **3b** as a white powder: ^{1}H NMR (500 MHz, C_6D_6) δ 7.28 (d, 2, *o*-Ph), 7.05 (m, 3, *o*/*p*-Ph), 6.92 (t, 1, aryl), 6.89 (s, 1, *m*-Mes), 6.85 (s, 1, *m*-Mes), 6.81 (t, 1, aryl), 6.66 (s, 1, *m*-Mes), 6.48 (m, 2, aryl), 6.05 (d, 1, aryl), 3.90 (td, 1, C*H*$_2$), 3.62 (td, 1, C*H*$_2$), 3.47 (dd, 1, C*H*$_2$), 3.37 (dd, 1, C*H*$_2$), 2.57 (s, 3, Mes-*Me*), 2.48 (s, 3, Mes-*Me*), 2.45 (s, 3, Mes-*Me*), 2.19 (s, 3, Mes-*Me*), 2.04 (s, 3, Mes-*Me*), 2.02 (s, 3, Mes-*Me*). Anal. Calcd for $C_{32}H_{35}Cl_2N_3Zr$: C, 61.62; H, 5.66; Cl, 11.37; N, 6.74. Found: C, 61.54; H, 5.73; Cl, 11.43; N, 6.79.

[MesNNPhNMes]ZrMe$_2$, 3c. A solution of 0.29 mL (0.87 mmol) of MeMgBr (3.0 M in Et_2O) was added dropwise to a cold (-25˚C) suspension of 0.256 g (0.410 mmol) of **3b** in 10 mL of diethyl ether. The reaction was allowed to warm to RT and stir for 1 hr. during which time the contents of the reaction went into solution and a small amount of precipitate formed. 1,4-Dioxane (0.1 mL, 1.17 mmol) was added to the reaction to precipitate the magnesium salts. The reaction was filtered through Celite and the volatiles removed in vacuo to give 0.225 g (90%) of **3c** as a white powder. Crystals suitable for X-ray diffraction were grown from a concentrated ether/pentane solution: ^{1}H NMR (500 MHz, C_6D_6) δ 7.25 (d, 2, *o*-Ph), 7.05 (s, 1, *m*-Mes), 7.04 (s, 1, *m*-Mes), 7.01 (t, 2, *m*-Ph), 6.91 (s, 1, *m*-Mes), 6.87 (m, 2, aryl), 6.80 (s, 1, *m*-Mes), 6.67 (d, 1, aryl), 6.46 (t, 1, aryl), 6.15 (d, 1, aryl), 3.78 (td, 1, C*H*$_2$), 3.53 (dd, 1, C*H*$_2$), 3.36 (m, 2, C*H*$_2$), 2.61 (s, 3, C*H*$_2$), 2.42 (s, 3, Mes-*Me*), 2.37 (s, 3, Mes-*Me*), 2.25 (s, 3, Mes-*Me*), 2.11 (s, 3, Mes-*Me*), 1.77 (s, 3, Mes-*Me*), 0.41 (s, 3, Zr*Me*), 0.40 (s, 3, Zr*Me*); ^{13}C NMR (125 MHz, C_6D_6) δ 153.5, 145.7, 143.9, 143.3, 141.8, 136.8, 136.5, 136.1, 135.8, 135.5, 135.1, 131.1, 130.7, 130.5, 130.3, 130.1, 129.8, 127.0, 125.2, 121.0, 117.7, 113.7, 57.5, 54.7, 49.2, 43.9, 21.5, 21.3, 19.7, 19.5, 18.7, 17.8. Anal. Calcd for $C_{34}H_{41}N_3Zr$: C, 70.05; H, 7.09; N, 7.21. Found: C, 69.87; H, 6.96; N, 7.12.

[MesNNPhNMes]Hf(NMe$_2$)$_2$, 4a. Compound **4a** was prepared in fashion that was strictly analogous to the synthesis of **3a** starting from 2.67 g (5.75 mmol) of H$_2$**1** and 2.044 g (5.76 mmol) of Hf(NMe$_2$)$_4$. Compound **4a** was isolated as 3.714 g (89%) of white cubes: ^{1}H NMR (500 MHz, C_6D_6) δ 7.03 (m, 5, aryl), 6.95 (s, 1, *m*-Mes), 6.92 (s, 1, *m*-Mes), 6.85 (m, 3, aryl), 6.51 (d, 1, aryl), 6.42 (t, 1, aryl), 6.20 (d, 1, aryl), 4.29 (td, 1, C*H*$_2$), 3.64 (m, 2, C*H*$_2$), 3.12 (dd, 1, C*H*$_2$), 2.50 (s, 9, N*Me*$_2$ + Mes-*Me*), 2.42 (s, 3, Mes-*Me*), 2.38 (s, 3, Mes-*Me*), 2.36 (s, 3, Mes-*Me*), 2.29 (s, 6, N*Me*$_2$), 2.25 (s, 3, Mes-*Me*), 2.19 (s, 3, Mes-*Me*). Anal. Calcd for $C_{36}H_{47}N_5Hf$: C, 59.37; H, 6.50; N, 9.62. Found: C, 59.46; H, 6.38; N, 9.55.

[MesNNPhNMes]HfCl$_2$, 4b. Compound **4b** was prepared in fashion similar to the synthesis of **3b** by treating **4a** (3.710 g, 5.095 mmol) with 2 equivalents of TMSCl. The reaction required additional heating at 45ºC for 3.5 days to go to completion (84% isolated yield): ^{1}H NMR (500 MHz, C_6D_6): δ 7.25 (d, 2, *o*-Ph), 7.03 (m, 3, aryl), 6.91 (m, 2, aryl), 6.87 (s, 1, *m*-Mes), 6.81 (t, 1, aryl), 6.68 (s, 1, *m*-Mes), 6.45 (t, 1, aryl), 6.40 (d, 1, aryl), 6.07 (d, 1, aryl), 4.08 (m, 1, C*H*$_2$), 3.57 (m, 1, C*H*$_2$), 3.42 (dd, 1, C*H*$_2$), 2.56 (s, 3, Mes-*Me*), 2.50 (s, 3, Mes-*Me*), 2.48 (s, 3, Mes-*Me*), 2.20 (s, 3, Mes-*Me*), 2.13 (s, 3, Mes-*Me*), 2.06 (s, 3, Mes-*Me*). Anal. Calcd for $C_{32}H_{35}Cl_2N_3Hf$: C, 54.05; H, 4.96; Cl, 9.97; N, 5.91. Found: C, 54.11; H, 5.06; Cl, 9.93; N, 5.88.

[MesNNPhNMes]HfMe$_2$, 4c. Compound **4c** was prepared in fashion analogous to the synthesis of **3c** from **4b** (0.8135 g, 1.144 mmol) and 2 equivalents of MeMgBr. The crude product was formed in 90% yield and could be recrystallized from toluene/ether: ^{1}H NMR (500 MHz, C_6D_6) δ 7.23 (d, 2, *o*-Ph), 7.02 (m, 4, aryl), 6.91 (s, 1, *m*-Mes), 6.87 (m, 2, aryl), 6.81 (s, 1, *m*-Mes), 6.61 (d, 1, aryl), 6.45 (t, 1, aryl), 6.15 (d, 1, aryl), 3.96 (td, 1, C*H*$_2$), 3.45 (m, 2, C*H*$_2$), 3.35 (m, 1, C*H*$_2$), 2.59 (s, 3, Mes-*Me*), 2.42 (s, 3, Mes-*Me*), 2.39 (s, 3, Mes-*Me*), 2.24 (s, 3, Mes-*Me*), 2.12 (s, 3, Mes-*Me*), 1.91 (s, 3, Mes-*Me*), 0.22 (s, 3, Hf*Me*), 0.11 (s, 3, Hf*Me*); ^{13}C NMR (125 MHz, C_6D_6) δ 154.2, 145.8, 144.4, 143.4, 141.8, 136.7, 136.5, 136.2, 135.9, 135.5, 134.8, 131.0, 130.7, 130.6, 130.1, 129.9, 129.9, 126.7, 125.5, 121.4, 118.0, 114.5, 58.8, 58.2, 56.6, 55.4, 21.5, 21.3,

19.5, 19.5, 18.7, 17.9. Anal. Calcd for $C_{34}H_{41}N_3Hf$: C, 60.93; H, 6.17; N, 6.27. Found: C, 61.08; H, 6.12; N, 6.23.

[*t*-BuNNPhNMes]Zr(NMe_2)$_2$, 5a. To a cold (-25 ºC) solution of 2.50 g (6.13 mmol) of H_2[*t*-BuNNPhNMes] in 50 mL of pentane was added dropwise a cold solution of 1.653 g (6.179 mmol) of Zr(NMe_2)$_4$ in 20 mL of pentane. The amber solution was allowed to warm to room temperature and stir for 15 h. The solution was then concentrated to ~10 mL and set aside at -25ºC for several hours during which time white crystals formed. The mother liquor was concentrated further and chilled to -25ºC yielding a second crop of crystals. The crystals were collected by filtration, washed with cold pentane, and dried in vacuo giving 2.245 g (63%) of **5a**. The crude residue also could be dissolved in toluene and used directly in the proceeding step without isolation of crystalline **5a**: ^{1}H NMR (500 MHz, C_6D_6) δ 7.15 (t, 1, aryl), 7.10 (d, 1, aryl), 7.04 (m, 4, aryl), 6.97 (s, 1, *m*-Mes), 6.83 (m, 1, aryl), 6.79 (s, 1, *m*-Mes), 6.73 (d, 1, aryl), 6.58 (t, 1, aryl), 4.03 (td, 1, C*H*$_2$), 3.39 (td, 1, C*H*$_2$), 3.20 (dd, 1, C*H*$_2$), 2.74 (dd, 1, C*H*$_2$), 2.71 (s, 6, N*Me*$_2$), 2.61 (br s, 6, N*Me*$_2$), 2.50 (s, 3, Mes-*Me*), 2.18 (s, 3, Mes-*Me*), 1.74 (s, 3, Mes-*Me*), 1.48 (s, 3, *t*-Bu-d_6).

[*t*-BuNNPhNMes]ZrCl_2, 5b. To a cold (-25 ºC) solution of 2.245 g (3.84 mmol) of **5a** in toluene was added 0.97 mL (7.6 mmol) of TMSCl. The reaction was allowed to stir at room temperature for 3 days. All volatiles were removed in vacuo and the residue treated with pentane giving 1.927 g (88%) of **5b** as a pale yellow crystalline powder: ^{1}H NMR (500 MHz, C_6D_6): δ 7.04 (m, 5, aryl), 6.92 (d, 1, aryl), 6.88 (s, 1, *m*-Mes), 6.87 (t, 1, aryl), 6.73 (s, 1, *m*-mes), 6.66 (t, 1, aryl), 6.60 (d, 1, aryl), 4.35 (td, 1, C*H*$_2$), 3.30 (td, 1, C*H*$_2$), 3.06 (dd, 1, C*H*$_2$), 2.67 (dd, 1, C*H*$_2$), 2.62 (s, 3, Mes-*Me*), 2.11 (s, 3, Mes-*Me*), 1.78 (s, 3, Mes-*Me*), 1.41 (s, 3, *t*-Bu-d_6). Anal. Calcd for $C_{27}H_{27}D_6Cl_2N_3Zr$: C, 57.12; H, 6.92; Cl, 12.49; N, 7.40. Found: C, 57.22; H, 7.08; Cl, 12.37; N, 7.34.

[*t*-BuNNPhNMes]ZrMe$_2$, 5c. Compound **5b** (1.010 g, 1.779 mmol) was suspended in 45 mL of diethyl ether and cooled to -25ºC. A 1.10 mL (3.60 mmol) quantity of chilled MeMgBr was added and the mixture allowed to stir at room temperature for 20 minutes. The ether was removed *in vacuo* and the residue was extracted into 70 mL of pentane and filtered through Celite. The pentane was removed *in vacuo* leaving 0.778 g (83 yield) of **5c** as an off white crystalline powder. Crystals suitable for X-ray diffraction were grown from a concentrated pentane solution at –25 ºC: ^{1}H NMR (500 MHz, C_6D_6) δ 7.13 (t, 1, aryl), 7.02 (m, 4, aryl), 6.89 (d, 2, *o*-Ph), 6.82 (m, 2, aryl), 6.77 (s, 1, *m*-Mes), 6.66 (t, 1, aryl), 3.83 (td, 1, C*H*$_2$), 3.53 (td, 1, C*H*$_2$), 3.19 (dd, 1, C*H*$_2$), 2.88 (dd, 1, C*H*$_2$), 2.73 (s, 3, Mes-*Me*), 2.15 (s, 3, Mes-*Me*), 1.81 (s, 3, Mes-*Me*), 1.42 (s, 3, *t*-Bu-*d*$_6$), 0.58 (s, 3, Zr*Me*), 0.29 (s, 3, Zr*Me*); ^{13}C NMR (125 MHz, C_6D_6) δ 149.6, 148.4, 148.1, 135.2, 135.0, 134.3, 132.1, 130.3, 130.0, 129.2, 125.2, 123.3, 121.9, 120.0, 118.4, 55.7, 55.5, 54.5, 45.6, 42.9, 31.0, 21.4, 19.6, 18.1. Anal. Calcd for $C_{29}H_{33}D_6N_3Zr$: C, 66.11; H, 8.61; N, 7.97. Found: C, 66.15; H, 8.48; N, 8.06.

[*t*-BuNNPhNMes]Hf(NMe$_2$)$_2$, 6a. To a cold (-25 ºC) solution of 1.51 g (3.70 mmol) of H_2[*t*-BuNNPhNMes] in 15 mL of toluene was added 1.317 g (3.712 mmol) of Hf(NMe$_2$)$_4$ in 15 mL of toluene. The resulting amber solution was heated at 70 ºC for 20 h. The toluene was removed in vacuo and the resulting residue dissolved in ~5 mL of pentane and the solution was set aside at -25 ºC for several h. During this time, white crystalline blocks formed in the solution. The crystals were collected by filtration and dried in vacuo giving 1.629 g (65%) of **6a**: ^{1}H NMR (500 MHz, C_6D_6) δ 7.14 (m, 2, aryl), 7.04 (m, 4, aryl), 6.99 (s, 1, *m*-Mes), 6.84 (m, 1, aryl), 6.80 (s, 1, *m*-Mes), 6.70 (d, 1, aryl), 6.58 (t, 1, aryl), 3.99 (td, 1, C*H*$_2$), 3.38 (td, 1, C*H*$_2$), 3.18 (dd, 1, C*H*$_2$), 2.89 (dd, 1, C*H*$_2$), 2.75 (s, 6, N*Me*$_2$), 2.66 (br s, 6, N*Me*$_2$), 2.52 (s, 3, Mes-*Me*), 2.19 (s, 3, Mes-*Me*), 1.74 (s, 3, Mes-*Me*), 1.49 (s, 3, *t*-Bu-*d*$_6$). Anal. Calcd for $C_{31}H_{39}D_6N_5Hf$: C, 55.39; H, 7.65; N, 10.42. Found: C, 55.46; H, 7.61; N, 10.47.

[*t*-BuNNPhNMes]HfCl$_2$, 6b. Compound **6b** was prepared in analogous fashion to **5b** starting from 0.512 g (0.762 mmol) of **6a** and 0.21 mL (1.7 mmol) of TMSCl. The reaction required heating at 100 ºC for 2.5 days to go to completion. The toluene was removed in vacuo and the residue treated with pentane to give 0.324 g (65%) of **6b** as a white crystalline powder which could be recrystallized from ether: ^{1}H NMR (500 MHz, C_6D_6) δ 7.09 (t, 1, aryl), 7.00 (m, 4, aryl), 6.97 (d, 1, aryl), 6.91 (s, 1, *m*-Mes), 6.86 (m, 1, aryl), 6.76 (s, 1, *m*-Mes), 6.63 (t, 1, aryl), 6.54 (d, 1, aryl), 4.31 (td, 1, C*H*$_2$), 3.31 (td, 1, C*H*$_2$), 3.06 (dd, 1, C*H*$_2$), 2.83 (dd, 1, C*H*$_2$), 2.62 (s, 3, Mes-*Me*), 2.13 (s, 3, Mes-*Me*), 1.82 (s, 3, Mes-*Me*), 1.44 (s, 3, *t*-Bu-d_6). Anal. Calcd for $C_{27}H_{27}D_6Cl_2N_3Hf$: C, 49.51; H, 6.00; Cl, 10.83; N, 6.42. Found: C, 49.62; H, 5.91; Cl, 10.87; N, 6.49.

[*t*-BuNNPhNMes]HfMe$_2$, 6c. Compound **6c** was prepared in analogous fashion to **5c** starting from 0.210 g (0.320 mmol) of **6b** and 0.20 mL (0.65 mmol) of MeMgBr. After stirring the reaction mixture at room temperature for 30 minutes, the ether was removed in vacuo and the resulting residue extracted into ~10 mL of toluene and the toluene solution was filtered through Celite. The toluene was removed in vacuo from the filtrate and the residue was dissolved in 1-2 mL of pentane. The pentane solution was set aside at -25ºC for several days during which time off-white crystals formed in solution. The material was isolated and dried in vacuo giving 0.173 g (88%) of **6c**: ^{1}H NMR (500 MHz, C_6D_6) δ 7.14 (t, 1, aryl), 7.00 (m, 4, aryl), 6.90 (m, 2, aryl), 6.83 (t, 1, aryl), 6.77 (s, 1, *m*-Mes), 6.74 (d, 1, aryl), 6.65 (t, 1, aryl), 3.96 (td, 1, C*H*$_2$), 3.44 (td, 1, C*H*$_2$), 3.14 (dd, 1, C*H*$_2$), 3.00 (dd, 1, C*H*$_2$), 2.69 (s, 3, Mes-*Me*), 2.16 (s, 3, Mes-*Me*), 1.81 (s, 3, Mes-*Me*), 1.45 (s, 3, *t*-Bu-d_6), 0.33 (s, 3, Hf*Me*), 0.10 (s, 3, Hf*Me*); ^{13}C NMR (125 MHz, C_6D_6) δ 149.5, 148.7, 148.4, 135.3, 135.2, 134.2, 132.2, 130.2, 130.1, 129.2, 129.0, 124.9, 123.6, 121.5, 120.5, 118.6, 56.4, 55.3, 54.4, 54.2, 53.9, 30.9, 30.4 (m, *C*D$_3$), 21.3, 19.5, 18.0. Anal. Calcd for $C_{29}H_{33}D_6N_3Hf$: C, 56.71; H, 7.38; N, 6.84. Found: C, 56.85; H, 7.32; N, 6.87.

Compound **6c** also was prepared using $^{13}CH_3MgI$ in ether: ^{13}C NMR (125 MHz, C_6D_5Br) δ 58.93 ppm (J_{CH} = 111 Hz, J_{CC} = 2.9 Hz), 57.17 ppm (J_{CH} = 112 Hz, J_{CC} = 2.9 Hz).

Observation of Cationic Initiators, 3d, 4d, 5d, 5e, 6d, and 6e by ^{1}H NMR. Equimolar amounts of the dimethyl precatalyst (**3c**, **4c**, **5c**, or **6c**) and trityl tetrakis(pentafluorophenyl)borate were measured out and each dissolved in ~0.4 mL of bromobenzene-d_5 (in the case of dimers **5e** and **6e**, half an equivalent of $\{Ph_3C\}\{B(C_6F_5)_4\}$ was used). The two solutions were chilled to –25 ºC in the glovebox freezer. The solutions were then mixed producing an orange-yellow solution that was immediately transferred to a J-Young tube and frozen in liquid nitrogen. The tube was transported to the NMR spectrometer, warmed until the solvent melted, and placed in the precooled spectrometer. The spectrum was then recorded giving the following spectra:

{[MesNNPhNMes]ZrMe}{B(C$_6$F$_5$)$_4$}, 3d. (500 MHz, 263 K) δ 7.26 (m, 2, aryl), 7.20 (t, 1, aryl), 7.16-6.99 (*Ph*$_3$CMe, and ligand), 6.95 (t, 1, aryl), 6.90 (s, 1, *m-Mes*), 6.88 (s, 1, *m*-Mes), 6.80 (d, 1, aryl), 6.66 (t, 1, aryl), 6.62 (br s, 1, *m*-Mes), 6.52 (br s, 1, *m*-Mes), 5.76 (d, 1, aryl), 4.04 (dd, 1, C*H*$_2$), 3.78 (m, 1, C*H*$_2$), 3.69 (m, 1, C*H*$_2$), 3.62 (m, 1, C*H*$_2$), 2.23 (s, 3, Mes-*Me*), 2.10 (s, 3, Mes-*Me*), 2.04 (s, 3, Ph$_3$C*Me*), 2.01 (s, 3, Mes-*Me*), 2.00 (s, 3, Mes-*Me*), 1.92 (br s, 3, Mes-*Me*), 1.40 (br s, 3, Mes-*Me*), -0.05 (s, 3, Zr*Me*).

{[MesNNPhNMes]HfMe}{B(C$_6$F$_5$)$_4$}, 4d. (500 MHz, 273 K) δ 7.27 (m, 4, aryl), 7.21 (t, 1, aryl), 7.17-7.02 (*Ph*$_3$CMe and ligand), 7.01 (br s, 1, *m*-Mes), 6.97 (t, 1, aryl), 6.90 (br s, 1, *m*-Mes), 6.65 (m, 3, aryl), 5.81 (d, 1, aryl), 4.03 (m, 2, C*H*$_2$), 3.91 (m, 1, C*H*$_2$), 3.74 (m, 1, C*H*$_2$), 2.25 (s, 3, Mes-*Me*), 2.12 (s, 3, Mes-*Me*), 2.08 (m, 6, Ph$_3$C*Me* and Mes-*Me*), 2.02 (br s, 3, Mes-*Me*), 1.57 (br s, 3, Mes-*Me*), -0.14 (s, 3, Hf*Me*).

{[*t*-BuNNPhNMes]ZrMe}{B(C$_6$F$_5$)$_4$}, 5d. (500 MHz, 263 K) δ 7.28 (m, 2, aryl), 7.24 (d, 1, aryl), 7.22-7.03, (*Ph*$_3$CMe and ligand), 6.95 (d, 1, aryl), 6.66 (d, 1, aryl), 3.86 (dd, 1, C*H*$_2$), 3.62 (td, 1, C*H*$_2$), 3.50 (td, 1, C*H*$_2$), 2.76 (dd, 1, C*H*$_2$), 2.2 (v br s, 3, Mes-*Me*), 2.08 (s, 3, Mes-*Me*), 2.02 (s, 3, Ph$_3$C*Me*), 1.3 (v br s, 3, Mes-*Me*), 0.90 (s, 3, *t*-Bu-d_6), 0.60 (s, 3, Zr*Me*).

{([*t*-BuNNPhNMes]Zr)$_2$μ-Me$_3$}{B(C$_6$F$_5$)$_4$}, 5e. (500 MHz, 273 K) δ 7.27 (m, 4, aryl), 7.16-6.90 (*Ph*$_3$CMe and ligand), 6.89 (s, 2, *m*-Mes), 6.80 (d, 2, aryl), 6.67 (d, 4, *o*-Ph), 6.53 (s, 2, *m*-Mes), 3.83 (m, 2, C*H*$_2$), 3.35 (dd, 2, C*H*$_2$), 3.24 (td, 2, C*H*$_2$), 2.76 (dd, 2, C*H*$_2$), 2.50 (s, 6, Mes-

Me), 2.09 (s, 6, Mes-*Me*), 2.02 (s, 3, Ph_3CMe), 1.11 (s, 6, Mes-*Me*), 0.90 (s, 6, *t*-Bu-d_6), 0.27 (s, 6, ZrMe_2), 0.01 (s, 3, bridging-Zr*Me*).

{[*t*-BuNNPhNMes]Hf)Me}{B(C_6F_5)$_4$}, 6d. (500 MHz, 273 K) δ 7.36 (t, 1, aryl), 7.28 (m, 2, aryl), 7.16-6.94, (Ph_3CMe and ligand), 6.75 (d, 2, aryl), 6.59 (br s, 2, *m*-Mes), 3.99 (td, 1, CH_2), 3.68 (dd, 1, CH_2), 3.15 (td, 1, CH_2), 2.96 (dd, 1, CH_2), 2.18 (v br s, 3, *o*-Me), 2.08 (s, 3, *p*-Me), 2.02 (s, 3, Ph_3CMe), 1.16 (v br s, 3, *o*-Me), 0.93 (s, 3, *t*-Bu-d_6), 0.68 (s, 3, Hf*Me*).

A ^{13}C-labeled version of **6d** also was prepared from ^{13}C-labeled **6e**: ^{13}C NMR (125 MHz, C_6D_5Br) δ 66.27 (J_{CH} =113.4 Hz).

{([*t*-BuNNPhNMes]Hf)$_2$μ-Me$_3$}{B(C_6F_5)$_4$}, 6e. (500 MHz, 273 K) δ 7.30 (m, 4, aryl), 7.16-6.92 (Ph_3CMe and ligand), 6.91 (s, 2, *m*-Mes), 6.84 (d, 2, aryl), 6.70 (d, 4, *o*-Ph), 6.52 (s, 2, *m*-Mes), 3.89 (td, 2, CH_2), 3.38 (dd, 2, CH_2), 3.14 (td, 2, CH_2), 2.85 (dd, 2, CH_2), 2.47 (s, 6, Mes-*Me*), 2.09 (s, 6, Mes-*Me*), 2.02 (s, 3, Ph_3CMe), 1.13 (s, 6, Mes-*Me*), 0.86 (s, 6, *t*-Bu-d_6), 0.13 (s, 3, bridging Hf*Me*), 0.06 (s, 6, HfMe_2).

A ^{13}C-labeled version of **6e** also was prepared from ^{13}C-labeled **6c**: ^{13}C NMR (125 MHz, C_6D_5Br) δ 64.78 (J_{CH} =113.6 Hz, HfMe_2), 50.20 ppm (J_{CH} = 132.6 Hz, bridging Hf*Me*).

General Procedure for Polymerization Experiments. In a general experiment, equimolar amounts of the dimethyl precatalyst (**3c**, **4c**, or **5c**) and trityl tetrakis(pentafluorophenyl)borate were measured out and dissolved in an equal amount of bromobenzene. The solutions were cooled to -25ºC, as was the 1-hexene. The cold bromobenzene solutions were mixed thoroughly and transferred to a sealable reaction vessel equipped with a stir bar. The 1-hexene was immediately added in one bulk portion and the contents allowed to react at either –25 ºC, or warmed to 0 ºC. Reaction times were 20 minutes for **3d** and **4d**, and 6 hours for **5d**. The reaction was quenched with MeOH/HCl (95/5 v/v). The volatiles were removed in vacuo and the polymer was extracted into pentane. The pentane solution was passed through a plug of silica gel and pentane was removed in vacuo at 60 ºC over a period of several hours leaving a colorless gel which was identified as atactic poly[1-hexene] by ^{13}C NMR.

1-(2-((6-methylpyridin-2-yl)methylamino)naphthalen-1-yl)-*N*-((6-methylpyridin-2-yl)methyl)naphthalen-2-amine, **H_2[MepyN]**. A two-neck round bottom flask was charged with 5.71 g (20.1 mmol) g of 2,2'-diamino-1,1'-binaphthalene, a magnetic stirbar and 50 mL of absolute ethanol. The flask was fitted with a reflux condensor and a pressure-equalizing addition funnel. To the addition funnel was added a solution of 5.61 g (46.3 mmol) of 6-methyl-2-pyridinecarboxaldehyde in 20 mL of absolute ethanol. The solution of the pyridine was added dropwise to the suspension of the diamine and then heated at reflux under nitrogen for 90 min. during which time the reaction mixture became a golden yellow solution. The solution was allowed to cool and the volatiles were removed in vacuo. An additional 150 mL of absolute ethanol was added, as was 2.28 g (60.3 mmol) of $NaBH_4$. The reaction mixture was heated again under nitrogen at reflux for 20 h. The mixture was cooled to room temperature and quenched by pouring onto 5 g of NH_4Cl. The ethanol was removed in vacuo and the resulting residue dissolved in methylene chloride, washed three times with 100 mL of water, dried over $MgSO_4$ and filtered through celite. The methylene chloride was removed in vacuo and the resulting amber residue dissolved in a minimal amount of hot toluene. Pentane was added until the solution became slightly turbid and was then set aside at -40ºC for 24 h during which time H_2[MepyN] precipitated as 8.13 g (82%) of off-white crystals. The compound was further purified by repeated crystallization from toluene/pentane: ^{1}H NMR (500 MHz, C_6D_6) δ 7.72 (t, 4, aryl), 7.40 (d, 2, aryl), 7.19 (d, 2, aryl), 7.10 (m, 4, aryl), 6.93 (t, 2, aryl), 6.82 (d, 2, aryl), 6.49 (d, 2, aryl), 4.87 (t, 2, N*H*), 4.15 (m, 4, CH_2), 2.27 (s, 6, py*Me*); ^{13}C NMR (125 MHz, C_6D_6) δ 159.5, 158.1, 144.9, 136.7, 135.2, 130.4, 129.0, 128.8, 127.5, 124.9, 122.7, 121.3, 118.1, 114.9, 113.1, 49.4 (*C*H_2), 24.7 (py*Me*). HRMS Calcd $[M+H]^+$: 495.2543. Found $[M+H]^+$: 495.2551. Anal. Calcd for $C_{34}H_{30}N_4$: C, 82.56; H, 6.11; N, 11.33. Found: C, 82.65; H, 6.04; N, 11.37.

[MepyN]Zr(NMe$_2$)$_2$, 7a. To 1.012 g (2.05 mmol) of H_2[MepyN] dissolved in 30 mL of toluene, was added a solution of 0.547 g (2.04 mmol) of $Zr(NMe_2)_4$ in 10 mL toluene. The solution was heated to 50ºC and stirred for 20 hours during which time it became golden yellow. The toluene

was concentrated in vacuo to ~10 mL and several volumes of pentane were added. The solution was set aside at –25ºC for several hours during which time yellow microcrystals precipitated. The crystals were isolated by filtration, washed with pentane and dried in vacuo; yield 1.343 g (98%): ^{1}H NMR (500 MHz, C_6D_6) δ 7.80 (d, 2, aryl), 7.70 (d, 2, aryl), 7.57 (d, 2, aryl), 7.04 (t, 2, aryl), 6.85 (t, 2, aryl), 6.68 (t, 2, aryl), 6.48 (d, 2, aryl), 6.36 (d, 2, aryl), 5.35 (d, *J* = 18.0 Hz, 2, CH_2), 5.05 (d, *J* = 18.0 Hz, 2, CH_2), 2.51 (s, 12, NMe_2), 2.26 (s, 6, py*Me*). Anal. Calcd for $C_{38}H_{40}N_6Zr$: C, 67.92; H, 6.00; N, 12.51. Found: C, 67.84; H, 6.09; N, 12.38.

[MepyN]Zr(NMe$_2$)Cl, 7a′. This compound was prepared in analogous fashion to [MepyN]Zr(NMe$_2$)$_2$ starting with ligand that contained approximately one-third of an equivalent of chloroform (65% yield, on ~1 gram scale). Crystals suitable for X-ray diffraction were grown by vapor diffusion of pentane into a saturated benzene solution: ^{1}H NMR (500 MHz, C_6D_6) δ 7.99 (d, 1, aryl), 7.90 (d, 1, aryl), 7.78 (d, 1, aryl), 7.55 (d, 1, aryl), 7.52 (d, 1, aryl), 7.31 (d, 1, aryl), 7.15 (m, 2, aryl), 7.05 (t, 1, aryl), 7.00 (t, 1, aryl), 6.90 (t, 1, aryl), 6.81 (m, 2, aryl), 6.51 (t, 1, aryl), 6.42 (m, 2, aryl), 6.28 (d, 1, aryl), 5.54 (d, 1, aryl), 5.36 (d, *J* = 20.0 Hz, 1, CH_2), 4.98 (d, *J* = 19.0 Hz, 1, CH_2), 4.49 (d, *J* = 20.0 Hz, 1, CH_2), 3.88 (d, *J* = 19.0 Hz, 1, CH_2), 2.95 (s, 3, py*Me*), 2.59 (br s, 6, NMe_2), 2.35 (s, 3, py*Me*). Anal. Calcd for $C_{36}H_{34}N_5ClZr$: C, 65.18; H, 5.17; N, 10.56; Cl, 5.34. Found: C, 65.26; H, 5.24; N, 10.44; Cl, 5.25.

[MepyN]ZrCl$_2$, 7b. A solution of 0.900 g (1.36 mmol) of [MepyN]Zr(NMe$_2$)$_2$ in 50 mL of toluene was treated with 0.38 mL (3.0 mmol) of TMSCl. The solution was heated to 80ºC and stirred for 24 hours during which time an off-white powder precipitated from solution. The material was collected by filtration, washed with pentane and dried *in vacuo*; yield 0.759 g (85%): ^{1}H NMR (500 MHz, CD_2Cl_2) δ 7.83 (m, 4, aryl), 7.68 (t, 2, aryl), 7.51 (d, 2, aryl), 7.34 (t, 2, aryl), 7.21 (m, 6, aryl), 7.04 (d, 2, aryl), 5.14 (d, *J* = 20.5 Hz, 2, CH_2), 4.73 (d, *J* = 20.5 Hz, 2, CH_2), 2.99 (s, 6, py*Me*).

[MepyN]Zr(OSO_2CF_3)$_2$, 7t. A solution of 1.052 g (1.57 mmol) of [MepyN]Zr(NMe_2)$_2$ in 50 mL of benzene was treated with 0.70 mL (3.6 mmol) of TMSOTf. The yellow solution was stirred at room temperature for 60 min. during which time the color became lighter. The solution was layered with several volumes of pentane and allowed to stand for 16 hrs. over which time the compound precipitated as 0.968 (68%) of white microcrystals. NMR spectra showed the presence of one equivalent of benzene, which was confirmed by analysis: ^{1}H NMR (500 MHz, C_6D_6) δ 8.15 (d, 2, aryl), 7.78 (d, 2, aryl), 7.63 (d, 2, aryl), 7.55 (d, 2, aryl), 7.15 (t, 2, aryl), 7.04 (t, 2, aryl), 6.52 (t, 2, aryl), 6.24 (d, 2, aryl), 5.75 (d, 2, aryl), 5.10 (d, *J* = 20.5 Hz, 2, C*H*$_2$), 4.23 (d, *J* = 20.5 Hz, 2, C*H*$_2$), 2.85 (s, 6, py*Me*); ^{19}F NMR (470 MHz, C_6D_6) δ -77.4 (OSO_2CF_3). Anal. Calcd for $C_{42}H_{34}N_4F_6O_6S_2Zr$: C, 52.54; H, 3.57; N, 5.84. Found: C, 52.33; H, 3.70; N, 5.62.

[MepyN]Zr(CH_2CHMe_2)$_2$, 7d. A flask was charged with 0.148 g (0.226 mmol) of [MepyN]$ZrCl_2$ and 15 mL of CH_2Cl_2 was added. The suspension was cooled to –25 ºC. Once cool, 0.24 mL of (0.58 mmol) *i*-BuMgBr (2.4 M in Et_2O) was added dropwise over the stirring suspension. The reaction mixture was allowed to stir for 10 minutes at room temperature during which time it became yellow-orange. 1,4-Dioxane (0.15 mL) was added at which point a white precipitate formed. The mixture was filtered through Celite and the volatiles removed in vacuo. The resulting orange residue was dissolved in 2 mL of toluene and several volumes of pentane were added. The solution was set aside at –25 ºC for several hours, during which time an orange microcrystalline material precipitated. The material was collected by filtration, washed with pentane and dried in vacuo to give 0.0696 g (44%, not optimized): ^{1}H NMR (500 MHz, C_6D_6) δ 7.83 (d, 2, aryl), 7.78 (d, 2, aryl), 7.61 (d, 2, aryl), 7.58 (d, 2, aryl), 7.17 (t, 2, aryl), 7.06 (t, 2, aryl), 6.85 (t, 2, aryl), 6.49 (d, 2, aryl), 6.39 (d, 2, aryl), 5.04 (d, *J* = 20.5 Hz, 2, C*H*$_2$,), 4.83 (d, *J* = 20.5 Hz, 2, C*H*$_2$), 2.81 (s, 6, py*Me*), 1.24 (m, 2, C*H*$_2$CHMe$_2$), 1.21 (m, 2, CH_2C*H*Me$_2$), 0.78 (d, 6, CH_2CH*Me*$_2$), 0.55 (dd, 2, C*H*$_2$CHMe$_2$), 0.41 (d, CH_2CH*Me*$_2$). Anal. Calcd for $C_{42}H_{46}N_4Zr$: C, 72.26; H, 6.64; N, 8.03. Found: C, 72.14; H, 6.57; N, 7.94.

[MepyN]Zr($CH_2C_6H_5$)$_2$, 7e. A reaction vessel was charged with 0.616 g (1.24 mmol) of H_2[MepyN] and 0.544 g (1.19 mmol) of $Zr(CH_2Ph)_4$. Benzene (35 mL) was added and the resulting orange solution was allowed to stand at room temperature for 20 hours. Pentane was added until the solution became turbid. The product precipitated from solution as over several hours at room temperature yielding 0.675 g (74%) of orange microcrystals. Crystals suitable for X-ray diffraction were grown by vapor diffusion of pentane into a saturated methylene chloride solution: ^{1}H NMR (500 MHz, CD_2Cl_2) δ 7.83 (m, 4, aryl), 7.54 (t, 2, aryl), 7.41 (d, 2, aryl), 7.28 (t, 2, aryl), 7.13 (m, 4, aryl), 7.06 (d, 2, aryl), 6.78 (d, 2, aryl), 6.13 (m, 6, *m*- and *p*-Bn), 5.63 (d, 4, *o*-Bn), 4.75 (d, *J* = 20.0 Hz, 2, C*H*$_2$), 4.12 (d, *J* = 20.0 Hz, 2, C*H*$_2$), 2.94 (s, 6, py*Me*), 2.26 (d, *J* = 10.0 Hz, 2, C*H*$_2$Ph), 1.89 (d, *J* = 10.0 Hz, 2, C*H*$_2$Ph); ^{13}C NMR (125 MHz, CD_2Cl_2) δ 163.7, 156.9, 153.7, 148.9, 137.9, 134.5, 130.6, 128.5, 128.2, 127.8, 127.3, 126.8, 126.1, 125.7, 124.9, 123.6, 123.3, 119.3, 119.1, 66.6, 61.7, 26.0. Anal. Calcd for $C_{48}H_{42}N_4Zr$: C, 75.25; H, 5.53; N, 7.31. Found: C, 75.18; H, 5.46; N, 7.22.

[MepyN]Hf(NMe_2)$_2$, 8a. This compound was prepared in similar fashion as **7a**, starting from 1.001 g (2.02 mmol) of H_2[MepyN] and 0.720 g (2.03 mmol) of $Hf(NMe_2)_4$. The reaction required heating at 60 ºC for 48 hours to go to completion; yield 1.178 g (77%): ^{1}H NMR (500 MHz, C_7D_8) δ 7.77 (d, 2, aryl), 7.66 (d, 2, aryl), 7.59 (d, 2, aryl), 7.03 (t, 2, aryl), 6.99 (d, 2, aryl), 6.81 (t, 2, aryl), 6.62 (t, 2, aryl), 6.34 (m, 4, aryl), 5.32 (d, *J* = 17.5 Hz, 2, C*H*$_2$), 5.01 (d, *J* = 17.5 Hz, 2, C*H*$_2$), 2.60 (s, 12, N*Me*$_2$), 2.28 (s, 6, py*Me*); ^{13}C NMR (125 MHz, CD_2Cl_2) δ 163.9, 158.2, 152.6, 137.3, 135.7, 129.7, 128.6, 127.8, 127.4, 125.6, 125.5, 122.7, 122.6, 122.0, 119.1, 61.4 (*C*H$_2$), 41.3 (N*Me*$_2$), 23.8 (py*Me*). Anal. Calcd for $C_{38}H_{40}N_6Hf$: C, 60.11; H, 5.31; N, 11.07. Found: C, 60.15; H, 5.40; N, 10.97.

[MepyN]Hf(OSO_2CF_3)$_2$, 8t. This compound was prepared in strictly analogous fashion as **7c** starting from 1.128 g (1.49 mmol) of [MepyN]Hf(NMe_2)$_2$ and 0.60 mL (3.1 mmol) of TMSOTf. One equivalent of benzene was present as judged by NMR/analysis. Crystals suitable for X-ray

diffraction were grown by vapor diffusion of pentane into a concentrated bromobenzene solution; yield 1.148 g (74%): ^{1}H NMR (C_6D_6) δ 7.90 (br s, 2, aryl), 7.79 (d, 2, aryl), 7.66 (d, 2, aryl), 7.49 (d, 2, aryl), 7.16 (t, 2, aryl), 7.04 (t, 2, aryl), 6.59 (t, 2, aryl), 6.29 (d, 2, aryl), 5.84 (br d, 2, aryl), 5.32 (d, *J* = 19.5 Hz, 2, C*H*$_2$,), 4.43 (br d, 2, C*H*$_2$), 2.77 (br s, 6, py*Me*); ^{13}C NMR (500 MHz, CD_2Cl_2): δ 164.5, 140.6, 134.0, 131.9, 129.9, 128.8, 127.5, 126.4, 125.5, 125.1, 124.7, 120.2, 199.7 (q, J_{CF} = 318 Hz, OSO_2CF_3,), 62.7 (br, *C*H$_2$), 23.6 (br, py*Me*); ^{19}F NMR (490 MHz, CD_2Cl_2) δ 78.1 (s, OSO_2CF_3). Three of the aromatic carbon peaks could not be unambiguously assigned; however, three very broad peaks appear in the spectrum between 120 and 160 ppm. Anal. Calcd for $C_{42}H_{34}N_4F_6O_6S_2Hf$: C, 48.16; H, 3.27; N, 5.35. Found: C, 48.59; H, 3.36; N, 5.10.

[MepyN]Hf(CH$_2$CHMe$_2$)$_2$, 8d. A flask was charged with 0.923 g (0.881 mmol) of **8c** and 30 mL of THF. The solution was chilled to –25 ºC at which point 0.82 mL (1.8 mmol) of Me_2CHCH_2MgBr was added dropwise. A precipitate formed immediately upon addition of the Grignard reagent. The mixture was allowed to stir at room temperature for 60 min. The THF was removed in vacuo and the residue extracted into toluene and filtered through Celite. The toluene solution was concentrated to ~10 mL, layered with several volumes of pentane and set aside at – 25ºC for several days during which time pale yellow crystals formed. The compound could be further purified by multiple recrystallizations from toluene/pentane. Crystals suitable for X-ray diffraction were grown by vapor diffusion of pentane into a concentrated benzene solution; yield 0.443 g (64%): ^{1}H NMR (500 MHz, C_6D_6) δ 7.85 (d, 2, aryl), 7.79 (d, 2, aryl), 7.63 (d, 2, aryl), 7.57 (d, 2, aryl), 7.18 (t, 2, aryl), 7.07 (d, 2, aryl), 6.85 (t, 2, aryl), 6.47 (d, 2, aryl), 6.38 (d, 2, aryl), 5.16 (d, *J* = 20.5 Hz, 2, C*H*$_2$), 4.86 (d, *J* = 20.5 Hz, 2, C*H*$_2$), 2.79 (s, 6, py*Me*), 1.25 (m, 2, CH_2CHMe_2), 1.01 (dd, 2, C*H*$_2$CHMe$_2$), 0.84 (d, 6, CH_2CHMe_2), 0.39 (d, 6, CH_2CHMe_2), 0.37 (dd, 2, C*H*$_2$CHMe$_2$); ^{13}C NMR (125 MHz, CD_2Cl_2) δ 164.1, 158.0, 153.7, 138.0, 134.3, 130.4, 128.1, 127.9, 127.8, 127.1, 126.9, 125.3, 123.6, 123.3, 119.1, 78.6, 66.8,

31.7, 30.5, 26.4, 25.9. Anal. Calcd for $C_{42}H_{46}N_4Hf$: C, 64.23; H, 5.90; N, 7.13. Found: C, 64.18; H, 5.86; N, 7.05.

{[MepyN]Zr($CH_2CH(CH_3)_2$)}{$HB(C_6F_5)_3$}. This species was observed spectroscopically by mixing equimolar amounts of **7d** and $B(C_6F_5)_3$ in benzene-d_6 at room temperature. ^{1}H NMR (293 K) δ 8.05 (d, 1, aryl), 7.75 (d, 1, aryl), 7.55 (d, 1, aryl), 7.46 (d, 1, aryl), 7.26 (d, 1, aryl), 7.22 (d, 1, aryl), 7.18 (m, 2, aryl), 7.01 (m, 3, aryl), 6.89 (m, 2, aryl), 6.84 (d, 1, aryl), 6.56 (m, 4, aryl), 5.17 (d, 1, C*H*$_2$), 4.97 (d, 1, C*H*$_2$), 4.51 (d, 1, C*H*$_2$), 4.24 (d, 1, C*H*$_2$), 1.56 (br s, 3, py*Me*), 1.40 (s, 3, py*Me*), 0.37 (m, 1, CH_2C*H*Me_2), 0.129 (d, 3, CH_2CH*Me*$_2$), -0.12 (dd, 1, C*H*$_2$$CHMe_2$), -0.45 (br d, 3, CH_2CH*Me*$_2$), -1.01 (br m, 1, C*H*$_2$$CHMe_2$); ^{19}F NMR (490 MHz) δ -132.7 (d, *o*-Ar*F*), -164.0 (t, *p*-Ar*F*), -166.8 (t, *m*-Ar*F*).

{[MepyN]Hf($CH_2CH(CH_3)_2$)}{A}. This species was observed spectroscopically by mixing equimolar amounts of **8d** and $B(C_6F_5)_3$, $\{Ph_3C\}\{B(C_6F_5)_4\}$, or $\{HNMe_2Ph\}\{B(C_6F_5)_4\}$ in bromobenzene-d_5 at room temperature. The ^{1}H NMR (500 MHz, 293 K) shifts for the cation formed by activation with $B(C_6F_5)_3$ are as follows: δ 8.13 (d, 1, aryl), 7.89 (d, 1, aryl), 7.67 (d, 1, aryl), 7.56 (d, 1, aryl), 7.47 (t, 1, aryl), 7.35 (m, 2, aryl), 7.15 (m, 5, aryl), 7.03 (m, 3, aryl), 6.81 (d, 1, aryl), 6.75 (d, 1, aryl), 6.38 (d, 1, aryl), 5.61 (d, 1, C*H*$_2$), 5.20 (d, 1, C*H*$_2$), 4.93 (d, 1, C*H*$_2$), 4.58 (d, 1, C*H*$_2$), 1.71 (s, 3, py*Me*), 1.57 (s, 3, py*Me*), 0.39 (m, 1, CH_2C*H*CMe_2), 0.10 (d, 3, CH_2CH*Me*$_2$), -0.21 (dd, 1, C*H*$_2$$CHMe_2$), -0.53 (d, 3, CH_2CH*Me*$_2$), -1.23 (dd, 1 C*H*$_2$$CHMe_2$).

Compound 7e′. This species has been observed spectroscopically by mixing equimolar amounts of **7e** and $\{HNMe_2Ph\}\{B(C_6F_5)_4\}$ in methylene chloride-d_2 at –25 ºC followed by warming to room temperature: ^{1}H NMR (500 MHz, 293 K) δ 8.30 (d, 1, aryl), 8.11 (t, 1, aryl), 8.07 (d, 1, aryl), 7.72 (d, 1, aryl), 7.68 (d, 1, aryl), 7.60 (m, 3, aryl), 7.56 (t, 1, aryl), 7.51 (t, 1, aryl), 7.42 (d, 1, aryl), 7.34 (d, 1, aryl), 7.28 (m, 3, aryl), 7.23 (m, 2, aryl), 7.18 (d, 1, aryl), 7.05 (d, 1, aryl), 6.73 (m, 4, aryl), 6.23 (t, 1, *p*-Ph), 5.93 (t, 2, *m*-Ph), 5.63 (d, $^3J_{HH}$ = 7.5 Hz, N*H*), 5.03

(d, 1, CH_2), 4.74 (d, 2, *o*-Ph), 4.21 (d, 1, CH_2), 4.14 (d, 1, CH_2), 3.44 (s, 3, py*Me*), 3.11 (d, 1, CH_2Ph), 2.98 (s, 3, py*Me*), 2.79 (dd, 1, CH_2), 2.71 (d, 1, CH_2Ph), 2.51 (d, 1, CH_2Ph), 1.41 (d, 1, CH_2Ph); ^{19}F NMR (490 MHz) δ -131.4 (d, 2, *o*-Ar*F*), -161.9 (t, 2, *p*-Ar*F*), -165.75 (t, 1, *m*-Ar*F*).

{[MepyN]Zr($CH_2C_6H_5$)}{A}. This species was observed spectroscopically by mixing equimolar amounts of [MepyN]Zr($CH_2C_6H_5$)$_2$ and {Ph_3C}{$B(C_6F_5)_4$} or $B(C_6F_5)_3$ in methylene chloride-d_2 at –25 ºC followed by warming to room temperature. The ^{1}H NMR (500 MHz, 203 K) shifts for the complex formed by activation with $B(C_6F_5)_3$ are as follows: δ 8.44 (d, 1, aryl), 7.95 (m, 3, aryl), 7.70 (m, 6, aryl), 7.41 (d, 1, aryl), 7.24 (m, 6, aryl), 7.12 (t, 1, aryl), 6.89 (t, 2, *m*-Ph of anion), 6.82 (t, 1, *p*-Ph of anion), 6.66 (d, 2, *o*-Ph of anion), 6.32 (m, 3, *m*/*p*-CH_2*Ph*), 5.75 (d, 1, CH_2), 5.66 (d, 1, CH_2), 5.46 (d, 2, *o*-CH_2*Ph*), 5.33 (d, 1, CH_2), 5.03 (d, 1, CH_2), 2.73 (s, CH_2 of anion), 1.81 (s, 3, py*Me*), 1.73 (s, 3, py*Me*), 1.44 (d, *J* = 12.5 Hz, 1, CH_2Ph), -0.56 (d, *J* = 12.5 Hz, 1, CH_2Ph).

***N*,*N*′-bis-(2′,2′′,4′,4′′,6′,6′′-hexaisopropyl-3,5-terphenyl)-1,1′-binaphthyl-2,2′-diamine, H_2[HIPTN$_2$]**. A 500 mL Schlenk flask was charged with 3.97 g (14.0 mmol) of 2,2′-diamino-1,1′-binaphthalene, 17.15 g (30.5 mmol) of 3,5-*bis*-(2,4,6-triisopropylphenyl)bromobenzene, 4.30 g (44.7 mmol) of NaO-*t*-Bu, and 300 mL of toluene. To the mixture was added a solution of 0.130 g (1 mol%) of $Pd_2(dba)_3$ and 0.138 g (2 mol%) of XPHOS dissolved in 5 mL of toluene. The resulting mixture was stirred at 90 ºC for 5 h during which time the mixture became brown and a large amount of precipitate had formed. The mixture was filtered through Celite and the volatiles were removed from the filtrate in vacuo. The brown residue was dissolved in a minimal amount of pentane and left to stand overnight. The compound precipitated as a white crystalline solid over a period of 18 h. The remaining mother liquor was purified by flash chromatography on silica gel eluting with 20% toluene in pentane. The pooled column fractions were evaporated to dryness *in vacuo* leaving a white solid; total yield 13.04 g (75%): ^{1}H NMR (500 MHz, CD_2Cl_2) δ 7.87 (d, 2, binaph), 7.82 (d, 2, binaph), 7.77 (d, 2, binaph), 7.26 (t, 2, binaph), 7.15 (t,

2, binaph), 7.09 (d, 2, binaph), 7.00 (m, 8, *m*-HIPT), 6.80 (s, 4, *o*-HIPT), 6.56 (s, 2, *p*-HIPT), 5.73 (s, 2, N*H*), 2.89 (sep, 4, *p*-C*H*Me$_2$), 2.73 (m, 8, *o*-C*H*Me$_2$), 1.26 (d, 24, *p*-CH*Me*$_2$), 1.09 (d, 12, *o*-CH*Me*$_2$), 1.03 (m, 36, *o*-CH*Me*$_2$); ^{13}C NMR (125 MHz, CD_2Cl_2) δ 148.6, 147.1, 142.5, 142.3, 141.5, 137.3, 134.4, 130.2, 123.0, 128.8, 127.5, 126.3, 124.6, 124.0, 121.0, 120.4, 118.5, 116.9, 34.9, 31.0, 24.8, 24.5, 24.5, 24.4; HRMS Calcd $[M+H]^+$ 1245.8898. Found $[M+H]^+$ 1245.8889. Anal. Calcd for $C_{92}H_{112}N_2$: C, 88.69; H, 9.06; N, 2.25. Found: C, 88.62; H, 8.94; N, 2.17.

[HIPTN$_2$]Ti(NMe$_2$)$_2$, 9a. A sealable Schlenk vessel was charged with 1.145 g (0.919 mmol) of H$_2$[HIPTN$_2$], 0.21 g (0.94 mmol) of Ti(NMe$_2$)$_4$, and 30 mL of toluene. The sealed vessel was heated at 110 ºC for 6 days during which time the solution became bright red-orange. The toluene was removed in vacuo and the residue was crystallized from a minimal amount of pentane at –25ºC to give 0.733 g (58%) of an orange powder: ^{1}H NMR (500 MHz, C_6D_6) δ 7.73 (m, 4, binaph), 7.47 (d, 2, binaph), 7.20 (s, 4, *m*-HIPT), 7.19 (s, 4, *m*-HIPT), 7.03 (d, 2, binaph), 7.02 (s, 4, *o*-HIPT), 6.98 (t, 2, binaph), 6.56 (s, 2, *p*-HIPT), 6.54 (t, 2, binaph), 3.15 (sep, 4, *o*-C*H*Me$_2$), 3.07 (sep, 4, *o*-C*H*Me$_2$), 2.87 (sep, 4, *p*-C*H*Me$_2$), 2.85 (s, 6, N*Me*$_2$), 1.30 (m, 48, CH*Me*$_2$), 1.21 (d, 12, CH*Me*$_2$), 1.08 (d, 12, CH*Me*$_2$). Anal. Calcd for $C_{96}H_{122}N_4Ti$: C, 83.56; H, 8.91; N, 4.06. Found: C, 83.37; H, 9.06; N, 3.94.

[HIPTN$_2$]Zr(NMe$_2$)$_2$, 10a. A round bottom flask was charged with 6.269 g (5.03 mmol) of H$_2$[HIPTN$_2$], 1.278 g (4.78 mmol) of Zr(NMe$_2$)$_4$, and 60 mL of pentane. The reaction mixture was allowed to stir for 2 days at room temperature during which time it became bright yellow. The solution was set aside at –25 ºC from which the compound crystallized as 5.538 g (82%) of yellow microcrystals: ^{1}H NMR (500 MHz, C_6D_6) δ 7.92 (d, 2, binaph), 7.75 (d, 2, binaph), 7.41 (d, 2, binaph), 7.22 (s, 4, *m*-HIPT), 7.21 (s, 4, *m*-HIPT), 7.16 (s, 4, *o*-HIPT), 7.08 (d, 2, binaph), 6.94 (t, 2, binaph), 6.60 (t, 2, binaph), 6.57 (s, 2, *p*-HIPT), 3.15 (m, 8, *o*-C*H*Me$_2$), 2.65 (s, 12,

N*Me*$_2$), 2.87 (sep, 4, *p*-C*H*Me$_2$), 2.64 (s, 12, N*Me*$_2$), 1.27 (m, 60, CH*Me*$_2$), 1.18 (d, 12, *o*-CH*Me*$_2$). Anal. Calcd for $C_{96}H_{122}N_4Zr$: C, 78.16; H, 8.40; N, 1.82. Found: C, 77.96; H, 8.31; N, 1.75.

[HIPTN$_2$]ZrCl$_2$(Et$_2$O)$_2$, 10b. A sealable Schlenk vessel was charged with 5.532 g (3.89 mmol) of [HIPTN$_2$]Zr(NMe$_2$)$_2$, 1.0 mL (8.1 mmol) of Me$_3$SiCl, and 70 mL of benzene. The reaction mixture was stirred at 70 ºC for 18 h during which time it became deep red. The benzene was removed *in vacuo* and the residue crystallized from diethyl ether at –25ºC. Attempts at crystallizing the compound from pentane were unsuccessful. The ^{1}H NMR spectrum of the orange-yellow compound was very broad and difficult to interpret with a peak assignable to ~2 equivalents of coordinated diethyl ether (see Section 1.3.1 above); yield 3.640 g (67%): ^{1}H NMR (500 MHz, C$_6$D$_6$) *all peaks very broad* δ 7.62, 7.37, 7.27, 7.16, 6.98, 6.85, 6.60, 6.38, 3.70 (*Et*$_2$O), 2.97 (C*H*Me$_2$), 2.87 (C*H*Me$_2$), 1.36 – 1.10 (CH*Me*$_2$), 1.01, 0.72. Anal. Calcd for $C_{100}H_{130}N_2Cl_2O_2Zr$: C, 77.28; H, 8.43; N, 1.80; Cl, 4.56. Found: C, 76.94; H, 8.12; N, 1.90; Cl, 4.75.

[HIPTN$_2$]ZrMe$_2$, 10c. A flask was charged with 2.005 g (1.43 mmol) of [HIPTN$_2$]ZrCl$_2$(Et$_2$O)$_2$ and dissolved in 40 mL of diethyl ether. The solution was chilled to –25 ºC at which point 0.91 mL (2.9 mmol) of MeMgBr (3.15 M in Et$_2$O) was added dropwise. The reaction mixture was allowed to stir at room temperature for 60 min. during which time the solution changed from orange to yellow, and a precipitate formed. The ether was removed in vacuo and the residue extracted with pentane and filtered through Celite. The pentane solution was concentrated to ~5 mL and set aside at –25 ºC for several days. The complex crystallized as 1.514 g (78%) of a yellow solid in three crops: ^{1}H NMR (500 MHz, C$_6$D$_6$) δ 7.84 (d, 2, binaph), 7.59 (d, 2, binaph), 7.47 (s, 4, *o*-HIPT), 7.26 (d, 2, binaph), 7.24 (s, 4, *m*-HIPT), 7.22 (s, 4, *m*-HIPT), 6.96 (d, 2, binaph), 6.90 (t, 2, binaph), 6.71 (s, 2, *p*-HIPT), 6.57 (t, 2, binaph), 3.13 (m, 8, *o*-C*H*Me$_2$), 2.88 (sep, 4, *p*-C*H*Me$_2$), 1.28 (m, 60, CH*Me*$_2$), 1.17 (d, 12, *o*-CH*Me*$_2$), 0.60 (s, 6, C*H*$_3$); ^{13}C NMR (125 MHz, CD$_2$Cl$_2$) δ 150.6, 148.5, 147.2, 147.2, 142.6, 138.3, 137.5, 135.1, 133.1, 131.6, 128.6,

128.0, 126.7, 126.0, 125.3, 124.9, 123.9, 121.1, 121.0, 119.3, 53.2 (*Me*), 34.9 (*p*-*C*HMe$_2$), 31.1 (*o*-*C*HMe$_2$), 31.0 (*o*-*C*HMe$_2$), 24.9, 24.8, 24.7, 24.6, 24.5, 24.4. Anal. Calcd for $C_{94}H_{116}N_2Zr$: C, 82.70; H, 8.56; N, 2.05. Found: C, 82.59; H, 8.50; N, 1.96.

[HIPTN$_2$]Zr(^{13}CH$_3$)$_2$ was prepared similarly from $^{13}CH_3MgI$: ^{13}C NMR (125 MHz, C_6D_6) δ 54.50 (q, *C*H$_3$, J_{CH} = 115 Hz).

[HIPTN$_2$]Zr(CH$_2$CMe$_3$)$_2$, 10f. This complex was prepared in a fashion analogous to that used to prepare [HIPTN$_2$]ZrMe$_2$ starting from 0.584 g (0.376 mmol) of [HIPTN$_2$]ZrCl$_2$(Et$_2$O)$_2$ and 0.54 mL (0.86 mmol) of Me$_3$CCH$_2$MgCl (1.6 M in Et$_2$O). The pentane extract was evaporated to dryness to give the complex as 0.538 g (88%) of a yellow solid: ^{1}H NMR (500 MHz, C_6D_6) δ 7.86 (d, 2, binaph), 7.80 (m, 2, binaph), 7.44 (s, 4, *o*-HIPT), 7.36 (d, 2, binaph), 7.21 (s, 4, *m*-HIPT), 7.20 (s, 4, *m*-HIPT), 6.89 (m, 4, binaph), 6.64 (s, 2, *p*-HIPT), 6.39 (t, 2, binaph), 3.16 (sep, 4, *o*-C*H*Me$_2$), 3.08 (sep, 4, *o*-C*H*Me$_2$), 2.86 (sep, 4, *p*-C*H*Me$_2$), 1.60 (d, *J* = 12.5 Hz, 2, C*H*$_2$CMe$_3$), 1.34 (d, 12, CH*Me*$_2$), 1.27 (m, 36, CH*Me*$_2$), 1.22 (d, 12, CH*Me*$_2$), 1.17 (d, 12, CH*Me*$_2$), 1.11 (d, *J* = 12.5 Hz, 2, C*H*$_2$CMe$_3$), 0.91 (s, 18, CH$_2$C*Me*$_3$); ^{13}C (125 MHz, CD_2Cl_2) δ 151.7, 148.3, 147.2, 147.1, 142.1, 139.3, 137.7, 135.2, 132.4, 131.6, 128.4, 127.7, 127.2, 126.5, 125.8, 125.5, 124.7, 120.9, 120.9, 120.5, 99.9 (*C*H$_2$CMe$_3$), 37.2 (*C*Me$_3$), 34.9 (*p*-*C*HMe$_2$), 34.8 (C*Me*$_3$), 30.9 (*o*-*C*HMe$_2$), 30.8 (*o*-*C*HMe$_2$), 25.0, 24.9, 24.9, 24.6, 24.5, 24.4 (CH*Me*$_2$). Anal. Calcd for $C_{102}H_{132}N_2Zr$: C, 82.92; H, 9.01; N, 1.90. Found: C, 82.84; H, 8.96; N, 1.86.

[HIPTN$_2$]Zr(C$_6$F$_5$)$_2$, 10g. A flask was charged with 0.343 g (0.251 mmol) of **10c** and dissolved in 30 mL of pentane. The yellow solution was chilled to –25 ºC at which point 0.135 g (0.264 mmol) of B(C_6F_5)$_3$ was added as a solid. The solution immediately became bright orange upon addition of borane. The orange solution was stirred at room temperature for 60 minutes and then evaporated to dryness. The orange residue was crystallized from hot hexane to give 0.318 g (76%) of orange needles: ^{1}H NMR (500 MHz, C_6D_6) δ 7.65 (d, 2, binaph), 7.41 (d, 2, binaph), 7.26 (d, 2, binaph), 7.16 (s, 4, *o*-HIPT), 7.12 (s, 4, *m*-HIPT), 7.11 (s, 4, *m*-HIPT), 7.00 (t, 2,

binaph), 6.84 (d, 2, binaph), 6.69 (s, 2, *p*-HIPT), 6.51 (t, 2, binaph), 2.92 (m, 8, *o*-C*H*Me$_2$), 2.79 (sep, 4, *p*-C*H*Me$_2$), 1.22 (d, 24, *p*-CH*Me*$_2$), 1.15 (m, 36, *o*-CH*Me*$_2$), 1.07 (d, 12, *o*-CH*Me*$_2$); ^{13}C NMR (125 MHz, CD_2Cl_2) δ 148.8, 148.7, 148.5 (dd, J_{CF} = 228 Hz, *o*-C_6F_5), 147.1, 146.8, 146.1 (t, J_{CF} = 65 Hz, *ipso*-C_6F_5), 143.0, 142.7 (d, J_{CF} = 257 Hz, *p*-C_6F_5), 137.5, 136.9, 136.5 (d, , J_{CF} = 261 Hz, *m*-C_6F_5), 135.0, 133.2, 132.6, 128.5, 128.5, 127.8, 127.7, 127.2, 126.7, 125.5, 120.9, 120.8, 119.7, 34.9 (*p*-*C*HMe$_2$), 31.0 (*o*-*C*HMe$_2$), 30.9 (*o*-*C*HMe$_2$), 24.7, 24.5, 24.4, 24.4, 24.3, 24.1; ^{19}F NMR (470 MHz, C_6D_6) δ -124.1 (d, 4, *o*-C_6F_5), -148.8 (t, 2, *p*-C_6F_5), -159.1 (t, 4, *m*-C_6F_5). Anal. Calcd for $C_{104}H_{110}N_2F_{10}Zr$: C, 74.83; H, 6.64; N, 1.68. Found: C, 74.91; H, 6.73; N, 1.66.

[HIPTN$_2$]Hf(NMe$_2$)$_2$, 11a. This complex was prepared in a manner strictly analogous to that used to prepare **10a** starting from 4.092 g (3.28 mmol) of H_2[HIPTN$_2$] and 1.189 g (3.35 mmol) of Hf(NMe$_2$)$_4$; yield 3.635 g (71%): ^{1}H NMR (500 MHz, C_6D_6) δ 7.90 (d, 2, binaph), 7.75 (d, 2, binaph), 7.41 (d, 2, binaph), 7.21 (s, 4, *m*-HIPT), 7.20 (s, 4, *m*-HIPT), 7.18 (s, 4, *o*-HIPT), 7.04 (d, 2, binaph), 6.95 (t, 2, binaph), 6.56 (m, 2, *p*-HIPT + 2 binaph), 3.13 (m, 8, *o*-C*H*Me$_2$), 2.87 (sep, 4, *p*-C*H*Me$_2$), 2.70 (s, 12, N*Me*$_2$), 1.27 (m, 60, CH*Me*$_2$), 1.15 (d, 12, CH*Me*$_2$). Anal. Calcd for $C_{96}H_{122}N_4Hf$: C, 76.33; H, 8.14; N, 3.71. Found: C, 76.25; H, 8.05; N, 3.57.

[HIPTN$_2$]HfCl$_2$, 11b. This complex was prepared in a manner similar to that used to prepare **10b** starting from 3.02 g (2.00 mmol) of **11a** and 0.53 mL (4.2 mmol) of Me_3SiCl. The reaction solution remained yellow after heating in contrast to the Zr complex. All volatiles were removed in vacuo giving 2.90 g (97%) of a yellow solid: ^{1}H NMR (500 MHz, C_6D_6) δ 7.64 (d, 2, binaph), 7.49 (d, 2, binaph), 7.34 (s, 4, *o*-HIPT), 7.16 (m, 2, binaph + 8 *m*-HIPT), 6.87 (m, 4, binaph), 6.63 (s, 2, *p*-HIPT), 6.50 (t, 2, binaph), 2.98 (m, 8, *o*-C*H*Me$_2$), 2.82 (sep, 4, *p*-C*H*Me$_2$), 1.20 (m, 60, CH*Me*$_2$), 1.11 (d, 12, *o*-CH*Me*$_2$). Anal. Calcd for $C_{92}H_{110}N_2Cl_2Hf$: C, 74.00; H, 7.42; N, 1.88; Cl, 4.75. Found: C, 73.85; H, 7.51; N, 1.83; Cl, 4.77.

[HIPTN$_2$]HfMe$_2$, 11c. A flask was charged with 1.138 g (0.762 mmol) of **11b** and dissolved in 20 mL of diethyl ether. The solution was chilled to –25 ºC at which point 0.47 mL (1.6 mmol) of MeMgBr (3.3 M in Et_2O) was added dropwise. The reaction mixture was allowed to stir at room temperature for 60 min. during which time a precipitate formed. The ether was removed in vacuo and the residue extracted with pentane and filtered through Celite. The pentane solution was evaporated to dryness yielding 0.978 g (88%) of a yellow solid: ^{1}H NMR (500 MHz, C_6D_6) δ 7.83 (d, 2, binaph), 7.60 (d, 2, binaph), 7.42 (s, 4, *o*-HIPT), 7.28 (d, 2, binaph), 7.23 (s, 4, *m*-HIPT), 7.21 (s, 4, *m*-HIPT), 6.96 (d, 2, binaph), 6.92 (t, 2, binaph), 6.68 (s, 2, *p*-HIPT), 6.55 (t, 2, binaph), 3.12 (m, 8, *o*-C*H*Me$_2$), 2.88 (sep, 4, *p*-C*H*Me$_2$), 1.30 – 1.20 (m, 72, CH*Me*$_2$), 0.46 (s, 6, C*H*$_3$). ^{13}C NMR (125 MHz, CD_2Cl_2) δ 150.7, 148.5, 147.2, 147.2, 142.5, 137.8, 137.6, 135.1, 133.1, 131.7, 128.6, 128.0, 126.8, 126.0, 125.4, 125.2, 124.6, 121.1, 121.0, 119.6, 63.2 (*Me*), 34.9 (*p*-*C*HMe$_2$), 31.1 (*o*-*C*HMe$_2$), 31.0 (*o*-*C*HMe$_2$), 24.9, 24.8, 24.7, 24.6, 24.5, 24.4. Anal. Calcd for $C_{94}H_{116}N_2Hf$: C, 77.73; H, 8.05; N, 1.93. Found: C, 77.62; H, 8.15; N, 1.87.

[HIPTN$_2$]Hf(*i*-Bu)$_2$, 11d. This compound was prepared in a manner analogous to that used to prepare **11c** starting from 1.076 g (0.721 mmol) of **11b** and 0.62 mL (1.5 mmol) of Me_2CHCH_2MgBr (2.4 M in Et_2O); yield 1.008 g (91%): ^{1}H NMR (C_6D_6) δ 7.87 (d, 2, binaph), 7.76 (d, 2, binaph), 7.39 (s, 4, *o*-HIPT), 7.37 (d, 2, binaph), 7.21 (s, 4, *m*-HIPT), 7.20 (s, 4, *m*-HIPT), 6.93 (m, 4, binaph), 6.64 (s, 2, *p*-HIPT), 6.43 (t, 2, binaph), 3.15 (sep, 4, *o*-C*H*Me$_2$), 3.07 (sep, 4, *o*-C*H*Me$_2$), 2.87 (sep, 4, *p*-C*H*Me$_2$), 2.25 (sep, 2, CH$_2$C*H*Me$_2$), 1.33 (d, 6, CH*Me*$_2$), 0.97 (dd, 2, C*H*$_2$CHMe$_2$), 0.85 (dd, 2, C*H*$_2$CHMe$_2$), 0.81 (d, 6, CH$_2$CH*Me*$_2$), 0.63 (d, 6, CH$_2$CH*Me*$_2$). ^{13}C NMR (CD_2Cl_2) δ 151.2, 148.4, 147.2, 147.1, 142.3, 138.5, 137.7, 135.2, 132.7, 131.6, 128.5, 127.8, 127.0, 126.1, 125.8, 125.3, 125.1, 121.0, 120.9, 120.3, 98.1 (*C*H$_2$CHMe$_2$), 34.9 (*p*-*C*HMe$_2$), 31.0 (*o*-*C*HMe$_2$), 30.9 (*o*-*C*HMe$_2$), 29.9, 29.0, 28.2, 24.9, 24.8, 24.7, 24.6, 24.5, 24.4. Anal. Calcd for $C_{100}H_{128}N_2Hf$: C, 78.16; H, 8.40; N, 1.82. Found: C, 77.96; H, 8.31; N, 1.75.

Activation experiments. Activation of $[HIPTN_2]ZrMe_2$, $[HIPTN_2]Zr(^{13}CH_3)_2$, and $[HIPTN_2]HfMe_2$ were conducted as follows. Equimolar amounts of the complex and activator were dissolved in ~0.4 mL of bromobenzene-d_5. The solutions were cooled to –30 ºC, at which point they were mixed and quickly transferred to the J-Young tube. The 500 MHz NMR data of the activated zirconium and hafnium species are listed below.

{[HIPTN$_2$]Zr(Me)(NMe$_2$Ph)}{B(C$_6$F$_5$)$_4$}. ^{1}H NMR (C_6D_5Br) δ 8.17 (d, 1, aryl), 7.87 (d, 1, aryl), 7.80 (d, 1, aryl), 7.77 (d, 2, aryl), 7.75 (t, 1, aryl), 7.69 (d, 1, aryl), 7.34 (t, 1, aryl), 7.23 (s, 2, HIPT), 7.21 (s, 2, HIPT), 7.19 (s, 2, HIPT), 7.15 (s, 2, HIPT), 7.05 – 6.85 (m, 7, aryl), 6.77 (s, 2, HIPT), 6.68 (t, 1, aryl), 6.62 (m, 4, aryl), 6.43 (t, 1, aryl), 3.01 – 2.79 (m, 12, C*H*Me$_2$), 2.21 (br s, 3, *Me*$_2$NPh), 1.47 (br s, 3, *Me*$_2$NPh), 1.35 – 1.12 (m, 72, CH*Me*$_2$), 0.53 (s, 3, *Me*).

{[HIPTN$_2$]Zr(Me)}{B(C$_6$F$_5$)$_4$} (*minor isomer only*). ^{1}H NMR (C_6D_5Br) δ 8.15 (d, 1, aryl), 7.78 (t, 2, aryl), 7.66 (d, 1, aryl), 7.21 – 6.98 (m, 32, aryl), 6.81 (m, 3, aryl), 6.73 (m, 2, aryl), 2.91 (m, 6, C*H*Me$_2$), 2.81 (m, 12, C*H*Me$_2$), 2.03 (s, 3, Ph_3CCH_3), 1.32 – 1.12 (m, 72, CH*Me*$_2$), 0.43 (s, 3, *Me*); ^{13}C NMR (125 MHz, C_6D_5Br) δ 49.76 (*Me*, minor isomer, J_{CH} = 120 Hz), 47.51 (*Me*, major isomer, J_{CH} = 120 Hz).

[HIPTN$_2$]Hf(C$_6$F$_5$)$_2$. ^{1}H NMR (C_6D_6) δ 7.68 (d, 2, binaph), 7.45 (d, 2, binaph), 7.31 (d, 2, binaph), 7.16 (s, 4, *o*-HIPT), 7.13 (s, 4, *m*-HIPT), 7.12 (s, 4, *m*-HIPT), 7.01 (t, 2, binaph), 6.85 (d, 2, binaph), 6.69 (s, 2, *p*-HIPT), 6.51 (t, 2, binaph), 2.94 (m, 8, *o*-C*H*Me$_2$), 2.82 (sep, 4, *p*-C*H*Me$_2$), 1.25 (d, 24, *p*-CH*Me*$_2$), 1.18 (m, 36, *o*-CH*Me*$_2$), 1.06 (d, 12, *o*-CH*Me*$_2$); ^{19}F NMR (470 MHz, C_6D_6) δ -122.9 (br s, 4, *o*-C_6F_5), -148.3 (br s, 2, *p*-C_6F_5), -159.0 (br s, 4, *m*-C_6F_5).

{[HIPTN$_2$]Hf(Me)(NMe$_2$Ph)}{B(C$_6$F$_5$)$_4$}. ^{1}H NMR (C_6D_5Br) δ 8.18 (d, 1, aryl), 7.82 (d, 1, aryl), 7.77 (d, 1, aryl), 7.72 (d, 1, aryl), 7.36 (d, 1, aryl), 7.22 – 7.14 (m, 10, aryl), 7.01 (m, 3, aryl), 6.93 (d, 1, aryl), 6.91 (s, 2, HIPT), 6.85 (t, 1, aryl), 6.83 (s, 2, HIPT), 6.71 (s, 2, HIPT), 6.66 (t, 1, aryl), 6.60 (s, 1, HIPT), 6.53 (m, 2, aryl), 6.36 (t, 1, aryl), 2.93 (m, 6, C*H*Me$_2$), 2.79 (m, 6, C*H*Me$_2$), 2.21 (br s, 3, *Me*$_2$NPh), 1.46 (br s, 3, *Me*$_2$NPh), 1.34 – 1.10 (m, 72, CH*Me*$_2$), 0.49 (s, 3, *Me*).

{[HIPTN$_2$]Hf(Me)}{B(C$_6$F$_5$)$_4$} (*major isomer only*). ^{1}H NMR (C_6D_5Br) δ 7.97 (br s, 1, aryl), 7.67 (t, 1, aryl), 7.56 (br d, 1, aryl), 7.31 (t, 2, aryl), 7.18 – 7.05 (m, 30, aryl), 7.01 (s, 1, HIPT) 6.80 (br d, 1, aryl), 6.74 (s, 2, HIPT), 6.62 (m, 2, aryl), 2.92 (m, 6, C*H*Me$_2$), 2.78 (m, 6, C*H*Me$_2$), 2.03 (s, 3, Ph_3CCH_3), 1.31 – 1.11 (m, 72, CH*Me*$_2$), 0.66 (s, 3, *Me*).

Crystal data and structure refinement for **1d**.

Identification code	**04038**	
Empirical formula	$C_{36}H_{60}N_8Zr_2$	
Formula weight	787.36 g/mol	
Temperature	193(2) K	
Wavelength	0.71073 Å	
Crystal system	Triclinic	
Space group	$P\bar{1}$	
Unit cell dimensions	a = 10.5468(4) Å	α = 94.063(1)°
	b = 13.1591(5) Å	β = 104.604(1)°
	c = 14.4106(5) Å	γ = 92.716(1)°
Volume	1926.10(12) $Å^3$	
Z	2	
Density (calculated)	1.358 g/cm^3	
Absorption coefficient	0.576 mm^{-1}	
F(000)	824	
Crystal size	0.18 × 0.13 × 0.08 mm^3	
Θ range for data collection	1.47 to 25.00°	
Index ranges	$-12 \le h \le 12$, $-15 \le k \le 13$, $-14 \le l \le 17$	
Reflections collected	10226	
Independent reflections	6707 [R(int) = 0.0356]	
Completeness to Θ = 25.00°	98.7%	
Absorption correction	None	
Max. and min. transmission	0.9554 and 0.9034	
Refinement method	Full-matrix least-squares on F^2	
Data / restraints / parameters	6707 / 0 / 431	
Goodness-of-fit on F^2	1.022	
Final R indices [I>2σ(I)]	R1 = 0.0291, wR2 = 0.0788	
R indices (all data)	R1 = 0.0326, wR2 = 0.0804	
Largest diff. peak and hole	0.393 and -0.446 $e \cdot Å^{-3}$	

Crystal data and structure refinement for **3c**.

Identification code	**00160**	
Empirical formula	$C_{38}H_{41}N_3OZr$	
Formula weight	646.96 g/mol	
Temperature	183(2) K	
Wavelength	0.71073 Å	
Crystal system	Monoclinic	
Space group	$P2_1/n$	
Unit cell dimensions	a = 11.1743(8) Å	α = 90°
	b = 19.3928(14) Å	β = 91.664(1)°
	c = 16.5054(12) Å	γ = 90°
Volume	3575.2(4) $Å^3$	
Z	4	
Density (calculated)	1.202 g/cm^3	
Absorption coefficient	0.338 mm^{-1}	
F(000)	1352	
Crystal size	0.30 × 0.15 × 0.15 mm^3	
Θ range for data collection	2.41 to 23.29°	
Index ranges	$-12 \le h \le 8$, $-21 \le k \le 21$, $-17 \le l \le 18$	
Reflections collected	14215	
Independent reflections	5143 [R(int) = 0.0394]	
Completeness to Θ = 25.00°	99.6%	
Absorption correction	Empirical	
Max. and min. transmission	0.2710 and 0.2316	
Refinement method	Full-matrix least-squares on F^2	
Data / restraints / parameters	5143 / 0 / 369	
Goodness-of-fit on F^2	1.062	
Final R indices [I>2σ(I)]	R1 = 0.0561, wR2 = 0.1489	
R indices (all data)	R1 = 0.0711, wR2 = 0.1568	
Largest diff. peak and hole	1.469 and -0.436 $e \cdot Å^{-3}$	

Crystal data and structure refinement for **5c**.

Identification code	**03238**	
Empirical formula	$C_{29}H_{39}N_3Zr$	
Formula weight	520.85 g/mol	
Temperature	193(2) K	
Wavelength	0.71073 Å	
Crystal system	Triclinic	
Space group	$P\bar{1}$	
Unit cell dimensions	a = 10.3983(9) Å	α = 89.535(2)°
	b = 15.5014(14) Å	β = 83.932(2)°
	c = 18.4205(17) Å	γ = 71.647(2)°
Volume	2801.4(4) $Å^3$	
Z	4	
Density (calculated)	1.235 g/cm^3	
Absorption coefficient	0.412 mm^{-1}	
F(000)	1096	
Crystal size	0.27 × 0.21 × 0.15 mm^3	
Θ range for data collection	1.11 to 24.00°	
Index ranges	$-10 \le h \le 11$, $-15 \le k \le 17$, $-21 \le l \le 21$	
Reflections collected	13921	
Independent reflections	8770 [R(int) = 0.0340]	
Completeness to Θ = 24.00°	99.8%	
Absorption Correction	Empirical	
Max. and min. transmission	0.9408 and 0.8969	
Refinement method	Full-matrix least-squares on F^2	
Data / restraints / parameters	8770 / 0 / 618	
Goodness-of-fit on F^2	1.075	
Final R indices [I>2σ(I)]	R1 = 0.0658, wR2 = 0.1510	
R indices (all data)	R1 = 0.0874, wR2 = 0.1604	
Largest diff. peak and hole	0.904 and -0.681 $e \cdot Å^{-3}$	

Crystal data and structure refinement for **7a′**.

Identification code	**04057**	
Empirical formula	$C_{42}H_{40}ClN_5Zr$	
Formula weight	741.46 g/mol	
Temperature	194(2) K	
Wavelength	0.71073 Å	
Crystal system	triclinic	
Space group	$P\bar{1}$	
Unit cell dimensions	a = 11.2241(8) Å	α = 105.3360(10)°
	b = 11.9467(8) Å	β = 103.6170(10)°
	c = 14.8348(10) Å	γ = 103.2950(10)°
Volume	1771.5(2) Å^3	
Z	2	
Density (calculated)	1.390 g/cm^3	
Absorption coefficient	0.424 mm^{-1}	
F(000)	768	
Crystal size	0.18 × 0.13 × 0.08 mm^3	
Θ range for data collection	1.50 to 28.25°	
Index ranges	$-12 \le h \le 14$, $-15 \le k \le 11$, $-17 \le l \le 19$	
Reflections collected	11351	
Independent reflections	7908 [R(int) = 0.0146]	
Completeness to Θ = 28.25°	90.2%	
Max. and min. transmission	0.9669 and 0.9276	
Refinement method	Full-matrix least-squares on F^2	
Data / restraints / parameters	7908 / 0 / 446	
Goodness-of-fit on F^2	1.046	
Final R indices [I>2σ(I)]	R1 = 0.0313, wR2 = 0.0796	
R indices (all data)	R1 = 0.0354, wR2 = 0.0822	
Largest diff. peak and hole	0.434 and -0.295 e·Å^{-3}	

Crystal data and structure refinement for **8t**.

Identification code	**04207**	
Empirical formula	$C_{44.96}H_{35.85}Br_{1.19}F_{5.86}HfN_4O_{5.86}S_{1.96}$	
Formula weight	1174.02	
Temperature	100(2) K	
Wavelength	0.71073 Å	
Crystal system	Triclinic	
Space group	$P\bar{1}$	
Unit cell dimensions	a = 11.7762(4) Å	α = 100.3660(10)°
	b = 12.9221(4) Å	β = 104.9870(10)°
	c = 17.4473(6) Å	γ = 112.6300(10)°
Volume	2247.97(13) $Å^3$	
Z	2	
Density (calculated)	1.734 g/cm^3	
Absorption coefficient	3.550 mm^{-1}	
F(000)	1157	
Crystal size	0.25 × 0.15 × 0.15 mm^3	
Θ range for data collection	1.27 to 26.02°	
Index ranges	$-14 \le h \le 13, -15 \le k \le 15, 0 \le l \le 21$	
Reflections collected	39931	
Independent reflections	8866 [R(int) = 0.0280]	
Completeness to Θ = 26.02°	100%	
Absorption correction	Semi-empirical from equivalents	
Max. and min. transmission	0.6180 and 0.4706	
Refinement method	Full-matrix least-squares on F^2	
Data / restraints / parameters	8866 / 849 / 743	
Goodness-of-fit on F^2	1.059	
Final R indices [I>2σ(I)]	R1 = 0.0370, wR2 = 0.0986	
R indices (all data)	R1 = 0.0389, wR2 = 0.1002	
Largest diff. peak and hole	2.143 and -1.553 $e \cdot Å^{-3}$	

Crystal data and structure refinement for **8d**.

Identification code	**04180**	
Empirical formula	$C_{48}H_{52}HfN_4$	
Formula weight	863.43 g/mol	
Temperature	100(2) K	
Wavelength	0.71073 Å	
Crystal system	Triclinic	
Space group	$P\bar{1}$	
Unit cell dimensions	a = 11.228(2) Å	α = 97.18(3)°
	b = 18.140(4) Å	β = 101.92(3)°
	c = 20.381(4) Å	γ = 90.73(3)°
Volume	4026.4(14) $Å^3$	
Z	4	
Density (calculated)	1.424 g/cm^3	
Absorption coefficient	2.629 mm^{-1}	
F(000)	1760	
Crystal size	0.25 × 0.20 × 0.20 mm^3	
Θ range for data collection	1.63 to 26.02°	
Index ranges	$-13 \le h \le 13$, $-22 \le k \le 22$, $-24 \le l \le 25$	
Reflections collected	70696	
Independent reflections	15780 [R(int) = 0.0270]	
Completeness to Θ = 26.02°	99.6%	
Max. and min. transmission	0.6214 and 0.5594	
Refinement method	Full-matrix least-squares on F^2	
Data / restraints / parameters	15780 / 0 / 955	
Goodness-of-fit on F^2	1.017	
Final R indices [I>2σ (I)]	R1 = 0.0268, wR2 = 0.0703	
R indices (all data)	R1 = 0.0295, wR2 = 0.0722	
Largest diff. peak and hole	2.231 and -0.659 $e \cdot Å^{-3}$	

Crystal data and structure refinement for **7e**.

Identification code	**04068**	
Empirical formula	$C_{49.5}H_{43.5}N_4Zr$	
Formula weight	785.60 g/mol	
Temperature	194(2) K	
Wavelength	0.71073 Å	
Crystal system	Triclinic	
Space group	$P\bar{1}$	
Unit cell dimensions	a = 12.3177(4) Å	α = 98.643(1)°
	b = 13.2063(5) Å	β = 91.127(1)°
	c = 13.8962(5) Å	γ = 116.507(1)°
Volume	1990.28(12) $Å^3$	
Z	2	
Density (calculated)	1.311 g/cm^3	
Absorption coefficient	0.316 mm^{-1}	
F(000)	817	
Crystal size	0.36 × 0.15 × 0.15 mm^3	
Θ range for data collection	1.49 to 28.33°	
Index ranges	$-16 \le h \le 14$, $-10 \le k \le 17$, $-18 \le l \le 18$	
Reflections collected	14821	
Independent reflections	9789 [Rint = 0.0145]	
Completeness to Θ = 28.33°	98.4%	
Absorption correction	Empirical	
Max. and min. transmission	0.2710 and 0.2316	
Refinement method	Full-matrix least-squares on F^2	
Data / restraints / parameters	9789 / 6 / 502	
Goodness-of-fit on F^2	1.095	
Final R indices [I>2σ(I)]	R1 = 0.0527, wR2 = 0.1595	
R indices (all data)	R1 = 0.0584, wR2 = 0.1654	
Largest diff. peak and hole	2.178 and -0.474 $e \cdot Å^{-3}$	

REFERENCES

1. Brintzinger, H. H.; Fischer, D.; Mülhaupt, R.; Rieger, B.; Waymouth, R. M. *Angew. Chem., Int. Ed. Engl.* **1995**, *34*, 1143.
2. McKnight, A. L.; Waymouth, R. M. *Chem. Rev.* **1998**, *98*, 2587.
3. Bochmann, M. J. Chem. Soc., Dalton Trans. **1996**, 255.
4. Kaminsky, W.; Ardnt, M. *Adv. Polym. Sci.* **1997**, *127*, 144.
5. Galimberti, M.; Martini, E.; Piemontesi, F.; Sartori, F.; Camurati, I.; Resconi, L.; Albizzati, E. *Macromol. Symp.* **1995**, *89*, 259.
6. Doi, Y.; Keii, T. *Adv. Polym. Sci.* **1986**, *73/74*, 201.
7. Britovsek, G. J. P.; Gibson, V. C.; Wass, D. F. *Angew. Chem., Int. Ed. Engl.* **1999**, *38*, 428.
8. Gibson, V. C.; Spitzmesser, S. K. *Chem. Rev.* **2003**, *103*, 283.
9. Matyjaszewski, K. *Macromolecules* **1993**, *26*, 1787.
10. Coates, G. W.; Hustad, P. D.; Reinartz, S. *Angew. Chem., Int. Ed. Engl.* **2002**, *41*, 2236.
11. Jayaratne, K. C.; Sita, L. J. *J. Am. Chem. Soc.* **2000**, *122*, 958.
12. Tshuva, E. Y.; Goldberg, I.; Kol, M. *J. Am. Chem. Soc.* **2000**, *122*, 10706.
13. Mitani, M.; Furuyama, R.; Mohri, J.; Saito, J.; Ishii, S.; Terao, H.; Kashiwa, N.; Fujita, T. *J. Am. Chem. Soc.* **2002**, *124*, 7888.
14. Mitani, M.; Furuyama, R.; Mohri, J.; Saito, J.; Ishii, S.; Terao, H.; Nakano, T.; Tanaka, H.; Fujita, T. *J. Am. Chem. Soc.* **2003**, *125*, 4293.
15. Busico, V.; Caporaso, L.; Cipullo, R.; Landriani, L.; Angelini, G.; Margonelli, A.; Segre, A. L. *J. Am. Chem. Soc.* **1996**, *118*, 2105.
16. Busico, V.; Cipullo, R.; Talarico, G. *Macromolecules* **1998**, *31*, 2387.
17. Corradini, P.; Busico, V.; Cipullo, R., In *Catalyst Design For Tailor-Made Polyolefins*, 1994; Vol. 89, pp 21.
18. Busico, V.; Cipullo, R.; Chadwick, J. C.; Modder, J. F.; Sudmeijer, O. *Macromolecules* **1994**, *27*, 7538.
19. Grubbs, R. H.; Coates, G. W. *Acc. Chem. Res.* **1996**, *29*, 85.
20. Coates, G. W. J. Chem. Soc., Dalton Trans. **2002**, 467.
21. Jayaratne, K. C.; Keaton, R. J.; Henningsen, D. A.; Sita, L. J. *J. Am. Chem. Soc.* **2000**, *122*, 10490.
22. Zhang, Y.; Keaton, R. J.; Sita, L. J. *J. Am. Chem. Soc.* **2003**, *125*, 9062.
23. Warren, T. H.; Schrock, R. R.; Davis, W. M. *Organometallics* **1996**, *15*, 562.
24. Baumann, R.; Davis, W. M.; Schrock, R. R. *J. Am. Chem. Soc.* **1997**, *119*, 3830.

25. Aizenberg, M.; Turculet, L.; Davis, W. M.; Schattenmann, F.; Schrock, R. R. *Organometallics* **1998**, *17*, 4795.
26. Schattenmann, F.; Schrock, R. R.; Davis, W. M. *Organometallics* **1998**, *17*, 989.
27. Schrock, R. R.; Schattenmann, F.; Aizenberg, M.; Davis, W. M. *Chem. Commun.* **1998**, 199.
28. Liang, L.-C.; Schrock, R. R.; Davis, W. M. *J. Am. Chem. Soc.* **1999**, *120*, 5797.
29. Mehrkhodavandi, P.; Bonitatebus, P. J., Jr.; Schrock, R. R. *J. Am. Chem. Soc.* **2000**, *122*, 7841.
30. Kempe, R. Angew. Chem., Int. Ed. Engl. **2000**, 39, 468.
31. Bradley, D. C.; Chisholm, M. H. *Acc. Chem. Res.* **1976**, *9*, 273.
32. Liang, L.-C.; Schrock, R. R.; Davis, W. M. *Organometallics* **2000**, *19*, 2526.
33. Schrock, R. R.; Baumann, R.; Reid, S. M.; Goodman, J. T.; Stumpf, R.; Davis, W. M. *Organometallics* **1999**, *18*, 3649.
34. Mehrkhodavandi, P.; Schrock, R. R.; Pryor, L. L. *Organometallics* **2003**, *22*, 4569.
35. Baumann, R. *Ph. D. Thesis*, Massachusetts Institute of Technology, 1998.
36. Flores, M. A.; Manzoni, M.; Baumann, R.; Davis, W. M.; Schrock, R. R. *Organometallics* **1999**, *18*, 3220.
37. Schrock, R. R. *Acc. Chem. Res.* **2006**, *39*, 167.
38. Tonzetich, Z. J.; Lu, C. C.; Schrock, R. R.; Hock, A. S.; Bonitatebus, P. J. *Organometallics* **2004**, *23*, 4362.
39. Fourneau, J.; Lestrange, M. Y. *Bull. Soc. Chim. Fr.* **1947**, 837.
40. Wolfe, J. P.; Wagaw, S.; Buchwald, S. L. *J. Am. Chem. Soc.* **1996**, *118*, 7215.
41. Wolfe, J. P.; Wagaw, S.; Marcoux, J.-F.; Buchwald, S. L. *Acc. Chem. Res.* **1998**, *31*, 805.
42. Schrock, R. R.; Casado, A. L.; Goodman, J. T.; Liang, L.-C.; Bonitatebus, P. J., Jr.; Davis, W. M. *Organometallics* **2000**, *19*, 5325.
43. Huang, X.; Anderson, K. W.; Zim, D.; Jiang, L.; Klapars, A.; Buchwald, S. L. *J. Am. Chem. Soc.* **2003**, *125*, 6653.
44. Diamond, G. M.; Jordan, R. F.; Petersen, J. L. *Organometallics* **1996**, *15*, 4030.
45. Mehrkhodavandi, P.; Schrock, R. R.; Bonitatebus, P. J. J. *Organometallics* **2002**, *21*, 5785.
46. Scollard, J. D.; McConville, D. H.; Payne, N. C.; Vittal, J. J. *Macromolecules* **1996**, *29*, 5241.
47. Ivin, K. J.; Kenwright, A. M.; Hofmeister, G. E.; McConville, D. H.; Schrock, R. R.; Amir-Ebrahimi, V.; Carbill, A. G.; Hamilton, J. G.; Rooney, J. J. *Macromol. Chem. Phys.* **1998**, *199*, 547.

48. Schrock, R. R.; Bonitatebus, P. J., Jr.; Schrodi, Y. *Organometallics* **2001**, *20*, 1056.
49. Schrodi, Y.; Schrock, R. R.; Bonitatebus, P. J. J. *Organometallics* **2001**, *20*, 3560.
50. Liu, Z.; Somsook, E.; White, C. B.; Rosaaen, K. A.; Landis, C. R. *J. Am. Chem. Soc.* **2001**, *123*, 11193.
51. Noyori, R. *Adv. Synth. Catal.* **2003**, *345*, 15.
52. Newkome, G. R.; Frere, Y. A.; Fronczek, F. R.; Gupta, V. K. *Inorg. Chem.* **1985**, *24*, 1001.
53. Kettunen, M.; Vedder, C.; Schaper, F.; Leskela, M.; Mutikainen, I.; Brintzinger, H. H. *Organometallics* **2004**, *23*, 3800.
54. Lawrance, G. A. *Chem. Rev.* **1986**, *86*, 17.
55. Wondimagegn, T.; Xu, Z.; Vanka, K.; Ziegler, T. *Organometallics* **2004**, *23*, 3847.
56. Scollard, J. D.; McConville, D. H.; Vittal, J. J. *Organometallics* **1995**, *14*, 5478.
57. Scollard, J. D.; McConville, D. H. *J. Am. Chem. Soc.* **1996**, *118*, 10008.
58. Warren, T. H.; Schrock, R. R.; Davis, W. M. *Organometallics* **1998**, *17*, 308.
59. Blackmore, I. J.; Gibson, V. C.; Hitchcock, P. B.; Rees, C. W.; Williams, D. J.; White, A. J. P. *J. Am. Chem. Soc.* **2005**, *127*, 6012.
60. Brown, K. J.; Berry, M. S.; Murdoch, J. R. *J. Org. Chem.* **1985**, *50*, 4345.
61. Yandulov, D. V.; Schrock, R. R.; Rheingold, A. L.; Ceccarelli, C.; Davis, W. M. *Inorg. Chem.* **2003**, *42*, 796.
62. Zucchini, U.; Albizzati, E.; Giannini, U. *J. Organomet. Chem.* **1971**, *26*, 357.
63. Tjaden, E. B.; Swenson, D. C.; Jordan, R. F. *Organometallics* **1995**, *14*, 371.
64. Schrock, R. R.; Sancho, J.; Pederson, S. F. *Inorg. Synth.* **1989**, *26*, 44.
65. Sheldrick, G. M. Acta Cryst. 1990, A46, 467.
66. Sheldrick, G. M (1997). SHELXL 97, University of Göttingen, Germany.

CHAPTER 2

Development of New Molybdenum Imido Alkylidene Initiators for the Controlled Polymerization of 1,6-Heptadiynes

Portions of this chapter have appeared in print:

Adamchuk, J. A.; Schrock, R. R.; Tonzetich, Z. J.; Müller, P. "Initiators of the Type $Mo(NR)(CHR')(OR'')_2$ for the Controlled Polymerization of Diethyldipropargylmalonate" *Organometallics* **2006**, *25*, 2364-2373.

Czekelius, C.; Hafer, J.; Tonzetich, Z. J.; Schrock, R. R.; Müller, P. "Synthesis of Oligoenes that Contain Up to 15 Double Bonds from 1,6-Heptadiynes" *J. Am. Chem. Soc.* **2006**, *128*, 16664-16675.

INTRODUCTION

Polyacetylene, the simplest π-conjugated organic polymer, has been the subject of intense investigation because of its fundamental electronic and photophysical properties.[1] The practical applications of π-conjugated polymers (polyenes) include uses in lasers, displays, and non-linear optical materials.[2] Limitations in the handling (oxygen sensitivity) and processing (insolubility) of traditional unsubstituted-polyacetylene has led to increased interest in preparing other well-characterized π-conjugated organic polymers. Soluble and more air-stable substituted polyenes have been prepared through polymerization of substituted phenylacetylenes[3,4,5,6,7] or 4,4-disubstituted 1,6-heptadiynes.[8,9,10,11] Although such polyenes are not highly conductive in the solid state, they demonstrate desirable electronic, linear or non-linear optical, and electrochemical (photoconductive or photorefractive) properties.[12] Moreover, these substituted polyenes serve as models for understanding the electronic and optical properties of one-dimensional, conjugated π-electron systems.[13]

Our laboratory has been interested in the synthesis of substituted poly[1,6-heptadiynes] via catalytic ring closing metathesis polymerization (RCMP). The RCMP of 1,6-heptadiynes such as diethyl dipropargylmalonate (DEDPM) to give substituted polyacetylenes has been known for several decades.[8] The polymers produced by the RCMP of heptadiynes are effectively polyacetylenes, but contain five and/or six-membered rings along the backbone of the polymer chain (Scheme 2.1). This substitution imparts a greater degree of stability and solubility to the polymers when compared with traditional polyacetylene. The catalyst systems traditionally used to affect RCMP comprise poorly defined ternary or quaternary mixtures of $MoCl_5$, EtOH, and alkylating agents such as $(n\text{-Bu})_4Sn$. Although these mixtures produce materials with interesting optical and electronic properties, the propagating catalyst was never identified, nor a mechanism postulated.[8] Despite this lack of understanding, recent work has demonstrated that living polymerization behavior can be achieved with these systems.[14]

Scheme 2.1. Five- and six-membered rings formed during polymerization of DEDPM.

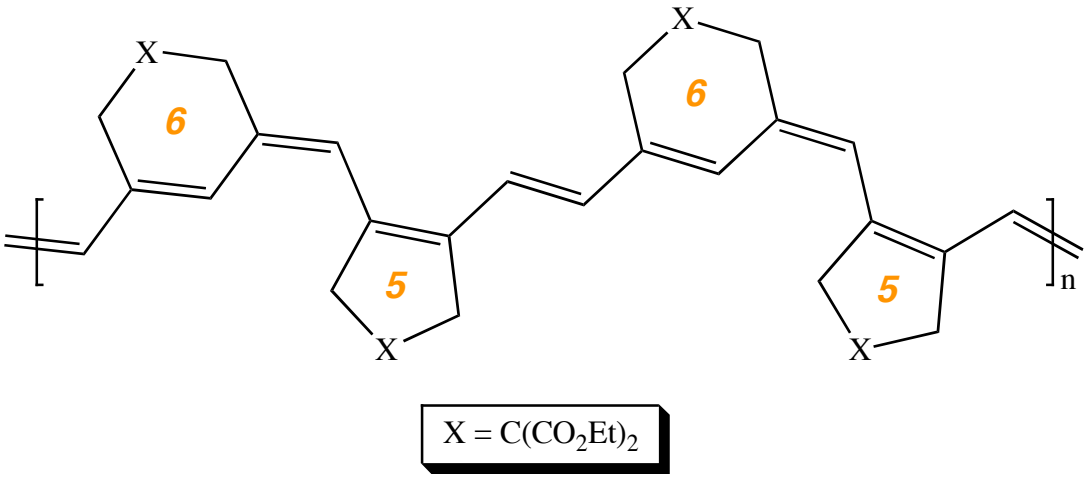

In 1992 our laboratory reported the first living polymerization of DEDPM catalyzed by high oxidation state molybdenum imido carbene (alkylidene) complexes of the type Mo(NAr)(CH-*t*-Bu)(O-*t*-Bu_{F6})$_2$ (Ar = 2,6-diisopropylphenyl; O-*t*-Bu_{F6} = $OC(CF_3)_2Me$).[15] These complexes yielded polymers with narrow polydispersities that resembled the polymers produced with the traditional metal halide-based catalyst systems. Owing to the well-defined nature of the catalyst precursors, a mechanism for the RCMP reaction was put forth which accounted for both the five- and six-membered ring topology of the polymer (Scheme 2.2). In this bifurcated mechanism, addition of the alkyne to the metal-carbon double bond can take place in either an α- or β- fashion. Approach of the terminal carbon of the alkyne to the alkylidene carbon (α-addition) results in formation of five-membered rings, whereas approach to the metal (β-addition) results in six-membered ring formation. Both addition processes take place competitively with catalysts bearing the O-*t*-Bu_{F6} ligand, giving rise to a polymer that possesses both five- and six-membered rings.

Since the initial report of living DEDPM polymerization, subsequent work by our laboratory and by others has resulted in new catalysts that are capable of producing polymers with 95+% enrichment in one type of ring.[16] Notably, the Mo(NAr)($CHCMe_2Ph$)(O-*t*-

$Bu)_2(quin)$[17] and $Mo(NAr'')(CH\text{-}t\text{-}Bu)(O_2CCPh_3)_2$[18] complexes produce polymers with greater than 95% enrichment in five-membered and six-membered rings, respectively. Although these catalysts give rise to homogenous ring composition, the precise structure of these polyenes was not elucidated. Knowledge of polyene structure is critical to an understanding of how steric interactions along the chain backbone determine effective conjugation length.

Scheme 2.2. Proposed mechanism for polymerization of 1,6-heptadiynes.

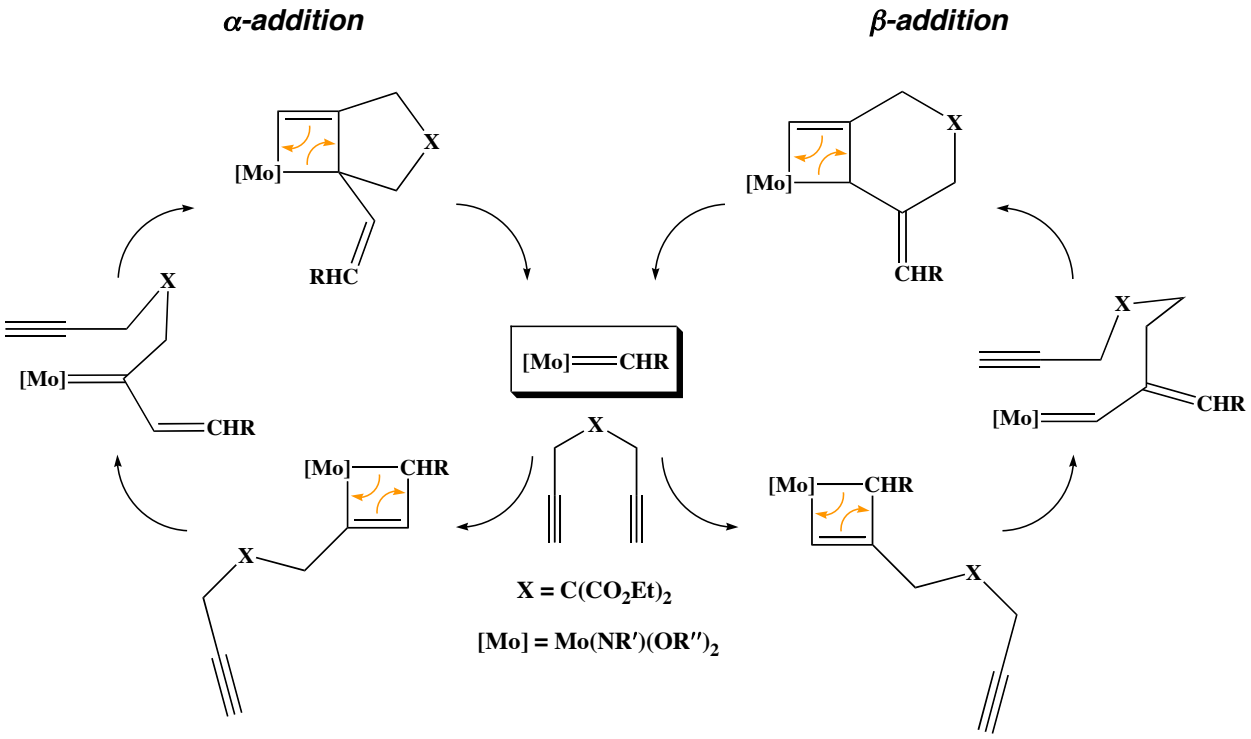

This chapter concerns the synthesis of molybdenum imido alkylidene complexes relevant to the polymerization of substituted 1,6-heptadiynes. The factors contributing to the formation of five- versus six-membered rings are examined in the context of modifications to the imido alkylidene framework. The synthesis of model polyenes is also presented and the implication to polymer structure discussed.

RESULTS

2.1 Preparation of alkylidene initiators possessing five- and six-membered ring vinyl alkylidenes

2.1.1 Five-membered ring initiators

Because of their well-defined structure, polyenes exclusively containing five-membered rings along the polymer backbone have the potential to display more interesting photophysical properties than their six-membered ring counterparts.[11] This potential lies in the fact that consecutive five-membered rings may adopt a less sterically demanding orientation, which leads to more planarity along the polyacetylene backbone.[19,20] Whereas the $A_{1,3}$ strain caused by the endocyclic methylene units forces the six-membered polymer to skew out of plane, the five-membered ring polymer may remain planar by adopting a perfectly alternating "up-down" geometry (Scheme 2.3).[21] Furthermore, polymers containing all five-membered rings have been shown to have lower energy absorption maxima than polymers of similar molecular weight containing only six- or both five- and six-membered rings.[17,22]

Scheme 2.3. Alternating *cis-trans* structure of five-membered poly[DEDPM].

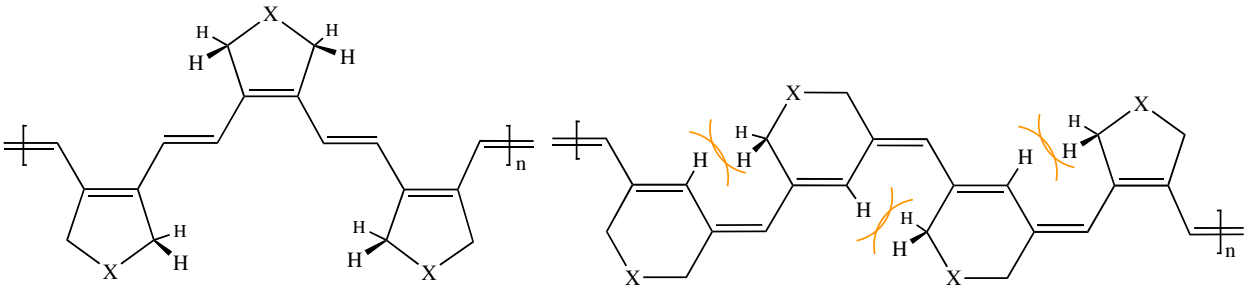

Buchmeiser's report of the regioselective polymerization of DEDPM by Mo(NAr)(CHCMe$_2$Ph)(O-*t*-Bu)$_2$(quin)[17] prompted an examination of alternate alkylidene

ligands. Slow initiation relative to propagation is a recurrent problem with many polymerization reactions initiated by bulky neophylidene or neopentylidene ligands.[23] As a result, polymers with unpredictable molecular weights are produced, and the ability to examine the detailed kinetics of initiation is limited. Information of this nature is useful in studying the origin of five- versus six-membered ring formation by imido alkylidene catalysts. Previous work in this laboratory demonstrated the viability of vinyl alkylidenes as initiators for both ROMP and alkyne polymerization reactions.[24] Although more effective initiating ligands than neopentylidene or neophylidene, vinyl alkylidenes such as but-2-enylidene are not perfect models of the growing polymer chain.

Ideally, a vinyl alkylidene ligand would contain a five- or six-membered ring analogous to that formed during RCMP of DEDPM. One strategy to prepare this type of alkylidene ligand is to prepare dienes or trienes resembling the conjugated rings of poly[DEDPM]. Cross-metathesis reactions of these alkenes with neopentylidene or neophylidene complexes then yields the corresponding vinyl alkylidenes.[25] Triene **1c** was prepared through a Wittig reaction with aldehyde **1b** (equation 2.1). The triene was isolated in 57% yield after column chromatography on silica gel and appears to be stable in air at room temperature for at least several days. The precursor aldehyde is readily available through the

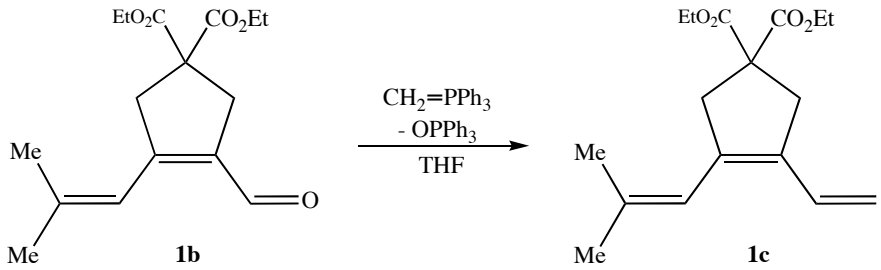

(2.1)

ruthenium catalyzed cycloisomerization of diynol **1a** according to methodology reported by Trost (equation 2.2).[26,27] The cyclization reaction shown in equation 2.2 was sensitive to the

amount of catalyst employed. Trost reports quantitative conversion in the case of the methyl ester analog of **1a** using 1 mol% $\{CpRu(CH_3CN)_3\}\{PF_6\}$. With the ethyl ester, the best yields were obtained by using 8 – 10 mol% ruthenium catalyst. Compound **1b** is a white,

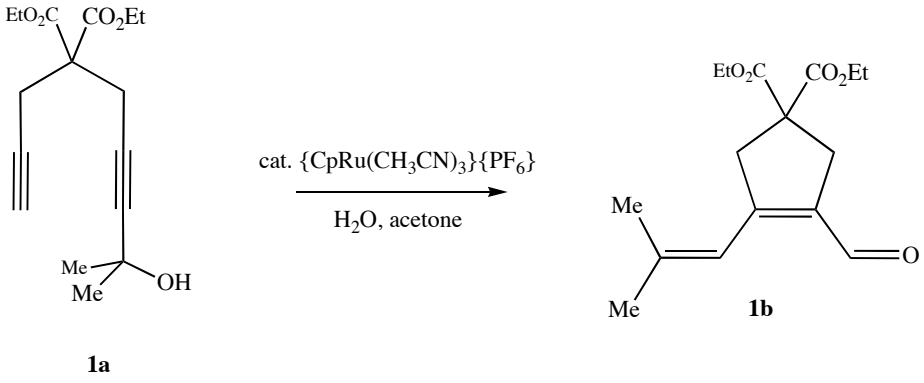

1a **1b** (2.2)

highly crystalline solid with a characteristic aldehyde ^{1}H NMR resonance at 9.85 ppm in chloroform-*d*. The compound is air and moisture stable, likely owing to the presence of the methyl groups on the exocyclic double bond. Diynol **1a** was prepared by deprotonation of DEDPM, followed by quenching with acetone (equation 2.3), and was obtained in good yield (~75%) after column chromatography, on scales as large as 12 g of DEDPM.[27]

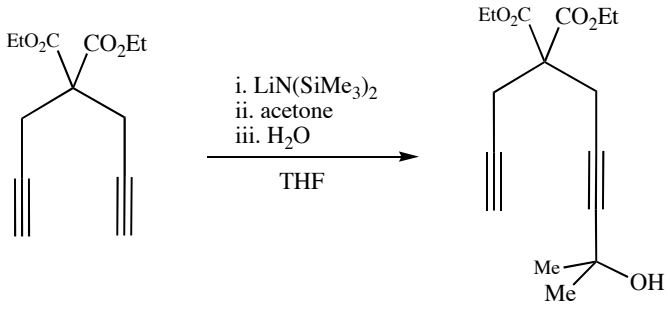

1a (2.3)

The five-membered ring-containing triene, **1c**, is a colorless crystalline solid. The NMR features of the compound are very straightforward showing the expected number of peaks for the structure depicted in equation 2.1. Of note is the ^{13}C NMR shift of the quaternary carbon, which

appears at 57.8 ppm in chloroform-*d*. This value should be compared to that of 56.7 ppm found for the ethyl ester substituted cyclopentene model synthesized previously by Fox (no mention of NMR solvent was made).[28] Addition of **1c** to Mo(NAr)(CHCMe$_2$R)(O-*t*-Bu$_{F6}$)$_2$ (R = Me, Ph) in pentane afforded the new vinyl alkylidene species, Mo(NAr)(CH[5])(O-*t*-Bu$_{F6}$)$_2$ (**2a**, equation 2.4). Complex **2a** is a flaky, orange-yellow solid with limited solubility in pentane. Only

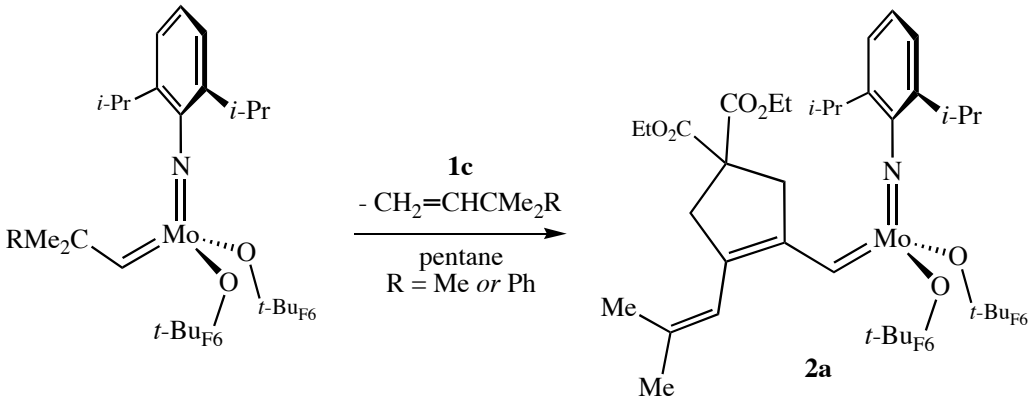

(2.4)

the *syn* isomer is observed in solution, with the alkylidene proton resonance appearing at 12.79 ppm (J_{CH} = 120 Hz) and the alkene proton resonance appearing at 5.96 ppm in methylene chloride-d_2. Unlike previous vinyl alkylidenes prepared our laboratory, compound **2a** is stable as a base-free species.[24,29] The stability of **2a** in the absence of Lewis bases such as THF or quinuclidine is likely a consequence of the bulky ester groups that shield the Mo=C bond, discouraging bimolecular coupling of alkylidenes.[30]

Ultra-violet irradiation of imido alkylidene species has been demonstrated to lead to alkylidene rotation (*syn* to *anti* interconversion) by excitation of the Mo=C π to π* transition.[31] This technique was previously employed to examine the effect of alkylidene rotation on the ROMP of norbornenes.[32] At that time it was found that *anti* alkylidenes give rise to *trans* double bonds along the polymer chain, while *syn* alkylidenes give rise to *cis*. In analogy to these experiments, irradiation of compound **2a** was investigated to determine if alkylidene rotation was important in the formation of five- and six-membered rings during polymerization of DEDPM.

Irradiation of compound **2** in toluene-d_8 at 366 nm with a medium pressure mercury lamp failed to yield any *anti* isomer as judged by ^{1}H NMR spectroscopy. Conducting the irradiation experiments at –78 ºC for up to six hours had no effect. Examination of the electronic absorption spectrum of **2** revealed an intense absorption centered at 360 nm (Figure 2.1). The electronic spectrum of the analogous neopentylidene compound did not show the same intense absorption at 360 nm, but instead was reported to display a broad absorption centered at 305 nm.[31] With compound **2**, conjugation of the alkylidene to the double bonds of the five-membered ring group likely lowers the energy of the π to π* transition.[22] Additionally, a substantial amount of double bond character between Mo and carbon may still remain even when the π* orbital is populated.

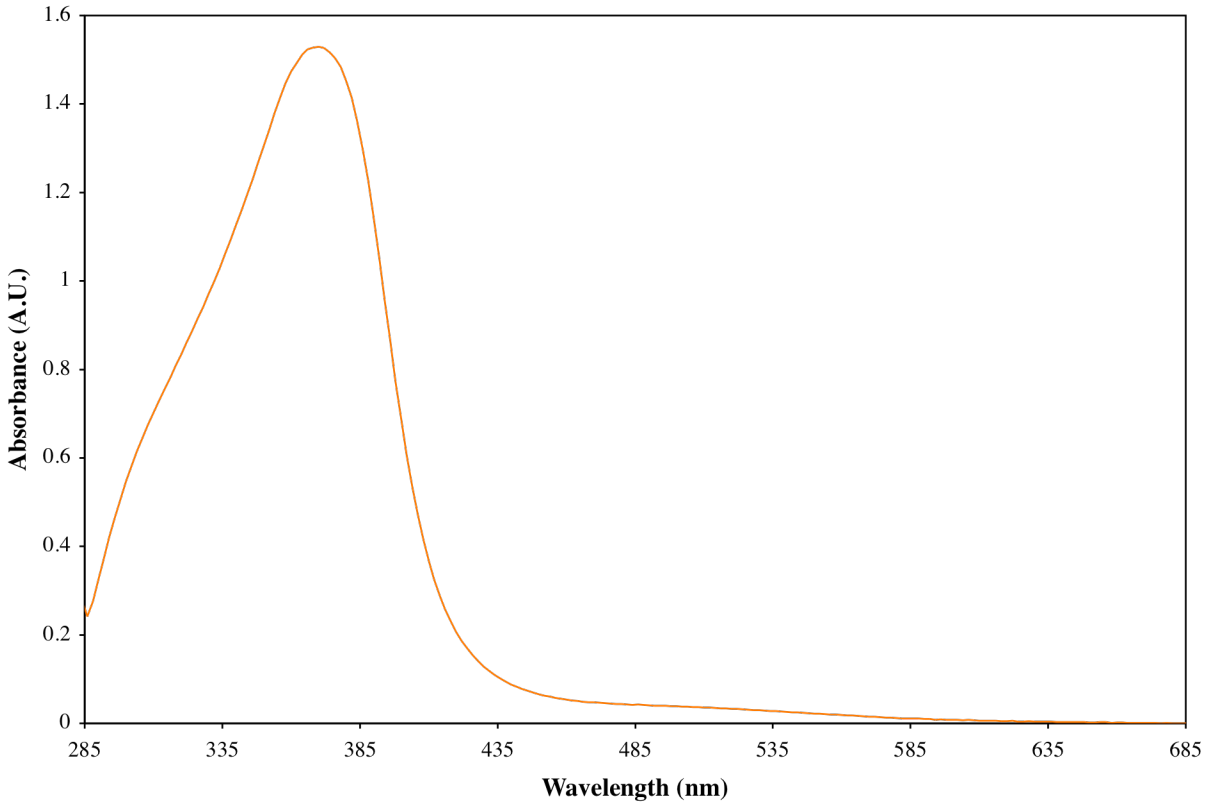

Figure 2.1. Electronic absorption spectrum of **2a** in toluene (66 μM).

2.1.2 Six-membered ring initiators

To complement the five-membered ring initiator described in the previous section, a six-membered ring containing vinyl alkylidene was targeted. Previously, our laboratory reported that 1-vinyl-3-methylene-5,5-*bis*-(carboxyethyl)cyclohex-1-ene (**3a**) is formed as a yellow solid when DEDPM is added to a solution of Mo(NAr)(CHCMe$_2$Ph)(O-*t*-Bu$_{F6}$)$_2$ in the presence of ethylene (Scheme 2.4).[28] The reaction was found to be reproducible in the present case, though

Scheme 2.4. Synthesis of triene **3a**.

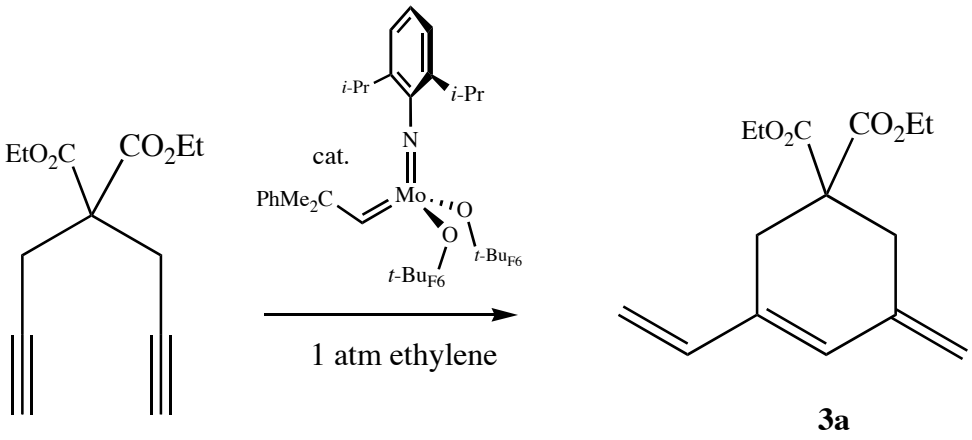

3a

isolated yields of the triene were relatively low (25 – 30%). Subsequent purification of **3a** by column chromatography revealed that the compound is in fact a colorless oil with limited stability in air at room temperature. Therefore, it must be used shortly after it is prepared. It was also reported that this triene reacts with Mo(NAr)(CH-*t*-Bu)(O-*t*-Bu$_{F6}$)$_2$ to produce Mo(NAr)[1-methylidene-3-methylen-5,5-*bis*-(carboxyethyl)cyclohex-1-ene)](O-*t*-Bu$_{F6}$)$_2$ (**4a**, equation 2.5) as a dark solid in low yield (< 12%). Reexamination of this reaction with purified **3a** demonstrated that no more than 45% of the starting neopentylidene complex is consumed over a period 24 hours in pentane, DME, or toluene. Several impurities are formed during this time, some of which are likely to arise from decomposition of the triene itself.

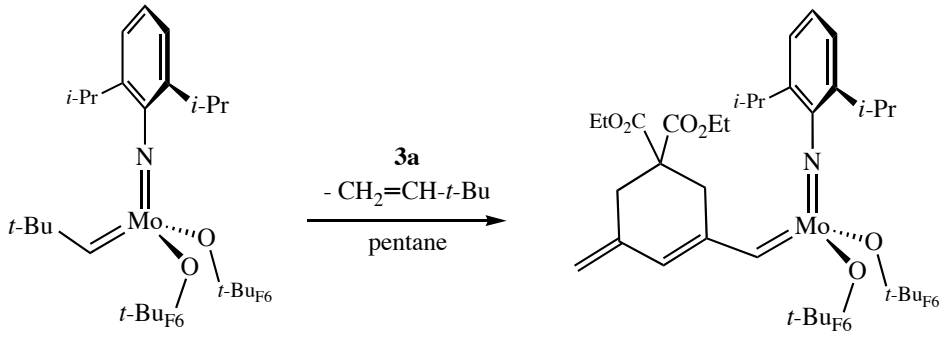

4a

(2.5)

To address the difficulties in preparing and metallating triene **3a**, a diene containing a six-membered ring that lacks the exo methylene group was prepared. Diene **3b** is a reported compound that can be isolated in good yield through an enyne reaction employing $Cl_2(PCy_3)_2Ru{=}CHPh$ as a catalyst (equation 2.6).[33] The diene is more stable than **3a** and can be

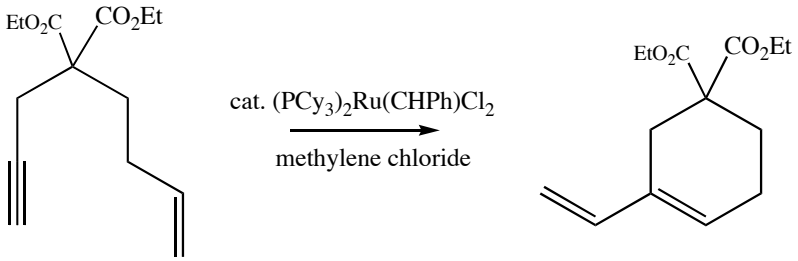

3b

(2.6)

stored at room temperature for short periods of time (1 to 2 days). Compound **3b** reacts readily with Mo(NAr)(CH-*t*-Bu)(O-*t*-Bu$_{F6}$)$_2$ to produce Mo(NAr)[1-methylidene-5,5-*bis*-(carboxyethyl)cyclohex-1-ene)](O-*t*-Bu$_{F6}$)$_2$ (Mo(NAr)(CH[6])(O-*t*-Bu$_{F6}$)$_2$, **4b**) in good yield as orange needle-like crystals (equation 2.7). The H_α resonance for **4b** appears at 12.52 in methylene chloride-d_2 (compare 12.44 ppm reported for **4a**) with a $^1J_{CH}$ value of 125 Hz suggestive of a syn alkylidene. Similar to **2a**, the complex shows limited solubility in pentane and may be crystallized readily.

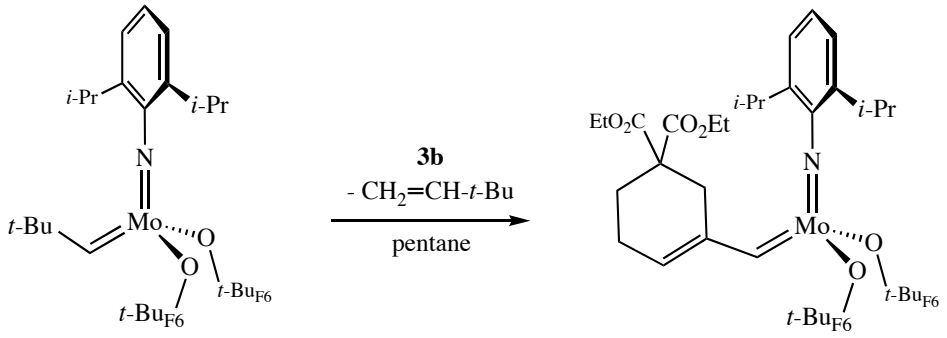

4b

(2.7)

Addition of 2 equivalents of LiO-*t*-Bu to **4b** yields complex **4c** (equation 2.8) as an orange-red crystalline solid. ^{1}H NMR spectra of **4c** indicate that the complex retains both equivalents of LiO-*t*-Bu$_{F6}$ even upon repeated crystallization from pentane. The lithium salt does not appear to interact with **4c** in solution; the CF_3 groups of the salt appear as a singlet in the

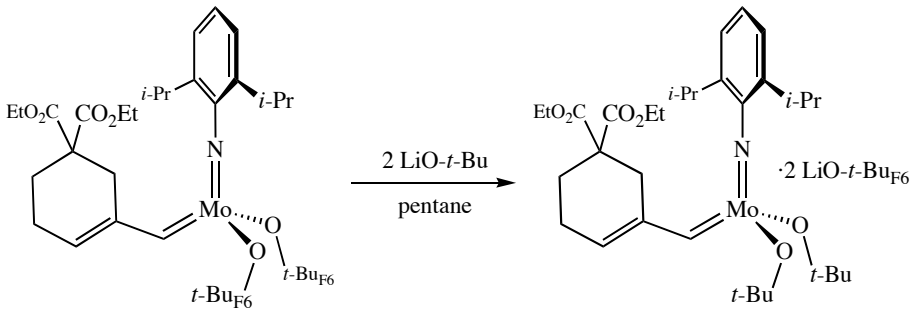

4b **4c**

(2.8)

^{19}F NMR, and the alkylidene H_α resonance displays the same chemical shift as that in samples free of the lithium salt (*vida infra*). Compound **4c** may be prepared free of the lithium salt by treating **4b** with 2 equivalents of TlO-*t*-Bu. Solid samples of **4c** prepared from TlO-*t*-Bu could not be isolated. Prolonged cooling at –25 ºC of a saturated pentane solution of **4c** (prepared from TlO-*t*-Bu) led to decomposition as judged by ^{1}H NMR. Olefinic resonances were observable consistent with bimolecular coupling of alkylidenes.[30] Apparently, the presence of LiO-*t*-Bu$_{F6}$ is beneficial to both the stability and crystallinity of **4c**. The H_α resonance for **4c** appears at 11.67 ppm in methylene chloride-d_2 with J_{CH} = 119 Hz, again consistent with a *syn* alkylidene. This

chemical shift value should be compared to that of 11.87 ppm reported for Mo(NAr)(CH[5])(O-*t*-Bu_{F6})$_2$ (**2c**).[34] The difference (0.20 ppm in methylene chloride-d_2) demonstrates the effect on chemical shift in moving from a six- (11.67 ppm) to a five-membered (11.87 ppm) ring.

Crystals of **4c**·2LiO-*t*-Bu_{F6} suitable for X-ray diffraction were grown by slow cooling of a saturated heptane solution. Two views of the solid state structure are depicted in Figures 2.2 and 2.3. Consistent with solution NMR, the alkylidene is the *syn* isomer and the structure contains two equivalents of LiO-*t*-Bu_{F6} per molybdenum atom. Four equivalents of the lithium salt crystallize in a Li_4O_4 heterocubane-type structure, coordinating to one ester moiety of two catalyst molecules (Figure 2.2).

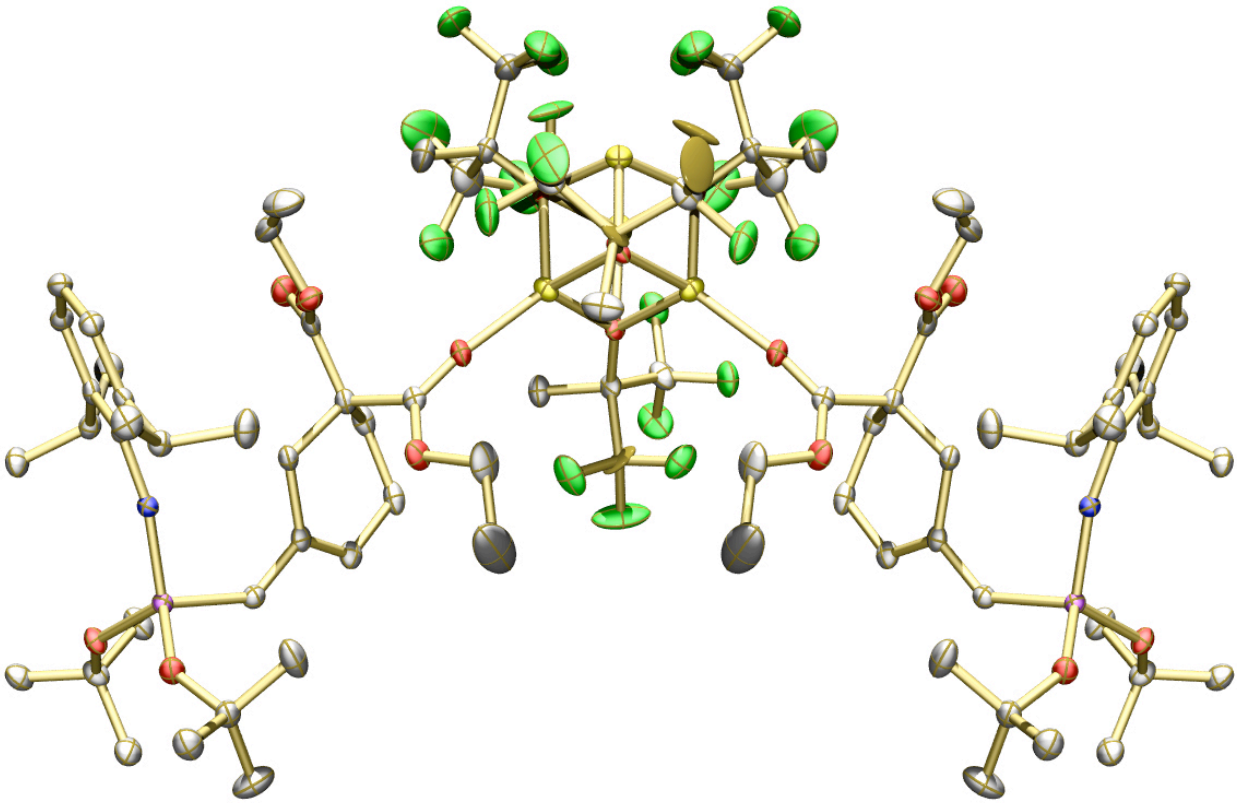

Figure 2.2. Thermal ellipsoid (35%) rendering of **4c**·2LiO-*t*-Bu_{F6}. Hydrogen atoms omitted for clarity.

The orientation of the six-membered ring is such that the ester groups are directed above the MoOO plane, as depicted in equation 2.8. The bond lengths and angles (caption to Figure 2.3) about Mo are similar to those of related five-membered ring alkylidene species, **2c**, prepared by Jennifer Adamchuk.[34] One notable difference between the two structures is the orientation of the isopropyl groups of the aryl imido. These groups appear to rotate in different directions to accommodate the spatial positions of the ester groups in the five- and six-membered rings.

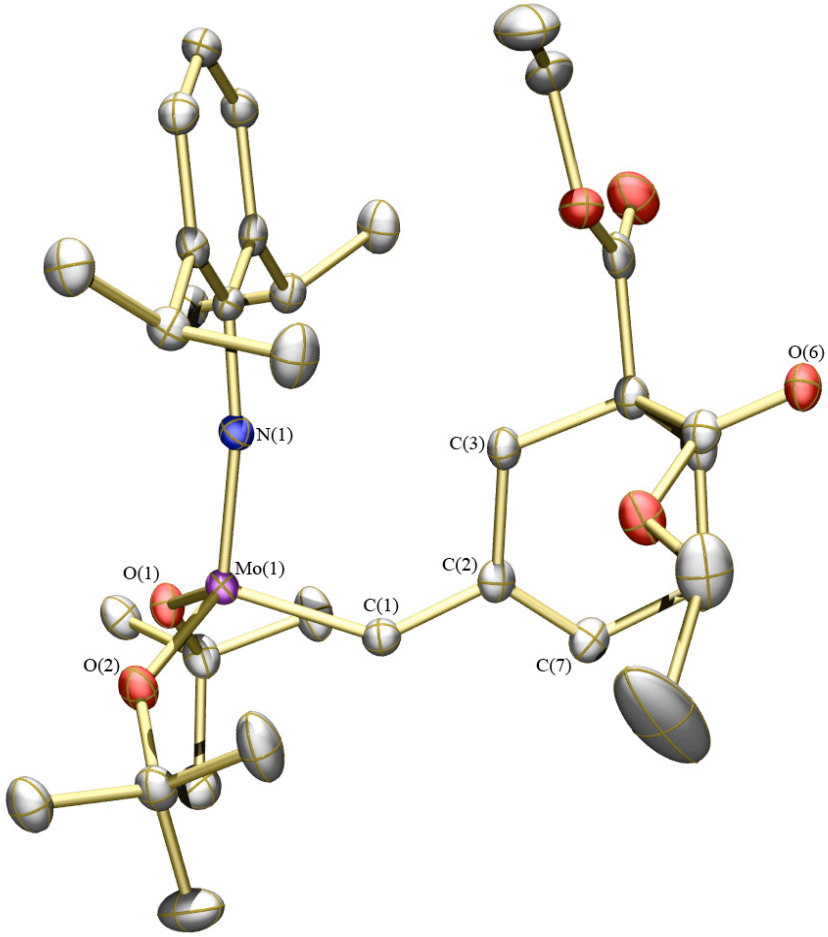

Figure 2.3. Thermal ellipsoid (50%) rendering of part of the solid state structure of **4c**. Hydrogen atoms omitted for clarity. Selected bond distances (Å) and angles (°): Mo(1)–C(1) = 1.911(2); Mo(1)–N(1) = 1.7345(19); Mo(1)–O(1) = 1.8897(16); Mo(1)–O(2) = 1.8845(16); C(1)–C(2) = ; C(2)–C(3) = ; C(3)–C(4) = ; N(1)–Mo(1)–C(1) = 101.02(9); Mo(1)–C(1)–C(2) = 138.18(17).

2.1.3 Initiation experiments

Initiation experiments employing compounds **2a**, **4b**, and **4c**, were examined to determine the effect of replacing the standard neopentylidene ligand with the model vinyl alkylidenes. These reactions also allow one to follow the formation of five- and six-membered rings during early stages of polymerization. ^{1}H NMR spectra of the alkylidene region for these reactions were used to determine the nature of the initial insertion products (five- versus six-membered ring). Assignments were made by comparison to the alkylidene resonances of the isolated complexes, **2c** and **4c**. In reactions with initiators **2a** and **4b**, excess LiO-*t*-Bu was added to the solutions after consumption of DEDPM. The more basic *tert*-butoxide ligand is capable of displacing the O-*t*-Bu$_{F6}$ ligand quickly and quantitatively. In this way, spectra obtained with initiators **2a** and **4b** can be compared directly to spectra obtained with initiator **2c**.

Addition of 1 – 5 equivalents of DEDPM to methylene chloride-d_2 solutions of initiators **2a** and **4b** (complexes bearing O-*t*-Bu$_{F6}$ ligands) gave rise to a mixture of products according to ^{1}H NMR. When less than 5 equivalents of DEDPM are employed in experiments with **2a** and **4b**, resonances for the initial alkylidenes remain visible, indicating that substantial amounts of **2a** and **4b** remain unreacted. The remaining alkylidene resonances are assignable to various insertion products (first, second, propagating species) containing five- or six-membered rings adjacent to molybdenum, Mo=CH(5) or Mo=CH(6). As demonstrated in part A of Figure 2.4, polymerizations initiated by **4b** show predominate formation of Mo=CH(6) insertion products. Minor resonances near 12 ppm are also visible for Mo=CH(5) species. Similar spectra were obtained with initiator **2c**. These observations suggest that at early stages of polymerization, six-membered rings are formed preferentially with O-*t*-Bu$_{F6}$ supported catalysts. This fact is somewhat surprising considered that bulk polymerizations initiated by **2a** and **4b** give rise to polymers possessing nearly equal amounts of five- and six-membered rings.

The *tert*-butoxide supported analog, **4c**, proved to be a more effective initiator than either **2a** or **4b**. NMR spectra of initiation reactions employing **4c** are consistent with predominant (90 – 95%) formation of five-membered rings. This observation is consistent with bulk

polymerizations employing **2c** and Mo(NAr)(CH-*t*-Bu)(O-t-Bu)$_2$, which were found to produce polymers with 95% five-membered rings. The initiation results are also very similar to those obtained by Jennifer Adamchuk for initiator **2c** and the vinyl alkylidene, Mo(NAr)(CHCH=CHMe)(O-*t*-Bu)$_2$.[34] The ^{1}H NMR spectrum of the alkylidene region for the reaction of **4c** with 1.9 equivalents of DEDPM is shown in part B of Figure 2.4. As evident from Figure 2.4, initiator **4c** is consumed to a greater extent than initiator **4b** in reactions involving 2 - 5 equivalents of DEDPM. These results are consistent with the smaller k_p/k_i ratios typically displayed by *tert*-butoxide catalysts in relation to their fluorinated counterparts.[35] The ratio of k_p/k_i for **4c** was calculated to be 0.60 in methylene chloride-d_2 at 23 ºC. This value is significantly lower than that found for the neopentylidene initiator, Mo(NAr)(CH-*t*-Bu)(O-*t*-Bu)$_2$.[17] The broad peak upfield of 12.1 ppm in part B of Figure 2.4 could not be assigned with certainty, though the chemical shift value is consistent with an *anti* alkylidene isomer, possibly coordinated to an ester oxygen of DEDPM.

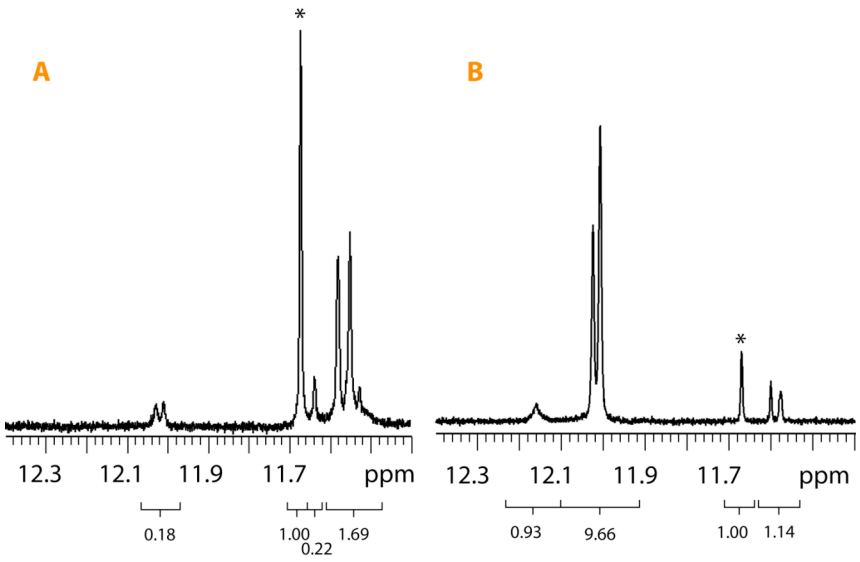

Figure 2.4. Alkylidene region of the 500 ^{1}H NMR spectrum (methylene chloride-d_2) of: (A) **4b** after addition of 4.4 equivalents of DEDPM followed by 2 equivalents of LiO-*t*-Bu; (B) **4c** upon addition of 1.9 equivalents of DEDPM. In each spectrum, the asterisk denotes the initial alkylidene (CH[6]).

2.2 Molybdenum imido alkylidene complexes supported by carboxylate ligands

2.2.1 Synthesis of carboxylate complexes

In contrast to imido alkylidene initiators supported by *tert*-butoxide ligands, initiators supported by carboxylate ligands give rise to 99% six-membered rings in polymers of DEDPM.[18] Carboxylate complexes were first examined by Florian Schattenmann in this laboratory.[36] An important finding from the original work was the fact that bulky carboxylate ligands are necessary to prevent formation of "ate" species (see later). Complexes of the triphenylacetate ligand can be prepared in straightforward fashion from the triflate precursor, $Mo(NR)(CHR')(OTf)_2(DME)$, by salt metathesis with NaO_2CCPh_3 in THF (equation 2.9).

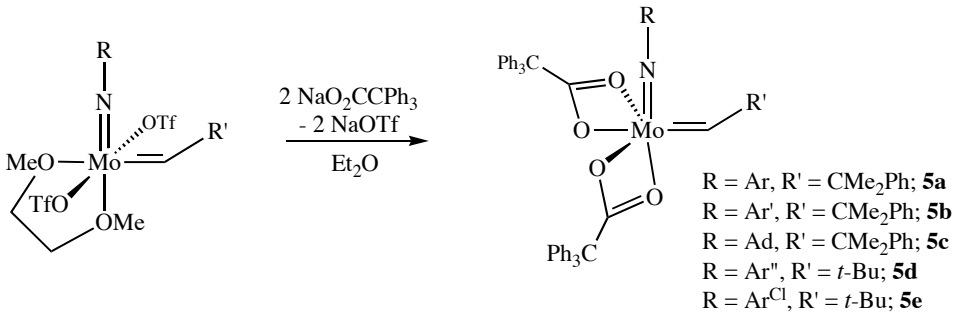

(2.9)

The reaction works well for the various imido groups listed in equation 2.9 (Ar = 2,6-diisopropylphenyl; Ar′ = 2,6-dimethylphenyl; Ad = 1-adamantyl; Ar′′ = 2-*tert*-butylphenyl; Ar^{Cl} = 2,6-dichlorophenyl). Compounds **5a**, **5c**, and **5d** were reported previously.[18]

All the complexes in equation 2.9, except **5b**, are soluble in organic solvents other than alkanes. Compound **5b** proved to be insoluble in common organic solvents with the exception of methylene chloride. Alkylidene H_α resonances for **5a**-**e** appear downfield of 13.1 ppm in benzene-d_6 or methylene chloride-d_2. To a degree, this chemical shift is a measure of the electrophilicity at the metal center and demonstrates the electron-deficient nature of these complexes. All alkylidenes appear to exist as the *syn* isomer in solution as judged by J_{CH} values in the range 117 to 125 Hz (see Experimental section). The imido groups for compounds **5a**-**e**

show free rotation about the N-C bond at room temperature. Spectra of the complexes also display time-averaged C_S symmetry, indicative of fast isomerization of the κ^1 and κ^2 modes of the carboxylate ligand. The crystal structure of **5d** was reported previously and demonstrated that both carboxylates are bound κ^2 in the solid state.[18]

Most carboxylate ligands other than triphenylacetate proved unsuitable in supporting well-defined monomeric complexes. For example, numerous attempts to prepare pivalate (O_2C-*t*-Bu) complexes yielded species that displayed several alkylidene peaks by ^{1}H NMR and could not be purified by repeated recrystallization. The nature of these complexes is at best a matter of speculation, though they appear to be oligomeric in nature based on their poor solubility in arene and ethereal solvents. The use of slightly larger carboxylates such as 2,6-dimethylbenzoate (O_2CAr') leads to the formation of "ate" complexes in which three carboxylate ligands bind to the imido alkylidene fragment creating an anionic complex. Such species do not react with alkynes or olefins and are therefore undesirable. In the case of the 1-adamantyl imido group, one of these compounds was isolated and characterized (**6c**, equation 2.10). Spectral features of **6c**

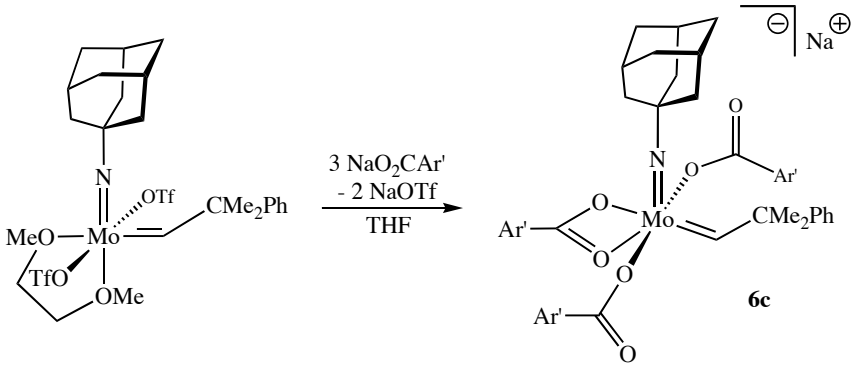

(2.10)

are similar to those of the triphenyl acetate complexes discussed above. Two of the carboxylate ligands are equivalent on the NMR timescale indicative of C_S symmetry in solution. No solvent incorporation is observable by NMR, which suggests that the sodium ion is bound to one or more of the terminal oxygen atoms of the benzoate ligands. An attempt at replacing the sodium cation with $\{(n\text{-Bu})_4N\}\{PF_6\}$ failed, further supporting a strong interaction between Na^+ and one of the

carboxylate oxygen atoms. Addition of PMe_3 to **6c** was observed to produce a PMe_3 adduct of a dicarboxylate species according to ^1H NMR spectroscopy (equation 2.11). A precipitate was observed several minutes after addition of PMe_3 to a methylene chloride-d_2 solution of **6c**. The resulting ^1H NMR spectrum displayed a doublet alkylidene resonance (J_{HP} = 6.0 Hz) and two singlet resonances of area six (each) for the methyl groups of the benzoate ligands, consistent with an unsymmetric carboxylate environment. It should be noted that coordination of Lewis bases has been used in the past to allow for isolation of alkylidene complexes bearing small alkoxide ligands that are otherwise unstable.[37]

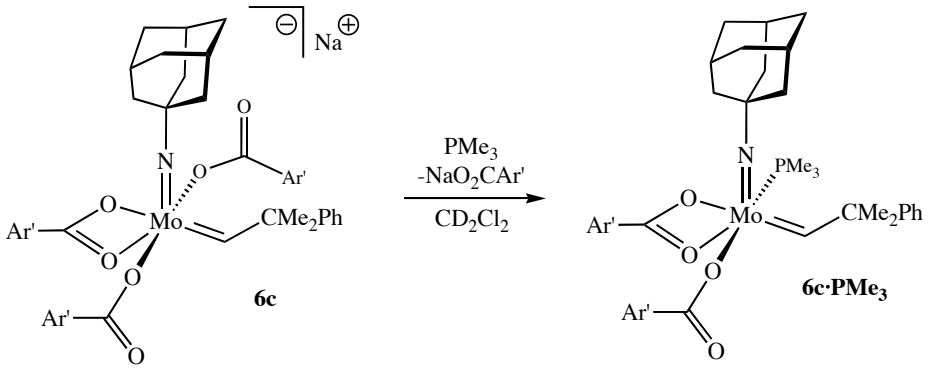

(2.11)

Diphenylmethylacetate ($Ph_2MeCO_2^-$) was reported by Schattenmann to support an alkylidene complex of the 2,6-diisopropylphenyl imido ligand[18] (**7a**, equation 2.12). The spectral features of **7a** are nearly identical to those of **1a**, showing the same time-averaged C_S symmetry by NMR. Examination of the methyl groups of the carboxylate ligand by NMR spectroscopy at temperatures down to 193 K (methylene chloride-d_2) revealed no descent in symmetry as expected for a locking out of the κ^2,κ^2-dicarboxylate structure observed in the solid-state. Complexes of diphenylmethylacetate possessing smaller imido groups could not be isolated. For example, attempts to prepare $Mo(NAr'')(CH\text{-}t\text{-}Bu)(O_2CCMePh_2)_2$ resulted in an insoluble yellow powder that resisted dissolution in dichloromethane.

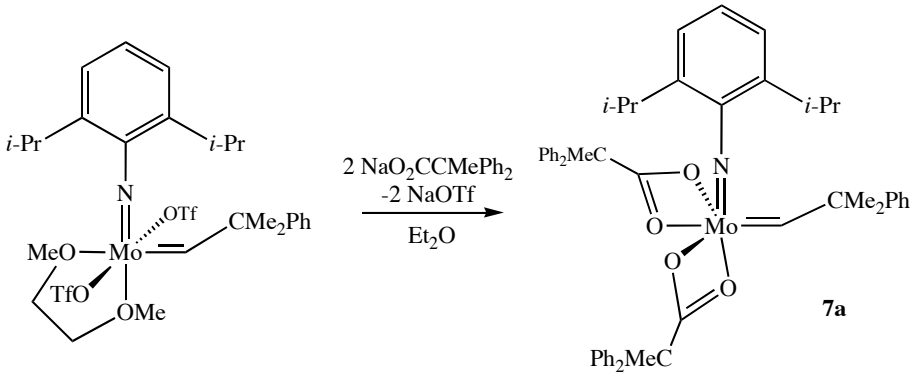

(2.12)

2.2.2 Base adducts of triphenylacetate complexes

Base adducts of imido alkylidene complexes are often prepared as simple models of substrate-catalyst complexes.[24] The carboxylate compounds may be viewed as 18 electron species if the imide is considered as a 5 electron ligand (neutral formalism) and the carboxylates are bound κ^2. As a result, the compounds are reluctant to bind Lewis bases even though they are sufficiently electron deficient. However, compounds **5b**-**d** will react with PMe_3 to give mono-adducts (**5b-d·PMe$_3$**, equation 2.13).

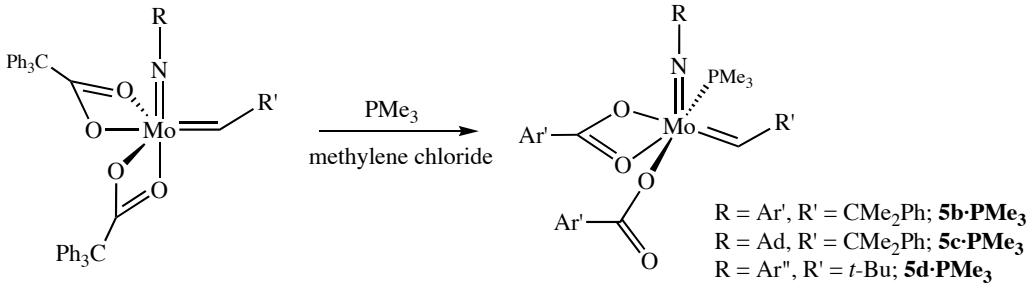

(2.13)

Compound **5d·PMe$_3$** was initially prepared by Schattenmann.[36] At that time it was also observed that compound **5a**, which possess the bulkier 2,6-diisopropylphenyl substituted imide, only binds PMe_3 reversibly. The phosphine adducts, **5b-d·PMe$_3$**, are similar to the base-free complexes and may be conveniently crystallized from methylene chloride/pentane mixtures. NMR spectra of **5c·PMe$_3$** and **5d·PMe$_3$** show inequivalent carboxylate environments, consistent with the structure depicted in equation 2.13. In contrast, compound **5b·PMe$_3$** shows equivalent

carboxylate ligands and a freely rotating 2,6-dimethylphenyl group. The methyl groups of the neophylidene ligand are inequivalent, eliminating the possibly that **5b·PMe$_3$** possesses C_S symmetry. Presumably, one of the carboxylate ligands must bind in a monodentate fashion due to the electronic and coordinative saturation at the metal, so the spectrum of **5b·PMe$_3$** is likely the result of a rapid exchange process.

The alkylidene protons of **1b-d·PMe$_3$** display coupling to phosphorous of 5-6 Hz, which is comparable to coupling constants for various phosphine adducts of imido alkylidene complexes possessing alkoxide ligands.[24] Spectra of freshly crystallized material show the presence of the *syn* isomer exclusively. However, upon standing at room temperature, the phosphine adducts convert over several days to the *anti* isomers. Compound **5e**, which contains the 2,6-dichlorophenyl substituted imide reacts with PMe_3 to give a mixture of two products. One product is the desired adduct, **5e·PMe$_3$**, while the second is proposed to be an amido alkylidyne (**5e′·PMe$_3$**, equation 2.14) as judged by ^{1}H NMR. Proton transfer reactions of the type shown in equation 2.14 have been observed before in complexes containing the 2,6-dichlorophenyl imide.[38] Typically, these isomerizations occur when the alkylidene proton is sufficiently acidic to be removed with a mild Brønsted base.[39] The electron deficient nature of the triphenylacetate ligands likely renders the alkylidene proton susceptible to deprotonation by PMe_3, ultimately resulting in the alkylidyne complex **5e′·PMe$_3$**. Attempts at isolation of **5e·PMe$_3$** or **5e′·PMe$_3$** resulted only in mixtures of the two tautomers that could not be separated.

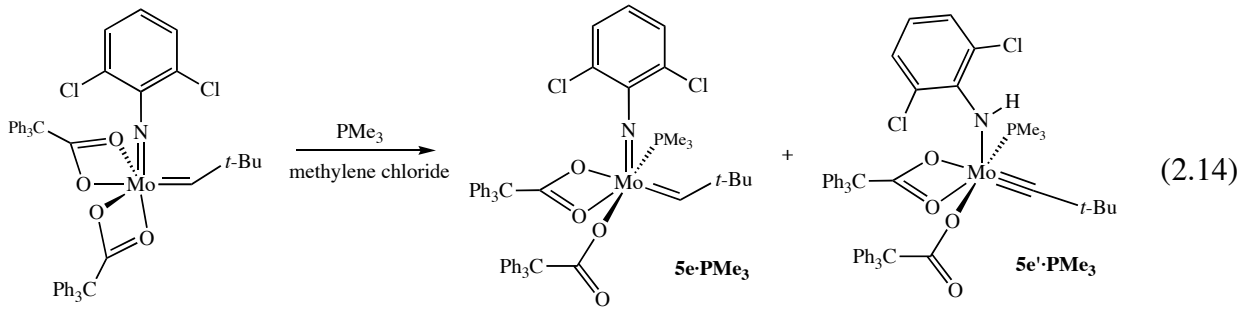

(2.14)

In order to better understand the nature of the PMe_3 adducts, an X-ray diffraction study of **5b·PMe$_3$** was undertaken. Suitable crystals of **5b·PMe$_3$** were grown from a saturated solution of 1:1 methylene chloride/pentane. The solid state structure is shown in Figure 2.5 (see caption for metric data).

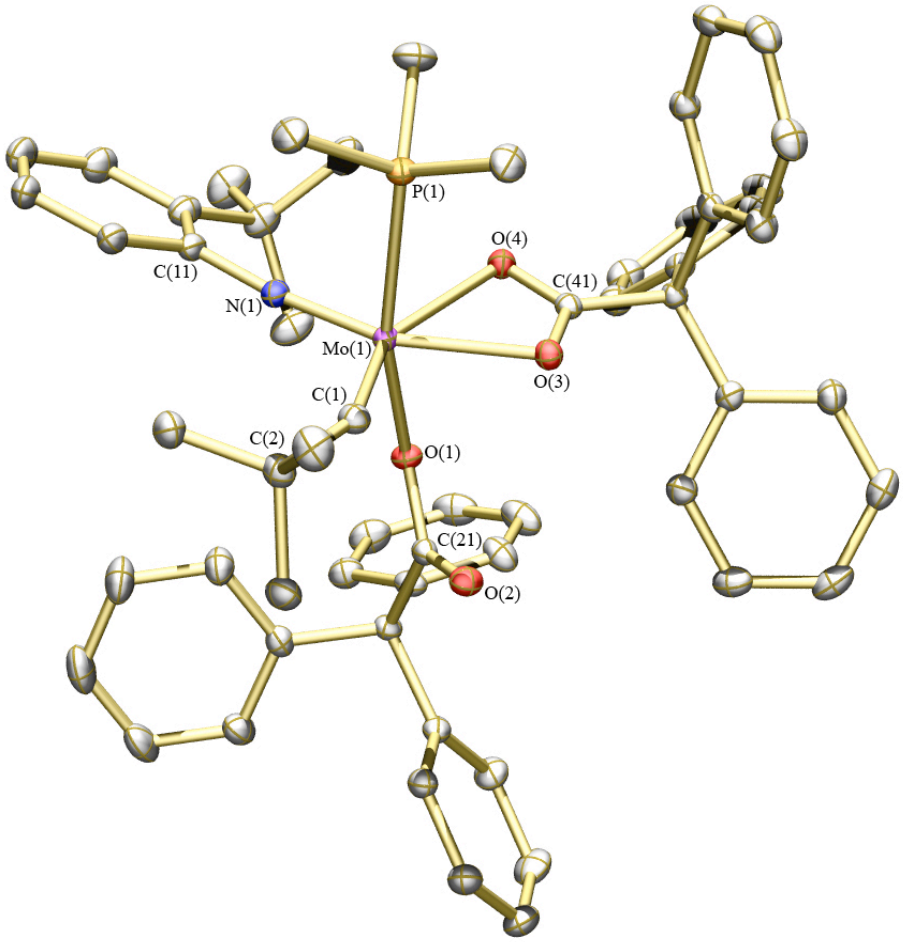

Figure 2.5. Thermal ellipsoid rendering (50%) of the solid state structure of **5d·PMe$_3$**. Hydrogen atoms and cocrystallized molecules of pentane and methylene chloride omitted for clarity. Selected bond distances (Å) and angles (°): Mo(1)–C(1) = 1.9107(18), Mo(1)–N(1) = 1.7402(15), Mo(1)–O(1) = 2.0822(13), Mo(1)–O(3) = 2.2597(13), Mo(1)–O(4) = 2.2873(13), Mo(1)–P(1) = 2.4967(5), N(1)–Mo(1)–C(1) = 106.04(8), P(1)–Mo(1)–O(1) = 164.68(4), O(3)–Mo(1)–O(4) = 57.27(5), Mo(1)–C(1)–C(2) = 152.65(15), Mo(1)–N(1)–C(11) = 173.51(13), O(1)–C(21)–O(2) = 124.63(16), O(3)–C(41)–O(4) = 118.94(16).

Compound **5d·PMe$_3$** displays a pseudo-octahedral geometry with one monodentate and one bidentate triphenylacetate ligand. The phosphine is bound to the CNOO-face of the molecule, which is reminiscent of the structure of Mo(NAr)(CH-*t*-Bu)(O-*t*-Bu$_{F6}$)$_2$(PMe$_3$), in which phosphine binds to the CNO face of the original CNOO tetrahedron.[24] The alkylidene exists as the *syn* isomer, consistent with solution NMR studies. The 2-*tert*-butylphenyl imide is oriented such that the aryl ligand lies nearly coplanar with the alkylidene and the *t*-Bu group (of the imide) is turned 180º away. As expected, the monodentate carboxylate ligand has a significantly shorter Mo-O bond length than the bidentate ligand. The bulky trityl groups of the carboxylate extend out into space shielding the periphery of the molecule and creating a very crowded coordination environment.

2.3 Oligomeric polyenes

2.3.1 Synthesis of a five-membered ring dimer

To examine the structure of polyenes prepared from DEDPM, oligomeric fragments of the polymer chain were synthesized in stoichiometric reactions. These reactions take advantage of the "Wittig-like" reactivity of Schrock-type carbenes with carbonyl groups.[40] The byproducts of these reactions are molybdenum-oxo species, although their exact composition is not known. Addition of aldehyde **1b** to complex **2a** yielded the dimeric pentaene, **8a** (equation 2.15). The pentaene is an ivory-colored solid with limited stability in air, though it may be purified by chromatography on silica gel. The NMR features of **8a** are consistent with the structure shown in equation 2.15. Two olefinic resonances are found at 6.35 and 5.99 ppm and two ring methylene resonances are found at 3.32 and 3.20 ppm in chloroform-*d*. Higher order oligomers (up to a heptamer) containing five-membered rings have subsequently been prepared in our laboratory following similar methodology.[41] These oligomers display a corresponding increase

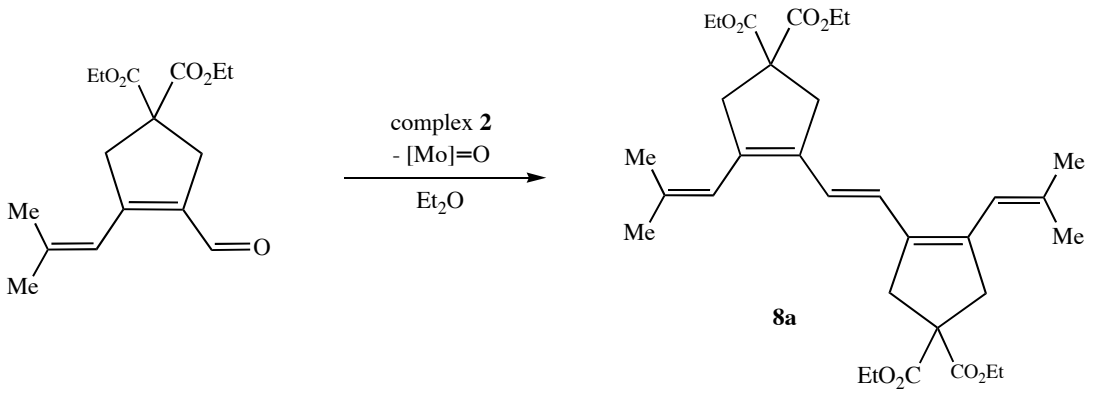

(2.15)

in E_{max} as a function of 1/N, where N represents the number of double bonds. Two examples of these oligomers, the dimer and trimer, have also been isolated and crystallographically characterized by Corina Scriban.[42] The structure of these two oligomers confirms the alternating *cis-trans* structure of the five-membered ring polyenes.

2.3.2 Synthesis of a trimer possessing five- and six-membered rings

To prepare an oligomer containing a six-membered ring, the reaction in equation 2.5 was reexamined using a molybdenum complex that contains the less sterically demanding 2-*tert*-butylphenyl (Ar′′) imido ligand. Reaction of Mo(NAr′′)(CH-*t*-Bu)(O-*t*-Bu_{F6})$_2$ with triene **3a** afforded the bimetallic species (**4d**) (equation 2.16). Compound **4d** is obtained as a pentane soluble brown powder. The complex can be freed of traces of the starting neopentylidene complex upon repeated recrystallization from pentane. The spectroscopic features

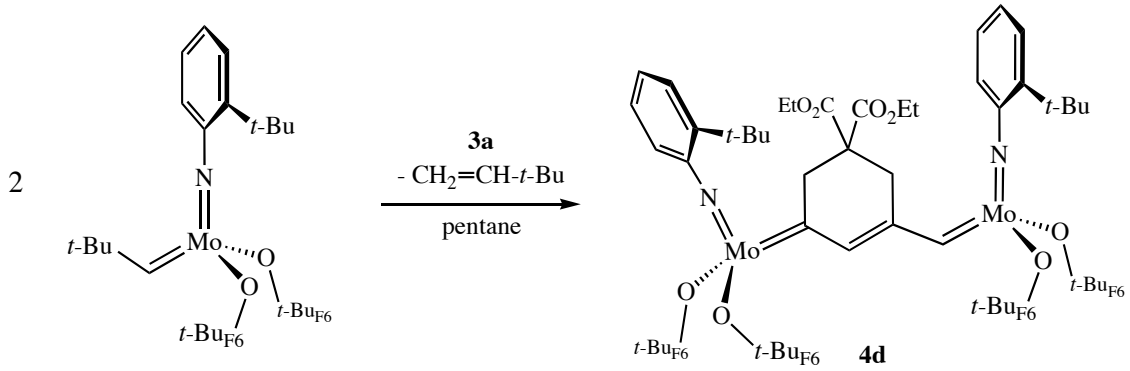

(2.16)

of the molecule are consistent with the proposed bimetallic structure shown in equation 2.16. The primary alkylidene proton resonance is found as a singlet at 12.38 ppm in benzene-d_6 with a J_{CH} value of 125 Hz, consistent with formulation of the species as a *syn* alkylidene. No information concerning the orientation of the secondary alkylidene could be obtained, and minor resonances in the ^{1}H NMR spectrum of **4d** suggest that rotational isomers about the Mo=C bond are present. The ^{13}C NMR spectrum shows two alkylidene resonances at 271.1 and 259.0 ppm. The upfield resonance is assigned to the primary alkylidene carbon on the basis of an observed coupling of the alkylidene carbon to one proton.

Reaction of two equivalents of aldehyde **1b** with complex **4d** afforded the trimeric heptaene, **8b** (equation 2.17). Two isomers of **8b** are observed in a ratio of ~2:1. All NMR data are consistent with formation of *E* and *Z* isomers, as shown in equation 2.17.

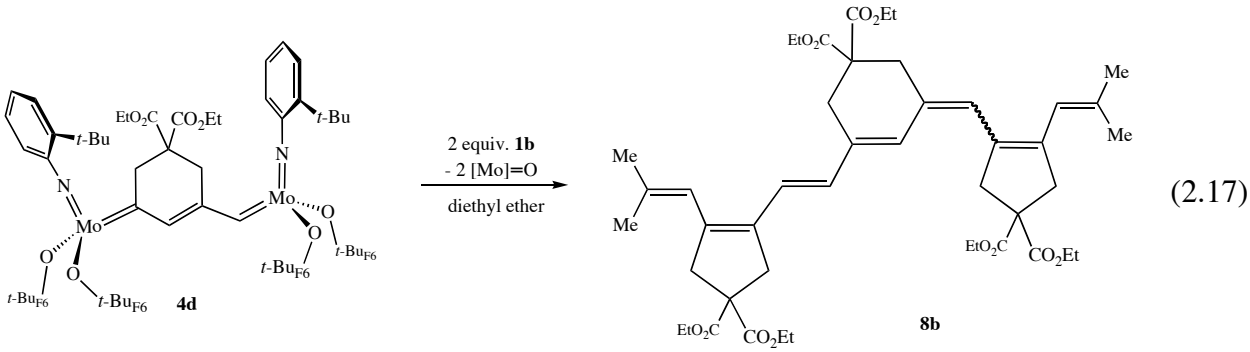

(2.17)

Consequently, polymers which contain both five-membered and six-membered rings are likely to display conformational disorder, owing to the likelihood of *E* and *Z* isomers being formed. This isomerism may be one reason why polymers that contain both five-membered and six-membered rings generally are more soluble than those that contain only five-membered rings. The λ_{max} value for **8b** is 384 nm (methylene chloride), 20 nm lower than the λ_{max} value for the corresponding all five-membered ring trimer in methylene chloride (404 nm). Although no other oligomeric polyenes that contain six-membered rings have been synthesized, it appears that the presence of one six-membered ring is necessary to effect a significant decrease in λ_{max}.

DISCUSSION

Catalysts now exist for the selective polymerization of DEDPM. As result, polymers with nearly exclusive five- and six-membered ring compositions can be prepared. However, no consistent explanation of the factors responsible (chain-end control, steric effects, electronic effects, alkylidene rotation, etc.) for the observed α- versus β-selectivity has emerged. Each set of catalysts (*tert*-butoxide supported and carboxylate supported) demonstrates properties consistent with living polymerization processes, though rates of initiation with neopentylidene or neophylidene versions of these catalysts are insufficiently low to allow for in-depth studies of ring formation during earlier stages of polymerization.

In the case of the alkoxide catalysts, substitution of the neopentylidene ligand with the five- and six-membered ring vinyl alkylidenes affords new initiators (**2a**, **4a**-**c**) that contain a fragment of the growing polymer chain as the alkylidene group. These complexes are effective initiators for the polymerization of DEDPM and serve as models for propagating species. Particularly diagnostic is the 0.2 ppm difference in ^{1}H chemical shift between five- and six-membered ring alkylidenes. This separation allows for quantification of ring formation during early stages of polymerization. Results from initiation experiments demonstrate that both the five- and six-membered ring initiators give rise to predominantly five-membered ring polymer when supported by *tert*-butoxide ligands. Therefore, chain-end control *is not* responsible for the observed regioselectivity. The percentage of five-membered ring polymers formed during early stages of polymerization (~10%) is slightly less than that observed in bulk polymers that are formed with initiators **2c** and **4c**. This fact suggests that the bulk of the propagating chain in tandem with the decreased steric hindrance of the *tert*-butoxide ligands may direct α-addition of the incoming alkyne. Unfortunately, due to failed attempts at generating *anti* alkylidene isomers of compound **2c**, the effect of alkylidene rotation on α- versus β-selectivity could not be examined.

An advantage of the vinyl alkylidene initiators is that they allow for the preparation of oligomeric fragments of the polymer chain. These oligomers confirm the alternating *cis-trans* structure of the five-membered ring polymers, and demonstrate the potential for *E*/*Z* isomerization in polymers containing six-membered rings. Unfortunately, analogous species to compounds **2a** and **4a** could not be prepared with carboxylate ligands. It appears that the ability to prepare and isolate stable, well-defined, carboxylate complexes depends critically on the steric encumbrance of the ligand (both alkylidene and carboxylate). Carboxylates that contain smaller substituents result in "ate" complexes or ill-defined oligomeric species.

Electronically, the carboxylate compounds are more electron deficient than corresponding alkoxide compounds (even those that contain the most electron withdrawing O-*t*-Bu_{F6} ligand). As a result, the compounds appear to favor κ^2 bonding of the carboxylate ligands, which renders the molybdenum center both electronically and coordinatively saturated. This saturation produces a metal center that remains unreactive toward all but the most potent Lewis bases. The reactivity of the carboxylate catalysts towards olefins and alkynes can therefore be reconciled by considering that the more reactive terminal alkyne is capable of capturing an unsaturated (κ^1, κ^1) metal fragment, whereas the alkene is not.

The true utility of the carboxylate species is their ability to selectively polymerize DEDPM to give a polymer containing all six-membered rings. The factors responsible for selective β-addition of alkynes to initiators **5c** and **5d** are intriguing and provide a contrast to the *tert*-butoxide supported catalysts. Chain-end control is unlikely, as demonstrated by experiments with related alkoxide systems. A space-filling diagram of the solid-state structure of **1d·PMe$_3$** viewed along the Mo-P bond vector is shown in Figure 2.6. Of note are the bulky trityl groups of the carboxylate ligands and the *tert*-butyl group of the imide that extend out above the CNOO face of the molecule. If PMe_3 is viewed as crude model of approaching alkyne, then it is evident from the space-filling diagram that α-addition will be sterically disfavored due to interaction between the alkyne substituents and the bulky ligands of the catalyst. Steric factors have been invoked before to explain the observed regioselectivity in alkyne and DEDPM polymerization.[29]

In support of this assertion is the observation that malonates with smaller ester groups (methyl) do not show the same degree of regioselectivity.[36] Furthermore, catalysts containing the 2,6-dimethylphenyl and 2,6-dichlorophenyl imides also do not produce poly-DEDPM with exclusively 6-membered rings. These imido groups do not extend above the CNOO face of catalyst to the same extent as the 2-*tert*-butylphenyl and 1-adamantyl imides. Thus, the three-dimensional nature of the imide substituents of catalysts **1c** and **1d** is more apparent during monomer enchainment than that of **1b** and **1e**. Such results further implicate the role of steric effects in controlling the regiochemistry of alkyne addition.

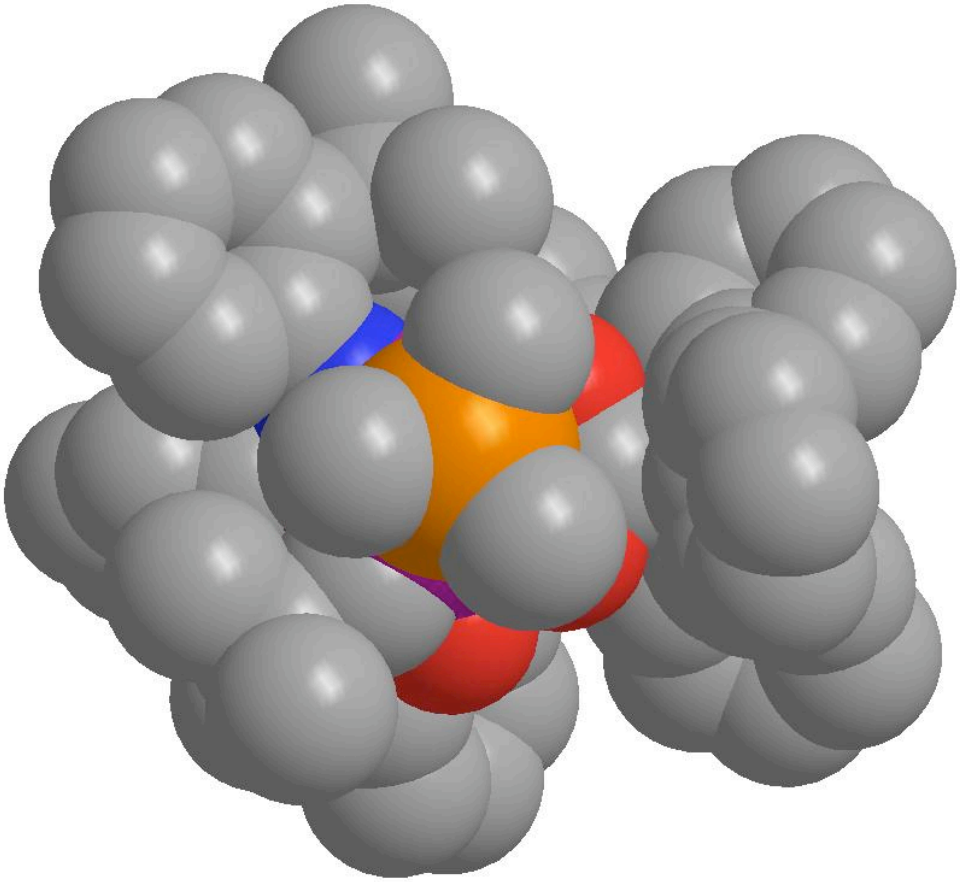

Figure 2.6. Space filling diagram of the structure of **5d·PMe$_3$**, as viewed down the P(1)–Mo(1) bond vector.

CONCLUSIONS

New molybdenum imido alkylidene initiators for the polymerization of DEDPM have been prepared and characterized. In the case of complexes supported by alkoxides (O-*t*-Bu_{F6} and O-*t*-Bu), vinyl alkylidene ligands containing five- and six-membered rings that mimic the propagating species have been isolated. These catalyst are excellent initiators for DEDPM polymerization, displaying k_p/k_i ratio less than one. Stoichiometric reaction of these vinyl alkylidenes with a five-membered ring aldehyde produced oligomer fragments of the polymer chain that serve as structural models. Carboxylate initiators were also prepared and shown to require substantial steric protection about the molybdenum to give stable species. Crystallographic characterization of a PMe_3 adduct of one carboxylate species revealed the bulky coordination sphere engendered by the triphenylacetate ligands. It is concluded that with both alkoxide and carboxylate initiators, subtle steric factors control the propensity for α- or β-addition of alkyne addition and that minor changes to the catalyst or substrate result in attenuated selectivity.

EXPERIMENTAL

General comments. All manipulations of air- and moisture-sensitive materials were performed in oven-dried (200 ºC) glassware under an atmosphere of nitrogen on a dual-manifold Schlenk line or in a Vacuum Atmospheres glovebox. HPLC grade organic solvents were sparged with nitrogen and dried by passage through activated alumina (for diethyl ether, toluene, pentane, THF, and methylene chloride) followed by passage through Q-5 supported copper catalyst (for benzene) prior to use, then stored over 4 Å Linde-type molecular sieves. Benzene-d_6 and toluene-d_8 was dried over sodium/benzophenone ketyl and vacuum-distilled. Methylene chloride-d_2 was dried over CaH_2, vacuum distilled and stored over 4 Å Linde-type molecular sieves. Chloroform-*d* was used as received. NMR spectra were recorded on Varian INOVA or

Varian Mercury spectrometers operating at 500 and 300 MHz (^{1}H), respectively. Chemical shifts for ^{1}H and ^{13}C spectra were referenced to the residual ^{1}H/^{13}C resonances of the deuterated solvent (^{1}H: $CDCl_3$, δ 7.26; C_6D_6, δ 7.16; CD_2Cl_2, δ 5.32; C_7D_8, δ 2.09. ^{13}C: $CDCl_3$, δ 77.23; C_6D_6, δ 128.39; CD_2Cl_2, δ 54.00) and are reported as parts per million relative to tetramethylsilane. ^{19}F NMR spectra were referenced externally to fluorobenzene (δ -113.15 ppm upfield of $CFCl_3$). ^{31}P NMR were referenced externally to 80% aqueous H_3PO_4 (δ 0.00 ppm). IR spectra were recorded on a Nicolet Avatar FT-IR spectrometer. High resolution mass spectrometry measurements were performed at the MIT Department of Chemistry Instrument Facility, and elemental analyses were performed by H. Kolbe Microanalytics Laboratory, Mülheim an der Ruhr, Germany. MALDI-ICR-FTMS spectra were obtained by L. Amundson and Professor E. A. Stemmler at Bowdoin College.

Materials. $\{CpRu(CH_3CN)_3\}\{PF_6\}$,[43] $Mo(NR)(CHR')(OTf)_2(DME)$,[44] $Mo(NR)(CH\text{-}t\text{-}Bu)(O\text{-}t\text{-}Bu_{F6})_2$, $Mo(Ar)(CHCMe_2Ph)(O_2CCMePh_2)_2$, $Mo(NAr'')(CH\text{-}t\text{-}Bu)(O_2CCPh_3)_2$, $Mo(NAd)(CHCMe_2Ph)(O_2CCPh_3)_2$[18] and compound **3a**[28] were prepared according to published procedures. Diethyl dipropargylmalonate (DEDPM) was synthesized by addition of NaOEt to an ethanol solution of diethylmalonate followed by addition of propargyl bromide. $LiOCMe(CF_3)_2$ and LiO-*t*-Bu were prepared by addition of *n*-BuLi (1.6 M in hexanes, Aldrich) to a pentane solution of the corresponding alcohols (Aldrich). The syntheses of diethyl 2-(4-hydroxy-4-methylpent-2-ynyl)-2-(prop-2-ynyl)malonate (**1a**) and diethyl 3-formyl-4-(2-methylprop-1-enyl)cyclopent-3-ene-1,1-dicarboxylate (**1b**) were carried out in similar fashion to the methyl ester derivatives reported by Trost.[27] Diethyl 2-(prop-2-ynyl)malonate,[45] diethyl 2-(but-3-enyl)-2-(prop-2-ynyl)malonate,[46] and diethyl 3-vinylcyclohex-3-ene-1,1-dicarboxylate[33] were prepared according to slightly modified published procedures and are described below for convenience. All carboxylate salts were prepared by addition of NaH to a THF solution of the corresponding acid (Aldrich) followed by crystallization from THF/pentane. PMe_3 (Strem), $Ru(=CHPh)(PCy_3)_2Cl_2$ (Aldrich), $LiN(TMS)_2$ (as a 1.0 M solution in THF), NaH, propargyl

bromide (as an 80% wt. soln. in toluene), 4-bromo-1-butene, and diethyl malonate were purchased from commercial vendors and used as received.

Crystallography. Mounting of crystals and refinement of X-ray diffraction data was performed by Dr. Peter Müller of the Department of Chemistry Diffraction Facility. Low temperature diffraction data were collected on a Siemens Platform three-circle diffractometer coupled to a Bruker-AXS Smart Apex CCD detector with graphite-monochromated Mo Kα radiation ($\lambda = 0.71073$ Å), performing φ- and ω-scans. All structures were solved by direct methods using SHELXS[47] and refined against F^2 on all data by full-matrix least squares with SHELXL-97.[48] All non-hydrogen atoms were refined anisotropically. All hydrogen atoms were included into the model at geometrically calculated positions and refined using a riding model. The isotropic displacement parameters of all hydrogen atoms were fixed to 1.2 times the *U* value of the atoms they are linked to (1.5 times for methyl groups).

Diethyl 2-(4-hydroxy-4-methylpent-2-ynyl)-2-(prop-2-ynyl)malonate, 1a. An oven dried three-neck round bottom flask equipped with a stir bar was fitted with an addition funnel, thermometer adapter, and stopcock. The flask was charged with 11.34 g (48.0 mmol) of DEDPM and 400 mL of THF. To the addition funnel was added a solution of 9.50 g (48.6 mmol) of $LiN(TMS)_2$ in 100 mL of THF. The contents of the flask were cooled to –65 ºC with a dry ice/acetone bath at which point the solution of $LiN(TMS)_2$ was added dropwise maintaining a temperature below –50 ºC. Once addition was complete, the mixture was stirred at –65 ºC for 15 minutes. Acetone (3.5 mL, 48 mmol) was then added via the addition funnel and the reaction allowed to warm to room temperature and stir overnight. The reaction was quenched with aqueous NH_4Cl, and the THF removed in vacuo. The product was extracted into Et_2O and dried over $MgSO_4$. The Et_2O was evaporated leaving a crude oil, which was purified by silica gel chromatography (40% Et_2O/hexanes) to yield 10.5 g (74%) of a colorless oil. IR (neat): 3488, 3283, 2981, 1731, 1303, 1249, 1184, 1055, 897. ^{1}H NMR (300 MHz, $CDCl_3$): δ 4.20 (q, 4, OCH_2), 2.94 (s, 2, CH_2), 2.92 (d, 2, J = 2.7 Hz, CH_2), 2.28 (br s, 1, O*H*), 2.00 (t, 1, J = 2.7 Hz,

≡C*H*), 1.44 (s, 6, *Me*), 1.24 (t, 6, CH_3). ^{13}C NMR (75.5 MHz, $CDCl_3$): δ 168.83, 88.83, 78.59, 76.14, 71.74, 64.84, 62.04, 56.59, 31.48, 22.66, 22.55, 14.06. HRMS (ESI, $[M+Na]^+$): Calcd for $C_{16}H_{22}NaO_5$: 317.1359; Found: 317.1311.

Diethyl 3-formyl-4-(2-methylprop-1-enyl)cyclopent-3-ene-1,1-dicarboxylate, 1b. An oven dried two-neck flask equipped with a stir bar was fitted with a stopcock and a septum. The flask was charged with 2.72 g (9.24 mmol) of diethyl 2-(4-hydroxy-4-methylpent-2-ynyl)-2-(prop-2-ynyl)malonate and 75 mL of acetone that had been sparged with N_2 for 20 minutes. To the solution was added 220 μL (12 mmol) of water and 330 mg (8 mol%) of $\{CpRu(CH_3CN)_3\}\{PF_6\}$. The orange solution was stirred at room temperature for 2 hours. The reaction was then filtered through a plug of silica gel, and the solvent removed in vacuo. The crude product was purified by silica gel chromatography (50% Et_2O/pentane) to yield 1.90 g (70%) of a white crystalline solid. IR (neat): 2978, 2874, 1726, 1648, 1626, 1573, 1369, 1260, 1216, 1186, 1078. ^{1}H NMR (300 MHz, $CDCl_3$): δ 9.85 (s, 1, C*H*O), 6.25 (s, 1, C*H*), 4.19 (q, 4, OCH_2), 3.39 (s, 2, CH_2), 3.23 (s, 2, CH_2), 1.90 (s, 3, *Me*), 1.85 (s, 3, *Me*), 1.24 (t, 6, CH_3). ^{13}C NMR (75.5 MHz, $CDCl_3$): δ 188.34, 171.52, 155.75, 144.08, 135.19, 117.49, 62.09, 57.45, 45.74, 37.90, 27.83, 20.87, 14.19. HRMS (EI, $[M]^+$): Calcd for $C_{16}H_{22}O_5$: 294.1462; Found: 294.1452.

Diethyl 3-(2-methylprop-1-enyl)-4-vinylcyclopent-3-ene-1,1-dicarboxylate, 1c. An oven-dried flask was charged with 0.860 g (2.13 mmol) of $MePPh_3I$ and 50 mL of THF. To the suspension was added 0.076 g (1.93 mmol) of NaH (60.8 wt.% dispersion in mineral oil). The mixture was allowed to stir at room temperature for 3 hours during which time it became bright yellow in color. To the mixture was added a solution of 0.505 g (1.72 mmol) of **1b** in 15 mL of THF. The reaction was then allowed to stir at room temperature overnight. The THF was removed in vacuo and the residue treated with diehthyl ether causing precipitation of NaI and $OPPh_3$. The ethereal solution was decanted away from the solids, washed three times with water

and dried over $MgSO_4$. The solvent was removed by rotary evaporation and the compound purified by silica gel chromatography (20% Et_2O/hexanes) to give 0.287 g (57%) of a colorless crystalline solid: ^{1}H NMR (300 MHz, $CDCl_3$) δ 6.57 (dd, $^3J_{cis}$ = 10.5 Hz, $^3J_{trans}$ = 18.0 Hz, 1, CH_2), 5.90 (s, 1, C*H*CMe$_2$), 5.11 (m, 1, C*H*CH$_2$), 5.06 (m, 1, CH_2), 4.20 (q, 4, OC*H*$_2$), 3.28 (s, 2, C*H*$_2$), 3.16 (s, 2, C*H*$_2$), 1.82 (s, 3, Me), 1.75 (s, 3, Me), 1.25 (t, 6, OCH$_2$C*H*$_3$); ^{13}C NMR (75 MHz, $CDCl_3$) δ 172.3, 137.0, 135.8, 133.5, 131.0, 119.1, 114.3, 61.8, 57.8, 44.7, 39.9, 27.4, 20.4, 14.3. IR (neat) cm^{-1} 2978, 1731, 1665, 1633, 1616, 1445, 1365, 1261, 1188, 1069, 895, 857. HRMS (EI, [M]$^+$) Calcd for $C_{17}H_{24}O_4$: 292.1669; Found: 292.1667.

Mo(NAr)(CH[5])(O-*t*-Bu$_{F6}$)$_2$, 2a. A solution of **1c** (0.359 g, 1.23 mmol) in 3 mL of pentane was added to a stirred suspension of Mo(NAr)(CHCMe$_2$Ph)(O-*t*-Bu$_{F6}$)$_2$ (0.683 g, 1.17 mmol) in 10 mL of pentane. The mixture was stirred at room temperature for 30 minutes during which time the suspension became homogeneous before an orange-yellow solid precipitated from solution. The precipitate was collected by filtration and dried *in vacuo*. The mother liquor was concentrated and a second batch of fluffy solid obtained as before; yield 0.847 g (84%): ^{1}H NMR (500 MHz, CD_2Cl_2) δ 12.79 (s, 1, $^1J_{CH}$ = 120 Hz, MoC*H*$_\alpha$), 7.19 (t, 1, *p*-Ar*H*), 7.19 (d, 2, *m*-Ar*H*), 5.96 (s, H, C*H*$_\delta$), 4.00 (q, 4, OC*H*$_2$), 3.71 (s, 2, C*H*$_2$), 3.51 (sep, 2, C*H*Me$_2$), 3.21 (s, 2, C*H*$_2$), 1.96 (s, 3, Me), 1.91 (s, 3, Me), 1.42 (s, 6, *t*-Bu$_{F6}$), 1.19 (d, 12, CH*Me*$_2$), 1.07 (t, 6, OCH$_2$C*H*$_3$); ^{19}F NMR (470 MHz, CD_2Cl_2) δ –78.50. Anal. Calcd for $C_{36}H_{45}F_{12}MoNO_6$: C, 47.43; H, 4.98; N, 1.54. Found: C, 47.55; H, 4.87; N, 1.48.

Diethyl 2-(prop-2-ynyl)malonate. A three-neck flask was charged with 13.0 g (0.33 mol) of NaH and 600 mL of THF. The solution was cooled to 0ºC and 50 mL (0.33 mol) of diethyl malonate was added dropwise via the addition funnel over 45 minutes. The mixture was warmed to room temperature and stirred for 90 minutes. The solution of was then transferred via cannula to a flask containing 37 mL (0.33 mol) of propargyl bromide (as an 80% solution in toluene) dissolved in 50 mL of THF. Rapid precipitation of salts occurred during addition, and once

complete, the mixture was allowed to stir at room temperature for 2 hours. The mixture was poured onto 100 mL of water and the THF removed in vacuo. The solution was extracted into ether and dried over $MgSO_4$. The crude compound was purified by vacuum distillation. The fraction at 39-45ºC (10 mTorr) was found by ^{1}H NMR to contain a ~2:1 mixture of the desired compound to twice alkylated product (DEDPM) and was used in the next step without further purification. The spectroscopic features of the molecule were identical to those reported in the literature. ^{1}H NMR (500 MHz, $CDCl_3$): δ 4.21 (q, 4, OCH_2), 3.55 (t, 1, CH), 2.77 (dd, 2, CH_2), 2.01 (t, 1, ≡CH), 1.27 (t, 6, CH_3).

Diethyl 2-(but-3-enyl)-2-(prop-2-ynyl)malonate. A three-neck flask was charged with 1.1 g (28 mmol) of NaH (60% wt. suspension in oil) and 80 mL of THF and fitted with a condensor, addition funnel, and gas inlet. The flask was cooled to 0ºC, at which point a solution of 8.0 g (25 mmol) of diethyl 2-(prop-2-ynyl)malonate (as a 2:1 mixture with diethyl dipropargylmalonate) in 25 mL of THF was added dropwise via the addition funnel. Once addition was complete, the solution was allowed to stir for 1 hour until the contents became homogeneous. The solution was warmed to room temperature and 4-bromo-1-butene was added via syringe. A catalytic amount of TBAI was added and the solution heated at reflux for 18 hours. After heating, the solution was cooled to room temperature and poured into ~100 mL of an ice water mixture. The THF was removed in vacuo and the remaining solution extracted with diethyl ether. The extract was dried over $MgSO_4$ and the volatiles removed in vacuo to yield a crude oil. The oil was purified by flash chromatography on silica gel (25:1 hexanes:EtOAc) to yield 4.29 g (68%) of a colorless oil. The spectroscopic features of the molecule were identical to those reported in the literature. ^{1}H NMR (300 MHz, $CDCl_3$): δ 5.80 (m, 1, CH), 5.05 (m, 1, CH_2), 4.98 (m, 1, CH_2), 4.20 (q, 4, OCH_2), 2.83 (d, 2, CH_2C≡CH), 2.16 (m, 2, CH_2), 2.00 (s, 1, ≡CH), 1.97 (m, 2, CH_2), 1.25 (t, 6, CH_3).

Diethyl 3-vinylcyclohex-3-ene-1,1-dicarboxylate, 3b. A flask was charged with 1.00 g (3.96 mmol) of diethyl 2-(but-3-enyl)-2-(prop-2-ynyl)malonate, 33 mg (1 mol%) of $Ru(=CHPh)(PCy_3)_2Cl_2$ and 50 mL of CH_2Cl_2. The head space in the flask was flushed with ethylene, and the mixture allowed to stir at room temperature under a balloon of ethylene for 20 hours. The volatiles were removed in vacuo and the crude material purified by flash chromatography on silica gel (30:1 hexanes:EtOAc) to yield 0.92 g (92%) of a colorless oil. The spectroscopic features of the molecule were identical to those in the literature. ^{1}H NMR (300 MHz, $CDCl_3$): δ 6.35 (dd, 1, C*H*), 5.70 (br s, 1, C*H*), 5.15 (d, 1, CH_2), 4.97 (d, 1, CH_2), 4.19 (q, 4, OCH_2), 2.68 (br s, 2, CH_2), 2.22 (v br, 2, CH_2), 2.11 (m, 2, CH_2), 1.24 (t, 6, CH_3).

Mo(NAr)(CH[6])(O-*t*-Bu$_{F6}$)$_2$, 4b. A solution of 0.505 g (0.718 mmol) of Mo(CH-t-Bu)(NAr)[OCMe$(CF_3)_2$]$_2$ in 20 mL of pentane was treated with a solution of 0.20 g (0.79 mmol) of diethyl 3-vinylcyclohex-3-ene-1,1-dicarboxylate in 5 mL of pentane. The solution was allowed to stir at room temperature for 3 h during which time the color changed from yellow to brown. All volatiles were removed *in vacuo* and the residue dissolved in a minimal amount of pentane. The solution was set aside at –25ºC for 18 h during which time the compound precipitated as fluffy, orange-red crystals; yield 0.404 g (65%): ^{1}H NMR (500 MHz, CD_2Cl_2) δ 12.52 (s, 1, $^1J_{CH}$ = 125 Hz, MoCH_α), 7.26 (t, 1, *p*-Ar*H*), 7.17 (d, 2, *m*-Ar*H*), 5.32 (m, 1, CH_γ), 3.98 (m, 2, OCH_2), 3.85 (m, 2, OCH_2), 3.52 (sep, 2, C*H*Me$_2$), 2.87 (s, 2, CH_2), 2.52 (br m, 2, CH_2), 1.97 (t, 2, CH_2), 1.43 (s, 6, *Me*-OR$_{F6}$), 1.19 (d, 12, CH*Me*$_2$), 1.05 (t, 6H, OCH$_2$CH_3); ^{19}F NMR (470 MHz, CD_2Cl_2) δ –78.40, -78.53. Anal. Calcd for $C_{33}H_{41}F_{12}MoNO_6$: C, 45.47; H, 4.74; N, 1.61. Found: C, 45.68; H, 4.67; N, 1.56.

Mo(NAr)(CH[6])(O-*t*-Bu)$_2$·2(LiO-*t*-Bu$_{F6}$)$_2$, 4c. To a suspension of 1.075 g (1.23 mmol) of Mo(NAr)(CH[6])(O-*t*-Bu$_{F6}$)$_2$ in 35 mL of pentane was added 0.202 g (2.52 mmol) of LiO-*t*-Bu as a solid in one portion. The solution became deep red within 5 minutes and was allowed to stir at room temperature for an addition 30 minutes. The volatiles were removed *in vacuo* and the

residue dissolved in a minmal amount of pentane. The solution was set aside at –25 ºC for two days during which time the compound crystallized as 1.082 g (85%) of red needles: ^{1}H NMR (500 MHz, CD_2Cl_2) δ 11.67 (s, 1, J_{CH} = 119 Hz, MoCH_α), 7.10 (m, 3, *m*- + *p*-Ar), 5.15 (br t, 1, CH_γ), 3.96 (m, 2, OCH_2), 3.83 (m, 2, OCH_2), 3.74 (sep, 2, C*H*Me$_2$), 2.85 (s, 2, CH_2), 2.42 (br m, 2, CH_2), 1.95 (t, 2, CH_2), 1.29 (s, 18, *t*-Bu), 1.78 (d, 12, CH*Me*$_2$), 1.01 (t, 6, OCH$_2$CH_3); ^{13}C NMR (125 MHz, CD_2Cl_2) δ 249.9 (MoC_α), 172.4 (*C*O), 153.4, 146.7, 142.6, 127.4, 123.2, 116.2, 78.4, 61.8, 54.6 (C_{quat} of [6]-ring), 36.3, 32.2 (C*Me*$_3$), 28.6, 27.7, 24.0, 22.3, 14.2 (OCH$_2$*C*H$_3$). Anal. Calcd for $C_{41}H_{59}F_{12}Li_2MoNO_8$: C, 47.73; H, 5.76; N, 1.36. Found: C, 47.66; H, 5.81; N, 1.41.

{Mo(NAr′′)(O-*t*-Bu$_{F6}$)$_2$}$_2$-μ-(CH[6]), 4d. A flask was charged with 0.203 g (0.301 mmol) of Mo(NAr′′)(CH-*t*-Bu)(O-*t*-Bu$_{F6}$)$_2$ and 5 mL of diethyl ether was added. To the stirring solution was added a solution of 70.0 mg (0.264 mmol) of diethyl 5-methylene-3-vinylcyclohex-3-ene-1,1-dicarboxylate in 10 mL of Et_2O. The solution became deep red and was allowed to stir at room temperature for 18 h. The volatiles were removed in vacuo and the residue dissolved in a minimal amount of pentane. The pentane solution was then set aside at –25ºC for several days during which time the desired complex precipitated as 0.100 g (45%) of a brown powder. Repeated crystallization from cold pentane removed any traces of Mo(N-2-*t*-BuC_6H_4)(CH-*t*-Bu)(OR$_{F6}$)$_2$: ^{1}H NMR (500 MHz, C_6D_6) δ 12.36 (s, 1H, J_{CH} = 125 Hz, Mo=CH_α), 7.74 (d, 1H, Ar*H*), 7.57 (d, 1H, Ar*H*), 7.52 (s, 1H, H_γ), 7.04 (m, 2H, Ar*H*), 6.86 (m, 4H, Ar*H*), 4.94 (s, 2H, CH_2), 3.69 (m, 4H, OCH_2), 3.67 (s, 2H, CH_2), 1.53 (s, 3H, *Me*-R$_{F6}$), 1.40 (s, 9H, C*Me*$_3$), 1.38 (s, 9H, C*Me*$_3$), 1.32 (br s, 3H, *Me*-R$_{F6}$), 0.75 (t, 6H, OCH$_2$CH_3); ^{13}C NMR (125 MHz, C_6D_6) δ 271.1 (MoC_α), 259.0 (MoC_αH), 170.3 (*C*O), 157.6, 156.3, 147.0, 146.7, 134.7, 134.2, 132.1, 130.2, 129.8, 127.5, 127.3, 127.1, 126.8, 113.7, 83.0 (br m, C_{quat}-R$_{F6}$), 82.7 (sep, J_{CF} = 29.9 Hz, C_{quat}-R$_{F6}$), 61.8 (O*C*H$_2$), 55.0 (C_{quat}-[6]), 47.2, 36.2, 36.1, 35.8, 30.7, 30.6, 19.6 (br, *Me*-R$_{F6}$), 19.1 (*Me*-R$_{F6}$), 14.2 (OCH$_2$*C*H$_3$). ^{19}F NMR (282 MHz, C_6D_6): δ –77.7 (q, 6 CF_3), –78.0 (q, 6 CF_3), –78.1 (br, 12 CF_3). Anal. Calcd for $C_{49}H_{54}F_{24}Mo_2N_2O_8$: C, 40.68; H, 3.76; N, 1.94. Found: C, 40.43; H, 3.82; N, 1.93.

Mo(N-2,6-$Me_2C_6H_3$)(CHCMe_2Ph)(O_2CCPh_3)$_2$, 5b. To a –25 ºC suspension of 0.525 g (0.714 mmol) of Mo(N-2,6-$Me_2C_6H_3$)(CHCMe_2Ph)(OTf)$_2$(DME) in 40 mL of diethyl ether was added 0.560 g (1.47 mmol) of NaO_2CCPh_3·THF as a solid in one portion. The mixture was allowed to warm to room temperature and stir for 1 hour. During this time, the mixture changed from yellow to orange and became homogeneous. The volatiles were removed in vacuo and the residue extracted into 60 mL of methylene chloride. The extract was filtered through Celite and the solution volume reduced in vacuo to ~10 mL. Several volumes of pentane were added resulting in precipitation of a yellow solid. The solid was collected by filtration and dried in vacuo to give 0.460 g (70%) of a yellow powder. Analytically pure material could be obtained by recrystallization from hot methylene chloride. Do to the insolubility of the complex in common solvents, a satisfactory ^{13}C NMR spectrum could not be obtained: ^{1}H NMR (300 MHz, CD_2Cl_2) δ 13.83 (br s, 1, MoCH_α), 7.29 - 6.96 (m, 38, aryl), 2.16 (s, 6, Ar′-*Me*), 1.50 (s, 6, CMe_2Ph). Anal. calcd for $C_{58}H_{51}MoNO_4$: C, 75.56; H, 5.58; N, 1.52. Found: C, 75.38; H, 5.65; N, 1.46.

Mo(N-2,6-$Cl_2C_6H_3$)(CH-*t*-Bu)(O_2CCPh_3)$_2$, 5e. To a suspension of 0.740 g (1.04 mmol) of Mo(CH-*t*-Bu)(N-2,6-$Cl_2C_6H_3$)(OTf)$_2$(DME) in 35 mL of diethyl ether was added 0.853 g (2.23 mmol) of NaO_2CCPh_3·(THF) as a solid in one portion. The resulting suspension was stirred at room temperature for 90 minutes during which time the reaction mixture became yellow and a precipitate formed. The volatiles were removed in vacuo and the residue extracted into 15 mL of methylene chloride. The extract was filtered through Celite and all volatiles removed in vacuo. The remaining residue was treated with pentane to give 0.640 g (68%) of a yellow crystalline powder. The crude material was pure by NMR but could be recrystallized from methylene chloride/pentane: ^{1}H NMR (500 MHz, CD_2Cl_2) δ 13.81 (s, 1, MoCH_α), 7.31 – 7.11 (m, 39, aryl), 1.16 (s, 9, *t*-Bu); ^{13}C (125 MHz, CD_2Cl_2) δ 315.8 (MoC_α, J_{CH} = 121 Hz,), 192.1 (CO_2), 150.5, 142.8, 134.5, 131.0, 128.7, 128.7, 128.2, 127.6, 69.4 (CCO_2), 49.9, 30.8. Anal. calcd for $C_{51}H_{43}Cl_2MoNO_4$: C, 68.00; H, 4.81; N, 1.56. Found: C, 67.68; H, 4.85; N, 1.48.

Mo(2,6-$Me_2C_6H_3$)(CHCMe_2Ph)(O_2CCPh_3)$_2$(PMe_3), 5b·PMe_3. To a suspension of 0.159 g (0.173 mmol) of Mo(N-2,6-$Me_2C_6H_3$)(CHCMe_2Ph)(O_2CCPh_3)$_2$ in 3 mL of methylene chloride was added 25 μL (0.24 mmol) of PMe_3 via microsyringe. The solution immediately became homogenous and was allowed to stand for 5 minutes. All volatiles were removed in vacuo and the residue dissolved in 1 mL of methylene chloride and layered with several volumes of pentane. Storage of the solution at –25 ºC afforded 0.155 g (90%) of yellow crystals that were dried in vacuo. Analytically pure material was obtained by recrystallization from methylene chloride/pentane. NMR and combustion analyses indicated the presence of two molecules of methylene chloride per Mo: ^{1}H NMR (500 MHz, CD_2Cl_2) δ 13.21 (d, 1, MoCH_α, J_{HP} = 5.5 Hz), 7.44 (d, 1, *o*-CMe_2*Ph*), 7.32 (d, 12, *o*-C*Ph*$_3$), 7.24 (t, 2, *m*-CMe_2Ph), 7.10 (m, 19, *m*/*p*-C*Ph*$_3$ + *p*-CMe_2*Ph*), 6.93 (m, 3, Ar′), 2.34 (s, 6, Ar′-*Me*), 1.88 (s, 3, C*Me*$_2$Ph), 1.47 (s, 3, C*Me*$_2$Ph), 0.59 (d, 9, P*Me*$_3$); ^{13}C NMR (125 MHz, CD_2Cl_2) δ 311.2 (d, MoC_α, J_{CH} = 118 Hz, J_{CP} = 19 Hz), 181.17 (br s, *C*O_2), 153.5 (d, J_{CP} = 3.1 Hz), 148.8 (d, J_{CP} = 2.3 Hz), 145.5, 137.7 (d, J_{CP} = 2.3 Hz), 131.4, 128.9, 128.3, 127.9, 127.6, 126.8, 126.7, 126.6, 69.8, 33.0, 29.4, 20.2, 15.6 (d, P*Me*$_3$, J_{CP} = 28 Hz). Anal calcd for $C_{63}H_{64}Cl_4MoNO_4P$: C, 64.79; H, 5.52; N, 1.20. Found: C, 65.15; H, 5.74; N, 1.16.

Mo(N-1-adamantyl)(CHCMe_2Ph)(O_2CCPh_3)$_2$(PMe_3), 5c·PMe_3. To a –25 ºC suspension of 0.293 g (0.308 mmol) of Mo(N-1-adamantyl)(CHCMe_2Ph)(O_2CCPh_3)$_2$ in 15 mL of toluene was added 35 μL (0.34 mmol) of PMe_3. The mixture was stirred at room temperature for 2 hours during which time it became homogeneous. All volatiles were removed in vacuo and the residue treated with pentane causing precipitation of a white solid. The solid was collected by filtration and dried in vacuo affording 0.271 g (85%) of the compound as a white powder: ^{1}H NMR (500 MHz, CD_2Cl_2) δ 13.17 (d, 1, MoCH_α, J_{HP} = 6.0 Hz), 7.45 (d, 2, *o*-CMe_2*Ph*), 7.34 (m, 5, aryl), 7.25 – 7.00 (m, 28, aryl), 2.15 (s, 3, C*Me*$_2$Ph), 2.01 (m, 3, Ad-C*H*), 1.91 (m, 6, Ad-CH_2), 1.58 (m, 6, Ad-CH_2), 1.37 (s, 3, C*Me*$_2$Ph), 0.58 (d, 9, P*Me*$_3$); ^{13}C NMR (125 MHz, CD_2Cl_2) δ 310.7 (d, MoC_α, J_{CH} = 120 Hz, J_{CP} = 18.0 Hz), 186.1 (br, *C*O_2), 176.4 (br, *C*O_2), 148.7 (d, J_{CP} = 3.0 Hz),

146.9 (br), 146.5, 144.8 (br), 131.5 – 131.4 (br m), 130.8, 128.8, 128.2 – 127.7 (br m), 127.9, 126.6, 126.5, 126.4 (br), 74.1 (N*C*), 70.5 (br, *C*CO_2), 69.0 (br, *C*CO_2), 51.1 (d, *C*Me_2Ph, J_{CP} = 3.1 Hz), 44.6, 36.2, 32.9 (d, J_{CP} = 3.0 Hz), 29.9, 29.6, 16.9 (d, P*Me*$_3$, J_{CP} = 28 Hz); ^{31}P NMR (121 MHz) δ 2.99. Anal. calcd for $C_{63}H_{66}MoNO_4P$: C, 73.60; H, 6.47; N, 1.36. Found: C, 73.81; H, 6.58; N, 1.31.

Mo(N-2-*t*-BuC_6H_4)(CH-*t*-Bu)(O_2CCPh_3)$_2$(PMe_3), 5d·PMe_3. To a solution of 0.315 g (0.355 mmol) of Mo(N-2-*t*-BuC_6H_4)(CH-*t*-Bu)(O_2CCPh_3)$_2$ in 10 mL of methylene chloride was added 80 μL (0.80 mmol) of PMe_3 via microsyringe. The mixture immediately became orange and was allowed to stir at room temperature for 2 hours. All volatiles were removed in vacuo and residue treated with pentane to give 0.291 g (85%) of an orange solid. Crystals suitable for X-ray diffraction were grown from a concentrated methylene chloride/pentane solution. NMR and combustion analyses indicated the presence of one molecule of methylene chloride per Mo: ^{1}H NMR (300 MHz, C_6D_6) δ 13.13 (d, 1, MoC*H*$_\alpha$, J_{HP} = 4.9 Hz), 7.92 (dd, 1, *o*-Ar′′), 7.62-7.57 (m, 12, aryl), 7.16 (dd, 1, *m*-Ar′′), 7.08-6.98 (m, 18, aryl), 6.91 (m, 1, *m*- or *o*-Ar′′), 6.84 (m, 1, *m*- or *o*-Ar′′), 1.38 (s, 9, *t*-Bu), 1.27 (s, 9, *t*-Bu), 0.63 (d, 9, P*Me*$_3$). Anal. calcd for $C_{59}H_{64}Cl_2MoNO_4P$: C, 67.56; H, 6.15; N, 1.34. Found: C, 67.83; H, 6.10; N, 1.15.

Mixture of compounds 5e·PMe_3 and 5e′·PMe_3. To a suspension of 0.209 g (0.232 mmol) of Mo(N-2,6-$Cl_2C_6H_3$)(CH-*t*-Bu)(O_2CCPh_3)$_2$ in toluene was added 50 mL (0.49 mmol) of PMe_3 via syringe. Upon addition of phosphine, the suspension immediately became homogeneous and took on deep red color. The mixture was stirred for 30 minutes at room temperature. All volatiles were removed in vacuo and the residue treated with pentane to afford 0.179 g (79%) of an orange powder. Examination of the material by ^{1}H NMR showed a 5:1 mixture of **5e′·PMe_3** to **5e·PMe_3**. Repeated crystallization from toluene/pentane resulted in the same mixture of products: ^{1}H NMR (500 MHz, C_6D_6) δ 13.47 (d, 1, MoC*H*$_\alpha$, J_{HP} = 5.0 Hz), 10.44 (br s, 1, N*H*Ar^{Cl}); ^{31}P NMR (121 MHz) δ 3.53 (**5e·PMe_3**), 0.21 (**5e′·PMe_3**).

{Na}{Mo(N-1-adamantyl)(CHCMe$_2$Ph)(O$_2$C-2,6-Me$_2$C$_6$H$_3$)$_3$}, 6c. To a –25 ºC solution of 0.423 g (0.553 mmol) of Mo(N-1-adamantyl)(CHCMe$_2$Ph)(OTf)$_2$(DME) in 30 mL of THF was added 0.456 g (1.87 mmol) of NaO$_2$C-2,6-Me$_2$C$_6$H$_3$·THF as a solid in one portion. The mixture was allowed to stir at room temperature for 90 minutes during which time it remained homogeneous. All volatiles were removed in vacuo and the residue extracted into 20 mL of methylene chloride. The extract was filtered through Celite and the solution volume reduced to ~1 mL in vacuo. The concentrated solution was layered with several volumes of pentane and set aside at –25 ºC overnight. The compound precipitated as 0.310 g (66%) of an off-white crystalline solid: ^{1}H NMR (300 MHz, CD$_2$Cl$_2$) δ 13.98 (br s, 1, MoC*H*$_\alpha$), 7.32 (d, 2, *o*-CMe$_2$*Ph*), 7.14 (m, 6, aryl), 6.91 (m, 6, aryl), 2.25 (s, 12, Ar′-*Me*), 2.09 (s, 6, Ar′-*Me*), 1.97 (br s, 9, Ad-C*H* + Ad-C*H*$_2$), 1.62 (s, 6, C*Me*$_2$Ph), 1.51 (s, 6, Ad-C*H*$_2$); ^{13}C (125 MHz) δ 310.4 (br, Mo*C*$_\alpha$), 179.8 (*C*O$_2$), 177.0 (*C*O$_2$), 151.6, 139.5, 137.1, 136.3, 134.5, 129.1, 128.4, 128.3, 128.1, 127.3, 126.1, 73.3 (N*C*), 52.4, 43.1, 36.3, 31.7, 29.8, 21.6, 20.5. Anal. calcd for C$_{47}$H$_{54}$MoNNaO$_6$: C, 66.58; H, 6.42; N, 1.65. Found: C, 66.41; H, 6.34; N, 1.53.

Spectroscopic observation of Mo(NAd)(CHCMe$_2$Ph)(O$_2$CAr′)$_2$(PMe$_3$), 6c·PMe$_3$. To a solution of 13.2 mg of **2** in CD$_2$Cl$_2$ was added 2 μL of PMe$_3$ via microsyringe. After 10 minutes, a precipitate was apparent and the NMR spectrum was recorded: ^{1}H (300 MHz) δ 13.15 (d, 1, MoC*H*$_\alpha$, J_{HP} = 6.0 Hz), 7.54 (d, 2, *o*-CMe$_2$*Ph*), 7.31 (t, 2, *m*-CMe$_2$*Ph*), 7.26 (t, 1, *p*-CMe$_2$*Ph*), 7.05 (br t, 2, *p*-Ar′), 6.90 (br d, 4, *m*-Ar′), 2.23 (m, 12, Ar′-*Me* + 3 C*Me*$_2$Ph + 6 Ad-C*H*$_2$), 2.13 (br s, 3, Ad-C*H*), 1.68 (br s, 6, Ad-C*H*$_2$), 1.52 (s, 3, C*Me*$_2$Ph), 1.23 (d, 9, P*Me*$_3$); ^{31}P (121 MHz) δ 4.22.

(E)-di-1,2-[1-(2-methyl-propenyl)-4,4-diethyl-carboxy-cyclopent-1-enyl]-ethene, 8a. To a solution of 0.303 g (0.33 mmol) of 2 in 10 mL of diethyl ether was added a solution of 0.100 g (0.34 mmol) of A in 5 mL of ether. The reaction was allowed to stir at room temperature for 60 minutes. The solution was filtered through a plug of silica gel, washed with 1 M HCl and dried

over $MgSO_4$. The crude material was then purified by chromatography on silica gel (40% Et_2O/hexanes) to yield the desired material as a pale yellow solid: ^{1}H NMR (500 MHz, $CDCl_3$) δ 6.35 (s, 2, C*H*), 5.99 (br s, 2, C*H*), 4.20 (q, 8, OCH_2), 3.32 (s, 4, CH_2), 3.20 (s, 4, CH_2), 1.87 (s, 6, *Me*), 1.80 (s, 6, *Me*), 1.25 (t, 12, OCH_2CH_3); ^{13}C NMR (125 MHz, $CDCl_3$) δ 172.2, 137.0, 135.8, 133.7, 123.4, 119.3, 61.8, 58.0, 44.6, 40.1, 27.7, 20.6, 14.2. MALDI-ICR-FTMS [M+Na$^+$]: Calcd for $C_{32}H_{44}NaO_8$: 579.2934; Found: 579.3033.

Diethyl 5-((4,4-di(ethoxycarbonyl)-2-(2-methylprop-1-enyl)cyclopent-1-enyl)methylene)-3-((1E)-2-(4,4-di(ethoxycarbonyl)-2-(2-methylprop-1-enyl)cyclopent-1-enyl)vinyl)cyclohex-3-ene-1,1-dicarboxylate, 8b. A flask was charged with 0.113 g (77.8 μmol) of compound **4d** and 8 mL of diethyl ether. To the stirring solution was added 56.9 mg (190 μmol) of aldehyde **1b**. Upon addition of the aldehyde, an immediate color change from brown to deep red occurred. The solution was stirred for 24 h at room temperature during which time the color lightened to yellow-brown. The solvent volume was reduced in vacuo to ~5 mL and 10 mL of pentane was added. The solution was loaded onto a short silica gel column and eluted with 2:1 hexanes:ethyl acetate. The product fractions (R_f = 0.45) were pooled and the solvent removed in vacuo yielding 50.0 mg (80%) of a bright yellow film. The compound exists as a 2:1 mixture of isomers as determined by NMR: ^{1}H NMR (500 MHz, $CDCl_3$) *Major isomer* δ 6.61 (s, 1, H), 6.56 (d, $^3J_{trans}$ = 16.0 Hz, 1, H), 6.25 (d, 1, H), 6.02 (s, 1, H), 5.97 (s, 1, H), 5.84 (s, 1, H), 4.20 (m, 12, OCH_2) 3.38 (s, 2, CH_2), 3.34 (s, 2, CH_2), 3.23 (s, 2, CH_2), 3.20 (s, 2, CH_2), 2.88 (s, 2, CH_2), 2.86 (s, 2, CH_2), 1.87 (s, 3, Me), 1.82 (s, 3, Me), 1.81 (s, 3, Me), 1.73 (s, 3, Me), 1.25 (m, 18, OCH_2CH_3); *Minor isomer* δ 6.51 (d, $^3J_{trans}$ = 16.0 Hz, 1, H), 6.19 (d, 1, H), 6.15 (s, 1, H), 6.08 (s, 1, H), 6.01 (s, 1, H), 5.84 (s, 1, H), 4.20 (m, 12, OCH_2), 3.40 (s, 2, CH_2), 3.32 (s, 2, CH_2), 3.20 (s, 2, CH_2), 3.18 (s, 2, CH_2), 3.07 (s, 2, CH_2), 2.85 (s, 2, CH_2), 1.87 (s, 3, Me), 1.83 (s, 3, Me), 1.80 (s, 3, Me), 1.71 (s, 3, Me), 1.25 (m, 18, OCH_2CH_3); ^{13}C NMR (125 MHz, $CDCl_3$) *Both isomers* δ 172.25, 172.23, 172.18, 171.21, 171.14, 138.41, 137.87, 137.60, 137.47, 137.22, 137.07, 136.41, 136.06, 136.01, 134.39, 133.77, 133.71, 133.17, 132.73, 132.70, 132.37, 131.89, 131.36, 130.82,

126.79, 125.40, 123.32, 122.51, 121.81, 120.12, 120.03, 119.47, 61.87, 61.83, 61.81, 61.76, 58.99, 58.86, 57.96, 57.92, 54.37, 54.21, 44.73, 44.68, 43.67, 43.44, 42.75, 40.34, 40.19, 38.54, 32.27, 30.77, 30.39, 27.81, 27.42, 20.67, 20.65, 20.57, 14.26, 14.24, 14.22, 14.17. HRMS (ESI, $[M+H]^+$): Calcd for $C_{45}H_{61}O_{12}$: 793.4158. Found: 793.4170. UV-VIS: λ_{max} = 384 nm (CH_2Cl_2).

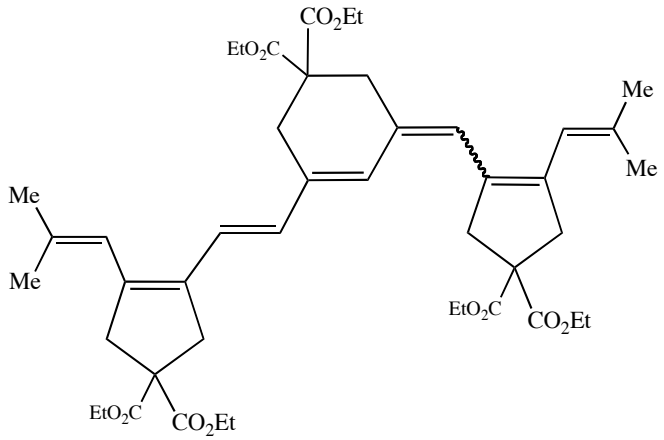

Crystal data and structure refinement for {Mo(NAr)(CH[6])(O-*t*-Bu_{F6})$_2$}$_2$-μ-[LiO-*t*-Bu_{F6}]$_4$, **4c**.

Reciprocal net identification code	**05248**	
Empirical formula	$C_{41}H_{59}F_{12}Li_2MoNO_8$	
Formula weight	1031.71 g/mol	
Temperature	100(2) K	
Wavelength	0.71073 Å	
Crystal system	Orthorhombic	
Space group	$Cmc2_1$	
Unit cell dimensions	a = 45.308(2) Å	α = 90°
	b = 10.0831(4) Å	β = 90°
	c = 21.3920(9) Å	γ = 90°
Volume	9772.9(7) Å^3	
Z	8	
Density (calculated)	1.402 g/cm^3	
Absorption coefficient	0.361 mm^{-1}	
F(000)	4256	
Crystal size	0.15 × 0.15 × 0.03 mm^3	
Θ range for data collection	1.80 to 29.57°.	
Index ranges	$-62 \le h \le 62$, $-14 \le k \le 14$, $-29 \le l \le 29$	
Reflections collected	106930	
Independent reflections	13844 [R(int) = 0.0670]	
Completeness to Θ = 29.57°	100.0%	
Absorption correction	Semi-empirical from equivalents	
Max. and min. transmission	0.9893 and 0.9478	
Refinement method	Full-matrix least-squares on F^2	
Data / restraints / parameters	13844 / 456 / 706	
Goodness-of-fit on F^2	1.042	
Final R indices [I>2σ(I)]	R1 = 0.0349, wR2 = 0.0731	
R indices (all data)	R1 = 0.0484, wR2 = 0.0784	
Absolute structure parameter	-0.025(18)	
Largest diff. peak and hole	0.594 and -0.261 e·Å^{-3}	

Crystal data and structure refinement for Mo(NAr′′)(CH-*t*-Bu)(O_2CCPh_3)$_2$(PMe_3), **5d·PMe_3**.

Reciprocal net identification code	**06052**	
Empirical formula	$C_{66.50}H_{82}Cl_2MoNO_4P$	
Formula weight	1157.14 g/mol	
Temperature	100(2) K	
Wavelength	0.71073 Å	
Crystal system	Triclinic	
Space group	$P\bar{1}$	
Unit cell dimensions	a = 12.7389(3) Å	α = 81.6190(10)°
	b = 14.0067(4) Å	β = 77.5020(10)°
	c = 17.7003(4) Å	γ = 88.9480(10)°
Volume	3050.21(13) Å^3	
Z	2	
Density (calculated)	1.260 g/cm^3	
Absorption coefficient	0.376 mm^{-1}	
F(000)	1222	
Crystal size	0.25 × 0.24 × 0.20 mm^3	
Θ range for data collection	1.64 to 29.57°	
Index ranges	$-17 \le h \le 17$, $-19 \le k \le 19$, $-24 \le l \le 24$	
Reflections collected	68763	
Independent reflections	17080 [R(int) = 0.0259]	
Completeness to Θ = 29.57°	99.7%	
Absorption correction	Semi-empirical from equivalents	
Max. and min. transmission	0.9286 and 0.9119	
Refinement method	Full-matrix least-squares on F^2	
Data / restraints / parameters	17080 / 299 / 717	
Goodness-of-fit on F^2	1.039	
Final R indices [I>2σ(I)]	R1 = 0.0390, wR2 = 0.1040	
R indices (all data)	R1 = 0.0434, wR2 = 0.1074	
Largest diff. peak and hole	2.425 and -1.172 e·Å^{-3}	

REFERENCES

1 For example see Sirringhaus, H.; Brown, P. J.; Friend, R. H.; Nielsen, M. M.; Bechgaard, K.; Langeveld-Voss, B. M. W.; Spiering, A. J. H.; Janssen, R. A. J.; Meijer, E. W.; Herwig, P.; De Leeuw, D. M. *Nature* **1999**, *401*, 685, and references therein.

2 Samuel, I. D. W. Philos. Trans. Royal Soc. London, Ser. A **2000**, 358, 193.

3 Masuda, T.; Abdul Karim, S. M.; Nomura, R. *J. Molec. Catal. A* **2000**, *160*, 125.

4 Masuda, T.; Higashimura, T. *Adv. Polym. Sci.* **1986**, *81*, 121.

5 Mizumoto, T.; Masuda, T.; Higashimura, T. *J. Polym. Sci. A - Polym. Chem.* **1993**, *31*, 2555.

6 Masuda, T.; Higashimura, T. *Acc. Chem. Res.* **1984**, *17*, 51.

7 Masuda, T.; Fujimori, J. I.; Abrahman, M. Z.; Higashimura, T. *Polym. J.* **1993**, *25*, 535.

8 Choi, S.-K.; Gal, Y.-S.; Jin, S.-H.; Kim, H. K. *Chem. Rev.* **2000**, *100*, 1645.

9 Lam, J. W. Y.; Tang, B. Z. *J. Poly. Sci.* **2003**, *41*, 2607.

10 Krause, J. O.; Wang, D.; Anders, U.; Weberskirch, R.; Zarka, M. T.; Nuyken, O.; Jaeger, C.; Haarer, D.; Buchmeiser, M. R. *Macromol. Symp.* **2004**, *217*, 179.

11 Buchmeiser, M. R. *Monats. Chem.* **2003**, *134*, 327.

12 Christensen, R. L., In *The Photochemistry of Carotenoids*, Frank, H. A.; Young, A. J.; Britton, G.; Cogdell, R. J., ed. Kluwer Academic Publishers: Dordrecht, 1999; Vol. 8, p 137.

13 Polivka, T.; Sundstrom, V. *Chem. Rev.* **2004**, *104*, 2021.

14 Anders, U.; Wagner, M.; Nuyken, O.; Buchmeiser, M. R. *Macromolecules* **2003**, *36*, 2668.

15 Fox, H. H.; Schrock, R. S. *Organometallics* **1992**, *11*, 2763.

16 Buchmeiser, M. R. *Adv. Polym. Sci.* **2005**, *176*, 89.

17 Anders, U.; Nuyken, O.; Buchmeiser, M. R.; Wurst, K. *Angew. Chem., Int. Ed. Engl.* **2002**, *41*, 4044.

18 Schattenmann, F. J.; Schrock, R. R.; Davis, W. M. *J. Am. Chem. Soc.* **1996**, *118*, 3295.

19 Anders, U.; Nuyken, O.; Buchmeiser, M. R.; Wurst, K. *Macromolecules* **2002**, *35*, 9029.

20 Anders, U.; Nuyken, O.; Buchmeiser, M. R. *J. Mol. Catal. A* **2004**, *213*, 89.

21 Wood, P.; Samuel, I. D. W.; Schrock, R.; Christensen, R. L. *J. Chem. Phys.* **2001**, *115*, 10955.

22 Christensen, R. L.; Faksh, A.; Meyers, J. A.; Samuel, I. D. W.; Wood, P.; Schrock, R. R.; Hultzsch, K. C. *J. Phys. Chem. A* **2004**, *108*, 8229.

23 Schrock, R. R., In *Metathesis Polymerization of Olefins and Polymerization of Alkynes*, Imamoglu, Y., Ed. Kluwer: 1998; p 1.

24 Schrock, R. R.; Crowe, W. E.; Bazan, G. C.; DiMare, M.; O'Regan, M. B.; Schofield, M. H. *Organometallics* **1991**, *10*, 1832.
25 Schrock, R. R.; Murdzek, J. S.; Bazan, G. C.; Robbins, J.; DiMare, M.; O'Regan, M. *J. Am. Chem. Soc.* **1990**, *112*, 3875.
26 Trost, B. M.; Rudd, M. T. *J. Am. Chem. Soc.* **2002**, *124*, 4178.
27 Trost, B. M.; Rudd, M. T. *J. Am. Chem. Soc.* **2005**, *127*, 4763.
28 Fox, H. H.; Wolf, M. O.; O'Dell, R.; Lin, B. L.; Schrock, R. R.; Wrighton, M. S. *J. Am. Chem. Soc.* **1994**, *116*, 2827.
29 Schrock, R. R.; Luo, S.; Lee, J. C. J.; Zanetti, N. C.; Davis, W. M. *J. Am. Chem. Soc.* **1996**, *118*, 3883.
30 Lopez, L. P. H.; Schrock, R. R. *J. Am. Chem. Soc.* **2004**, *126*, 9526.
31 Oskam, J. H.; Schrock, R. R. *J. Am. Chem. Soc.* **1992**, *114*, 7588.
32 Oskam, J. H.; Schrock, R. R. *J. Am. Chem. Soc.* **1993**, *115*, 11831.
33 Mori, M.; Sakakibara, N.; Kinoshita, A. *J. Org. Chem.* **1998**, *63*, 6082.
34 Adamchuk, J.; Schrock, R. R.; Tonzetich, Z. J.; Müller, P. *Organometallics* **2006**, *25*, 2364.
35 Bazan, G.; Khosravi, E.; Schrock, R. R.; Feast, W. J.; Gibson, V. C.; O'Regan, M. B.; Thomas, J. K.; Davis, W. M. *J. Am. Chem. Soc.* **1990**, *112*, 8378.
36 Schattenmann, F. J. *Ph.D. Thesis*, Massachusetts Institute of Technology, 1995.
37 Schrock, R. R.; Luo, S.; Zanetti, N.; Fox, H. H. *Organometallics* **1994**, *13*, 3396.
38 Schrock, R. R.; Jamieson, J. Y.; Araujo, J. P.; Bonitatebus, P. J. J.; Sinha, A.; Lopez, L. P. H. *J. Organometal. Chem.* **2003**, *684*, 56.
39 Tonzetich, Z. J.; Schrock, R. R.; Müller, P. *Organometallics* **2006**, *25*, 4301.
40 Schrock, R. R. *J. Am. Chem. Soc.* **1976**, *98*, 5399.
41 Czekelius, C.; Hafer, J.; Tonzetich, Z. J.; Schrock, R. R.; Christensen, R. L.; Müller, P. *J. Am. Chem. Soc.* **2006**, *128*, 16664.
42 Scriban, C., Unpublished results, **2006**
43 Trost, B. M.; Older, C. M. *Organometallics* **2002**, *21*, 2544.
44 Oskam, J. H.; Fox, H. H.; Yap, K. B.; McConville, D. H.; O'Dell, R.; Lichtenstein, B. J.; Schrock, R. R. *J. Organometal. Chem.* **1993**, *459*, 185.
45 Wu, Z.; Minhas, G. S.; Wen, D.; Jiang, H.; Chen, K.; Zimniak, P.; Zheng, J. *J. Med. Chem.* **2004**, *47*, 3282.
46 Pagenkopf, B. L.; Livinghouse, T. *J. Am. Chem. Soc.* **1996**, *118*, 2285.
47 Sheldrick, G. M. Acta Cryst. 1990, A46, 467.
48 Sheldrick, G. M (1997). SHELXL 97, University of Göttingen, Germany.

CHAPTER 3

Molybdenum Imido Alkylidene Complexes Supported by β-Diketonate and β-Diketiminate Ligands: Synthesis and Metathetical Reactivity

Portions of this chapter have appeared in print:

Tonzetich, Z. J.; Jiang, A. J.; Schrock, R. R.; Müller, P. "Molybdenum Imido Alkylidene Complexes that Contain a β-Diketiminate Ligand" *Organometallics* **2007**, submitted.

Tonzetich, Z. J.; Jiang, A. J.; Schrock, R. R.; Müller, P. "Cationic Imido Alkylidene Complexes of Molybdenum Supported by β-Diketonate and β-Diketiminate Ligands" *Organometallics* **2006**, *25*, 4725-4727.

INTRODUCTION

The olefin metathesis reaction now stands at the forefront of synthetic tools available to the organic chemist.[1,2,3] A primary driving force in the development of the metathesis reaction has been the synthesis and characterization of high-oxidation state carbene complexes of the early to mid transition series.[4,5] For the most part, high oxidation state carbene (alkylidene) compounds capable of catalyzing metathesis reactions have been limited to molybdenum or tungsten,[6] though examples from vanadium,[7,8] tantalum,[9] and rhenium[10] chemistry should be noted. Group VI alkylidene catalysts have almost invariably contained alkoxide or aryloxide ligation leading to the belief that such ligands were necessary for metathetical activity.[11] However, recent studies in homogeneous solution[12,13] and on silica support[14,15] have revealed that in certain instances, supporting ligands other than alkoxides can lead to active catalysts. Particularly significant is the work of Boncella, which concerns molybdenum and tungsten alkylidene complexes of the {1,2-([Me_3Si]N)$_2C_6H_4$} ligand.[16,17] This work demonstrated that limited metathetical activity could be realized for alkylidene complexes supported by nitrogen ligation.

Along these lines, our laboratory has been exploring variations to the traditional imido alkylidene dialkoxide framework in hopes of preparing more reactive and/or selective catalysts.[18] An especially intriguing variation to the imido alkylidene platform is the introduction of a *positive* charge. Electrophilic attack of the d^0 metal center on incoming alkene has been proposed as the initial step in olefin metathesis catalyzed by high oxidation state alkylidenes compounds.[19,20,21,22] One possible means of improving the catalytic activity of these compounds is to create a cationic metal center that serves as a more potent electrophile. This strategy has been successfully employed with olefin polymerization catalysts of the Group IV metals (see Chapter 1). Additionally, recent work with imido alkylidenes of tungsten has demonstrated that bimolecular coupling of alkylidene ligands to give reduced metal-metal bonded species can be a detrimental deactivation mode during olefin metathesis.[23] Imparting a positive charge to the

catalyst molecule may therefore discourage such reactions because of the resultant coulombic repulsion.

Reports of high-oxidation state alkylidene cations of molybdenum and tungsten are rare. Boncella has reported a series of cationic molybdenum and tungsten imido alkylidenes supported by the *tris*-pyrazolylborate ligand. The counterion in these complexes was the weakly coordinating B[3,5-$(CF_3)_2C_6H_3$] (BAr_{f4}) anion.[24] Such compounds were prepared by alkylide abstraction (see Chapter 1) and isolated as six-coordinate solvent adducts.[25] As a result of the coordinative and electronic saturation, these species demonstrated no reactivity toward olefins.[26] Osborn reported the sole example of a catalytically active cationic alkylidene complex based on tungsten.[27] In the Osborn system, halide abstraction of a dibromide precursor by $GaBr_3$ afforded a four-coordinate species of the type {W(CHR)(OCH_2-*t*-Bu)$_2$(Br)}{$GaBr_4$}.[28] The anion in this instance was found to coordinate to the metal center, rendering the complexes Zwitterionic. Addition of excess $GaBr_3$ to the Zwitterion afforded a new salt with the weakly coordinating Ga_2Br_7 anion. Despite the paucity of Group VI alkylidene cations, several catalytically active ruthenium alkylidene cations have been published, and these complexes display excellent reactivity toward olefins.[29,30,31,32,33,34]

Ideally, supporting ligands for cationic imido alkylidenes should provide stability (steric bulk) while engendering a reactive metal center (low coordination number). The β-diketonate (acac)[35] and β-diketiminate (nacnac)[36] ligands (Scheme 3.1) were chosen in this regard because they fulfill the aforementioned criteria and are readily available either commercially or through well-established synthetic procedures. The ligands also offer the advantage of being symmetric, which limits potential complications arising from the formation of diastereomeric mixtures. As depicted in Scheme 3.1, each ligand class may be modified at the indicated positions to accommodate different steric and electronic requirements. Previous work with alkoxide based imido alkylidenes has demonstrated that changes in the steric and electronic properties of the coordinating alkoxide can dramatically effect catalyst reactivity.[1] Therefore, the ability to modify the acac and nacnac ligands was deemed necessary to fully explore their potential

chemistry. No previous examples of alkylidene complexes supported by β-diketonates appear in the literature, though recent work by Mindiola has shown the proficiency of the β-diketiminate in supporting earlier transition metal alkylidenes and alkylidynes.[37,38] Notably, the nacnac scaffold was shown to support neutral as well as cationic alkylidenes of titanium[39] and vanadium.[40]

Scheme 3.1. β-Diketonate and β-diketiminate ligands.

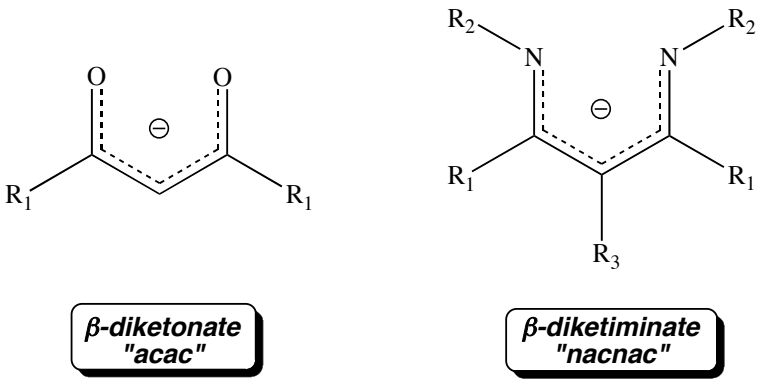

This chapter concerns the synthesis, characterization, and reactivity of alkylidene complexes supported by acac and nacnac ligands. Both neutral and cationic alkylidene species have been prepared, and their proficiency as catalysts in metathesis reactions has been examined through experiments with selected olefins. The chemistry of these compounds is discussed in terms of the relevance to catalytic activity.

RESULTS

3.1. Synthesis and reactivity of neutral and cationic β-diketonate complexes.

The acac ligand was initially targeted because of its similarity to alkoxides, and the commercial availability of several diketones and diketonate salts. Reaction of $Mo(NAr)(CHCMe_2Ph)(OTf)_2(DME)$ with one equivalent of an alkali metal diketonato salt

(Li{TMHD}, TMHD = 2,2,6,6-tetramethylheptane-3,5-dionato; or Na{HFAC}, HFAC = 1,1,1,5,5,5-hexafluoropentane-2,4-dianato) in the presence of a coordinating Lewis base afforded a variety of six-coordinate mono-triflate complexes in modest to good yield (Scheme 3.2, **1a–c** and **2a**). The adducts are all crystalline solids that demonstrate moderate solubility in pentane and dissolve readily in aromatic and ethereal solvents. When the salt metathesis reaction with Li{TMHD} is carried out in the absence of THF, the base free species, Mo(NAr)(CHCMe$_2$Ph)(TMHD)(OTf) (**1d**), can be isolated albeit in lower yield (equation 3.1). The ^{1}H NMR features of **1d** show the lack of any symmetry, consistent with the possible structure depicted in equation 3.1. Unlike the THF adduct **1a**, compound **1d** is insoluble in pentane, suggesting that it may possess a dimeric or oligomeric structure in the solid state. Addition of THF to a solution of **1d** in methylene chloride-d_2 immediately afforded the THF adduct, **1a**, according to ^{1}H NMR spectroscopy.

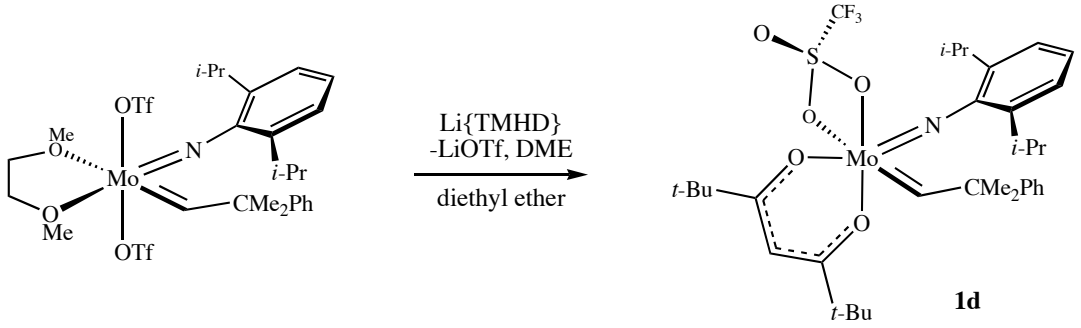

1d (3.1)

The spectral features of **1a** and **1d** are nearly identical, with resonances for the THF ligand appearing very close to those observed for the free solvent (see Experimental). Addition of excess THF to a methylene chloride-d_2 solution of **1a** does not alter the appearance of the ^{1}H NMR spectrum, suggesting that THF may be rapidly dissociating on the NMR timescale at 20 ºC. All other ^{1}H NMR resonances for **1a** appear sharp with inequivalencies observed for both the methyl protons of the isopropyl groups and the neophylidene ligand. Resonances for the H_α and C_α atoms of the alkylidene ligand are found at 13.45 ppm and 326.3 ppm, respectively

(methylene chloride-d_2). The J_{CH} value of 127 Hz for these two atoms is consistent with a *syn* orientation of the alkylidene ligand.[41] Free rotation about the N_{imido}-C_{ipso} bond is apparent as judged by the presence of a single sharp septet resonance for the methine protons of the isopropyl group. The location of the THF ligand (*cis* versus *trans*) relative to the alkylidene could not be determined by NMR spectroscopy, but was elucidated by means of an X-ray diffraction study. The solid-state structure of compound **1a** is shown in Figure 3.1.

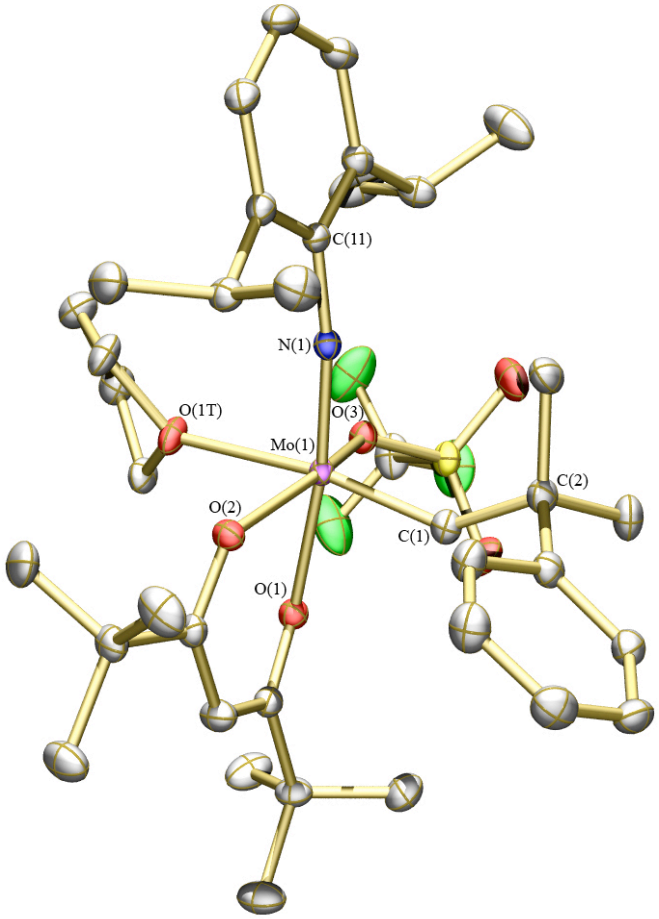

Figure 3.1. Thermal ellipsoid rendering (50%) of **1a**. Hydrogen atoms omitted for clarity. Selected bond distances (Å) and angles (°): Mo(1)–C(1) = 1.9176(17); Mo(1)–N(1) = 1.7488(13); Mo(1)–O(1) = 2.1038(11); Mo(1)–O(2) = 2.0579(11); Mo(1)–O(1T) = 2.3525(12); Mo(1)–O(3) = 2.1351(11); Mo(1)–C(1)–C(2) = 141.95(13); N(1)–Mo(1)–C(1) = 99.59(7); Mo(1)–N(1)–C(11) = 170.21(12); O(1)–Mo(1)–O(2) = 81.99(4); C(1)–Mo(1)–O(1T) = 168.92(6).

Metric parameters are listed in the caption to Figure 3.1 and refinement data can be found in the Experimental section. The complex displays octahedral geometry about the Mo atom with the THF ligand bound *trans* to the alkylidene. The alkylidene is the *syn* isomer, consistent with solution studies. All bond lengths and angles fall within the range commonly encountered for six-coordinate imido alkylidenes of this type (c.f. $Mo(NAr)(CHCMe_2Ph)(OTf)_2(DME)$[42]). Of note is the acute O(1)–Mo(1)–O(2) angle of 89.99(4)º, which is significantly smaller than the bite angles typically observed for chelating diolate ligands.[43]

Scheme 3.2. Preparation of various imido alkylidene complexes of the acac ligand.

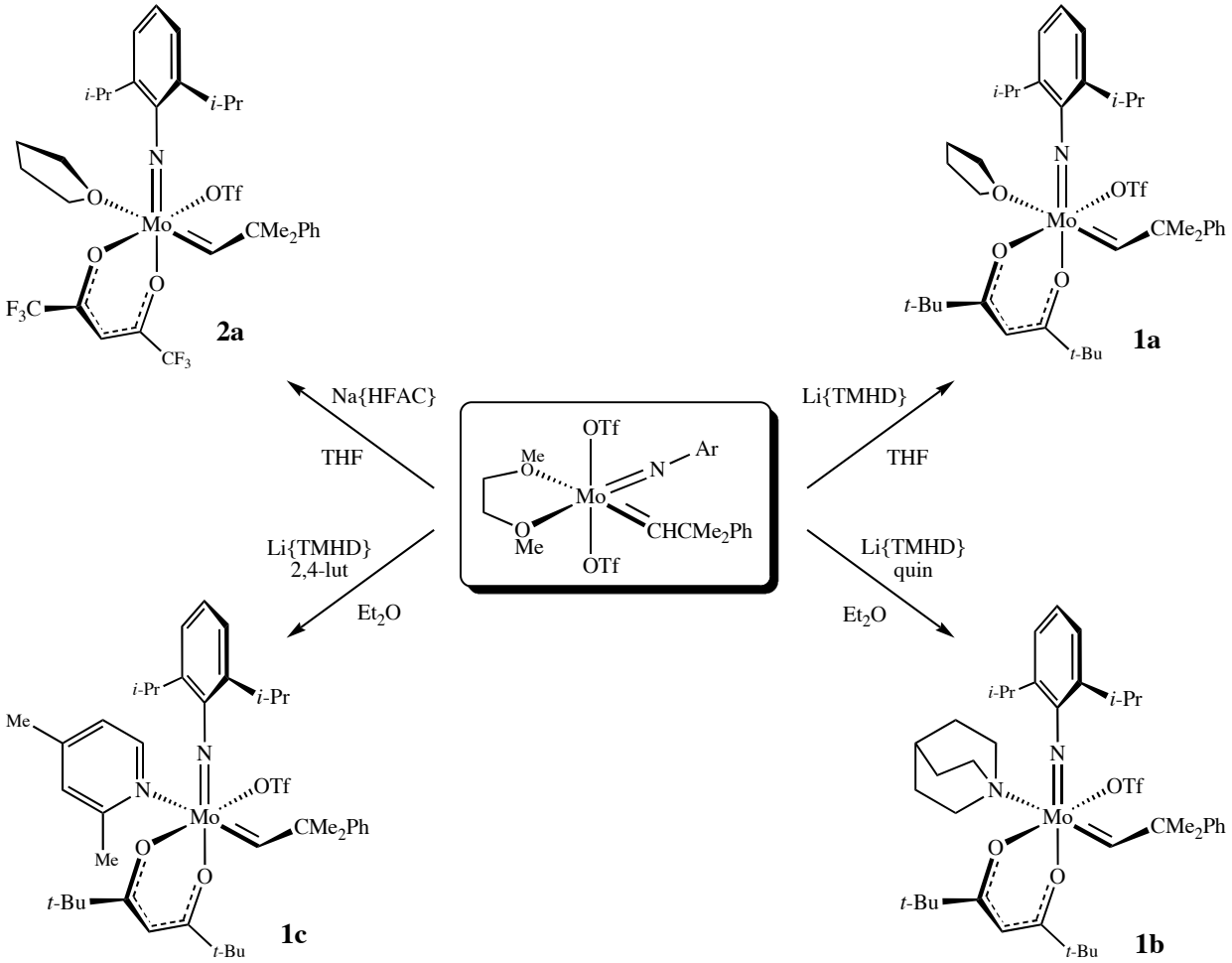

In contrast to the THF adduct, the quinuclidine adduct (**1b**, Scheme 3.2) displays hindered rotation about the N_{imido}-C_{ipso} bond in solution as judged by ^{1}H NMR spectroscopy. Resonances for the quinuclidine ligand are sharp as expected for a tightly bound adduct, and the alkylidene exists solely as the *syn* isomer (J_{CH} = 127 Hz, benzene-d_6). Unlike **1a** and **1b**, the lutidine adduct (**1c**, Scheme 3.2) exists as two isomers. The ^{1}H NMR spectrum of **1c** reveals a 1.3:1 ratio of isomers that remains unchanged upon repeated recrystallization of the compound from pentane or diethyl ether. The nature of the isomerism is not known at this time, and the two compounds may be coordination isomers (lutidine bound *cis* or *trans* to alkylidene) or simply rotational isomers of the 2,4-lutidine ligand and/or alkylidene ligand. The J_{CH} value could not be determined due to broadening of the alkylidene proton resonances.

An attempt to prepare a PMe_3 adduct similar to compounds **1a**-**c** resulted in isolation of the *bis*-trimethylphosphine complex, **1e** (equation 3.2). Addition of Li{TMHD} to an ethereal solution of Mo(NAr)($CHCMe_2Ph$)$(OTf)_2$(DME) in the presence of several equivalents of PMe_3 led to precipitation of a bright yellow powder. The insolubility of the powder in common

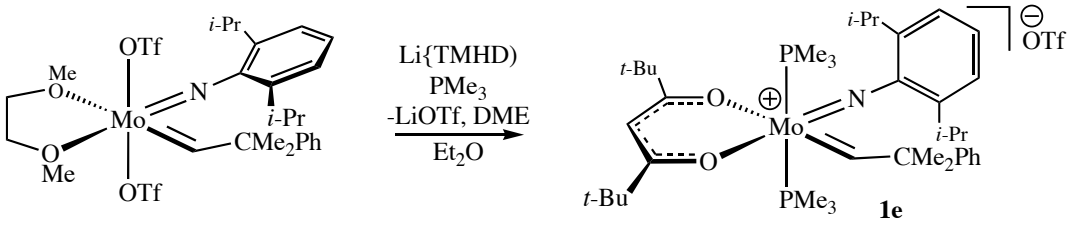

(3.2)

solvents other than THF and methylene chloride is consistent with its formulation as a charged species such as that shown in equation 3.2. The ^{1}H NMR spectrum of **1e** demonstrates that the molecule possesses a mirror plane. A pseudo-triplet resonance is observed for the methyl groups of the PMe_3 ligands, consistent with *trans* disposed phosphines. The six-coordinate nature of **1e** (18 electron) renders the complex relatively inert. Consequently, no further examination of the species was undertaken.

Reaction of Mo(NAr)(CHCMe$_2$Ph)(OTf)$_2$(DME) with Na{HFAC} in THF afforded compound **2a** (Scheme 3.2) as a pentane soluble orange-red crystalline material. The ^{1}H NMR spectrum of the material contains three alkylidene resonances with one species predominating in >90 %. The resonances for all three species are broadened slightly, as are the resonances for THF (contrast **1a** where the protons for THF appear as sharp multiplets). The spectrum remains unchanged after repeated recrystallization of **2a** from pentane.

Conversion of the triflate complexes to the corresponding cationic complexes was accomplished by reaction with NaB[3,5-(CF$_3$)$_2$C$_6$H$_3$]$_4$ (NaBAr$_{f4}$) in methylene chloride (equation 3.3). The complex salt, **3a**, forms large yellow cubes that desolvate quickly at room temperature

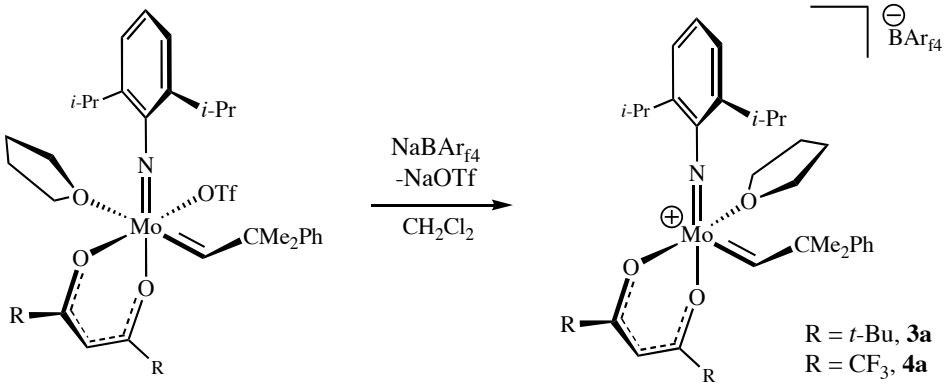

(3.3)

or *in vacuo*. The NMR features of the complex are similar to those of **1a**. The alkylidene resonance is found at 13.02 ppm (methylene chloride-d_2) and remains the *syn* rotamer as judged by a J_{CH} value of 121 Hz. The methyl protons of the neophylidene ligand appear as two distinct singlets indicating that no major rearrangement of the TMHD ligand has taken place to increase the symmetry of the complex. The methine proton of the isopropyl group appears as a single sharp septet indicating free rotation of the aryl ring. Layering of a saturated methylene chloride solution of **3a** with heptane afforded crystals suitable for X-ray diffraction. Several views of the solid-state structure are depicted in Figure 3.2 and metric parameters are listed in the caption.

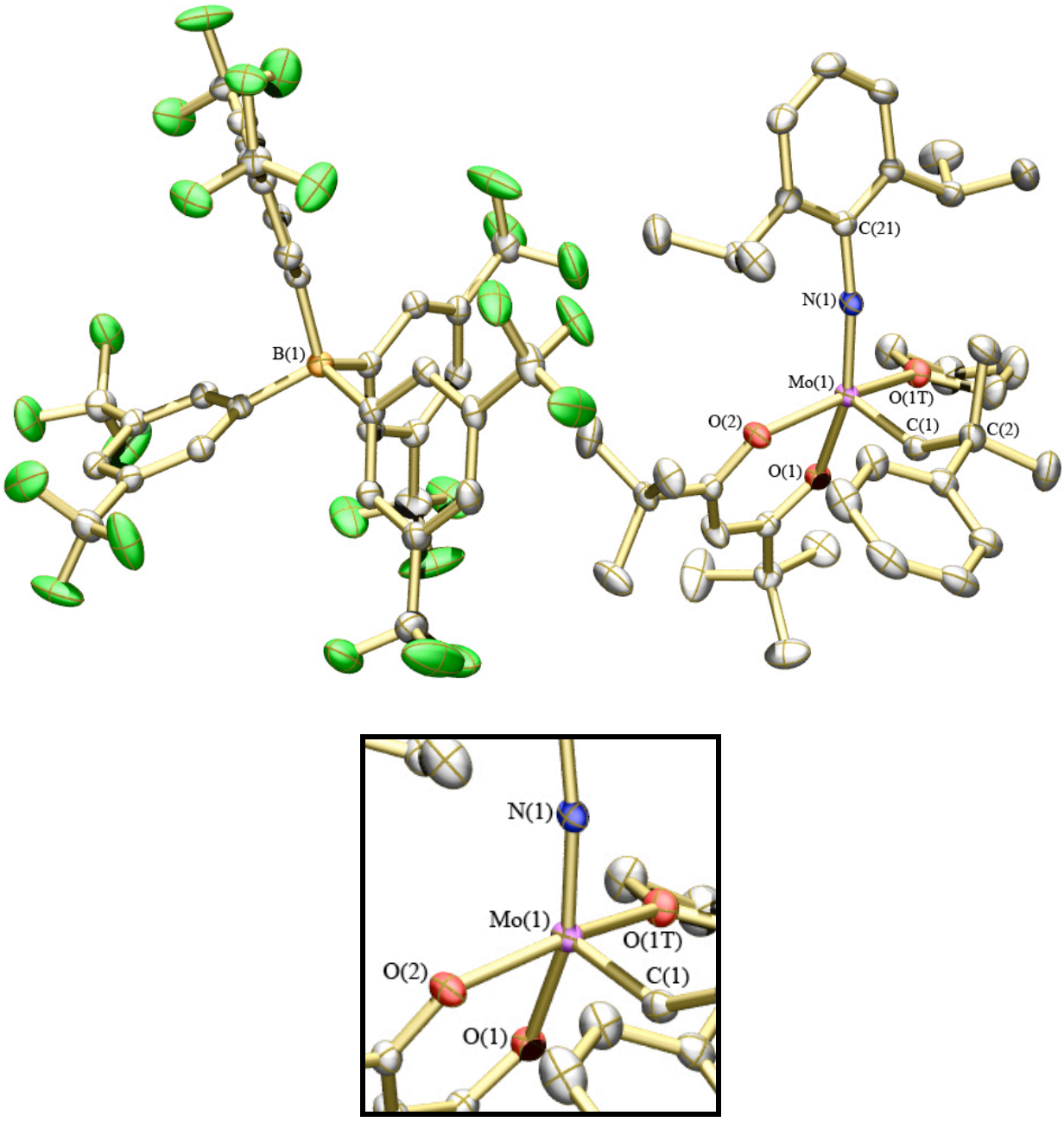

Figure 3.2. Above: thermal ellipsoid drawing (50%) of compound **3a**. Hydrogen atoms, minor components of disordered atoms, and cocrystallized molecules of heptane and methylene chloride omitted for clarity. Below: enlargement of the coordination sphere in **3a**. Selected bond distances (Å) and angles (°): Mo(1)–C(1) = 1.893(3); Mo(1)–N(1) = 1.745(2); Mo(1)–O(1) = 2.0677(18); Mo(1)–O(2) = 2.0540(18); Mo(1)–O(1T) = 2.1385(18); Mo(1)–F(anion) > 5.7; Mo(1)–C(1)–C(2) = 142.4(2); N(1)–Mo(1)–C(1) = 101.07(10); Mo(1)–N(1)–C(11) = 167.89(18); O(1)–Mo(1)–O(2) = 81.95(7).

The asymmetric unit of the crystal contained one molecule of both CH_2Cl_2 and heptane, consistent with NMR spectra of freshly crystallized material. The heptane molecule was disordered but could be modeled satisfactorily. The most interesting feature of the structure is the pseudo-square pyramidal geometry. The Mo atom sits ~0.3 Å above the best-formed plane through the four equatorial atoms. The solid state structure of **3a** is reminiscent of the structure of Re(N-2,6-*i*-$Pr_2C_6H_3$)(CH-*t*-Bu)$(OAr)_3$, which also displays a pseudo-square pyramidal geometry with the alkylidene ligand occupying the axial position.[10] The bond lengths and angles of **3a** are unremarkable, with the exception of the Mo(1)–O(1T) bond length of 2.1385(18) Å. This bond distance is 0.2 Å shorter than the dative Mo(1)–O(1T) bond in **1a**. The structure shows no close contacts with the anion or the cocrystallized solvent molecules (see caption to Figure 3.2).

The cationic species, **4a**, formed cleanly upon addition of $NaBAr_{f4}$ to a solution of **2a** in methylene chloride-d_2. Unfortunately, solid samples of **4a** contained substantial amounts of 2,6-diisopropylanilinium borate presumably via decomposition. Repeated recrystallization of **4a** did not free the complex of the anilinium salt. As a result no further study of **4a** was carried forward. Cationic species containing quinuclidine or 2,4-lutidine in place of THF could not be isolated, though NaOTf was observed to precipitate upon addition of $NaBAr_{f4}$ to methylene chloride solutions of **1b** and **1c**.

To determine the utility of **3a** as a metathesis catalyst, reactions with several olefins were investigated. Upon addition of 20 equivalents of diallyl ether to a methylene chloride-d_2 solution of the **3a**, consumption of the initial neophylidene was apparent, but no ring-closed product was observed via ^{1}H NMR. Likewise, addition of excess diallyltosylamine or norbornene led to disappearance of the starting neophylidene, but in each case no metathesis products were formed in substantial quantities.

In order to probe the apparent lack of metathetical reactivity towards olefins, the reaction of **3a** with ethylene was examined. Upon exposure of **3a** to 1 atm of ethylene or ethylene-$^{13}C_2$ in methylene chloride-d_2 at room temperature, an immediate darkening of the yellow solution was

apparent. Observation of the reaction by NMR revealed a variety of reaction products. Spectroscopic data for several of the observed species appear in Scheme 3.3. Consumption of the original neophylidene was complete within 10 minutes as judged by NMR. The principal end-products of the reaction were cyclopropane and an ethylene complex (Scheme 3.3). Also observable in the ^{13}C NMR spectrum was the unsubstituted metallacyclobutane complex (J_{CC} = 11.6 Hz), as well as minor amounts of propylene and the neophyl-substituted cyclopropane. The presence of cyclopropanes and propylene is indicative of rearrangement of intermediate metallacyclobutane species.[44] Formation of cyclopropane in reactions of alkylidenes with ethylene has only been observed as a minor reaction pathway in previous experiments with neutral alkoxide-supported catalysts.[45,46]

Scheme 3.3. Proposed reaction pathway for reaction of **3a** with ethylene-$^{13}C_2$.

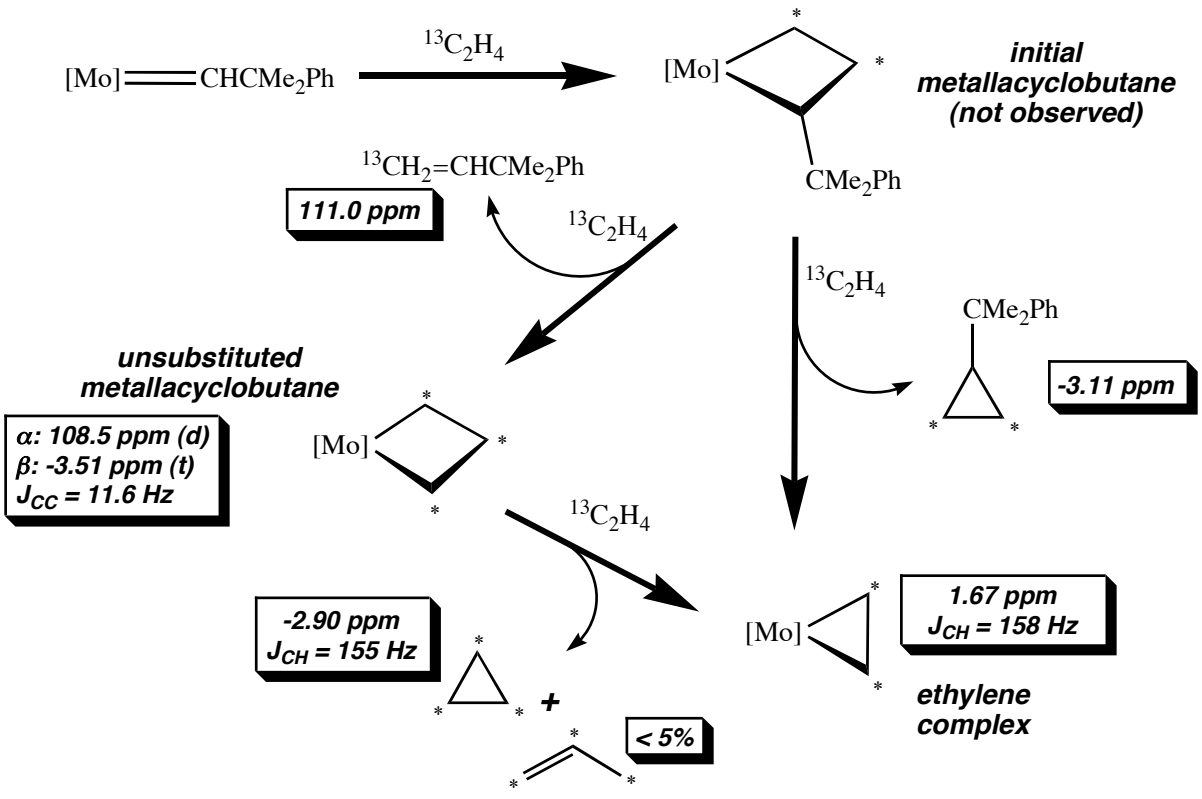

Results from the experiments with metathesis substrates clearly demonstrate that initial reactivity of olefins with **3a** is not the cause of the poor catalytic efficacy. In each case, consumption of the initial alkylidene is observed although only very small amounts of the metathesis products are observed. The reaction with ethylene is more enlightening, and reveals several possible deactivation modes that may destroy intermediate metallacycles.

3.2 Synthesis and reactivity of neutral β-diketiminate complexes

The larger steric protection afforded by nacnac ligands and their success in supporting reactive metal fragments[36] led to the exploration of this class of ligands as an alternative to β-diketonates. Unlike β-diketonates, β-diketiminate salts are not commercially available, although a variety of different substituted β-diketimines can be prepared in simple fashion by condensation of the desired aniline with pentanedione in the presence of *p*-toluenesulfonic acid. The first nacnac ligand examined was $\{[(2,6\text{-}Me_2C_6H_3)NC(Me)]_2CH\}^-$ (Ar′-nacnac).[47] In analogous fashion to diketonate complexes, salt metathesis reactions of Li{Ar′-nacnac} with $Mo(NR)(CHCMe_2R')(OTf)_2(DME)$ (R = Ar, Ar^{Cl}, or Ar″; R′ = Me or Ph) in ether afforded the corresponding nacnac complexes (**5a**-**c**) in good yield (equation 3.4).

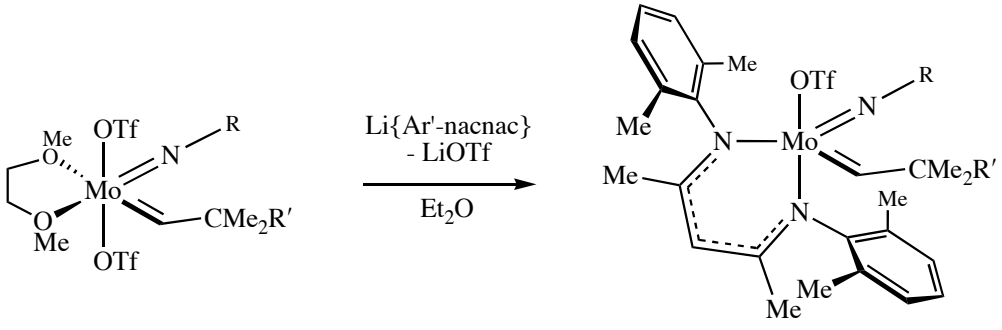

(3.4)

R = Ar, R′ = Ph, **5a**
R = Ar^{Cl}, R′ = Me, **5b**
R = Ar″, R′ = Me, **5c**

Compounds **5a**-**c** are all pentane insoluble microcrystalline powders that may be conveniently crystallized from diethyl ether. Compounds **5a** and **5c** are orange, while compound **5b** is deep red. ^{1}H NMR spectra of **5a**-**c** are consistent with the structure depicted in equation 3.3. The molecular geometry shown in equation 3.3 is inferred from a crystal structure of a related complex possessing the Ar^{Cl}-nacnac ligand (Ar^{Cl} = 2,6-dichlorophenyl) prepared by Annie Jiang.[48] Compound **5a** predominantly exists as the *syn* isomer (97%) in solution as judged by a J_{CH} value of 116 Hz. In general, coupling constants observed for the *syn* isomers of the nacnac complexes are 10 – 12 Hz smaller than those observed for the corresponding acac complexes (e.g. **5a** versus **1a**). The attenuated coupling may result from an opening of the Mo–C_α–C_β angle imposed by the steric constraints of the nacnac ligand. The alkylidene H_α resonance for **5a** is found at 11.56 ppm in benzene-d_6. This value is nearly 2 ppm upfield of that for **1a** highlighting the electronic differences between the acac and nacnac ligands. Rotation about the N-aryl bond of the diketiminate is locked, and sharp singlet resonances are observed for each of the Ar′-methyl groups. Compound **5a** also displays locked rotation about the N_{imido}-C_{ipso} bond as evidenced by inequivalent broadened methine resonances. Spectroscopic features for **5b** and **5c** are nearly identical to those of **5a** with the exception of free rotation about the N_{imido}-C_{ipso} bond in **5b**. Unlike the diketonate complexes, the diketiminate complexes show no tendency to bind Lewis bases such as THF or quinuclidine, presumably due to the bulkier, more electron rich nature of the nacnac ligand.

A variety of decomposition modes of the nacnac ligand have been reported for complexes across the transition series.[49,50,51] In many instances these decomposition reactions occur in a well-defined manner to yield new ligand architectures.[52] Such was the case with compounds **5a**-**c**. These compounds were found to decompose to the molybdaziridine[53] species, **6a**-**c** (equation 3.5), when heated at or above 60 ºC in solvents such as benzene or toluene.

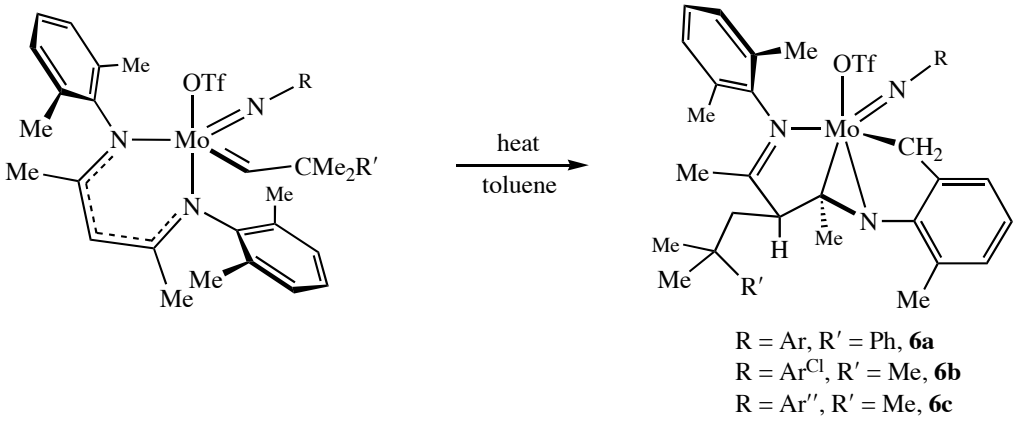

(3.5)

R = Ar, R′ = Ph, **6a**
R = Ar^{Cl}, R′ = Me, **6b**
R = Ar″, R′ = Me, **6c**

The structure of **6a** was determined by X-ray crystallography. The compound crystallized as a non-merohedral twin, with two chemically identical but crystallographically independent molecules in the asymmetric unit. One of the molecules is shown in Figure 3.3 and metric parameters are listed in the caption. The most striking structural feature of **6a** is the apparent addition of an alkyl group derived from the former neophylidene ligand to the γ carbon of the nacnac ligand. One of the CH bonds of the *ortho*-methyl groups has also been activated resulting in a new metal-carbon bond. The nacnac ligand is now best described as a chelating κ^1/η^2-diimine ligand with an additional bond from the benzylic methyl group of the η^2-coordinated imine substituent. This description is borne out in the bond lengths tabulated in the caption to Figure 3.3.

The spectroscopic features of **6a** in solution are also in accord with the solid state structure. The proton attached to C(2) appears at 4.12 ppm as a triplet with J_{HH} = 4.5 Hz in benzene-d_6. The ^{13}C NMR was assigned with the help of HSQC and HMBC experiments, which located carbon atoms C(1) and C(3) at 197.8 ppm and 82.83 ppm, respectively in benzene-d_6. Though not isolated, derivatives **6b** and **6c** form smoothly at 90 ºC in toluene-d_8, and display spectral features nearly identical to those of **6a**. Several reports of benzylic CH activation reactions of aryl-nacnac ligands have appeared,[54,55] but there are no reports of decomposition modes such as that shown in equation 3.5. The qualitative rate of decomposition of the different imide derivatives roughly follows the order **5a** ≈ **5c** > **5b**.

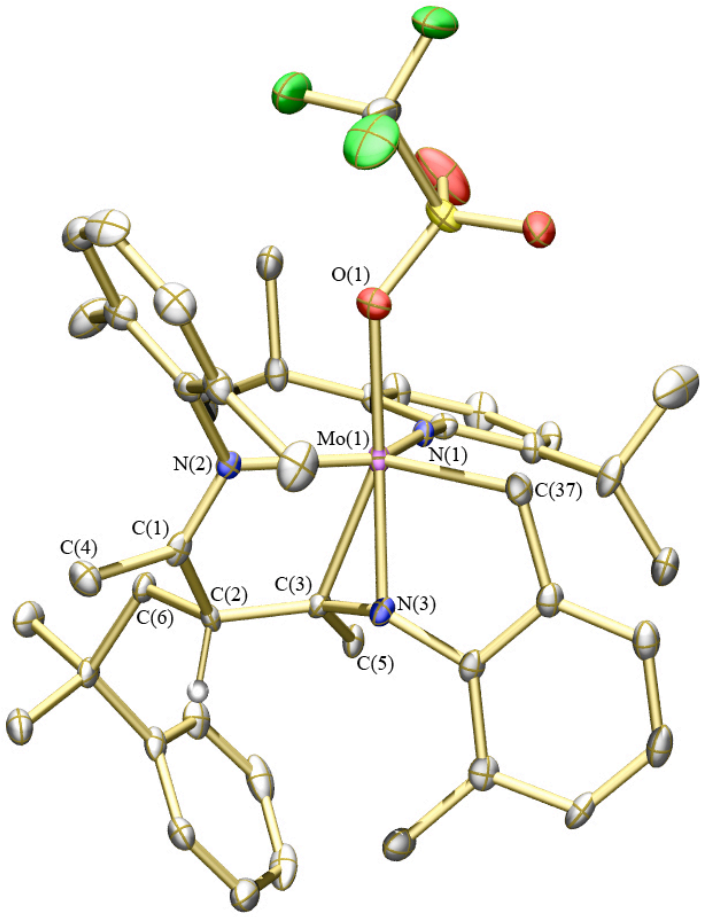

Figure 3.3. Thermal ellipsoid drawing (50%) of one of two independent molecules of **6a** in the asymmetric unit. Hydrogen atoms omitted for clarity. Selected bond distances (Å) and angles (º): Mo(1)–N(1) = 1.723(3); Mo(1)–N(2) = 2.239(3); Mo(1)–O(1) = 2.127(2); Mo(1)–N(3) = 1.992(3); Mo(1)–C(3) = 2.207(3); Mo(1)–C(37) = 2.165(3); C(1)–N(2) = 1.285(4); C(1)–C(2) = 1.505(5); C(2)–C(3) = 1.541(4); C(3)–N(3) = 1.380(4); N(2)–Mo(1)–N(3) = 85.10(10); N(3)–Mo(1)–C(37) = 126.67(12).

In order to better understand the thermal degradation process, the reaction shown in equation 3.5 was examined by NMR spectroscopy for **5a**. Formation of the molybdaziridine in toluene-d_8 followed smooth first order kinetics in the temperature range examined (333 to 363 K) with no observable intermediates (Figure 3.4). An Eyring plot is shown in Figure 3.5.

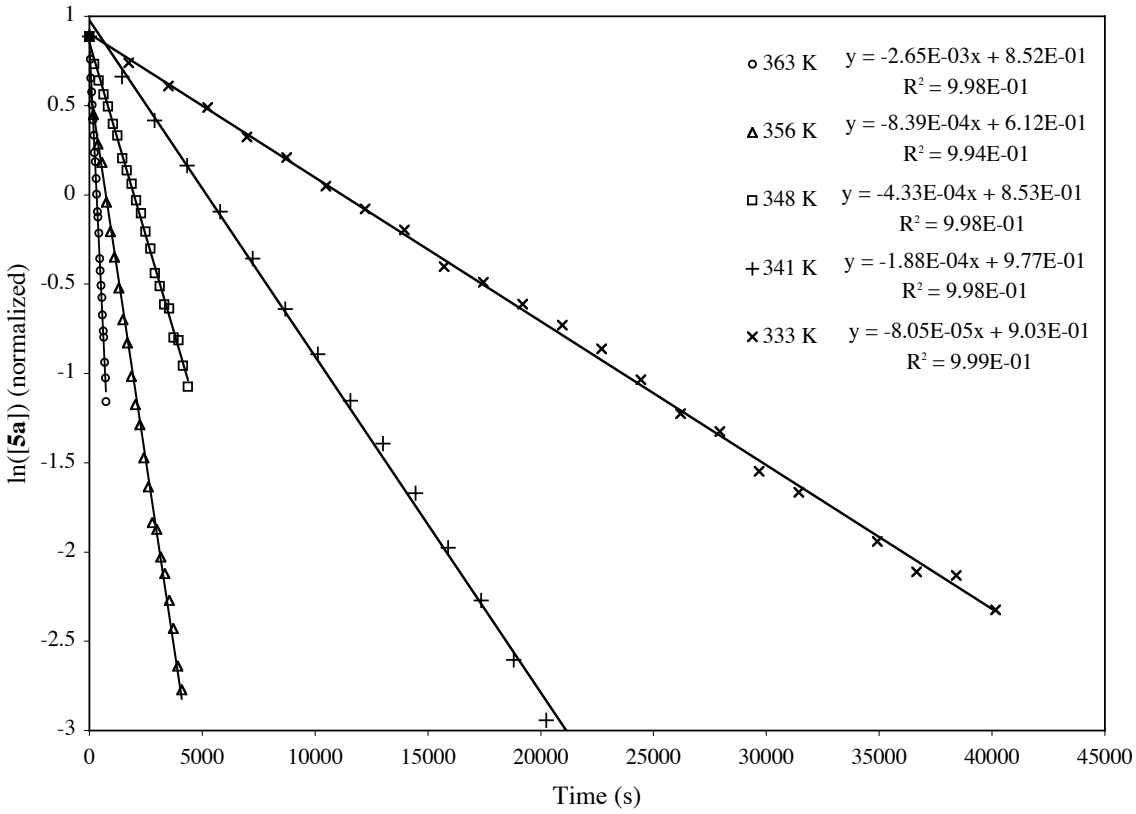

Figure 3.4. Kinetic plots for the conversion **5a** to **6a** at various temperatures in toluene-d_8 (18.0 mM).

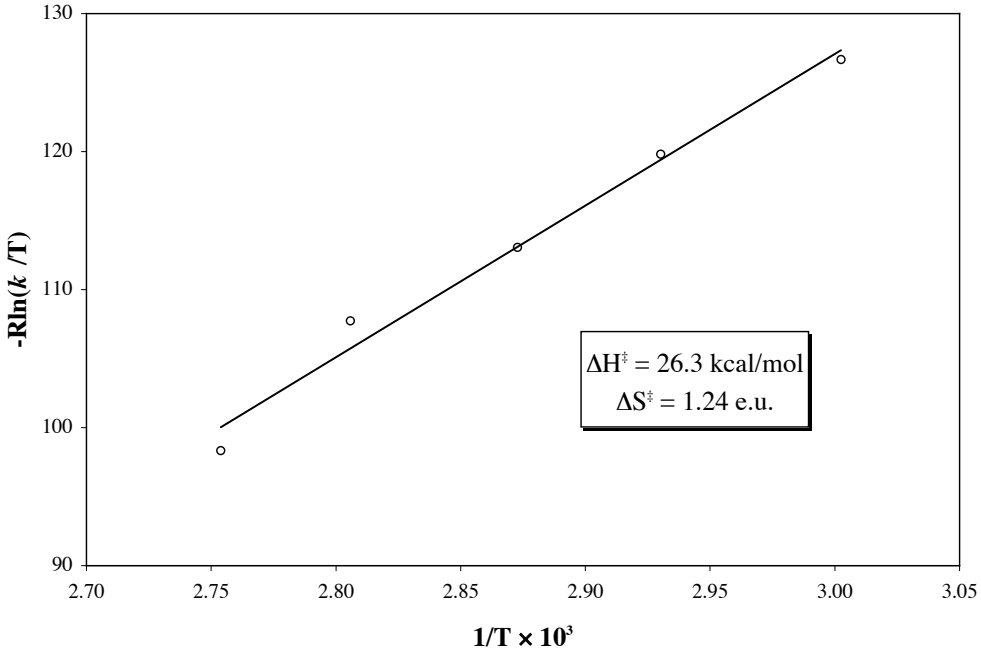

Figure 3.5. Eyring plot for the conversion of **5a** to **6a** in toluene-d_8.

The large activation enthalpy for formation of **6a** is consistent with rate-determining C-H bond cleavage. However, the small positive activation entropy is curious and no concise explanation for this value can be put forth at this time.

A possible mechanism for the formation of the molybdaziridine begins with rate-determining proton transfer from a benzylic methyl group to the alkylidene ligand (Scheme 3.4). This proton transfer generates a putative dialkyl intermediate that immediately undergoes migratory insertion into the C-C double bond of the nacnac ligand. The ability of the dialkyl

Scheme 3.4. Possible reaction pathway for conversion of **5a** to **6a**.

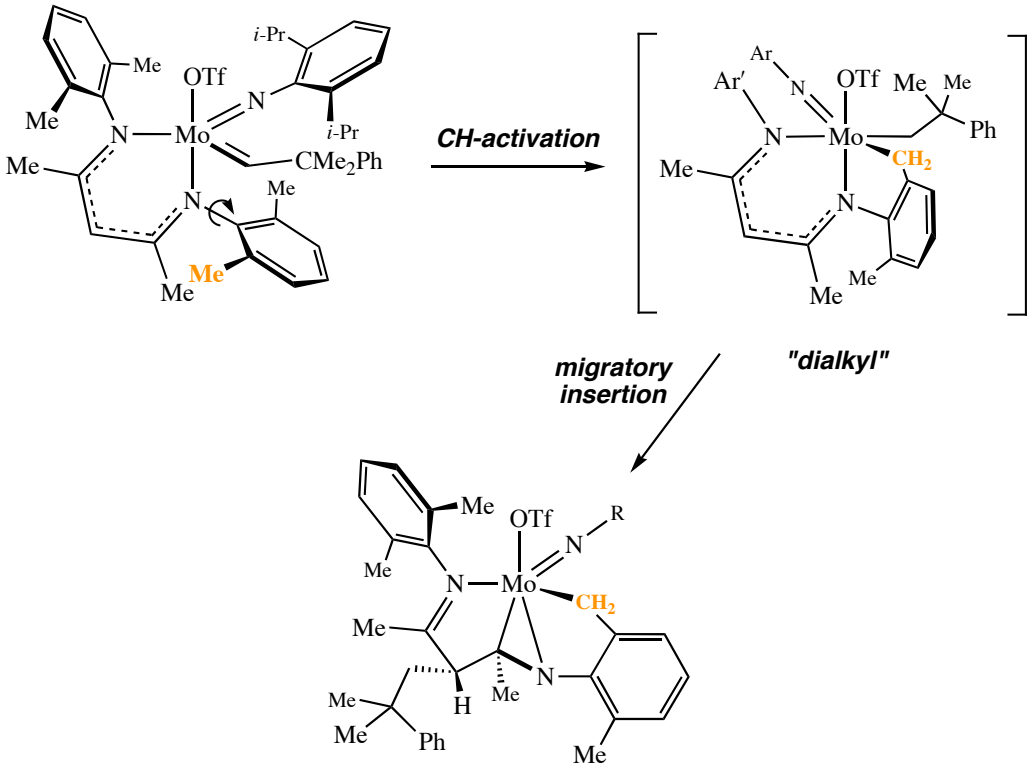

intermediate to insert into the nacnac backbone may be rationalized by considering that benzylic activation of the aryl substituent destroys the symmetry in the nacnac ligand rendering the backbone more olefinic. The migratory insertion step is almost certainly unimolecular as demonstrated by crossover experiments (70 °C, benzene-d_6) between **6a** and **6c**, which fail to

show any scrambling of the initial neophylidene/neopentylidene ligands. Also note from Figure 3.3 that C(6) and the Mo atom are on the same side of the C(2)–C(3) bond, consistent with *cis* addition across the C(2)=C(3) bond. It is likely that CH addition across the alkylidene ligand is influenced by steric congestion about the coordination sphere of the Mo atom. Not surprisingly, the qualitative trend in decomposition rates observed for **5a**-**c** roughly parallel the steric properties of the respective imides.

Initial success with the Ar^{Cl}-nacnac ligand, and potential complications stemming from benzylic activation of the Ar′-nacnac ligand next prompted an examination of Ar^{F}-nacnac[56]. Unfortunately, salt metathesis reactions similar to those in equation 3.4 with Li{Ar^{F}-nacnac} did not afford the desired diketiminate complex, instead resulting in isolation of the starting materials. However, transmetallation of the ligand was achieved through use of the thallium complex, Tl(Ar^{F}-nacnac),[56] in toluene (equation 3.6). The thallium salt was prepared in straightforward fashion from Li{Ar^{F}-nacnac} and Tl(O_2CCH_3) in THF.

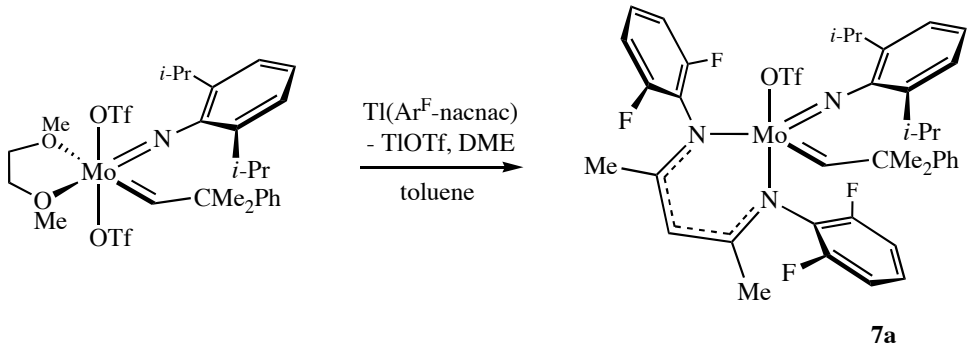

7a (3.6)

Mo(NAr)($CHCMe_2Ph$)(Ar^{F}-nacnac)(OTf) (**7a**) is similar to compounds discussed above. Despite the presence of the more electron-withdrawing difluorophenyl substituents, the compound shows no affinity toward THF or quinuclidine. Additionally, compound **7a** is quite thermally robust. Solutions of **7a** in benzene-d_6 are stable at 70 ºC for at least 18 hours. The spectroscopic features are complicated by the presence of substantial amounts of both *syn* and *anti* isomers that appear in 1:1.2 ratio. The alkylidene H_α resonance for the *syn* isomer appears at

12.42 ppm (benzene-d_6). This chemical shift is nearly a full ppm downfield of the analogous species possessing the Ar′-nacnac ligand, and demonstrates the pronounced electronic effect of replacing the methyl groups with fluorine atoms. The alkylidene resonance for the *anti* isomer appears at 14.90 ppm in benzene-d_6 and shows a small splitting (J = 2.0 Hz), presumably due to H-F coupling. This small coupling may be indicative of fluorine coordination in the *anti* isomer, though a corresponding J_{CF} could not be identified by ^{13}C NMR spectroscopy. No ^{19}F-coupling of any kind could be resolved for the *syn*.

In addition to the *ortho*-substituted aryl nacnac ligands, the 3,5-dimethylphenyl nacnac ligand (Ar*-nacnac)[57] was studied, partly in order to avoid the benzylic activation observed with Ar′-nacnac. Reaction of Li{Ar*-nacnac} with Mo(NAr)(CHCMe$_2$Ph)(OTf)$_2$(DME) in diethyl ether afforded the corresponding triflate species, **8a**, in good yield as an orange-red crystalline solid (equation 3.7). Unlike **5a**, the spectral features of **8a** indicate free rotation about the N_{imido}-C_{ipso} bond at room temperature. The 3,5-dimethylphenyl rings appear to be rotating slowly on the NMR timescale, as judged by broadened resonances for the *o*-H resonances.

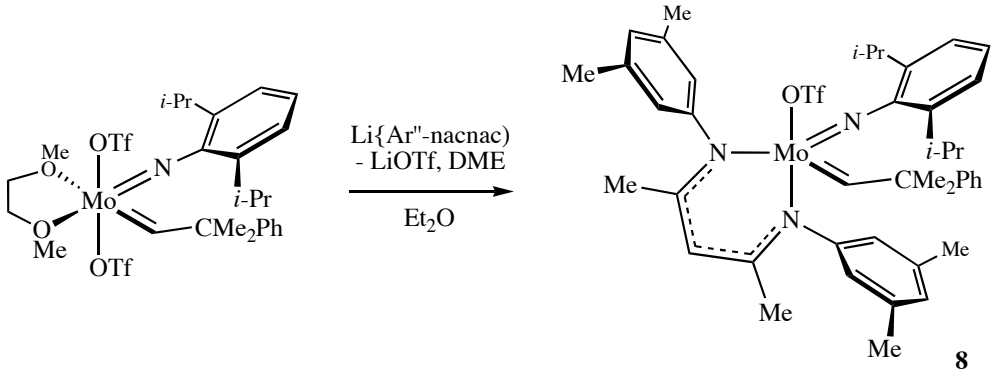

8 (3.7)

Recrystallized samples of **8a** show predominantly the *syn* isomer (92%), with the alkylidene H_α resonance appearing at 12.12 ppm (benzene-d_6). The alkylidene chemical shift of **8a** is substantially farther downfield than that of **5a** (11.56 ppm), possibly a consequence of the attenuated inductive effects of placing the methyl groups in the *meta* versus *ortho* positions. Thermolysis of **8** in benzene-d_6 at 40 ºC for 4 hours led to decomposition as judged by ^{1}H NMR

spectroscopy. The nature of the decomposition product is not known at this time, although spectra are consistent with destruction of the alkylidene ligand and formation of a compound containing diastereotopic methylene resonances. The decomposition product could not be isolated and bulk thermolysis of **8a** always results in substantial amounts of the starting material. This result suggests that the decomposition mode may be bimolecular. Such a reaction pathway would be consistent with the smaller steric protection afforded by the Ar*-nacnac ligand. Thus, removal of the benzylic methyl groups from the 2 and 6 positions of the aryl substituents *is not* sufficient to eliminate thermal decomposition processes.

Various attempts to alkylate compounds **5a** and **8a** with a variety of alkylating agents such as *t*-$BuCH_2MgCl$, *t*-$BuCH_2Li$, and MeMgBr were unsuccessful. The nature of the reaction products in these experiments could not be identified spectroscopically, but in each case a darkening of the reaction solution was observed. The thermal sensitivity of **5a** and **8a** suggests that increasing the steric environment around Mo may be detrimental to complex stability. It is also possible that the nacnac ligands may be attacked by aggressive alkylating agents, leading to rampant decomposition. The nacnac imido framework remains an intriguing platform in which to study possible α-elimination processes if suitable alkylating agents could be found.

3.3 Synthesis and reactivity of cationic β-diketiminate complexes

Synthesis of the cationic nacnac complexes **9a** and **9b** was carried out in methylene chloride with $NaBAr_{f4}$ in the presence of several equivalents of THF, or with $NaB(C_6F_5)_4 \cdot THF$ (equation 3.8). Spectral features of the cations with either anion (BAr_{f4} or $B(C_6F_5)_4$) are identical. The BAr_{f4} anion was used preferentially because its salts were more crystalline and easier to handle than the corresponding $B(C_6F_5)_4$ salts. Attempts at preparing the tetraphenylborate salt of **9a** were unsuccessful and yielded only oils. Reaction of **5a** or **5c** with $NaBAr_{f4}$ in the absence of THF led to unidentifiable decomposition products. Examination of the decomposition products by ^1H NMR spectroscopy showed evidence of benzylic activation of

the nacnac ligand, although in no case could any product be isolated. THF appears necessary to stabilize the cationic species. This requirement is consistent with the observed intramolecular coordination of Cl to cations prepared with the Ar^{Cl}-nacnac ligand.[58]

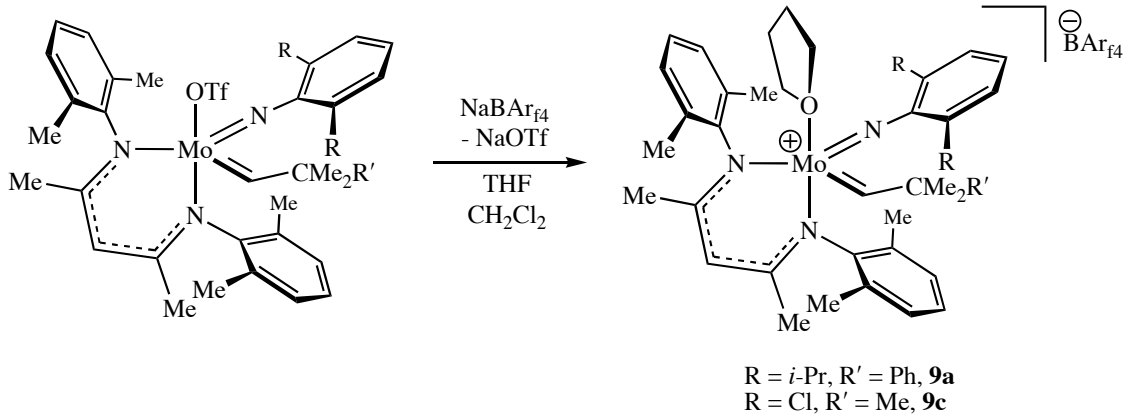

(3.8)

In the case of both **9a** and **9b**, isolated yields exceed 85%. Complex **9a** is an orange crystalline solid, whereas **9b** is deep red; both compounds are insoluble in aromatic and aliphatic solvents. The spectroscopic features of each complex are similar and display broadened ^{1}H NMR spectra at room temperature. In solution at 20 ºC, coordinated THF appears to exchange rapidly with free THF for both compounds. Thus, the appearance of spectra at room temperature is most likely a consequence of both THF dissociation and geometrical rearrangement (pseudo-rotation) of the coordination sphere. Each complex exists as the *syn* isomer as judged by J_{CH} values of 108 Hz for **9a** and 117 Hz for **9b** in methylene chloride-d_2. The alkylidene proton chemical shifts for each compound are shifted downfield from those of the neutral triflate compounds (see Experimental section), indicating that the cations are more electron deficient. Variable temperature spectra of both compounds at low temperature show locking out of rotational processes for each of the aryl substituents. In the low temperature limit, inequivalencies for the protons of the THF ligand (Figures 3.6 and 3.7) are observed. Such spectra are consistent with tight binding of THF at low temperature, and a structure resembling that in equation 3.8.

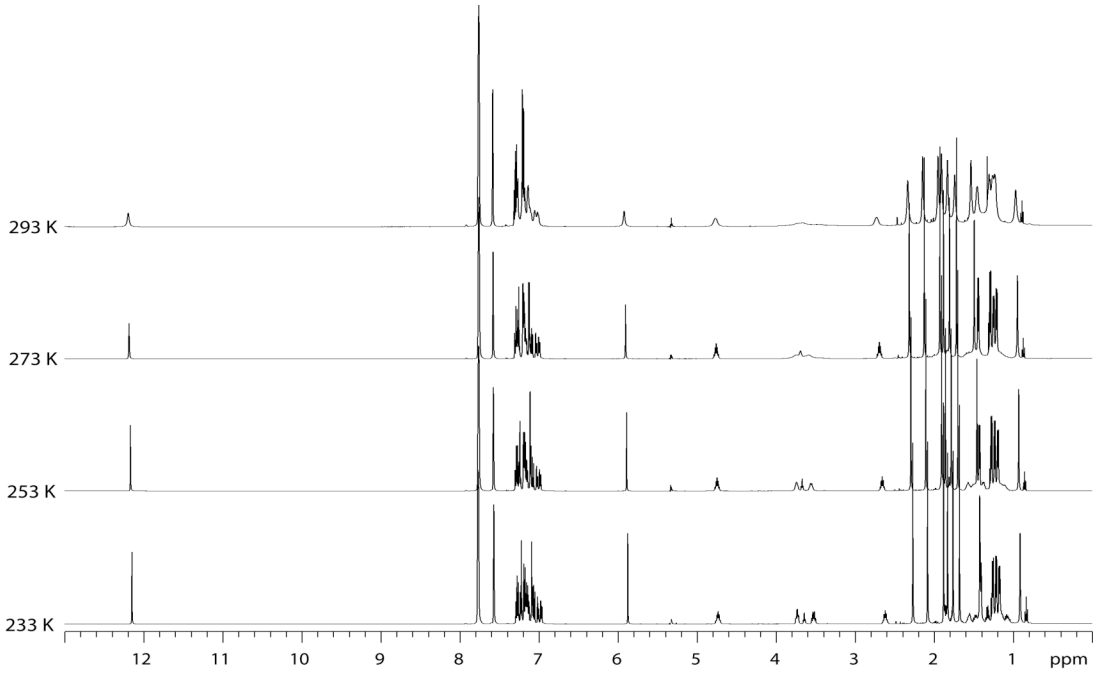

Figure 3.6. Variable temperature 500 MHz ^{1}H NMR spectrum of **9a** in methylene chloride-d_2.

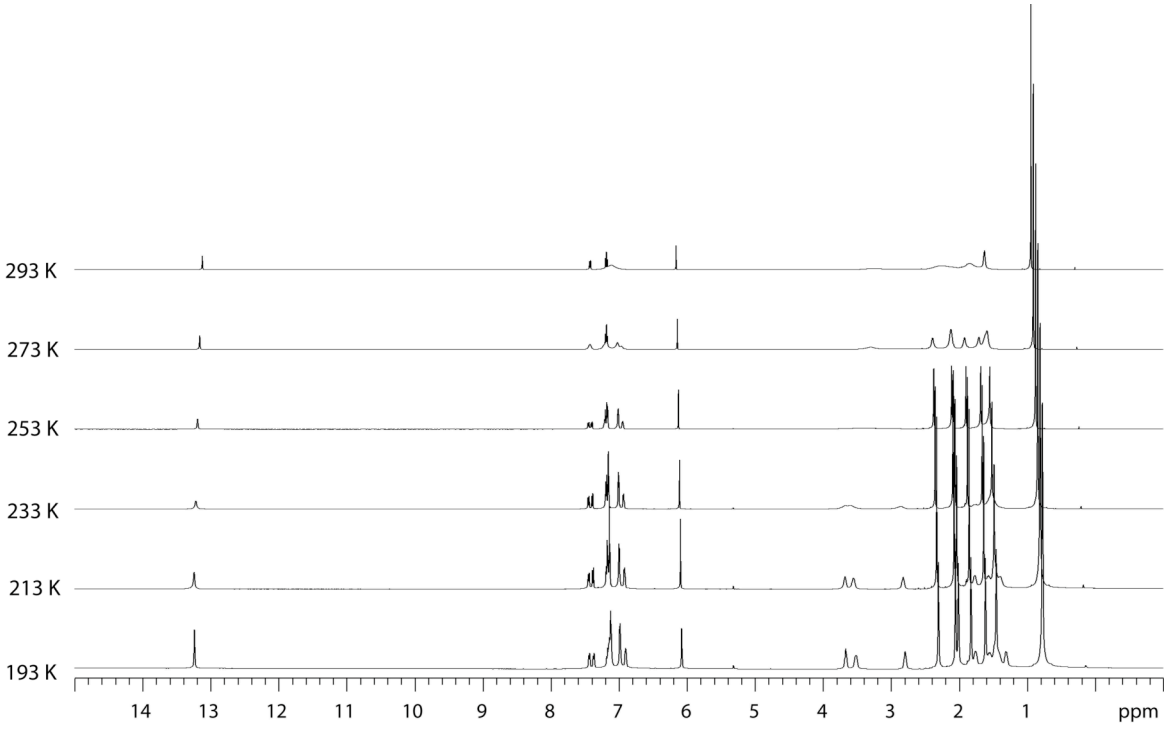

Figure 3.7. Variable temperature 500 MHz ^{1}H NMR spectrum of **9b** ($B(C_6F_5)_4$ salt) in methylene chloride-d_2.

Crystals of **9a** suitable for X-ray diffraction were grown by cooling of a saturated methylene chloride/pentane solution to –25 ºC. The solid state structure of the cation of **9a** is displayed in Figure 3.8 and metric data are listed in the caption. The solid state structure of **9a** is

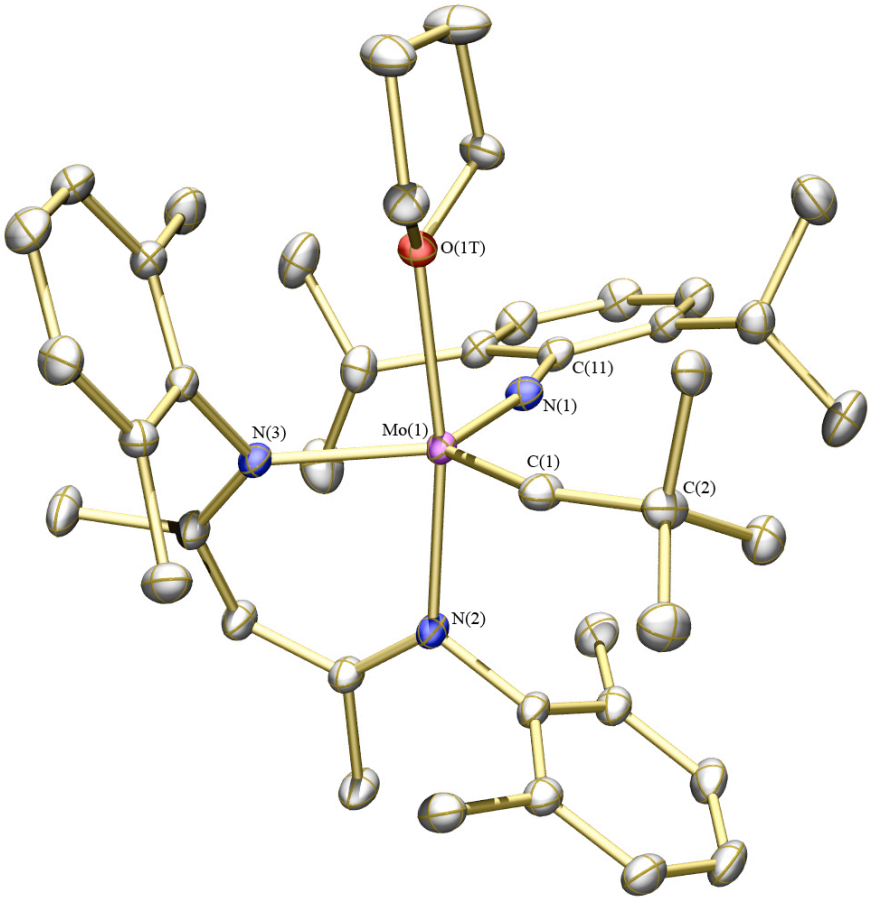

Figure 3.8. Thermal ellipsoid drawing of the cation of **9a**. Anion, hydrogen atoms, phenyl group of neophylidene ligand, and cocrystallized CH_2Cl_2 molecule omitted for clarity. Selected bond distances (Å) and angles (º): Mo(1)–C(1) = 1.909(2); Mo(1)–N(1) = 1.7460(16); Mo(1)–N(2) = 2.1435(16); Mo(1)–N(3) = 2.1220(16); Mo(1)–O(1T) = 2.2417(13); Mo(1)–C(1)–C(2) = 155.26(17); N(1)–Mo(1)–C(1) = 110.49(9); Mo(1)–N(1)–C(11) = 162.68(15); N(2)–Mo(1)–N(3) = 84.99(6).

consistent with the low temperature spectral limit observed in solution. As with BAr_{f4} salts of the other alkylidene cations, no close contact exists between the cation and anion.[58] The

alkylidene and imide bond lengths are consistent with other five-coordinate solvent adducts of this type.[41] The Mo(1)–O(1T) bond length of 2.2417(13) Å is consistent with a dative interaction, though markedly shorter than the dative Mo–Cl interaction (2.53432(s) Å) observed in the solid state structure of {Mo(NAr)(CHCMe$_2$Ph)(Ar^{Cl}-nacnac)}{BAr$_{f4}$}.[58]

Triflate abstraction from compound **5c** was found to give an orange solid after crystallization from methylene chloride/pentane (Equation 3.9). Spectroscopic examination of the solid material revealed it to be a mixture of two compounds, one that contains an alkylidene (**9c**), and one that does not (**10c**). Compound **9c** contains several alkylidene resonances consistent with a mixture of *syn* and *anti* isomers, and slow rotation about the N$_{imido}$–C$_{ipso}$ bond of the *syn* isomer (see Experimental section). Subsequent experiments examining the

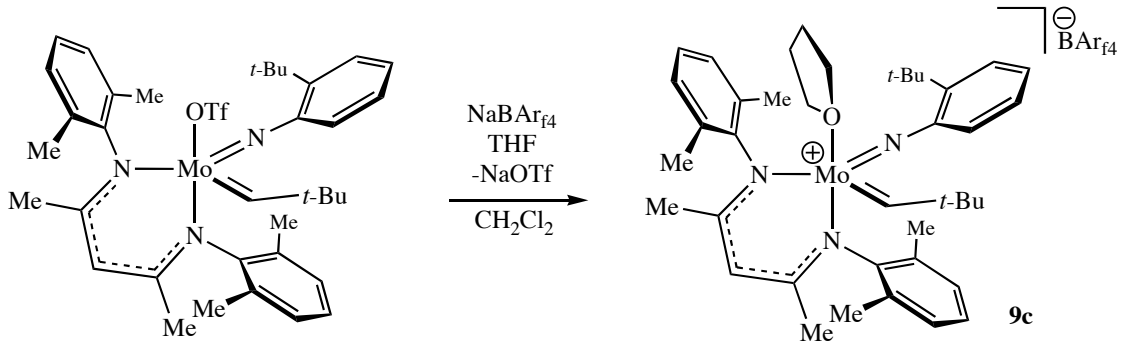

9c (3.9)

reaction of **5c** with NaBAr$_{f4}$ *in situ* demonstrated that the desired cationic complex (**9c**) is formed initially, but decomposes after several hours at room temperature to a new complex (**10c**). A possible structure for **10c** is shown in Scheme 3.5. Four methylene proton doublets are expected for a compound with this structure, though the complexity of the NMR spectrum and the presence of significant quantities of **9c** prevented assignment of the full spectrum. Compound **10c** is not stable and decomposes further at 20 ºC to a new complex that contains an alkylidene resonance (**11c**). The new alkylidene resonance appears several ppm downfield of the initial *anti* resonance of **9c**, though no J_{CH} was determined (see Experimental section). The intermediate

species, **10c**, likely undergoes α-elimination to generate **11c** and neopentane (observed in *in situ* experiments). The tentative reaction pathway is shown in Scheme 3.5.

Scheme 3.5. Possible reaction pathway for conversion of **9c** to **11c**.

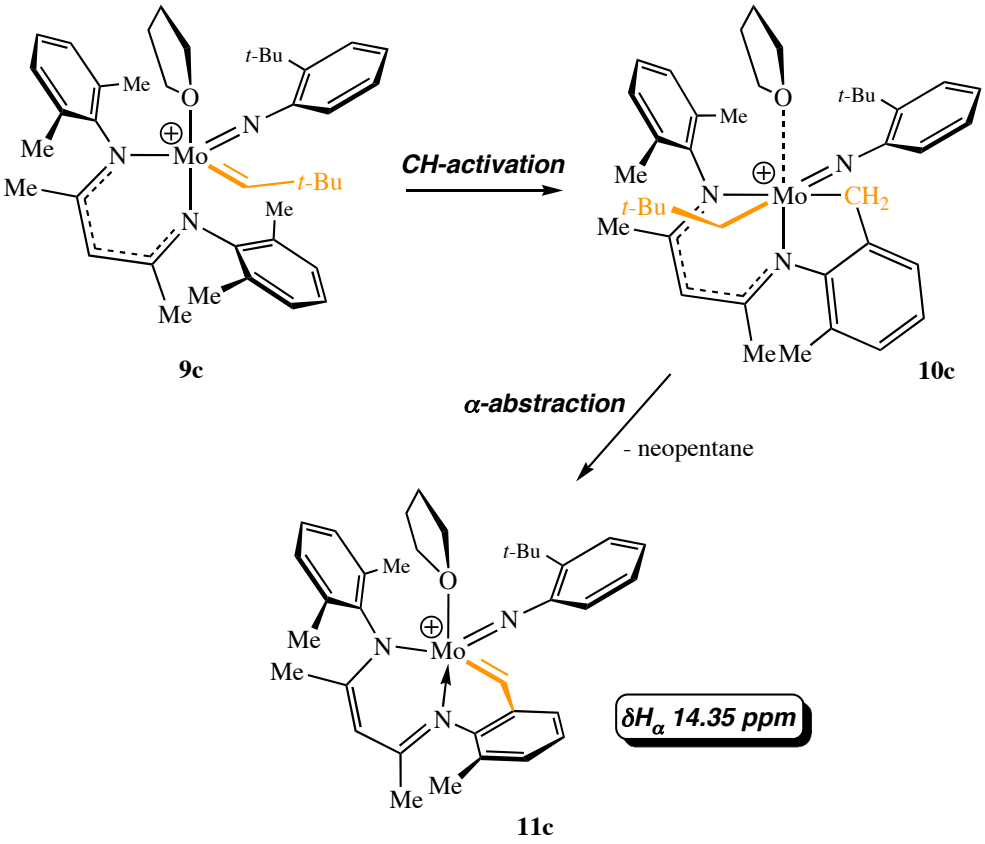

As with compounds **5a**-**c**, decomposition is most likely initiated by proton transfer to the alkylidene from a benzylic CH to generate the dialkyl complex, **10c**. Instead of undergoing migratory insertion, **10c** undergoes a second α-abstraction to generate a new benzylidene, **11c**. The divergent reactivity of **9c** versus **5c** may be a consequence of the labile THF ligand, which may dissociate from **10c** to relieve the steric congestion in the molecule and render it observable for a short time. Reassociation of THF then promotes a second proton transfer to yield **11c**. The thermal stability of compounds **5c** with **9c** make for an interesting comparison. Whereas the

neutral triflate complex does not begin decomposing until about 50 ºC, the cation is thermally sensitive below room temperature. Therefore, introduction of the positive charge imparts a great deal of reactivity even though compounds **5c** and **9c** are both five-coordinate species.

Results stemming from the thermal decomposition of **9c** led to a reexamination of compounds **9a** and **9b**. Solutions of **9a** stored at or even below 20 ºC led to degradation of the neophylidene species in similar fashion to that of **9c**, albeit more slowly. The decomposition product appears to be the analogous benzylidene species, **11a** (equation 3.10). In this case, *tert*-butylbenzene was observed by NMR, as expected from protonation of the original neophylidene ligand. Compound **9b** proved significantly more robust than **9a** or **9c**. Thermolysis of **9b** at 50 ºC in methylene chloride-d_2 eventually led to observation of species analogous to **10c** and **11c** according to ^{1}H NMR spectroscopy.

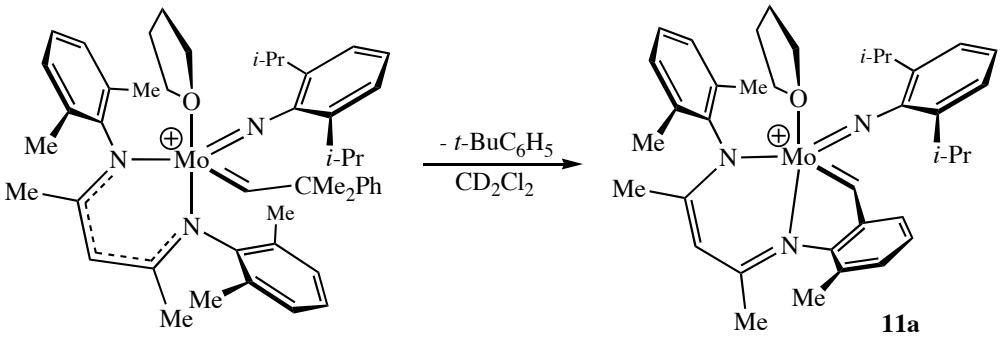

(3.10)

Monitoring of methylene chloride-d_2 solutions of **9a** by NMR led to observation of **11a**, but in no case were intermediate dialkyl species analogous to **10c** observed. Identification of **10c** was thus quite fortuitous, as the nature of this intermediate is critical to understanding the decomposition processes in these cations. Compound **10c** can be observed, unlike **10a**, since the 2-*tert*-butylphenylimido group is less sterically demanding than the 2,6-diisopropylphenylimido group and the subsequent α-abstraction in **10c** to yield **11c** is relatively slow. It is not known whether THF is coordinated strongly to the metal in **10c**, but it should be noted that coordination of THF (and other donor ligands) accelerates α-abstraction reactions in tantalum neopentyl

species.[59,60] Multiple attempts at isolating crystalline samples of compounds **11a** and **11c** have met with failure, yielding only oils. Decomposition of **9c** appears to be substantially slower than that of **9a** or **9c**, consistent with the trends observed for **5a**-**c**.

The spectroscopic features of **11a** are similar to those of **11c**. The alkylidene proton and carbon atoms resonate at 14.28 and 299.5 ppm, respectively in methylene chloride-d_2. The J_{CH} value for the alkylidene ligand is 150 Hz, consistent with an *anti* isomer. The fact that only the *anti* isomer is present is consistent with the proposed structure in equation 3.10. The kinetics of decomposition of **9a** were examined by ^{1}H NMR spectroscopy at 40 ºC in methylene chloride-d_2. As seen in Figure 3.9, decomposition of **9a** occurs in a first order manner with $k = 3.23 \times 10^{-4}$ $M^{-1}s^{-1}$. This transformation is considerably faster than conversion of **5a** to **6a** (compare Figure 3.4).

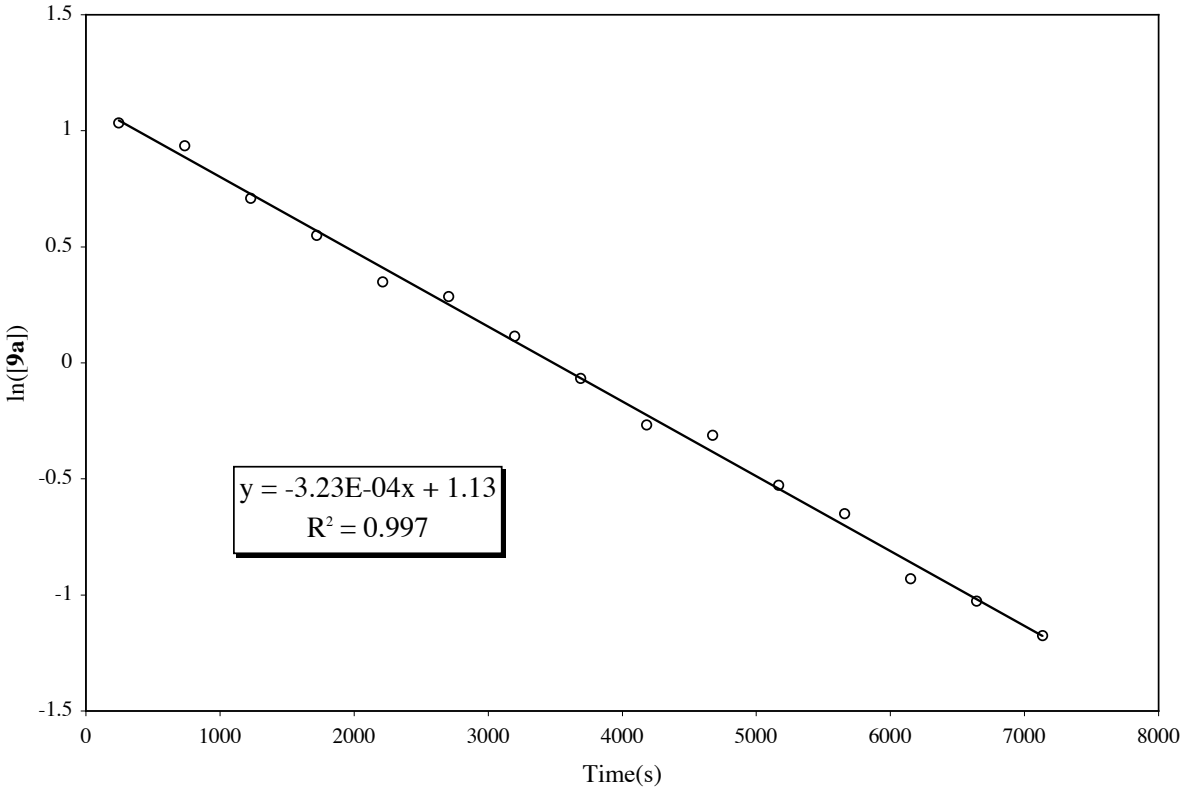

Figure 3.9. Kinetic profile for the conversion of **9a** to **11a** at 40 ºC in methylene chloride-d_2.

An intriguing possibility is the intermediacy of a cationic version of **6a** in the decomposition of **9a** to **11a** (i.e. compound **10c** is a cationic version of **6c**). To test this possibility, compound **6a** was allowed to react with $NaB(C_6F_5)_4 \cdot THF$ in methylene chloride-d_2. Observation of the reaction by ^1H NMR spectroscopy demonstrated slow conversion ($t_{1/2} \sim 30$ min) to a new species with very similar spectral features to **6a** (see Experimental section). This species is assigned as the cationic THF adduct (**12a**) shown in equation 3.11. The THF molecule is bound strongly to Mo as evidenced by the absence of exchange with free THF. Compound **12a** is stable at room temperature and does not undergo further transformation to a species analogous to **11a**. This fact rules out the possibility of a species analogous to **12a** serving as the dialkyl intermediate along the pathway from **9a** to **11a**. Unfortunately, **12a** has resisted attempts at crystallization, giving only oils.

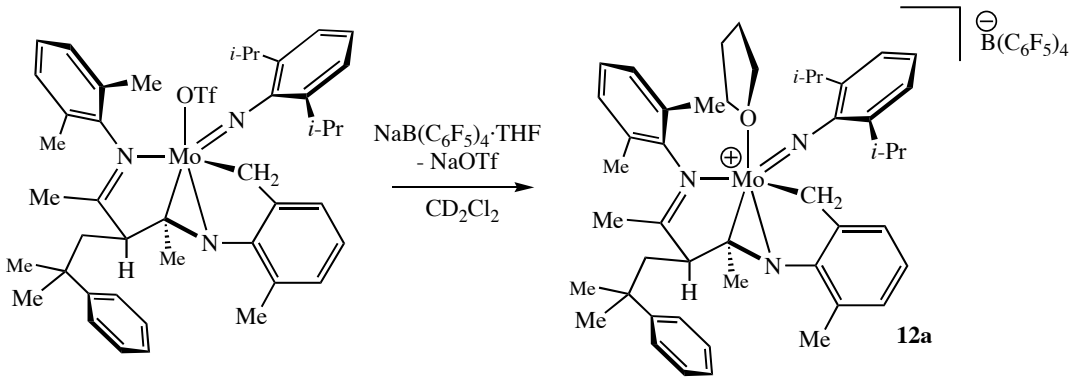

(3.11)

Formation of a cationic complex from **7a** met with limited success. Reaction of **7a** with $NaBAr_{f4}$ in the absence of THF led only to decomposition. Such instability contrasts that of the cationic complex supported by the Ar^{Cl}-nacnac ligand, where intramolecular chlorine coordination is sufficient to stabilize the cation. In the presence of THF, a cationic species may be isolated in moderate yield (**13a**, equation 3.12). The spectroscopic features of **13a** are consistent with the structure depicted in equation 3.12. The THF ligand shows distinct

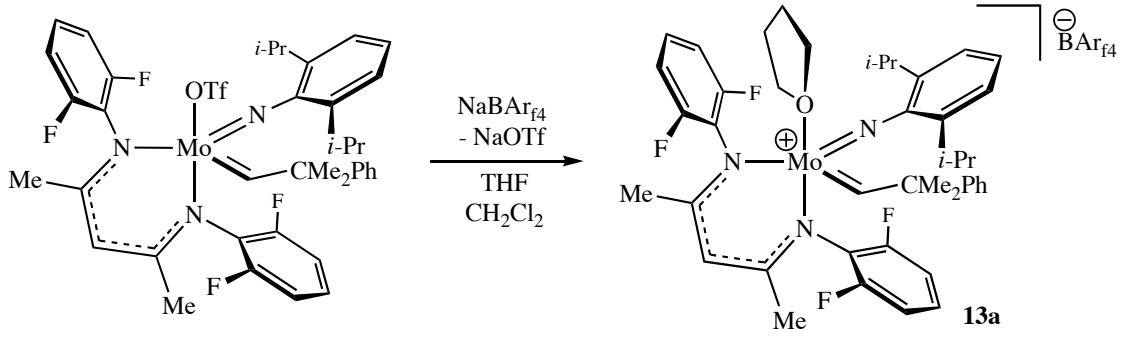

(3.12)

resonances at room temperature unlike compounds **9a**-**c**. Coordinated THF does not appear to exchange readily with free THF. The *anti* isomer is present in ~20% and shows a coupling to fluorine of 3.5 Hz; no such coupling is apparent in the *syn* isomer. The alkylidene chemical shifts of **13a** are both downfield of the other cations prepared (see Experimental), again highlighting the electron-withdrawing nature of the Ar^F-nacnac ligand. Compound **13a** requires several days to precipitate from concentrated solutions. This fact casts some doubt on the nature of **13a**, since decomposition may have occurred in the time required for crystallization. Due to the difficulty in preparing and handling **13a**, no reactivity was examined.

Addition of NaB(C$_6$F$_5$)$_4$·THF to a methylene chloride-d_2 solution of **8a** produced what is tentatively assigned as the cationic complex **14a** (equation 3.13). Complex **14a** exists as a single isomer as judged by the appearance of a lone alkylidene resonance at 14.23 ppm

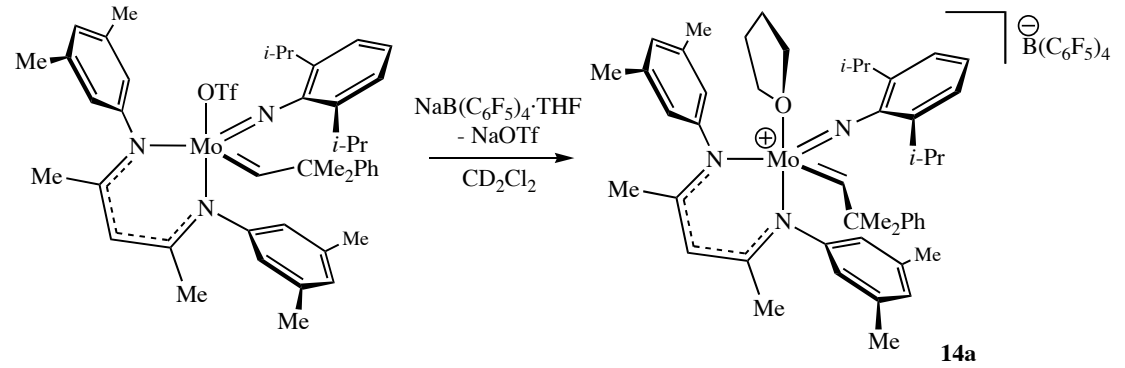

(3.13)

(methylene chloride-d_2). The remainder of the spectrum is broad and coordinated THF appears to exchange readily with free THF. A single septet resonance for the 2,6-diisopropylphenyl

indicates free rotation about the N_{imido}-C_{ipso} bond on the NMR timescale. Attempts to isolate the BAr_{f4} salt of the cation were unsuccessful, and preparative scale reactions have resulted in oils. The stability of complex **14a** is questionable based on the thermal sensitivity of **8a** and the similar relationship between compounds **5a**-**c** and **9a**-**c**. It is probable that the insufficient steric protection provided by the Ar^*-nacnac ligand renders it unsuitable for supporting a cationic species of the type discussed above.

3.4. Metathesis reactivity of cationic nacnac complexes

The metathetical reactivity of compounds **9a** and **9b** proved more promising than those of compound **3a**. Three metathesis substrates were chosen to examine the proficiency of the nacnac cations towards olefin metathesis. The substrates chosen were vinyltrimethylsilane, *N*-diallyltosylamine, and norbornene. Conditions for a series of test reactions and results are summarized in Table 3.1. The ability of each cation to polymerize norbornene is not surprising in view of the relative ease in which this monomer is polymerized. Reaction with vinyltrimethylsilane did not produce the expected cross metathesis product with complex **9a**. Consumption of olefin was slow and the final product could not be identified by NMR. After prolonged time, decomposition of **9a** is likely a competing factor. In contrast, reaction of vinyltrimethylsilane with complex **9b** led instantly to the TMS-methylidene as judged by alkylidene resonances at 15.35 ppm and 16.47 ppm for the syn and anti isomers, respectively.[42] The reduced steric bulk of the 2,6-dichlorophenyl imide may allow for better access to the Mo center in **9b** versus **9a**. Of particular interest are the results with the ring closing metathesis substrate, *N*-diallyltosylamine. Both catalysts reacted with the substrate initially, but complete conversion to the ring-closed product was not achieved in either case. Monitoring of the reactions over the course of 24 hours by NMR spectroscopy demonstrated that the conversions listed in Table 3.1 remained unchanged, indicating catalyst deactivation.

In order to examine the nature of metathesis reactions with complexes **9a** and **9b**, each was exposed to one atmosphere of ethylene gas. Observation of the reaction by ^{1}H NMR spectroscopy demonstrated that both compounds give rise to an ethylene complex (**15a** and **15b**, equation 3.14). The structure shown in equation 3.14 is consistent with the spectroscopic features of the ethylene complexes, namely C_S symmetry. In both **15a** and **15b**, the aryl imide appears to be rotating rapidly at 20 ºC. Resonances for the protons of the ethylene ligand in **15a** appear as a set of multiplets at 2.57 and 0.86 ppm (methylene chloride-d_2). The byproducts

Table 3.1. Reaction of complexes **9a** and **9b** with selected olefins.

Catalyst	Substrate	Comments
9a	vinyltrimethylsilane	Slow consumption of substrate; unidentifiable prodcut
9a	*N*-diallytosylamine	12% Ring closed product after 10 minutes; no further reactivity.
9a	norbornene	Complete in seconds; 70:30 *trans*:*cis* polymer.
9b	vinyltrimethylsilane	Rapid quantitative formation of TMS methylidene; syn: 15.35 ppm, anti: 16.47 ppm.
9b	*N*-diallyltosylamine	33% Ring closed product after 10 minutes; no further reactivity.
9b	norbornene	Complete in seconds; 90:10 *cis*:*trans* polymer.

[†]All reactions performed in CD_2Cl_2 with millimolar catalyst concentrations. Substrate amounts are as follows: 1.5 equiv. vinylTMS, 20 equiv. *N*-diallyltosylamine, 100 equiv. norbornene.

observed in the formation of **15a** and **15b** are 3-methyl-3-phenyl-butene (initial metathesis product) and propylene; no cyclopropane is observed. The presence of propylene is indicative of β-H elimination from an unsubstituted metallacyclobutane species (Scheme 3.6).[45] Further support for the reaction sequence shown in Scheme 3.6 was garnered from experiments involving ethylene-$^{13}C_2$. From such experiments, the chemical shift of the ethylene ligand was identified at 70.31 ppm (J_{CH} = 157 Hz, methylene chloride-d_2) for compound **15a**.

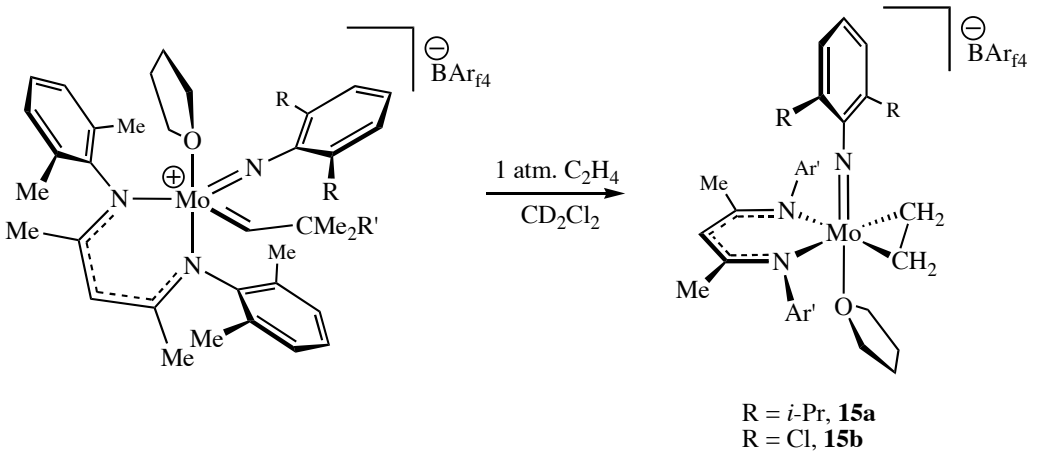

R = *i*-Pr, **15a**
R = Cl, **15b**

(3.14)

^{13}C NMR resonances for the initial metathesis product and propylene are also present. Attempts to isolate **15a** or **15b** on a preparative scale have failed, and it does not appear that either compound is stable for prolonged time.

Scheme 3.6. Proposed reaction pathway for reaction of **9a** with ethylene-$^{13}C_2$.

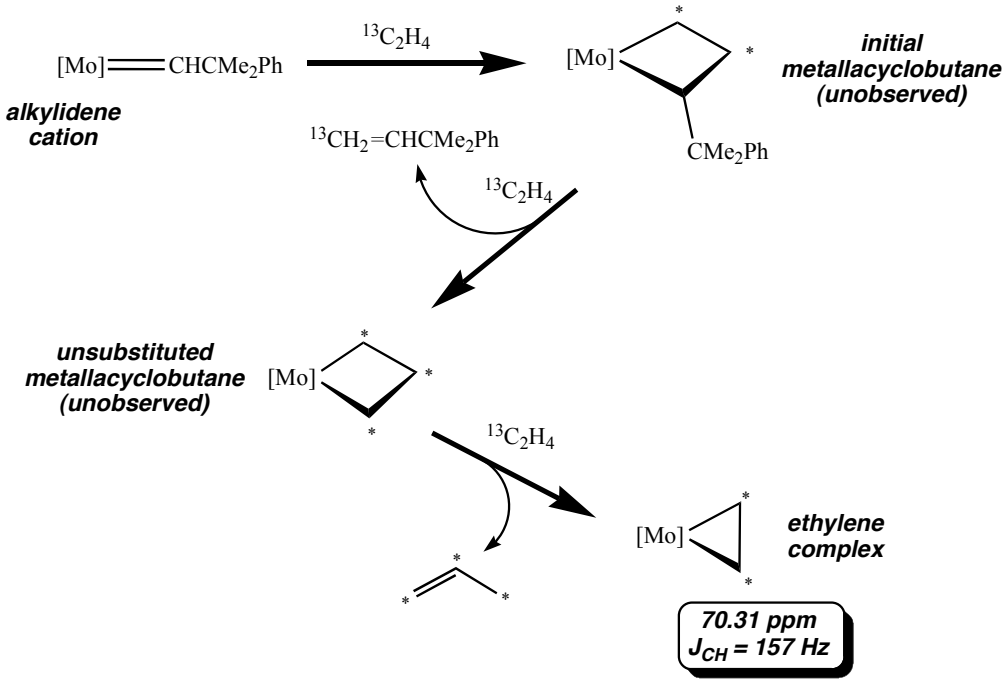

DISCUSSION

The reactivity of the complexes described in the preceding pages appears to be dictated by two major factors: the inability of intermediate metallacyclobutane species to rearrange effectively and the propensity for proton transfer reactions in nacnac ligands. Whereas complexes **3a**, **9a**, and **9b** react with terminal olefins readily, the lack of catalytic and/or sustained catalytic activity in each case suggests that the intermediate metallacycles are not stable with respect to formation of catalytically inactive species. Reactions with ethylene demonstrate several possible decomposition modes of these metallacycles and offer a potential explanation to the lack of catalysis. In order for metathesis to occur, the intermediate metallacyclobutane must rearrange in a fashion that allows for elimination of new olefin. If this rearrangement is retarded, the metallacycles persist and are subject to decomposition. This particular situation is apparent with compound **3a**, where the unsubstituted metallacycle is actually observable by NMR. We can only speculate about the factors contributing to sluggish metallacycle rearrangement at this point, but the chelating nature of the acac and nacnac ligands may be an important determinant. The very acute bite angle of these ligands in comparison to other chelating diolates examined in this laboratory probably hinders the geometric reorganization necessary for productive metathesis. Thus, the chelating nature of the acac and nacnac ligands, which imparts stability to the cationic alkylidenes, may serve the same role in stabilizing metallacyclobutanes, leading to poor catalyst lifetime.

The persistence of metallacycles is not, in it of itself, a determining factor in catalyst efficacy (c.f. W alkylidenes, where metallacycles are readily observable and still serve as catalysts in certain instances[4]); yet, the metallacycles in the present study appear to decompose readily. The fact that these compounds are cationic may favor reductive processes such as β-elimination, leading to increased rates of metallacycle decomposition. The most electron deficient complex, **3a**, prefers to undergo C–C bond reductive elimination to generate cyclopropanes in the presence of ethylene. Evidence of such reactions has been seen before, but

this decomposition mode was never observed to account for anything more than a very minor pathway.[46]

The second factor dictating the chemistry of these compounds is the propensity for facile proton transfer reactions with certain β-diketiminate ligands. The thermolysis reactions observed for **5a**-**c** demonstrate that clean benzylic activation about the periphery of the nacnac ligand is an accessible reaction pathway. When these benzylic groups are moved away from the metal center, bimolecular reactivity appears to take place as evidenced by the thermal degradation of **8a**. Thermal instability is more manifest in the cationic species **9a** and **9b**, where decomposition reactions occur at 23 ºC. The most successful nacnac ligand appears to be the one containing 2,6-dichlorophenyl substituents. The chlorine atom is unique in that, unlike fluorine, it is sterically encumbering enough to protect the cationic Mo center, yet may also participate in dative interactions with its lone pairs. However, even complexes of this ligand fail to serve as competent olefin metathesis catalysts.

CONCLUSIONS

This chapter has explored the synthesis and reactivity of a series of new imido alkylidene complexes supported by acac and nacnac ligands. Both of these ligands support isolable, well-defined, neutral and cationic complexes. The compounds represent the first examples of nacnac complexes of Mo and demonstrate both the advantages and disadvantages of this ligand class. In comparison to the acac species, the nacnac species proved to be both more facile to prepare and to function as better metathesis catalysts (in a limited sense). Results from reactions with olefins suggest that with both ligand classes, decomposition of metallacyclobutane species through reactions other than metathesis is the major deterrent to sustained catalytic activity. It is concluded that, whereas the cations prepared in this study may show excellent affinity towards olefins, decomposition of intermediates along the metathesis pathway prevent such species from serving as efficient catalysts.

EXPERIMENTAL

General comments. All manipulations were performed in oven-dried (200ºC) glassware under an atmosphere of nitrogen on a dual-manifold Schlenk line or in a Vacuum Atmosphere's glovebox. HPLC grade organic solvents were sparged with nitrogen and dried by passage through activated alumina, then stored over 4 Å Linde-type molecular sieves prior to use. Benzene-d_6 and toluene-d_8 and were dried over sodium/benzophenone ketyl and vacuum distilled prior to use. Methylene chloride-d_2 and bromobenzene-d_5 were dried over CaH_2 and vacuum distilled prior to use. NMR spectra were recorded on a Varian Mercury or Varian INOVA spectrometers operating at 300 and 500 MHz (^{1}H), respectively. Chemical shifts for ^{1}H and ^{13}C spectra were referenced to the residual ^{1}H/^{13}C resonances of the deuterated solvent (^{1}H: C_6D_6, δ 7.16; $C_6D_5CD_3$, δ 2.09; CD_2Cl_2, δ 5.32; C_6D_5Br, δ 7.29; ^{13}C: C_6D_6, δ 128.39; CD_2Cl_2, δ 54.00) and are reported as parts per million relative to tetramethylsilane. ^{19}F NMR spectra were referenced externally to fluorobenzene (δ -113.15 ppm upfield of $CFCl_3$). Elemental analyses were performed by H. Kolbe Microanalytics Laboratory, Mülheim an der Ruhr, Germany.

Materials. Mo(NR)(CHCMe$_2$R′)(OTf)$_2$(DME) complexes,[61] NaBAr$_{f4}$,[62] Ar′-nacnac,[47] Ar^F-nacnac,[56] Ar′′-nacnac,[57] and were prepared according to published procedures. The lithium salts of the various acac and nacnac ligands were prepared by addition of *n*-BuLi to a pentane solution of the corresponding acid. Na{HFAC}, TlOAc, and PMe_3 were purchased from commercial vendors and used as received. Quinuclidine and 2,4-lutidine were purchased from Aldrich and sublimed and distilled prior to use, respectively.

Crystallography. Mounting of crystals and refinement of X-ray diffraction data were performed by Dr. Peter Müller of the Department of Chemistry Diffraction Facility. Low temperature diffraction data were collected on a Siemens Platform three-circle diffractometer coupled to a Bruker-AXS Smart Apex CCD detector with graphite-monochromated Mo Kα radiation (λ = 0.71073 Å), performing φ- and ω-scans. All structures were solved by direct methods using SHELXS[63] and refined against F^2 on all data by full-matrix least squares with

SHELXL-97[64]. All non-hydrogen atoms were refined anisotropically. All hydrogen atoms were included into the model at geometrically calculated positions and refined using a riding model. The isotropic displacement parameters of all hydrogen atoms were fixed to 1.2 times the *U* value of the atoms they are linked to (1.5 times for methyl groups).

Mo(NAr)(CHCMe$_2$Ph)(TMHD)(OTf)(THF), 1a. A flask was charged with 1.453 g (1.83 mmol) of Mo(N-2,6-*i*-Pr$_2$C$_6$H$_3$)(CHCMe$_2$Ph)(OTf)$_2$(DME) and 40 mL of THF and chilled to –25ºC. To the cold solution was added 0.379 g (1.99 mmol) of Li{TMHD} as a solid in one portion. The reaction was stirred at room temperature for one hour during which time the solution color changed from yellow to red-orange. All volatiles were removed in vacuo and the residue extracted into ~80 mL pentane. The extract was filtered through a plug of Celite and the solution volume reduced to 20 mL in vacuo. The product precipitated during concentration of the solvent as 1.029 g (70%) of a yellow crystalline solid. Crystals suitable for X-ray diffraction were grown by slow cooling of a saturated pentane solution: ^{1}H NMR (500 MHz, C$_6$D$_6$) δ 13.45 (s, 1, MoC*H*$_\alpha$, J_{CH} = 127 Hz), 7.20 (d, 2, *o*-CMe$_2$*Ph*), 7.09 (m, 4, aryl), 6.98 (m, 2, aryl), 6.14 (s, 1, acac-C*H*), 4.33 (sep, 2, C*H*Me$_2$), 3.51 (m, 4, OC*H*$_2$CH$_2$) 1.96 (s, 3, C*Me*$_2$Ph), 1.76 (s, 3, C*Me*$_2$Ph), 1.40 (app dd, 12, CH*Me*$_2$), 1.31 (s, 9, *t*-Bu), 1.15 (m, 4, OCH$_2$C*H*$_2$), 1.07 (s, 9, *t*-Bu); ^{13}C NMR (125 MHz, CD$_2$Cl$_2$): δ 324.3 (Mo*C*H), 202.0 (*C*O), 201.9 (*C*O), 151.7, 151.1, 150.8, 128.7, 128.5, 126.5, 126.2, 124.2, 120.1 (*C*F$_3$, J_{CF} = 318 Hz), 95.1, 69.4, 57.7, 42.3, 41.9, 32.1, 30.0, 28.8, 28.7, 28.2, 28.1, 25.8, 25.1, 24.3; ^{19}F NMR (282 MHz, C$_6$D$_6$) δ –77.9. Anal. Calcd for C$_{38}$H$_{56}$F$_3$MoNO$_6$S: C, 56.50; H, 6.99; N, 1.73. Found: C, 56.94; H, 6.88; N, 1.65.

Mo(NAr)(CHCMe$_2$Ph)(TMHD)(OTf)(quin), 1b. A flask was charged with 1.262 g (1.59 mmol) of Mo(CHCMe$_2$Ph)(NAr)(OTf)$_2$(DME) and 45 mL of Et$_2$O. The solution was cooled to –25ºC at which point 0.178 g (1.60 mmol) of quinuclidine and 0.308 g (1.62 mmol) of Li{TMHD} were added successively as solids. The mixture was stirred at room temperature for two hours during which time the solution turned from yellow to brown. All volatiles were

removed in vacuo, and the residue extracted into 70 mL of pentane. The mixture was filtered through Celite and the solution volume reduced ~10 mL in vacuo. The solution was stored at –25ºC for 24 hrs. yielding 0.582 g (43%) of orange-red crystals: ^{1}H NMR (500 MHz, C_6D_6) δ 13.48 (s, 1, MoC*H*$_\alpha$, J_{CH} = 129 Hz), 7.20 (d, 2, *o*-CMe$_2$Ph), 7.10 (t, 2, *m*-CMe$_2$*Ph*), 7.03 (br, 2, *m*-Ar), 6.97 (m, 2, *p*-Ar + *p*-CMe$_2$*Ph*), 6.13 (s, 1, acac-C*H*), 4.42 (br s, 1, C*H*Me$_2$), 4.17 (br s, 1, C*H*Me$_2$), 2.80 (br s, 6, quin), 1.95 (s, 3, C*Me*$_2$Ph), 1.82 (s, 3, C*Me*$_2$Ph), 1.57 (br s, 3, CH*Me*$_2$), 1.48 (br s, 3, CH*Me*$_2$), 1.34 (s, 9, *t*-Bu), 1.26 (br s, 6 CH*Me*$_2$), 1.18 (m, 1 quin), 1.07 (m, 6 quin), 1.05 (s, 9 *t*-Bu). Anal. Calcd for $C_{41}H_{61}F_3MoN_2O_5S$: C, 58.14; H, 7.26; N, 3.31. Found: C, 58.34; H, 6.86; N, 3.28.

Mo(NAr)(CHCMe$_2$Ph)(TMHD)(OTf)(2,4-lut), 1c. A flask was charged with 1.080 g (1.36 mmol) of Mo(CHCMe$_2$Ph)(NAr)(OTf)$_2$(DME), 0.16 mL (1.4 mmol) of 2,4-lutidine, and 20 mL of diethyl ether. To the orange-red solution was added 0.273 g (1.44 mmol) of Li{TMHD} as a solid in one portion. The mixture was stirred at room temperature for 90 minutes during which time the color became brown-yellow. All volatiles were removed in vacuo and the residue extracted into 60 mL of a 2:1 mixture of pentane to CH_2Cl_2. The mixture was filtered through Celite and the filtrate concentrated to ~5 mL in vacuo. The solution was then set aside at –25ºC for 24 hours to yield 0.584 g (51%) of a yellow microcrystalline solid. The ^{1}H NMR spectrum of the material showed two sets of alkylidene resonances in a ~1:1.3 ratio that did not change upon repeated crystallization from pentane or ether. The spectrum is very complicated by the presence of two isomers and could not be completely assigned: ^{1}H NMR (500 MHz, C_6D_6) δ *selected peaks* 13.82 (*minor isomer*, s, 1 MoC*H*$_\alpha$), 13.42 (*major isomer*, br s, 1 MoC*H*$_\alpha$), 9.17 (br d, 1, *o*-lut), 8.80 (d, 1, *o*-lut), 7.18 – 6.96 (m, 16, aryl), 6.46 (d, 1, *m*-lut), 6.43 (d, 1, *m*-lut), 6.37 (s, 2, acac-C*H* + *m*-lut), 6.22 (br s, 1, *m*-lut), 6.13 (s, 1, acac-C*H*), 4.28 (sep, 2, C*H*Me$_2$), 2.41 (s, 3, lut-*Me*), 2.38 (v br s, 2, C*H*Me$_2$), 2.14 (s, 3, Me), 1.80 (s, 3, Me), 1.79 (s, 3, Me), 1.62 (br s, 3, lut-*Me*), 1.55 (s, 3, Me), 1.49 (s, 3, Me), 1.39 (s, 3, Me), 1.37 (s, 9, *t*-Bu), 1.19 (s, 9, *t*-Bu), 1.08 (br

s, 3, lut-*Me*), 1.06 (s, 9, *t*-Bu). Anal. Calcd for $C_{41}H_{57}F_3MoN_2O_5S$: C, 58.42; H, 6.82; N, 3.32. Found: C, 58.75; H, 7.17; N, 3.24.

Mo(NAr)(CHCMe$_2$Ph)(TMHD)(OTf), 1d. A flask was charged with 1.119 g (1.41 mmol) of Mo(CHCMe$_2$Ph)(NAr)(OTf)$_2$(DME) and 20 mL of diethyl ether and chilled to –25 ºC. To the solution was added 0.302 g of Li{TMHD} as a solid. The solution was stirred at room temperature for 30 minutes. The volatiles were removed in vacuo and the residue extracted into methylene chloride. The extract was filtered through a plug of Celite and the methylene chloride removed in vacuo. The residue was treated with pentane and set aside at –25 ºC overnight. The crude material precipitated as 0.624 g (60%) of a yellow crystalline solid. The crude material was purified (to remove traces of DME) by repeated recrystallization from CH_2Cl_2/pentane: ^{1}H NMR (500 MHz, CD_2Cl_2) δ 13.12 (s, 1, MoC*H*$_\alpha$), 7.19 (m, 8, aryl), 6.41 (s, 1, acac-C*H*), 3.89 (sep, 2, C*H*Me$_2$), 1.84 (s, 3, C*Me*$_2$Ph), 1.55 (s, 3, C*Me*$_2$Ph), 1.35 (s, 9, *t*-Bu), 1.24 (d, 6, CH*Me*$_2$), 1.21 (s, 9, ^{t}Bu), 1.19 (d, 6, CH*Me*$_2$). Anal. Calcd for $C_{34}H_{48}F_3MoNO_5S$: C, 55.50; H, 6.58; N, 1.90. Found: C, 56.31; H, 6.70; N, 1.79.

{Mo(NAr)(CHCMe$_2$Ph)(TMHD)(PMe$_3$)$_2$}{OTf} 1e. A flask was charged with 1.200 g (1.52 mmol) of Mo(CHCMe$_2$Ph)(NAr)(OTf)$_2$(DME), 0.15 mL (1.5 mmol) of PMe$_3$ and 25 mL of diethyl ether. To the solution was added 0.293 g (1.54 mmol) of Li{TMHD} as a solid in one portion. Initially the mixture became homogeneous, then a yellow precipitate formed after stirring for 15 minutes at room temperature. The mixture was stirred for an additional 30 minutes. The precipitate was collected by filtration and washed with diethyl ether to yield 0.770 g (98% based on PMe$_3$) of a yellow microcrystalline solid: ^{1}H NMR (300 MHz, CD_2Cl_2) δ 15.00 (t, J_{HP} = 4.7 Hz, 1, MoC*H*$_\alpha$), 7.48 (d, 2, *o*-CMe$_2$*Ph*), 7.33 (m, 6, aryl), 6.13 (t, J_{HP} = 0.9 Hz, 1, acac-C*H*,), 3.87 (sep, 2, C*H*Me$_2$), 1.79 (s, 6, C*Me*$_2$Ph), 1.33 (d, 12, CH*Me*$_2$), 1.26 (s, 9, *t*-Bu), 1.23 (s, 9, *t*-Bu), 1.16 (app t, 18, P*Me*$_3$); ^{31}P NMR (121 MHz) δ –6.8. Anal. Calcd for $C_{40}H_{66}F_3MoNO_5P_2S$: C, 54.11; H, 7.49; N, 1.58. Found: C, 53.95; H, 7.56; N, 1.52.

Mo(NAr)(CHCMe$_2$Ph)(HFAC)(OTf)(THF), 2a. A flask was charged with 1.015 g (1.28 mmol) of Mo(NAr)(CHCMe$_2$Ph)(OTf)$_2$(DME) and 20 mL of THF and chilled to –25 ºC. To the solution was added 0.311 g (1.35 mmol) of Na{HFAC} as a solid in one portion. The mixture was allowed to stir at room temperature for one hour during which time the color became deep red. All volatiles were removed in vacuo and the residue extracted into 70 mL of warm pentane. The pentane extract was filtered through a plug of Celite and the solution volume concentrated in vacuo to ~10mL. The solution was set aside at –25 ºC overnight during which time the compound precipitated as 0.811 g (76%) of an orange microcrystalline powder. The NMR spectrum of **2a** showed the presence of one major isomer and two very minor isomers: ^{1}H NMR (500 MHz, C_6D_6) δ 13.51 (s, 1, MoCH_α, J_{CH} = 125 Hz), 13.29 (*minor isomer*, s, 1, MoCH_α), 13.05 (*minor isomer*, s, 1, MoCH_α), 7.09 (m, 4, aryl), 6.96 (m, 4, aryl), 6.25 (s, 1, acac-C*H*), 4.15 (v br, 2, C*H*Me$_2$), 3.38 (br s, 4, OCH_2CH$_2$), 1.97 (br s, 3, C*Me*$_2$Ph), 1.59 (s, 3, C*Me*$_2$Ph), 1.33 (br m, 12, CH*Me*$_2$), 0.98 (br s, 4, OCH$_2$CH_2); ^{13}C NMR (125 MHz, CD) *selected peaks* δ 337.6 (MoC_α), 179.9 (q, J_{CF} = 37 Hz, *C*=O), 178.5 (q, J_{CF} = 37 Hz, *C*=O), 93.5 (acac-*C*H), 70.2 (O*C*H$_2$), 60.4 (*C*Me$_2$Ph); ^{19}F NMR (470 MHz) δ –74.7, -75.4, -76.6. Anal. Calcd for $C_{32}H_{38}F_9MoNO_6S$: C, 46.22; H, 4.61; N, 1.68. Found: C, 46.46; H, 4.71; N, 1.68.

{Mo(NAr)(CHCMe$_2$Ph)(TMHD)(THF)}{BAr$_{f4}$}, 3a. A flask was charged with 0.444 g (0.550 mmol) of Mo(NAr)(CHCMe$_2$Ph)(TMHD)(OTf)(THF) and 10 mL of methylene chloride and chilled to –25 ºC. To the solution was added 0.478 g (0.552 mmol) of NaBAr$_{f4}$ as a solid. The solution was stirred at room temperature for two hours during which time the solution color darkened and a precipitate formed. The reaction mixture was filtered through a plug of Celite, and the solution volume concentrated to 1-2 mL in vacuo. The solution was layered with several volumes of pentane and set aside at –25 ºC for several days. The product crystallized as 0.465 g (55%) of yellow blocks. Crystals suitable for X-ray diffraction were grown by liquid-liquid diffusion of heptane into a saturated methylene chloride solution: ^{1}H NMR (500 MHz, CD_2Cl_2) δ 13.02 (s, 1, J_{CH} = 125 Hz, MoCH_α), 7.72 (d, 8, *o*-Ar$_{f4}$), 7.56 (s, 4 *p*-Ar$_{f4}$), 7.27 (m, 8, aryl), 6.57

(s, 1, acac-C*H*), 4.13 (m, 4, OC*H*$_2$CH$_2$), 3.59 (sep, 2, C*H*Me$_2$), 2.14 (m, 4, OCH$_2$C*H*$_2$), 1.80 (s, 3, C*Me*$_2$Ph), 1.78 (s, 3, C*Me*$_2$Ph), 1.34 (s, 9, *t*-Bu), 1.28 (d, 6, CH*Me*$_2$), 1.24 (d, 6, CH*Me*$_2$), 1.23 (s, 9, *t*-Bu); ^{13}C NMR (125 MHz, CD_2Cl_2) δ 323.3 (Mo*C*$_\alpha$), 206.9, 201.8, 162.4 (q, J_{CB} = 50 Hz, *ipso-C* of anion), 151.4, 149.0, 146.8, 135.4, 130.6, 129.5 (q, J_{CF} = 31 Hz, *m*-Ar$_{f4}$), 129.4, 127.7, 126.2, 125.2 (q, J_{CF} = 272 Hz, *C*F$_3$), 124.7, 118.1 (m, *p*-Ar$_{f4}$ of anion), 97.9, 80.9, 58.3, 43.6, 41.9, 31.2, 29.4, 29.1, 28.5, 28.4, 26.9, 24.7, 24.5; ^{19}F NMR (282 MHz, CD_2Cl_2) δ –62.8. Anal. Calcd for $C_{69}H_{68}BF_{24}NO_3Mo$: C, 54.45; H, 4.50; N, 0.92. Found: C, 54.80; N, 4.59; N, 0.89.

{Mo(NAr)(CHCMe$_2$Ph)(HFAC)(THF)}{BAr$_{f4}$}, 4a. A flask was charged with 0.424 g (0.51 mmol) of Mo(NAr)(CHCMe$_2$Ph)(HFAC)()Tf)(THF) and 10 mL of methylene chloride. The solution was chilled to –25ºC at which point 0.446 g (0.52 mmol) of NaBAr$_{f4}$ was added as a solid in one portion. The mixture was stirred at room temperature for 30 minutes then filtered through a plug of Celite. The filtrate was concentrated in vacuo to ~3 mL and layered with several volumes of pentane. The solution was stored at –25ºC for two weeks after which time **4a** crystallized as 0.260 g (40%) of yellow needles, NMR examination showed the product to contain significant quantities of {H$_3$N-2,6-*i*-Pr$_2$C$_6$H$_3$}{BAr$_{f4}$}: ^{1}H NMR (500 MHz, CD_2Cl_2) δ 13.48 (br s, 1, MoC*H*$_\alpha$), 7.72 (s, 8, *o*-Ar$_f$), 7.56 (s, 4, *p*-Ar$_f$), 7.43 (t, 1, *p*-CMe$_2$*Ph*), 7.32 (d, 2, *o*-CMe$_2$*Ph*), 7.27 (t, 2, *m*-CMe$_2$*Ph*), 7.21 (t, 1, *p*-Ar), 7.07 (d, 2, *m*-Ar), 6.94 (br s, 1, acac-C*H*), 4.19 (br s, 4, OC*H*$_2$CH$_2$), 3.54 (br m, 2, C*H*Me$_2$), 2.19 (m, 4, OCH$_2$C*H*$_2$), 1.78 (br s, 3, C*Me*$_2$Ph), 1.63 (br s, 3, C*Me*$_2$Ph), 1.31 (br d, 12, CH*Me*$_2$); ^{19}F NMR (470 MHz) δ -62.8 (Ar$_f$), -74.8 (C*F*$_3$), -75.4 (br, C*F*$_3$).

Mo(NAr)(CHCMe$_2$Ph)(Ar′-nacnac)(OTf), 5a. A flask was charged with 1.650 g (2.08 mmol) of Mo(NAr)(CHCMe$_2$Ph)(OTf)$_2$(DME) and 40 mL of diethyl ether. The mixture was chilled briefly at –25 ºC before 0.656 g (2.10 mmol) of Li{Ar′-nacnac} was added as a solid in one portion. The mixture was allowed to stir at room temperature for 20 hours during which time it became homogeneous and took on an orange-yellow color. All volatiles were removed in vacuo

and the residue was extracted with 30 mL of toluene. The extract was filtered through a plug of Celite and evaporated to dryness. The residue was dissolved in a minimal amount of diethyl ether and set aside at –25 ºC overnight to yield 1.413 g (79%) of orange needles: ^{1}H NMR (500 MHz, C_6D_6) δ 11.56 (s, 1, MoCH_α, J_{CH} = 118 Hz), 7.25 (d, 2, *o*-CMe$_2$*Ph*), 7.14 (t, 2, *m*-CMe$_2$*Ph*), 7.12 (br t, 1, *p*-Ar′), 7.06 (t, 1, *p*-CMe$_2$*Ph*), 7.04 (br d, 2, *m*-Ar), 6.93 (br d, 1, *m*-Ar′), 6.82 (t, 1, *p*- Ar), 6.74 (br d, 1, *m*-Ar′), 6.61 (br d, 1 *m*-Ar′), 6.54 (br m, 2, *m*/*p*-Ar′), 5.39 (s, 1, nacnac-C*H*), 4.94 (sep, 1, C*H*Me$_2$), 2.75 (sep, 1, C*H*Me$_2$), 2.35 (s, 3, Me), 2.21 (s, 3, Me), 2.15 (s, 3, Me), 1.81 (s, 3, Me), 1.77 (s, 3, Me), 1.65 (s, 3, Me), 1.60 (d, 3, CH*Me*$_2$), 1.59 (s, 3, Me), 1.34 (m, 6, Me + CH*Me*$_2$), 1.20 (d, 3, CH*Me*$_2$), 1.14 (d, 3, CH*Me*$_2$); ^{13}C NMR (125 MHz, CD_2Cl_2) *many peaks broad* δ 299.1 (MoC_α), 167.7 (2, *C*=N), 153.5, 153.3, 149.9, 148.4, 147.8, 145.5, 133.6, 132.5, 131.9, 131.3, 129.6, 129.3, 128.9, 128.8 128.7, 126.7, 126.4, 126.3, 125.8, 123.5, 122.9, 119.5 (q, J_{CF} = 319 Hz, *C*F$_3$), 104.8 (nacnac-*C*H), 56.7 (*C*Me$_2$Ph), 33.6, 32.1, 28.1, 26.4, 25.5, 25.3 (nacnac-*Me*), 24.3 (nacnac-*Me*), 23.9, 20.2, 19.2; ^{19}F NMR (282 MHz) δ –76.1. Anal. Calcd for $C_{44}H_{54}F_3MoN_3O_5S$: C, 61.60; H, 6.34; N, 4.90. Found: C, 61.72; H, 6.46; N, 4.81.

Mo(NAr^{Cl})(CH-*t*-Bu)(Ar′-nacnac)(OTf), 5b. A flask was charged with 0.714 g (1.00 mmol) of Mo(NAr^{Cl})(CH-*t*-Bu)(OTf)$_2$(DME) and 20 mL of diethyl ether. To the solution was added 0.319 g (1.02 mmol) of Li{Ar′-nacnac} as a solid in one portion. The reaction was stirred at room temperature for 18 hours. All volatiles were removed in vacuo, and the residue extracted into a 4:1 mixture of toluene to methylene chloride. The mixture was filtered through a bed of Celite and the solution volume concentrated to ~3 mL in vacuo. Several volumes of pentane were added until wine-red precipitate persisted. The mixture was set aside at –25 ºC for 30 minutes to encourage more precipitation. The solid was collected by filtration and washed with pentane to yield 0.595 g (71%) of a deep red microcrystalline powder: ^{1}H NMR (500 MHz, C_6D_6) δ 11.93 (s, 1, MoCH_α, J_{CH} = 115 Hz), 7.12 (d, 1, *m*-Ar′), 7.04 (t, 1, *p*-Ar′), 7.01 (d, 1, *m*-Ar′), 6.79 (d, 1, *m*-Ar′), 6.64 (t, 1, *p*-Ar′), 6.56 (m, 3, *m*-Ar′ + *m*-Ar^{Cl}), 6.10 (t, 1, *p*-Ar^{Cl}), 5.47 (s, 1, nacnac-C*H*), 2.44 (s, 3, Me), 2.31 (s, 3, Me), 2.13 (s, 3, Me), 1.91 (s, 3, Me), 1.58 (s, 3, nacnac-*Me*), 1.51 (s, 9,

t-Bu), 1.45 (s, 3, nacnac-*Me*); ^{13}C NMR (125 MHz, CD_2Cl_2) δ 311.9 (MoC_α), 167.4 (*C*=N), 166.8 (*C*=N), 153.8, 149.6, 147.7, 140.0, 134.3, 131.8, 131.6, 130.1, 129.6, 128.9, 128.5, 128.4, 128.2, 126.9, 126.5, 125.7, 119.4 (q, J_{CF} = 319 Hz, *C*F_3), 104.6 (nacnac-*C*H), 50.4 (*C*Me_3), 30.7 (C*Me*$_3$), 25.8, 23.7, 21.5, 20.9, 19.6, 18.8; ^{19}F NMR (282 MHz) δ –77.2. Anal. Calcd for $C_{33}H_{38}Cl_2F_3MoN_3O_3S$: C, 50.78; H, 4.91; N, 5.38. Found: C, 52.06; H, 5.10; N, 5.15.

Mo(NAr′′)(CH-*t*-Bu)(Ar′-nacnac)(OTf), 5c. A flask was charged with 0.792 g (1.13 mmol) of Mo(NAr′′)(CH-*t*-Bu)$(OTf)_2$(DME) and 35 mL of diethyl ether. To this stirring solution was added 0.390 g (1.25 mmol) of Li{Ar′-nacnac} as a solid in one portion. The mixture was stirred at room temperature for two hours during which time it became homogeneous and turned yellow-brown in color. All volatiles were removed in vacuo, and the residue was extracted into 30 mL of toluene. The solution was filtered through Celite and evaporated to dryness. The residue was dissolved in a minimal amount of diethyl ether and set aside at –25 ºC for 24 hours during which time the compound precipitated as 0.693 g (74%) of an orange, microcrystalline solid: ^{1}H NMR (500 MHz, C_6D_6) δ 11.43 (s, 1, MoC*H*$_\alpha$, J_{CH} = 116 Hz), 8.18 (v br, 1, *o*-Ar′′), 7.09 (t, 1, Ar), 7.03 (m, 3, Ar), 6.90 (t, 1, Ar), 6.76 (t, 1, Ar*)*, 6.65 (m, 3, Ar), 5.36 (s, 1, nacnac-C*H*), 2.39 (s, 3, Me), 2.18 (s, 6, Me), 1.58 (s, 3, Me), 1.42 (s, 3, Me), 1.37 (s, 9, *t*-Bu), 1.35 (s, 9, *t*-Bu); ^{13}C NMR (125 MHz, CD_2Cl_2) *many peaks broad* δ 310.3 (MoC_α), 167.7 (*C*=N), 167.4 (*C*=N), 154.6, 154.2, 147.9, 132.9, 132.8, 132.5, 131.5, 129.5, 129.4, 129.3, 129.2, 129.1, 128.4, 128.3, 126.0, 125.7, 119.5 (q, J_{CF} = 319 Hz, *C*F_3), 104.5 (nacnac-*C*H), 51.3 (*C*Me_3), 36.7, 32.7, 30.7, 25.5, 24.4, 20.8, 20.7, 20.1, 19.5; ^{19}F NMR (282 MHz) δ –77.2. Anal. Calcd for $C_{37}H_{48}F_3MoN_3O_3S$: C, 57.88; H, 6.30; N, 5.47. Found: C, 57.89; H, 6.39; N, 5.41.

Mo(NAr)(κ^1-κ^1-η^2-[Ar^x/Ar′-NC(Me)]$_2$CHCMe$_2$Ph)(OTf), 6a. A flask was charged with 0.103 g (0.119 mmol) of Mo(NAr)(CHCMe$_2$Ph)(Ar′-Nacnac)(OTf) and 10 mL of toluene. The orange solution was heated to 90 ºC for 45 minutes. All volatiles were removed in vacuo and the residue crystallized from a minimal amount of diethyl ether at –25 ºC to give 0.090 g (89%) of

an orange-yellow crystalline solid. Crystals suitable for X-ray diffraction were grown by slow cooling of a saturated diethyl ether solution at 23 ºC: *NMR assignments are based on ^{1}H, ^{13}C, HSQC, and HMBC experiments*; ^{1}H NMR (300 MHz, C_6D_6) δ 7.11 (m, 2, Ar), 6.97 (m, 6, Ar), 6.79 (m, 4, Ar), 5.38 (d, J_{HH} = 14 Hz, 1, $C^{37}H_2$), 4.14 (m, 1, C*H*Me$_2$), 4.12 (t, J_{HH} = 4.5 Hz, 1, $C^{2}H$), 3.70 (d, J_{HH} = 14 Hz, 1, $C^{37}H_2$), 2.63 (dd, J_{HH} = 15 Hz, 4.5 Hz, 1, $C^{6}H_2$), 2.59 (m, 1, C*H*Me$_2$), 2.19 (s, 3, Me), 2.02 (s, 3, Me), 1.77 (dd, J_{HH} = 15 Hz, 4.5 Hz, 1 $C^{6}H_2$), 1.61 (d, 3, CH*Me*$_2$), 1.57 (s, 3, Me), 1.41 (d, 3, CH*Me*$_2$), 1.34 (d, 3, CH*Me*$_2$), 1.23 (s, 3, Me), 1.21 (s, 3, Me), 1.09 (s, 3, Me), 0.65 (d, 3, CH*Me*$_2$), 0.57 (s, 3, Me); ^{13}C NMR (125 MHz, C_6D_6) δ 197.80 (C^{1}), 158.03, 153.78, 150.22, 147.89, 146.67, 145.36, 143.92, 129.90, 129.54, 129.50, 129.33, 128.53, 128.52, 128.03, 127.51, 127.31, 126.86, 125.84, 123.68, 123.63, 123.31, 123.05, 120.52 (q, J_{CF} = 319 Hz, *C*F$_3$), 82.83 (C^{3}), 66.76 (C^{37}), 59.61 (C^{2}), 46.60 (C^{6}), 38.61 (C^{7}), 31.12, 30.70, 28.63, 27.75, 25.88, 25.73, 24.15, 22.20 (C^{5}), 21.84, 19.84 (C^{4}), 18.77 (C^{38}), 18.21, 18.18. ^{19}F NMR (282 MHz) δ –77.3 (C*F*$_3$). Anal. calcd for $C_{44}H_{54}F_3MoN_3O_3S$: C, 61.60; H, 6.34; N, 4.90. Found: C, 61.78; H, 6.42; N, 4.81.

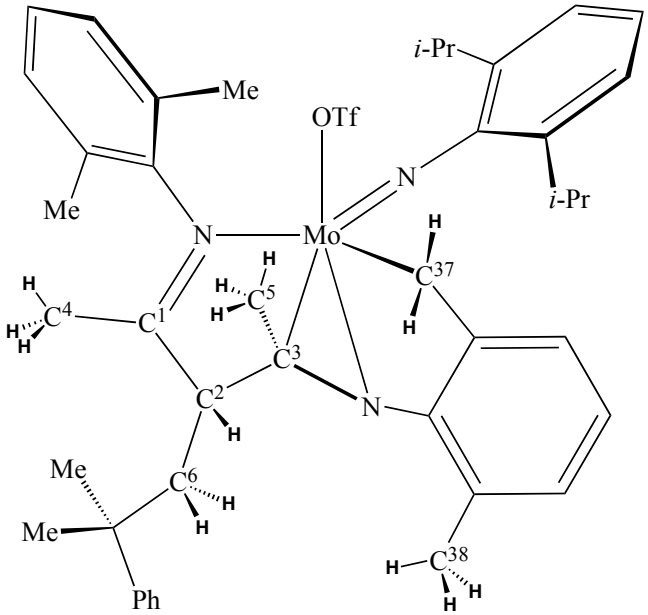

Compounds 6b and 6c. These species were observed spectroscopically upon thermolysis of solutions of **5b** and **5c** in toluene-d_8: NMR (300 MHz, toluene-d_8) *selected peaks* **6b** δ 5.66 (d, J_{HH} = 14 Hz, CH_2), 4.15 (t, J_{HH} = 3.3 Hz, C*H*), 3.59 (d, J_{HH} = 14 Hz, CH_2), 2.64 (dd, J_{HH} = 16 Hz, J_{HH} =3.3 Hz, CH_2); **6c** δ 5.44 (br d, J_{HH} = 14 Hz, 1, CH_2), 4.11 (t, J_{HH} = 3.2 Hz, C*H*), 3.75 (d, J_{HH} = 14 Hz, CH_2), 2.37 (dd, J_{HH} = 16 Hz, J_{HH} = 3.2 Hz, CH_2).

Tl(Ar^F-Nacnac). A flask was charged with 0.519 g (1.58 mmol) of Li{Ar^F-Nacnac} and 25 mL of tetrahydrofuran. To the solution was added 0.415 g (1.58 mmol) of Tl(OAc) as a solid in one portion. The mixture was allowed to stir in the dark for 24 hours at room temperature. All volatiles were removed in vacuo and the residue extracted into diethyl ether. The solution was filtered through Celite and the solvent volume reduced to ~7 mL in vacuo. The solution was set aside at –25 ºC for several days affording a yellow solid that was isolated by filtration and dried in vacuo to afford 0.515 g (62%) of the desired compound: ^{1}H NMR (300 MHz, C_6D_6) δ 6.67 (m, 4, *m*-Ar^F), 6.49 (m, 2, *o*-Ar^F), 4.92 (br s, 1, nacnac-C*H*), 1.90 (s, 6, Me); ^{19}F NMR (282 MHz) δ 121.3 (d, J_{TlF} = 753 Hz, Ar^F).

Mo(NAr)(CHCMe$_2$Ph)(Ar^F-Nacnac)(OTf), 7a. A flask was charged with 0.724 g (0.913 mmol) of Mo(NAr)(CHCMe$_2$Ph)(OTf)$_2$(DME) and 25 mL of toluene. To the solution was added 0.482 g (0.916 mmol) of Tl(Ar^F-Nacnac) as a solid in one portion. The mixture was set in a dark corner of the glove box and allowed to stir at room temperature for 40 hours. All volatiles were removed in vacuo and the residue extracted into 25 mL of toluene. The extract was filtered through a pad of Celite and evaporated to dryness. The residue was then dissolved in a minimal amount of diethyl ether and set aside at –25 ºC. The product precipitated in two crops as 0.630 g (79%) of yellow microcrystals that exist as a 1:1.5 mixture of syn to anti isomers: ^{1}H NMR (300 MHz, C_6D_6) δ 14.90 (s, 1, *anti* MoCH_α, J_{CH} = 145 Hz), 12.42 (s, 1, *syn* MoCH_α, J_{CH} = 117 Hz), 7.42 (d, 2, *anti o*-CMe$_2$*Ph*), 7.35 (d, 2, *syn o*-CMe$_2$*Ph*), 7.18 (t, 2, *anti m*-CMe$_2$*Ph*), 7.16 (t, 2, *syn m*-CMe$_2$Ph), 7.07 (t, 1, *syn p*-CMe$_2$*Ph*), 7.05 (t, 1, *p*-CMe$_2$*Ph*), 6.91 – 6.58 (m, 13, *syn*/*anti* Ar^F +

m/*p*-2,6-*i*-$Pr_2C_6H_3$), 6.26 (m, 2, *syn* Ar^F), 6.00 (m, 3, *anti* Ar^F), 5.15 (s, 1, *syn* nacnac-C*H*), 5.14 (s, 1, *anti* nacnac-C*H*), 4.08 (br m, 1, *anti* C*H*Me_2), 3.81 (sep, 2, *syn* C*H*Me_2), 3.37 (br m, 1, *anti* C*H*Me_2), 2.12 (s, 3, *anti* Me), 2.01 (s, 3, *syn* Me), 1.90 (s, 3, *syn* Me), 1.88 (s, 3, *anti* Me), 1.70 (br, 3, *anti* CH*Me*$_2$), 1.64 (s, 3, *anti* Me), 1.42 (d, 6, *syn* CH*Me*$_2$), 1.41 (s, 3, *syn* Me), 1.40 (br, 3, *anti* CH*Me*$_2$), 1.39 (s, 3, *anti* Me), 1.34 (d, 6, *syn* CH*Me*$_2$), 1.21 (br, 6, *anti* CH*Me*$_2$); ^{13}C NMR (125 MHz, C_6D_6) *selected peaks only* δ 322.8 (*anti* Mo*C*$_\alpha$), 303.1 (*syn* Mo*C*$_\alpha$), 169.8 (*syn C*=N), 169.5 (*anti C*=N), 169.0 (*syn C*=N), 167.2 (*anti C*=N), 104.7 (*syn* nacnac-*C*H), 103.7 (*anti* nacnac-*C*H), 56.8 (*syn C*Me_2Ph), 54.9 (*anti C*Me_2Ph); ^{19}F NMR (282 MHz) δ –76.7 (C*F*$_3$), –114.3 (*anti* Ar*F*), –114.5 (*syn* Ar*F*), –116.2 (*anti* Ar*F*), –117.5 (2, *syn* Ar*F*), –118.4 (*syn* Ar*F*), –119.7 (*anti* Ar*F*), –120.1 (*anti* Ar*F*). Anal. Calcd for $C_{40}H_{42}F_7MoN_3O_3S$: C, 54.98; H, 4.84; N, 4.81. Found: C, 55.05; H, 4.88; N, 4.70.

Mo(NAr)(CHCMe$_2$Ph)(Ar*-nacnac)(OTf), 8a. A flask was charged with 1.190 g (1.50 mmol) of Mo(NAr)(CHCMe$_2$Ph)(OTf)$_2$(DME) and 25 mL of diethyl ether. The solution was chilled to –25 ºC at which point 0.473 g (1.51 mmol) of Li{Ar*-nacnac} was added as a solid in one portion. The mixture was allowed to stir at room temperature for two hours, during which time the solution color darkened from yellow to yellow-brown. All volatiles were removed in vacuo and the residue extracted into 20 mL of toluene. The extract was filtered through Celite and evaporated to dryness in vacuo. The resulting solid was recrystallized from a minimal amount of diethyl ether yielding 0.970 g (75%) of an orange-red crystalline solid. The compound was found to exist as a 15:1 mixture of syn to anti isomers: ^{1}H NMR (300 MHz, C_6D_6) δ 14.30 (s, 1, *anti* MoC*H*$_\alpha$, J_{CH} = 145 Hz), 12.12 (s, 1, *syn* MoC*H*$_\alpha$, J_{CH} = 117 Hz), *syn isomer only* 7.35 (d, 2, *o*-CMe$_2$*Ph*), 7.17 (t, 2, *m*-CMe$_2$*Ph*), 7.05 (t, 1, *p*-CMe$_2$*Ph*), 6.94 (br s, 2, *o*-Ar*), 6.81 (m, 3, *m*/*p*-Ar), 6.74 (s, 1, *p*-Ar*), 6.26 (s, 1, *p*-Ar*), 5.91 (br s, 2, *o*-Ar*), 5.28 (s, 1, nacnac-C*H*), 3.56 (sep, 2, C*H*Me$_2$), 2.30 (s, 3, Me), 2.27 (s, 6, Ar*-*Me*), 1.87 (br s, 6, Ar*-*Me*), 1.77 (s, 3, Me), 1.70 (s, 3, Me), 1.47 (s, 3, Me), 1.34 (d, 6, CH*Me*$_2$), 1.04 (d, 6, CH*Me*$_2$); ^{13}C NMR (125 MHz, C_6D_6) δ 297.8 (MoC_α), 167.1 (*C*=N), 165.4 (*C*=N), 154.5, 152.2, 149.4, 149.0, 147.6 (br), 138.6 (br),

129.1, 128.9, 127.3, 126.9, 126.6, 126.1 (br), 123.0, 122.2 (br), 120.7 (q, *C*F_3, J_{CF} = 319 Hz), 104.8 (nacnac-*C*H), 55.3 (*C*Me_2Ph), 32.6 (br), 31.0, 27.9, 24.7 (br m), 24.1, 21.6 (br); ^{19}F NMR (282 MHz) δ -76.7. Anal. Calcd for $C_{44}H_{54}F_3MoN_3O_3S$: C, 61.60; H, 6.34; N, 4.90. Found: C, 61.54; H, 6.31; N, 4.86.

{Mo(NAr)(CHCMe$_2$Ph)(Ar′-nacnac)(THF)}{BAr$_{f4}$}, 9a. A flask was charged with 0.502 g (0.585 mmol) of Mo(N-2,6-*i*-$Pr_2C_6H_3$)(CHCMe$_2$Ph)(Ar′-nacnac)(OTf), 1 mL of THF, and 25 mL of methylene chloride. The solution was cooled to –25 ºC and 0.513 g (0.592 mmol) of solid $NaBAr_{f4}$ was added in one portion. The mixture was stirred at room temperature for 5 minutes. All volatiles were removed *in vacuo*. The residue was extracted with methylene chloride and the mixture was filtered through Celite. The extract's volume was reduced to ~5 mL *in vacuo* and the solution was layered with several volumes of pentane. The product crystallized at –25 ºC as an orange microcrystalline solid; yield 0.887 g (92%). Crystals suitable for X-ray diffraction were grown by slowly cooling a saturated solution of methylene chloride and pentane at –25 ºC: ^{1}H NMR (238 K, 500 MHz, CD_2Cl_2) δ 12.18 (s, 1, MoC*H*$_\alpha$, J_{CH} = 108 Hz), 7.75 (s, 8, *o*-Ar_f), 7.58 (s, 4, *p*-Ar_f), 7.28 (m, 3, aryl), 7.23 (m, 2, aryl), 7.19-7.12 (m, 4, aryl), 7.09-7.05 (m, 3, aryl), 7.01 (br d, 1, Ar′), 6.97 (br d, 1, Ar′), 5.89 (s, 1, nacnac-C*H*), 4.73 (sep, 1, C*H*Me_2), 3.73 (m, 2, OC*H*$_2$), 3.52 (m, 2, OC*H*$_2$), 2.62 (sep, 1, C*H*Me_2), 2.27 (s, 3, Me), 2.08 (s, 3, Me), 1.88 (s, 3, Me), 1.83 (m, 3, Me), 1.76 (s, 3, Me), 1.68 (s, 3, Me), 1.55 (br m, 2, OC*H*$_2$), 1.43 (s, 3, Me), 1.41 (d, 3, CH*Me*$_2$), 1.32 (m, 2, OCH_2), 1.26 (d, 3, C*H*Me_2), 1.21 (d, 3, C*H*Me_2), 1.17 (d, 3, C*H*Me_2), 0.91 (s, 3, Me); ^{13}C NMR (253 K, 125 MHz, CD_2Cl_2) δ 317.6 (Mo*C*$_\alpha$), 168.9 (*C*N), 167.4 (*C*N), 161.9 (q, J_{CB} = 49.6 Hz, *ipso*-Ar_f), 154.3, 153.9, 148.0, 147.1, 143.9, 143.1, 135.1, 134.9 (*o*-Ar_f), 132.7, 131.1, 131.0, 130.4, 129.7, 129.5, 129.4, 129.1, 128.9 (qq, J_{CF} = 31.3 Hz, *m*-Ar_f), 127.8, 127.4, 126.7, 125.9, 124.7 (q, J_{CF} = 272 Hz, *C*F_3), 124.6, 124.5, 117.7 (m, *p*-Ar_f), 105.7 (nacnac-*C*H), 80.2 (O*C*H_2), 79.3 (O*C*H_2), 56.6 (*C*Me_2Ph), 31.3, 29.7, 28.2, 27.3, 26.5, 25.5, 25.3, 25.2, 25.1, 25.0, 23.8, 19.6, 19.4, 19.3, 18.8; ^{19}F NMR (293 K, 472 MHz) δ –62.4. Anal. Calcd for $C_{79}H_{74}BF_{24}MoN_3O$: C, 57.71; H, 4.54; N, 2.53. Found: C, 57.48; H, 4.68; N, 2.45.

{Mo(NAr^{Cl})(CH-*t*-Bu)(Ar′-nacnac)(THF)}{BAr$_{f4}$}, 9b. A flask was charged with 0.183 g (0.235 mmol) of Mo(NAr^{Cl})(CH-*t*-Bu)(Ar′-nacnac)(OTf), 1 mL of THF, and 20 mL of methylene chloride. The solution was cooled to –25 ºC, at which point 0.255 g (0.257 mmol) of NaBAr$_{f4}$ was added as a solid in one portion. The mixture was allowed to stir at room temperature for 10 minutes. All volatiles were removed in vacuo and the residue extracted into methylene chloride and filtered through Celite. The solvent volume was reduced to ~2 mL in vacuo and layered with several volumes of pentane. The mixture was set aside at –25 ºC for two days to afford 0.322 g (87%) of red crystals: ^{1}H NMR (300 MHz, CD_2Cl_2) δ 13.11 (s, 1, MoC*H*$_\alpha$, J_{CH} = 116 Hz), 7.72 (s, 8, *o*-Ar$_f$), 7.56 (s, 4, *p*-Ar$_f$), 7.41 (d, 2, *m*-Ar^{Cl}), 7.16 (t, 1, *p*-Ar^{Cl}), 7.11 (br, 6, Ar′), 6.15 (s, 1, nacnac-C*H*), 3.1 (v br, 4, OC*H*$_2$), 2.26 (br, 6, Me), 1.84 (br m, 12, Me), 1.62 (m, 4, OCH$_2$C*H*$_2$), 0.94 (s, 9, *t*-Bu); ^{13}C NMR (125 MHz, CD_2Cl_2) δ 332.8 (Mo*C*$_\alpha$), 168 (v br, *C*=N), 162.4 (q, J_{CB} = 49.9 Hz, *ipso*-Ar$_f$), 151.4 (*ipso*-Ar^{Cl}), 135.4 (*m*-Ar$_f$), 130.3 (*m*-Ar^{Cl}), 130.2 (*o*-Ar^{Cl}), 130.1 (*p*-Ar^{Cl}), 129.5 (q, J_{CF} = 32.5 Hz, *m*-Ar$_f$), 129.1 (br, Ar'), 128.0 (br, Ar'), 125.2 (q, J_{CF} = 271 Hz, *C*F$_3$), 118.0 (sep, J_{CF} = 3.8 Hz, *p*-Ar$_f$), 106.9 (nacnac-*C*H), 80.6 (br, OCH$_2$CH$_2$), 51.8 (*C*Me$_3$), 31.4 (C*Me*$_3$), 26.1, 25.2, 19.5; ^{19}F NMR (282 MHz) δ –63.3. Anal. Calcd for $C_{68}H_{58}BCl_2F_{24}MoN_3O$: C, 52.13; H, 3.73; N, 2.68. Found: C, 52.19; H, 3.80; N, 2.64.

{Mo(NAr′′)(CH-*t*-Bu)(Ar′-nacnac)(THF)}{BAr$_{f4}$}, 9c. This compound was prepared in analogous fashion to complex **9a** starting from 0.155 g (0.20 mmol) of Mo(N-2-*t*-BuC$_6$H$_4$)(CH-*t*-Bu)(Ar′-nacnac)(OTf) and 0.192 g (0.22 mmol) of NaBAr$_{f4}$. Upon recrystallization from methylene chloride/pentane, 0.279 g of a bright orange powder was obtained. ^{1}H NMR spectra showed the compound to be a mixture of two compounds, **9c** and **10c**, as well as a mixture of syn and anti isomers of **9c**: ^{1}H NMR (500 MHz, CD_2Cl_2) δ 14.52 (s, *anti* MoC*H*$_\alpha$), 11.85 (v br s, *syn* MoC*H*$_\alpha$), 11.08 (v br s, *syn* MoC*H*$_\alpha$), 7.75 (s, *o*-Ar$_f$), 7.60 (s, *p*-Ar$_f$), 7.2 (v br m, aryl), 6.15 (s, *anti* nacnac-C*H*), 6.0 (v br s, *syn* nacnac-C*H*), 3.6 (v br m, THF), 2.60 (s, Me), 2.30 (br s, Me), 2.10 (br m, Me), 1.90 (s, *t*-Bu), 1.83 (br s, Me), 1.75 (br m, THF), 1.65 (s, *t*-Bu), 1.56 (s, *t*-Bu), 1.1 (br, Me).

Compound 11a. This species was observed spectroscopically upon thermolysis of a 15 mM solution of **4a** in methylene chloride-d_2 at 40 ºC for 3 hours: ^{1}H NMR (500 MHz) δ *including* tert-*butylbenzene* δ 14.28 (br s, 1, MoCH_α, J_{CH} = 150 Hz), 8.26 (s, 8, *o*-Ar$_f$), 7.64 (s, 4, *p*-Ar$_f$), 7.34 (d, 2, Ar), 7.27 (t, 1, Ar), 7.22 (d, 1, Ar), 7.14 (m, 3, Ar), 6.99 (d, 1, Ar), 6.83 (t, 1, Ar), 6.69 (d, 2, Ar), 6.53 (d, 1, Ar), 4.85 (br s, 1, nacnac-C*H*), 3.32 (sep, 2, C*H*Me$_2$), 3.28 (m, 2, THF), 2.98 (m, 2, THF), 2.29 (s, 3, Me), 2.10 (br s, 3, Me), 1.87 (s, 3, Me), 1.65 (s, 3, Me), 1.4 – 1.1 (br m, 19, THF + CH*Me*$_2$ + Me), 0.74 (br s, 6, CH*Me*$_2$).; ^{13}C NMR (258 K, 125 MHz) δ 299.5 (MoC_α), 166.2 (*C*N), 162.1 (q, J_{CB} = 49.7 Hz, *ipso*-Ar$_f$), 152.5, 151.4, 150.7, 147.0, 146.7 (v br), 143.2, 135.1 (*o*-Ar$_f$), 133.0, 131.5, 129.9, 129.2, 129.1, 129.1 (qq, J_{CF} = 31.3 Hz, *m*-Ar$_f$), 129.0, 127.9, 126.1, 124.9 (q, J_{CF} = 272 Hz, *C*F$_3$), 124.6, 123.8, 119.4, 81.5, 75.8, 28.7, 26.7, 25.4 (br), 24.1, 23.5, 22.1, 19.3, 17.7, 17.5.

Compound 11c. This species was observed spectroscopically upon thermolysis of a mixture of **9c** and **10c** at 40 ºC for 3 hours in methylene chloride-d_2: ^{1}H NMR (300 MHz) δ 14.13 (s, 1, MoCH_α), 7.73 (s, 8, *o*-Ar$_f$), 7.56 (s, 4, *p*-Ar$_f$), 7.40 (d, 1, aryl), 7.15 (m, 3, aryl), 6.98 (t, 1, aryl), 6.90 (t, 1, aryl), 6.81 (t, 1, aryl), 6.74 (d, 1 aryl), 6.65 (d, 1, aryl) 5.89 (d, 1, aryl), 5.35 (s, 1, nacnac-C*H*), 3.78 (m, 2, OCH_2CH$_2$), 3.41 (m, 2, OCH_2CH$_2$), 2.57 (s, 3, Me), 2.48 (s, 3, Me), 2.06 (s, 3, Me), 1.97 (s, 3, Me), 1.85 (m, 4, OCH$_2$CH_2), 1.58 (s, 9, *t*-Bu), 1.17 (s, 3, Me).

{Mo(NAr)(κ^1-κ^1-η^2-[Ar^x/Ar′-NC(Me)]$_2$CHCMe$_2$Ph)(THF)}{B(C$_6$F$_5$)$_4$}, 12a. This species was observed spectroscopically by mixing equimolar amounts of **6a** and NaB(C$_6$F$_5$)$_4$·THF in methylene chloride-d_2: ^{1}H NMR (300 MHz) δ 7.49 (d, 2, *o*-CMe$_2$*Ph*), 7.35 (t, 2, *m*-CMe$_2$*Ph*), 7.22 (t, 1, *p*-CMe$_2$*Ph*), 7.16 (m, 4, aryl), 7.08 (d, 1, *m*-Ar′), 7.07 (t, 1, *p*-Ar′), 6.95 (d, 1, *m*-Ar′), 6.89 (m, 2, *m* + *p*-Ar′), 4.54 (d, J_{HH} = 12.9 Hz, CH_2), 4.50 (t, J_{HH} = 3.0 Hz, C*H*), 3.93 (m, 3, C*H*Me$_2$ + OCH_2CH$_2$), 3.52 (m, 2, OCH_2CH$_2$), 3.01 (d, J_{HH} = 12.9 Hz, 1, CH_2), 2.79 (dd, J_{HH} = 15.6 Hz, J_{HH} = 3.0 Hz, 1, CH_2), 2.31 (s, 1, Me), 2.15 (sep, 1, C*H*Me$_2$), 2.14 (s, 3, Me), 1.97 (dd, J_{HH} = 15.6 Hz, J_{HH} = 3.0 Hz, 1, CH_2), 1.86 (s, 3, Me), 1.82 (m, 4, OCH$_2$CH_2), 1.63 (s, 3, Me),

1.60 (s, 3, Me), 1.51 (d, 3, CH*Me*$_2$), 1.33 (d, 3, CH*Me*$_2$), 1.17 (s, 3, Me), 1.04 (s, 3, Me), 1.03 (d, 3, CH*Me*$_2$), 0.44 (d, 3, CH*Me*$_2$).

{Mo(NAr)(CHCMe$_2$Ph)(Ar^F-nacnac)(THF)}{BAr$_{f4}$}, 13a. This compound was prepared in analogous fashion to complex **9a** starting from 0.327 g (0.374 mmol) of **8a** and 0.330 g (0.381 mmol) of NaBAr$_{f4}$. The complex was observed to form an oil during attempts at crystallization, and finally precipitated as 0.421 g (68%) of a yellow-brown powder: ^{1}H NMR (300 MHz, CD_2Cl_2) δ 14.86 (d, J_{HF} = 3.5 Hz, *anti* MoC*H*), 12.75 (s, 1, *syn* MoC*H*), 7.75 (s, 8, *o*-Ar$_f$), 6.58 (s, 4, *p*-Ar$_f$), 7.4 – 6.9 (m, 9, Ar), 5.94 (s, 1, nacnac-C*H*), 3.7 (v br m, 1, C*H*Me$_2$), 2.84 (m, 2, OC*H*$_2$CH$_2$), 2.45 (m, 2, OC*H*$_2$CH$_2$), 2.17 (s, 3, C*Me*$_2$Ph), 1.94 (s, 3, C*Me*$_2$Ph), 1.57 (s, 3, nacnac-*Me*), 1.36 (m, 4, OCH$_2$C*H*$_2$), 1.28 (br, 6, CH*Me*$_2$), 1.22 (d, 6, CH*Me*$_2$), 1.10 (s, 3, nacnac-*Me*); ^{19}F NMR (470 MHz) δ -62.5 (Ar$_f$), -115.4 (Ar^F), -115.7 (Ar^F), -117.2 (Ar^F), -119.5 (Ar^F). Anal. Calcd for $C_{75}H_{62}BF_{28}MoN_3O$: C, 54.26; H, 3.76; N, 2.53. Found: C, 54.33; H, 3.68; N, 2.46.

Compound 14a. This compound was observed spectroscopically upon mixing equimolar amounts of **8a** and NaB(C$_6$F$_5$)$_4$·THF in methylene chloride-d_2: ^{1}H NMR (300 MHz) *selected peaks* δ 14.23 (s, 1, MoC*H*), 5.89 (s, 1, nacnac-C*H*), 3.17 (sep, 2, C*H*Me$_2$).

{Mo(NAr)(CH$_2$CH$_2$)(Ar′-nacnac)(THF)}{BAr$_{f4}$}, 15a. This species was observed spectroscopically by exposing a solution of **9a** to one atmosphere of ethylene at 23 ºC in methylene chloride-d_2: ^{1}H NMR (300 MHz) δ 7.73 (s, 8, *o*-Ar$_f$), 7.56 (s, 4, *p*-Ar$_f$), 7.40 (t, 2, aryl), 7.36 – 7.26 (m, 5, aryl), 7.15 (d, 2, aryl), 6.46 (s, 1, nacnac-C*H*), 3.65 (br s, 4, OC*H*$_2$CH$_2$), 2.85 (sep, 2, C*H*Me$_2$), 2.57 (m, 2, C*H*$_2$CH$_2$), 2.33 (s, 6, Me), 1.93 (s, 6, Me), 1.80 (br s, 4, OCH$_2$C*H*$_2$), 1.77 (s, 6, Me), 1.16 (d, 12, CH*Me*$_2$), 0.86 (m, 2, CH$_2$C*H*$_2$).

{Mo(NAr^{Cl})(CH_2CH_2)(Ar′-nacnac)(THF)}{BAr_{f4}}, 15b. This compound was observed in analogous fashion to **15a**: ^{1}H NMR (500 MHz, CD_2Cl_2) *selected peaks* δ 6.51 (s, 1, nacnac-C*H*), 2.90 (m, 2, CH_2CH$_2$), 1.15 (m, 2, CH$_2$CH_2).

Crystal data and structure refinement for **1a**.

Reciprocal net identification code	**05097**	
Empirical formula	$C_{38}H_{56}F_3MoNO_6S$	
Formula weight	807.84 g/mol	
Temperature	100(2) K	
Wavelength	0.71073 Å	
Crystal system	Monoclinic	
Space group	$P2_1/n$	
Unit cell dimensions	a = 13.2044(4) Å	α = 90°
	b = 16.9843(5) Å	β = 97.7710(10)°
	c = 18.0952(5) Å	γ = 90°
Volume	4020.9(2) $Å^3$	
Z	4	
Density (calculated)	1.334 g/cm^3	
Absorption coefficient	0.435 mm^{-1}	
F(000)	1696	
Crystal size	0.20 × 0.09 × 0.06 mm^3	
Θ range for data collection	1.80 to 29.57°	
Index ranges	$-17 \le h \le 18$, $-23 \le k \le 23$, $-25 \le l \le 24$	
Reflections collected	88513	
Independent reflections	11285 [R(int) = 0.0490]	
Completeness to Θ = 29.57°	100.0 %	
Absorption correction	Semi-empirical from equivalents	
Max. and min. transmission	0.9744 and 0.9180	
Refinement method	Full-matrix least-squares on F^2	
Data / restraints / parameters	11285 / 1 / 466	
Goodness-of-fit on F^2	1.067	
Final R indices [I>2σ(I)]	R1 = 0.0338, wR2 = 0.0785	
R indices (all data)	R1 = 0.0444, wR2 = 0.0840	
Largest diff. peak and hole	0.854 and -0.262 $e \cdot Å^{-3}$	

Crystal data and structure refinement for **3a**.

Reciprocal net identification code	**05220**	
Empirical formula	$C_{77}H_{86}BCl_2F_{24}MoNO_3$	
Formula weight	1707.12 g/mol	
Temperature	100(2) K	
Wavelength	0.71073 Å	
Crystal system	Triclinic	
Space group	$P\bar{1}$	
Unit cell dimensions	a = 12.5398(3) Å	α = 73.0120(10)°
	b = 15.8864(4) Å	β = 88.1790(10)°
	c = 20.9492(5) Å	γ = 80.2490(10)°
Volume	3932.88(17) $Å^3$	
Z	2	
Density (calculated)	1.442 g/cm^3	
Absorption coefficient	0.338 mm^{-1}	
F(000)	1752	
Crystal size	0.30 × 0.25 × 0.20 mm^3	
Θ range for data collection	1.92 to 29.13°	
Index ranges	$-17 \le h \le 17$, $-21 \le k \le 21$, $-28 \le l \le 28$	
Reflections collected	85713	
Independent reflections	21129 [R(int) = 0.0264]	
Completeness to Θ = 29.13°	99.7 %	
Absorption correction	Semi-empirical from equivalents	
Max. and min. transmission	0.9354 and 0.9053	
Refinement method	Full-matrix least-squares on F^2	
Data / restraints / parameters	21129 / 1383 / 1282	
Goodness-of-fit on F^2	1.051	
Final R indices [I>2σ(I)]	R1 = 0.0578, wR2 = 0.1673	
R indices (all data)	R1 = 0.0671, wR2 = 0.1763	
Largest diff. peak and hole	2.107 and -1.180 $e \cdot Å^{-3}$	

Crystal data and structure refinement for **6a**.

Reciprocal net identification code	**06187**	
Empirical formula	$C_{44}H_{54}F_3MoN_3O_3S$	
Formula weight	857.90 g/mol	
Temperature	100(2) K	
Wavelength	0.71073 Å	
Crystal system	Monoclinic	
Space group	$P2_1$	
Unit cell dimensions	a = 10.7550(5) Å	α = 90°
	b = 17.4054(9) Å	β = 92.020(2)°
	c = 22.5561(12) Å	γ = 90°
Volume	4219.8(4) Å^3	
Z	4	
Density (calculated)	1.350 g/cm^3	
Absorption coefficient	0.415 mm^{-1}	
F(000)	1792	
Crystal size	0.30 × 0.10 × 0.08 mm^3	
Θ range for data collection	1.48 to 29.13°	
Index ranges	$-14 \le h \le 14$, $-23 \le k \le 23$, $0 \le l \le 30$	
Reflections collected	26565	
Independent reflections	26569	
Completeness to Θ = 29.13°	99.5 %	
Absorption correction	Semi-empirical from equivalents	
Max. and min. transmission	0.9675 and 0.8855	
Refinement method	Full-matrix least-squares on F^2	
Data / restraints / parameters	26569 / 986 / 1026	
Goodness-of-fit on F^2	1.009	
Final R indices [I>2σ(I)]	R1 = 0.0389, wR2 = 0.0765	
R indices (all data)	R1 = 0.0450, wR2 = 0.0782	
Absolute structure parameter	-0.017(15)	
Largest diff. peak and hole	0.970 and -0.647 e·Å^{-3}	

Crystal data and structure refinement for **9a**.

Reciprocal net identification code	**06192**	
Empirical formula	$C_{80}H_{76}BCl_2F_{24}MoN_3O$	
Formula weight	1729.09 g/mol	
Temperature	100(2) K	
Wavelength	0.71073 Å	
Crystal system	Triclinic	
Space group	$P\bar{1}$	
Unit cell dimensions	a = 11.4290(4) Å	α = 95.7510(10)°
	b = 18.7038(7) Å	β = 94.0100(10)°
	c = 19.0217(7) Å	γ = 101.9670(10)°
Volume	3940.6(2) $Å^3$	
Z	2	
Density (calculated)	1.457 g/cm^3	
Absorption coefficient	0.338 mm^{-1}	
F(000)	1764	
Crystal size	0.35 × 0.25 × 0.10 mm^3	
Θ range for data collection	1.65 to 29.57°	
Index ranges	$-15 \le h \le 15$, $-25 \le k \le 25$, $-26 \le l \le 26$	
Reflections collected	88758	
Independent reflections	22050 [R(int) = 0.0316]	
Completeness to Θ = 29.57°	99.7 %	
Absorption correction	Semi-empirical from equivalents	
Max. and min. transmission	0.9670 and 0.8909	
Refinement method	Full-matrix least-squares on F^2	
Data / restraints / parameters	22050 / 2444 / 1192	
Goodness-of-fit on F^2	1.025	
Final R indices [I>2σ(I)]	R1 = 0.0407, wR2 = 0.1056	
R indices (all data)	R1 = 0.0471, wR2 = 0.1099	
Largest diff. peak and hole	1.103 and -0.589 $e \cdot Å^{-3}$	

REFERENCES

1. Schrock, R. R.; Hoveyda, A. H., *Angew. Chem. Int. Ed.* **2003**, *42*, 4592.
2. Grubbs, R. H., *Handbook of Metathesis.* Wiley-VCH: Weinheim, 2003.
3. Grubbs, R. H.; Miller, S. J.; Fu, G. C., *Acc. Chem. Res.* **1995**, *28*, 446.
4. Schrock, R. R.; Feldman, J., *Prog. Inorg. Chem.* **1991**, *39*, 1.
5. Schrock, R. R., *Chem. Rev.* **2002**, *102*, 145.
6. Schrock, R. R., *Chem. Comm.* **2005**, 2773.
7. Nomura, K.; Sagara, A.; Imanishi, Y., *Macromolecules* **2002**, *35*, 1583.
8. Yamada, J.; Fujiki, M.; Nomura, K., *Organometallics* **2005**, *24*, 2248.
9. Wallace, K. C.; Liu, A. H.; Dewan, J. C.; Schrock, R. R., *J. Am. Chem. Soc.* **1988**, *110*, 4964.
10. Schofield, M. H.; Schrock, R. R.; Park, L. Y., *Organometallics* **1991**, *10*, 1844.
11. Schrock, R. R., *Polyhedron* **1995**, *14*, 3177.
12. Sinha, A.; Schrock, R. R., *Organometallics* **2004**, *23*, 1643.
13. Sinha, A.; Lopez, L. P. H.; Schrock, R. R.; Hock, A. S.; Mueller, P., *Organometallics* **2006**, *25*, 1412.
14. Blanc, F.; Coperet, C.; Thivolle-Cazat, J.; Basset, J.-M.; Lesage, A.; Emsley, L.; Sinha, A.; Schrock, R. R., *Angew. Chem. Int. Ed.* **2006**, *45*, 1216.
15. Rhers, B.; Salameh, A.; Baudouin, A.; Quadrelli, E. A.; Taoufik, M.; Coperet, C.; Lefebvre, F.; Basset, J.-M.; Solans-Monfort, X.; Eisenstein, O.; Lukens, W. W.; Lopez, L. P. H.; Sinha, A.; Schrock, R. R., *Organometallics* **2006**, *25*, 3554.
16. Cameron, T. M.; Ortiz, C. G.; Ghiviriga, I.; Abboud, K. A.; Boncella, J. M., *Organometallics* **2001**, *20*, 2032.
17. VanderLende, D. D.; Abboud, K. A.; Boncella, J. M., *Polymer Preprints (American Chemical Society, Division of Polymer Chemistry)* **1994**, 35, 691.
18. Sinha, A.; Schrock, R. R.; Mueller, P.; Hoveyda, A. H., *Organometallics* **2006**, *25*, 4621.
19. Eisenstein, O.; Hoffmann, R.; Rossi, A. R., *J. Am. Chem. Soc.* **1981**, *103*, 5582.
20. Anderson, D. R.; Hickstein, D. D.; O'Leary, D. J.; Grubbs, R. H., *J. Am. Chem. Soc.* **2006**, *128*, 8386.
21. Goumans, T. P. M.; Ehlers, A. W.; Lammertsma, K., *Organometallics* **2005**, *24*, 3200.
22. Kress, J.; Osborn, J. A., *Angew. Chem.* **1992**, *104*, 1660.
23. Lopez, L. P. H.; Schrock, R. R., *J. Am. Chem. Soc.* **2004**, *126*, 9526.
24. Blosch, L. L.; Gamble, A. S.; Abboud, K.; Boncella, J. M., *Organometallics* **1992**, *11*, 2342.
25. Vaughan, W. M.; Abboud, K. A.; Boncella, J. M., *Organometallics* **1995**, *14*, 1567.

26. Vaughan, W. M.; Abboud, K. A.; Boncella, J. M., *J. Organomet. Chem.* **1995**, *485*, 37.
27. Kress, J.; Osborn, J. A., *J. Am. Chem. Soc.* **1983**, *105*, 6346.
28. Youinou, M. T.; Kress, J.; Fischer, J.; Aguero, A.; Osborn, J. A., *J. Am. Chem. Soc.* **1988**, *110*, 1488.
29. Furstner, A., Chemical Communications (Cambridge) **1998**, 1315.
30. Sanford, M. S.; Henling, L. M.; Grubbs, R. H., *Organometallics* **1998**, *17*, 5384.
31. Hansen, S. M.; Volland, M. A. O.; Rominger, F.; Eisentrager, F.; Hofmann, P., *Angew. Chem. Int. Ed.* **1999**, *38*, 1273.
32. Furstner, A.; Liebl, M.; Lehmann, C. W.; Picquet, M.; Kunz, R.; Bruneau, C.; Touchard, D.; Dixneuf, P. H., *Chem. Eur. J.* **2000**, *6*, 1847.
33. Hofmann, P.; Volland, M. A. O.; Hansen, S. M.; Eisentrager, F.; Gross, J. H.; Stengel, K., *J. Organomet. Chem.* **2000**, *606*, 88.
34. Bassetti, M.; Centola, F.; Semeril, D.; Bruneau, C.; Dixneuf, P. H., *Organometallics* **2003**, *22*, 4459.
35. Thompson, D. W., *Structure and Bonding* (Berlin, Germany) **1971**, 9, 27.
36. Bourget-Merle, L.; Lappert, M. F.; Severn, J. R., *Chem. Rev.* **2002**, *102*, 3031.
37. Basuli, F.; Bailey, B. C.; Tomaszewski, J.; Huffman, J. C.; Mindiola, D. J., *J. Am. Chem. Soc.* **2003**, *125*, 6052.
38. Mindiola, D. J., *Acc. Chem. Res.* **2006**, *39*, 813.
39. Basuli, F.; Bailey, B. C.; Watson, L. A.; Tomaszewski, J.; Huffman, J. C.; Mindiola, D. J., *Organometallics* **2005**, *24*, 1886.
40. Basuli, F.; Kilgore, U. J.; Hu, X.; Meyer, K.; Pink, M.; Huffman, J. C.; Mindiola, D. J., *Angew. Chem. Int. Ed.* **2004**, *43*, 3156.
41. Schrock, R. R.; Crowe, W. E.; Bazan, G. C.; DiMare, M.; O'Regan, M. B.; Schofield, M. H., *Organometallics* **1991**, *10*, 1832.
42. Schrock, R. R.; Murdzek, J. S.; Bazan, G. C.; Robbins, J.; DiMare, M.; O'Regan, M., *J. Am. Chem. Soc.* **1990**, *112*, 3875.
43. For example of a structurally determined diolate complex see: Pilyugina, T. S.; Schrock, R. R.; Müller, P.; Hoveyda, A. H., *Organometallics* **2007**, *26*, 831.
44. Robbins, J.; Bazan, G. C.; Murdzek, J. S.; O'Regan, M. B.; Schrock, R. R., *Organometallics* **1991**, *10*, 2902.
45. Tsang, W. C. P.; Hultzsch, K. C.; Alexander, J. B.; Bonitatebus, P. J.; Schrock, R. R.; Hoveyda, A. H., *J. Am. Chem. Soc.* **2003**, *125*, 2652.
46. Tsang, W. C. P.; Jamieson, J. Y.; Aeilts, S. L.; Hultzsch, K. C.; Schrock, R. R.; Hoveyda, A. H., *Organometallics* **2004**, *23*, 1997.

47. Budzelaar, P. H. M.; Moonen, N. N. P.; De Gelder, R.; Smits, J. M. M.; Gal, A. W., *Eur. J. Inorg. Chem.* **2000**, 753.
48. Tonzetich, Z. J.; Jiang, A. J.; Schrock, R. R.; Müller, P., *Organometallics* **2007**, *submitted*.
49. Yokota, S.; Tachi, Y.; Itoh, S., *Inorg. Chem.* **2002**, *41*, 1342.
50. Basuli, F.; Huffman, J. C.; Mindiola, D. J., *Inorg. Chem.* **2003**, *42*, 8003.
51. Basuli, F.; Bailey, B. C.; Huffman, J. C.; Mindiola, D. J., *Organometallics* **2005**, *24*, 3321.
52. Basuli, F.; Huffman, J. C.; Mindiola, D. J., *Inorg. Chim. Acta* **2007**, *360*, 246.
53. Stephens, F. H.; Figueroa, J. S.; Cummins, C. C.; Kryatova, O. P.; Kryatov, S. V.; Rybak-Akimova, E. V.; McDonough, J. E.; Hoff, C. D., *Organometallics* **2004**, *23*, 3126.
54. Basuli, F.; Bailey, B. C.; Watson, L. A.; Tomaszewski, J.; Huffman, J. C.; Mindiola, D. J., *Organometallics* **2005**, *24*, 1886.
55. Li, X.; Cheng, X.; Song, H.; Cui, C., *Organometallics* **2007**, *26*, 1039.
56. Dai, X, *Ph.D. Thesis*, Georgetown University **2003**.
57. Laitar, D. S.; Mathison, C. J. N.; Davis, W. M.; Sadighi, J. P., *Inorg. Chem.* **2003**, *42*, 7354.
58. Tonzetich, Z. J.; Jiang, A. J.; Schrock, R. R.; Mueller, P., *Organometallics* **2006**, *25*, 4725.
59. Schrock, R. R., in *Reactions of Coordinated Ligands*, Braterman, P. R., Ed. Plenum: New York, 1986; Vol. 1, pp 221-283.
60. Rupprecht, G. A.; Messerle, L. W.; Fellmann, J. D.; Schrock, R. R. *J. Am. Chem. Soc.* **1980**, *102*, 6236.
61. Oskam, J. H.; Fox, H. H.; Yap, K. B.; McConville, D. H.; O'Dell, R.; Lichtenstein, B. J.; Schrock, R. R., *J. Organomet. Chem.* **1993**, *459*, 185.
62. Yakelis, N. A.; Bergman, R. G., *Organometallics* **2005**, *24*, 3579.
63. Sheldrick, G. M. Acta Cryst. 1990, A46, 467.
64. Sheldrick, G. M (1997). SHELXL 97, University of Göttingen, Germany.

CHAPTER 4

Organometallic Chemistry of Tungsten(VI) Alkyl Alkylidyne Complexes

A portion of this chapter has appeared in print:

Tonzetich, Z. J.; Lam, Y. C.; Schrock, R. R.; Müller, P. " Facile Synthesis of a Tungsten Alkylidyne Catalyst for Alkyne Metathesis" *Organometallics* **2007**, *26*, 475-477.

INTRODUCTION

The ability of high-oxidation state carbyne (alkylidyne) compounds to effect the catalytic redistribution of carbon-carbon triple bonds (alkyne metathesis) is a remarkable feat.[1,2,3] Unfortunately, alkylidyne complexes capable of catalyzing this reaction are typically difficult to prepare. The usual methods of synthesizing alkyne metathesis precatalysts involve several steps, some of which may be low yielding and/or highly sensitive to the reaction conditions.[4] Three common synthetic routes are outlined in Scheme 4.1. The standard tungsten alkylidyne trialkoxide alkyne metathesis catalysts were discovered in 1981 (part I, Scheme 4.1).[5] The first synthesis of these species consisted of the reaction of W(C-*t*-Bu)(CH_2-*t*-Bu)$_3$[6] with HCl to yield W(C-*t*-Bu)Cl_3(DME), followed by displacement of the chlorides with the desired alkoxide.[7] The key synthesis of volatile, yellow, crystalline W(C-*t*-Bu)(CH_2-*t*-Bu)$_3$ in 50-60% yield consists of a reaction between W(OMe)$_3Cl_3$ and six equivalents of *t*-BuCH_2MgCl, five of which ultimately are sacrificed.[8] Other routes have been developed that consist of cleavage of a tungsten-tungsten triple bond upon reaction with an alkyne or nitrile (part II, Scheme 4.1).[9,10,11,12] Recent advances in alkyne metathesis have included syntheses of Mo-based catalysts[13] as well as supported Mo-based catalysts.[14] Many of the recently employed molybdenum catalysts have taken advantage of Cummins' molybdenum anilide complexes (part III, Scheme 4.1), as a starting material.[15,16,17,18,19,20] Anilide ligands containing both *tert*-butyl (Scheme 4.1) and isopropyl substitution have been used in this role.

A more convenient preparation of catalytically active tungsten or molybdenum alkylidynes would be of great value. Although metathesis of internal alkynes catalyzed by high oxidation state alkylidyne species[1,21,22] has not received the exposure enjoyed by alkene metathesis in the last decade,[23,24] alkyne metathesis is becoming of greater use for synthesizing certain organic molecules. Of note is the work by Fürstner concerning compounds that contain a *cis* C=C bond in a large ring.[25] These macrocycles are formed through selective *cis* hydrogenation of the triple bond with a Lindlar catalyst.[26] This method circumvents the still

unsolved problem in alkene metathesis of selectively forming *cis* double bonds. Other uses of the alkyne metathesis reaction include cross metathesis and step growth polymerization of highly-functionalized monomers.[27,28]

Scheme 4.1. Common routes to alkyne metathesis precatalysts.

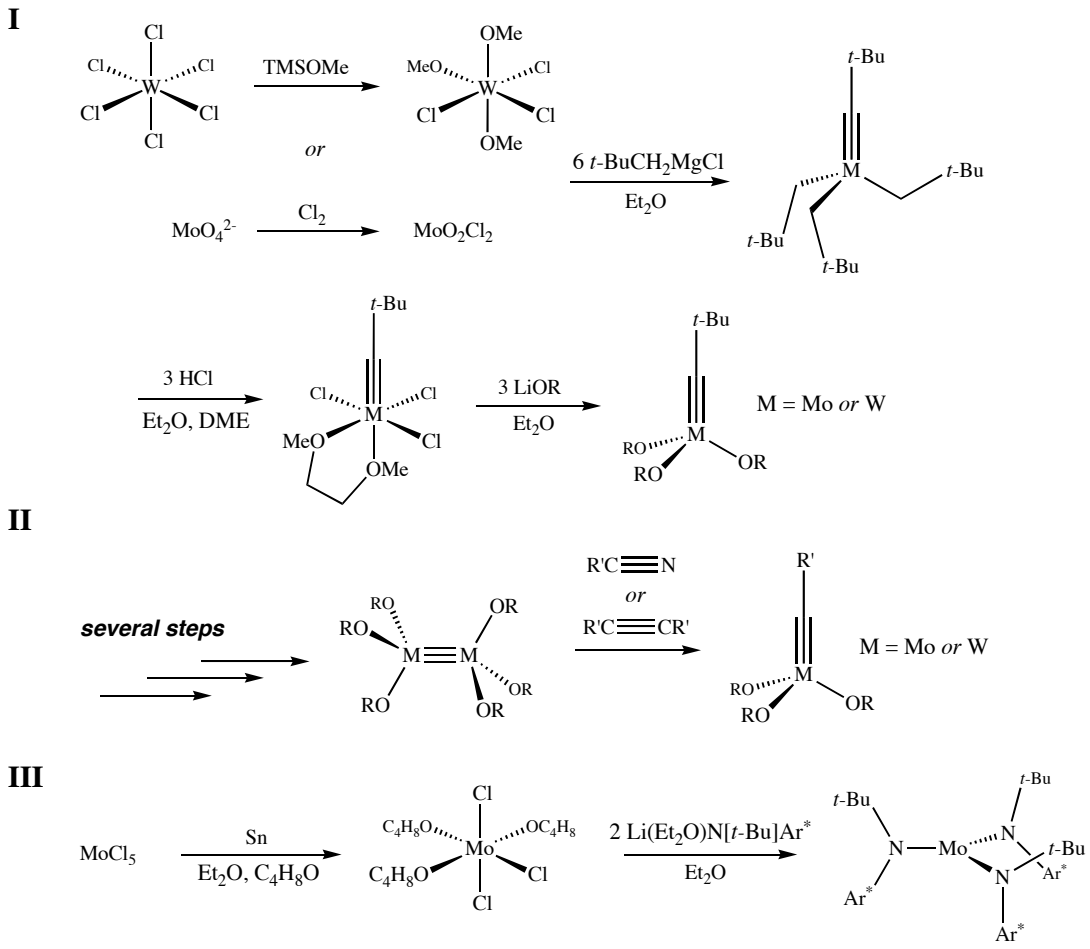

The mechanism of the alkyne metathesis reaction is similar to that of the olefin metathesis reaction.[29,30,31] The initial step is [2 + 2] cycloaddition of a carbon-carbon triple bond to the metal-carbon triple bond of an alkylidyne (Scheme 4.2).[32] The resultant metallacyclobutadiene may be viewed as a delocalized π-system with equivalent C−C bonds. Cycloreversion of the metallacyclobutadiene in a non-degenerate fashion yields a new alkyne,

and a new alkylidyne that serves as the propagating species in the catalytic cycle. Examples of high-oxidation state metallacyclobutadienes of tungsten and molybdenum have been isolated for various alkoxides.[33,34,35] Fast rearrangement of these intermediates is critical to catalyst efficiency, and prolonged lifetimes can lead to poor catalytic turnover or polymerization of the alkyne. Additionally, metallacyclobutadienes have been observed to add additional equivalents of alkyne to afford metallacycloheptatrienes and larger macrocycles.[34] Rapid formation of large macrocycles is one proposed mechanism by which alkynes are polymerized by high-oxidation state alkylidynes.[1] Formation of large metallacycles has also been implicated in formation of cyclopentadienyl species, a decomposition pathway that results in catalyst deactivation.[36]

Scheme 4.2. Mechanism of the alkyne metathesis reaction.

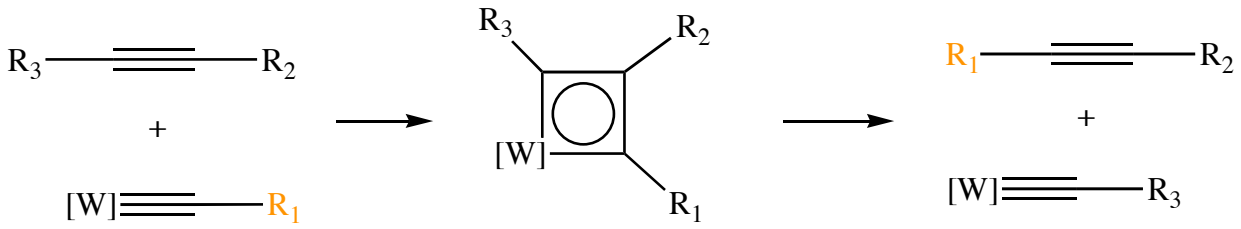

metallacyclobutadiene

This chapter details the synthesis and reactivity of the alkylidyne complex W(C-*t*-Bu)(CH_2-*t*-Bu)$(OAr)_2$ (Ar = 2,6-*i*-$Pr_2C_6H_3$). Most notably, the tungsten alkylidyne complex can be prepared in only two steps from commercially available reagents and displays metathetical reactivity toward alkynes. Reactions of W(C-*t*-Bu)(CH_2-*t*-Bu)$(OAr)_2$ with a variety of organic molecules are also presented, and compared with the organometallic chemistry of previously reported tungsten alkylidynes.

RESULTS

4.1 Preparation of W(C-*t*-Bu)(CH_2-*t*-Bu)($OAr)_2$

The tungsten alkylidyne complex, W(C-*t*-Bu)(CH_2-*t*-Bu)($OAr)_2$, was first identified in crude reaction mixtures during the attempted preparation of W(C-*t*-Bu)(CH_2-*t*-Bu)$_3$ from $WCl_3(OAr)_3$ and *t*-$BuCH_2MgCl$. Unlike alkylation of $WCl_3(OMe)_3$, addition of *t*-$BuCH_2MgCl$ to the bulkier $WCl_3(OAr)_3$ did not result in displacement of all three alkoxide ligands, and no amount of W(C-*t*-Bu)(CH_2-*t*-Bu)$_3$ was obtained after attempted distillation of the reaction mixture.[8] A rational synthesis of W(C-*t*-Bu)(CH_2-*t*-Bu)($OAr)_2$ consists of addition of four equivalents of *t*-$BuCH_2MgCl$ to $W(OAr)_3Cl_3$ in diethyl ether (equation 4.1).[37] The neopentylidyne complex can be isolated from the crude reaction mixture as a highly crystalline yellow complex in 40-50 % yield. The starting material, *mer*-$W(OAr)_3Cl_3$ is prepared from WCl_6 and three equivalents of ArOH (Ar = 2,6-diisopropylphenyl) in high yield and on a large scale.[38] Precipitation of *mer*-$W(OAr)_3Cl_3$ from pentane circumvents the need for chromatographic purification as reported previously.[39]

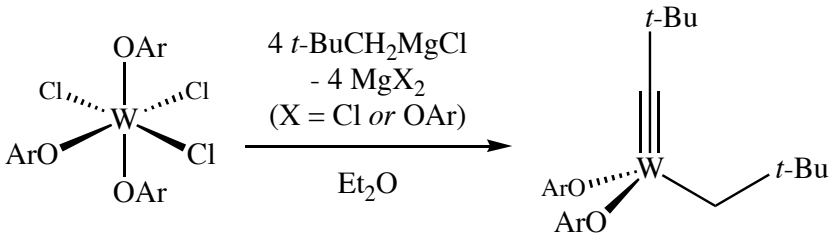

(4.1)

It seems likely that tungsten remains in its highest oxidation state and that at least two diisopropylphenoxide ligands are bound to the metal at all times. Formation of the alkylidyne ligand through sequential α-abstractions (alkyl to alkylidene followed by alkylidene to alkylidyne) is a logical proposal in light of similar reactions with tantalum.[40] Exactly when and how these abstractions take place is not known. Overall, the synthesis is analogous to that of

W(C-*t*-Bu)(CH_2-*t*-Bu)$_3$ from $WCl_3(OMe)_3$, but has the advantage of ready isolation of the product. The good yield of W(C-*t*-Bu)(CH_2-*t*-Bu)$(OAr)_2$ is probably a consequence of its relatively crowded nature, which slows further attack by *t*-BuCH_2MgCl on W(C-*t*-Bu)(CH_2-*t*-Bu)$(OAr)_2$. In support of this notion, addition of one to two equivalents of *t*-BuCH_2MgCl to isolated W(C-*t*-Bu)(CH_2-*t*-Bu)$(OAr)_2$ showed no signs of reaction over several hours at 23 ºC according to ^{1}H NMR spectroscopy. Not surprisingly, similar reactions involving W(O-2,6-$Me_2C_6H_3)_3Cl_3$ did not produce an analogous product in a relatively large and/or easily isolated amount. The attenuated steric bulk of the 2,6-dimethylphenoxide ligand is likely insufficient to prevent further attack by *t*-BuCH_2MgCl.

The NMR spectroscopic parameters of W(C-*t*-Bu)(CH_2-*t*-Bu)$(OAr)_2$ are typical for high oxidation state alkylidyne species of this general type[4] with C_α resonating at 303.0 ppm (J_{CW} = 271 Hz) in benzene-d_6. The methylene protons of the neopentyl ligand appear as a sharp singlet resonance in the ^{1}H NMR spectrum at 3.02 ppm and display a coupling to ^{183}W of 10.5 Hz. The solid state structure of W(C-*t*-Bu)(CH_2-*t*-Bu)$(OAr)_2$ was confirmed by an X-ray study and is shown in Figure 4.1 (see caption for bond metrics). The W(1)–C(1) bond length of 1.755(2) Å and W(1)–C(6) bond length of 2.119(2) Å are typical of W–C triple and single bonds, respectively. The W(1)–C(1)–C(2) bond angle of 175.62(17)° and W(1)–C(6)–C(7) bond angle of 114.70(13)° are also not unusual.[21] Both aryl groups of the phenoxide ligands reside above the $C_{alkyl}OO$ face, while the *tert*-butyl group of the neopentyl ligand resides below, presumably for steric reasons. It should be noted that Chisholm has prepared a related alkyl alkylidyne species, W(CCH_2CH_3)(CH_2-*t*-Bu)(O-*i*-Pr)$_2$, through a reaction between W_2(O-*i*-Pr)$_4$(CH_2-*t*-Bu)$_2$(*W≡W)* and 3-hexyne.[41] This compound was found to be dimeric in the solid state by virtue of bridging isopropoxide ligands. No reactivity (including metathesis) was reported for the propylidyne complex.

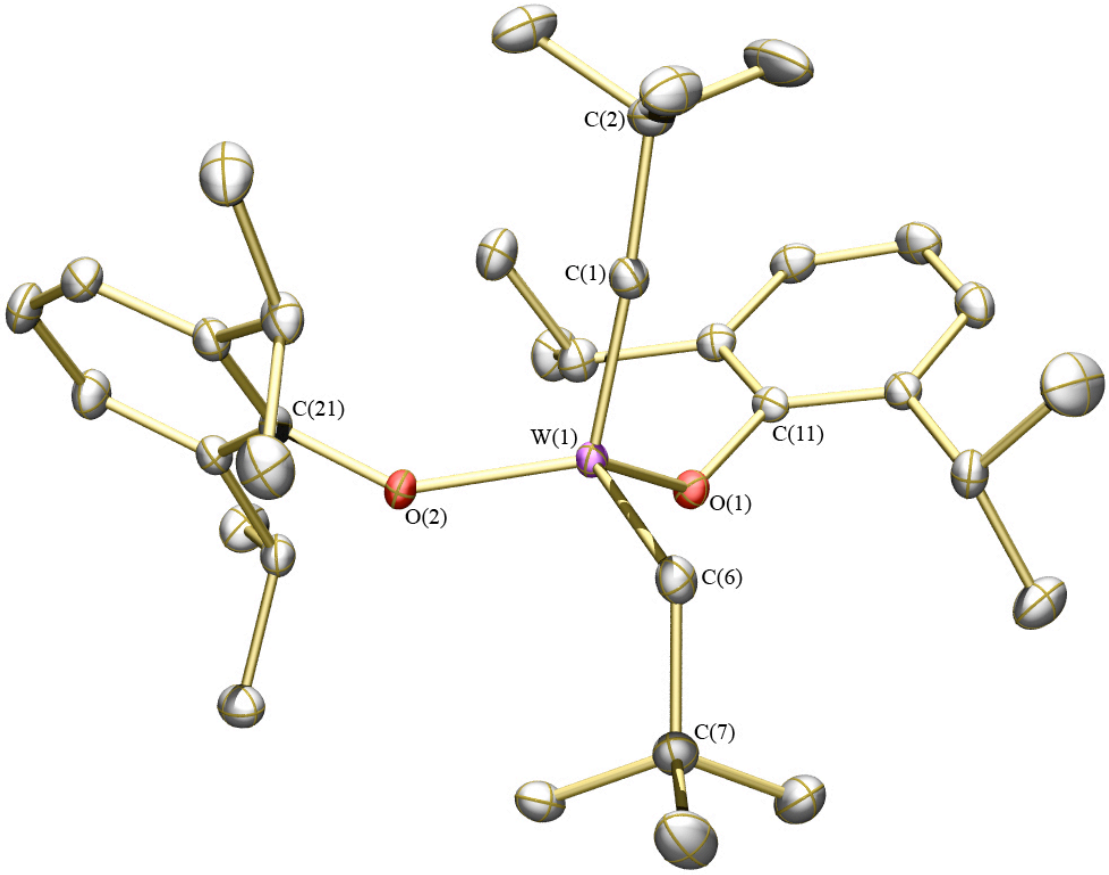

Figure 4.1. Thermal ellipsoid rendering (50%) of W(C-*t*-Bu)(CH_2-*t*-Bu)($OAr)_2$. Hydrogen atoms omitted for clarity. Selected bond distances (Å) and angles (°): W(1)–C(1) = 1.755(2); W(1)–C(6) = 2.119(2); W(1)–O(1) = 1.8982(14); W(1)–O(2) = 1.8920(14); W(1)–C(1)–C(2) = 175.62(17); W(1)–C(6)–C(7) = 114.70(13); W(1)–O(1)–C(11) = 132.76(12); W(1)–O(2)–C(21) = 145.95(13); C(1)–W(1)–C(6) = 100.04(9).

Attempted optimization of the synthesis of W(C-*t*-Bu)(CH_2-*t*-Bu)($OAr)_2$ through use of alkylating agents other than neopentyl Grignard was unsuccessful. For example, use of neopentyl lithium in toluene resulted in formation of significant quantities of W(C-*t*-Bu)(CH_2-*t*-Bu)$_3$, and none of the desired W(C-*t*-Bu)(CH_2-*t*-Bu)($OAr)_2$ could be isolated. Alkylation with (*t*-$BuCH_2)_2Mg$[42] in diethyl ether was found to give similar results as *t*-$BuCH_2MgCl$. In a non-ethereal solvent such as pentane, reaction of *mer*-$W(OAr)_3Cl_3$ with (*t*-$BuCH_2)_2Mg$ was found to give predominantly W(C-*t*-Bu)(CH_2-*t*-Bu)$_3$. Use of less aggressive alkylating agents such as

$Zn(CH_2\text{-}t\text{-}Bu)_2$ led to incomplete alkylation according to ^1H NMR experiments. Variations in temperature and the amount of $t\text{-}BuCH_2MgCl$ did not lead to better yields than those obtained with four equivalents of Grignard reagent at room temperature. ^1H NMR observation of crude reaction mixtures indicates that the desired alkylidyne complex is the main component (70%), with unidentifiable minor products comprising the remainder of the mixture. Thus, crystallization of the complex away from the minor reaction products appears to be the limiting factor in obtaining better yields. Such a finding is not surprising considering the problems in isolating both $W(C\text{-}t\text{-}Bu)(CH_2\text{-}t\text{-}Bu)_3$[5] and $W(C\text{-}t\text{-}Bu)(OAr)_3$[33]. Performing the reaction on scales greater than five grams of $WCl_3(OAr)_3$ also resulted in poorer yields.

4.2 Reaction of $W(C\text{-}t\text{-}Bu)(CH_2\text{-}t\text{-}Bu)(OAr)_2$ with alkynes

The alkyl alkylidyne complex reacts readily with alkynes to give metallacyclobutadiene complexes. At short reaction times, the metallacycle resulting from addition of one equivalent of alkyne can be observed (equation 4.2). Upon prolonged reaction with excess alkyne at room temperature, the symmetric metallacycles may be isolated cleanly. Preparative scale reactions with 3-hexyne and 2-butyne give rise to the metallacyclobutadienes depicted in equation 4.3.

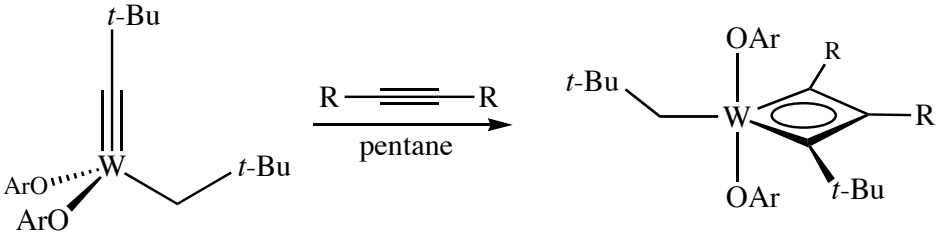

(4.2)

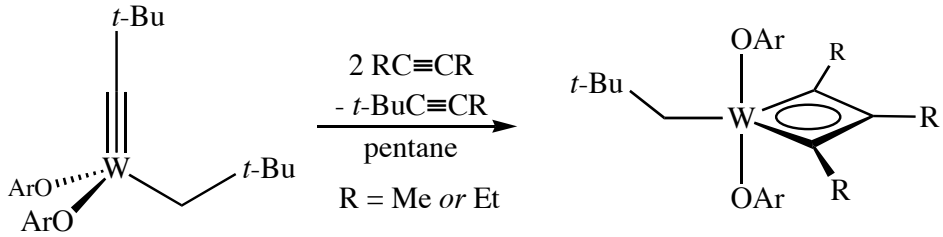

(4.3)

The symmetric metallacyclobutadiene species are red (R = Me) to orange (R = Et), pentane soluble fibrous needles. $W[C_3R_3](CH_2\text{-}t\text{-}Bu)(OAr)_2$ (R = Me and Et) are analogous to related trialkoxide species that contain OAr or $OCH(CF_3)_2$ groups.[33,34] NMR spectra at 20 ºC in benzene-d_6 are consistent with a species possessing time-averaged C_{2V} symmetry. The apparent symmetry may arise from a molecule with the structure depicted in equation 4.3 where both diisopropylphenyl and neopentyl groups are rotating rapidly on the NMR time scale. The carbon resonances are found at chemical shift values that are typical for high oxidation state metallacyclobutadiene species. For example, in $W[C_3Et_3](CH_2\text{-}t\text{-}Bu)(OAr)_2$, C_α and C_β resonate at 242.7 ppm (J_{CW} = 122 Hz) and 146.8 ppm (J_{CW} = 21 Hz), respectively in benzene-d_6. A substantial amount of polyalkyne is formed during the synthesis of each $W[C_3R_3](CH_2\text{-}t\text{-}Bu)(OAr)_2$ species, though the insoluble polymers are easily removed from the solution and $W[C_3R_3](CH_2\text{-}t\text{-}Bu)(OAr)_2$ thereby isolated cleanly.

The initial metallacycle formed with 3-hexyne, $W[C(t\text{-}Bu)CRCR](CH_2\text{-}t\text{-}Bu)(OAr)_2$ (equation 4.2, R = Et), can be observed by NMR, and even cocrystallizes with the $W[C_3Et_3](CH_2\text{-}t\text{-}Bu)(OAr)_2$ species when the reaction is run for less than one hour. The asymmetric metallacycle crystallizes as red urchins from pentane, and may be separated mechanically from $W[C_3Et_3](CH_2\text{-}t\text{-}Bu)(OAr)_2$. Spectroscopic features of $W[C(t\text{-}Bu)C(Et)C(Et)](CH_2\text{-}t\text{-}Bu)(OAr)_2$ are consistent with a species lacking any symmetry element. The ^{1}H NMR spectrum at 20 ºC displays broadened resonances for all protons of the aryloxide ligands suggesting hindered rotation about the C_{ipso}-O bonds. Resonances for the methylene protons of the neopentyl ligand appear at 0.78 ppm and 0.45 ppm as a pair of doublets (J_{HH} = 14.0 Hz) in benzene-d_6. Full characterization of $W[C(t\text{-}Bu)C(Et)C(Et)](CH_2\text{-}t\text{-}Bu)(OAr)_2$ was hampered by slow decomposition of the complex in solution. The asymmetric metallacycle was observed to transform to the symmetric metallacycle through loss of the *t*-Bu-substituted alkyne in solution. This process is presumably non-stoichiometric, as only $W[C_3Et_3](CH_2\text{-}t\text{-}Bu)(OAr)_2$ is detectable by ^{1}H NMR after prolonged time.

To test the catalytic efficacy of W(C-*t*-Bu)(CH_2-*t*-Bu)$(OAr)_2$ in alkyne metathesis reactions, experiments were conducted employing 3-heptyne as substrate. Exposure of a pentane *or* diethyl ether solution of W(C-*t*-Bu)(CH_2-*t*-Bu)$(OAr)_2$ to 50 equivalents of 3-heptyne led to formation of the expected 3-hexyne and 4-octyne metathesis products, but relatively slowly. The reaction required more than 24 hours to reach equilibrium at 23 ºC as determined by gas chromatography. Also, significant amounts of polyalkyne were formed during the reaction, hindering rigorous kinetic analyses. These results are consistent with sluggish break up of the metallacyclobutadiene intermediate (see Discussion section). Similar results have been observed with W(C-*t*-Bu)$(OAr)_3$.[33]

The reactivity of W(C-*t*-Bu)(CH_2-*t*-Bu)$(OAr)_2$ with terminal alkynes was also examined briefly. Addition of one to five equivalents of phenylacetylene to benzene-d_6 solutions of W(C-*t*-Bu)(CH_2-*t*-Bu)$(OAr)_2$ resulted in complex ^{1}H NMR spectra. Peaks displaying tungsten satellites downfield of 9 ppm were apparent, indicative of either a methylidyne species or metallacyclobutadiene species possessing hydrogen substituents. Also observable by ^{1}H NMR was 2,6-diisopropylphenol. The presence of the free phenol suggests that deprotonation of intermediate metallacycles may be occurring. Previous work with terminal alkynes has demonstrated the tendency for deprotonation of metallacyclobutadiene intermediates.[43,44,45,46] Due to the complicated results with phenylacetylene, no further reactivity with terminal alkynes was pursued.

4.3 Reaction of W(C-*t*-Bu)(CH_2-*t*-Bu)$(OAr)_2$ with carbonyl compounds

Alkylidyne complexes of tungsten have been demonstrated to react with carbonyl functionalities to give oxo complexes.[47] This reaction proceeds through a putative oxametallacyclobutene (Scheme 4.3) and may result in several different isomeric products depending on the nature of the carbonyl compound employed (aldehyde, ketone, ester, etc.). Grubbs has utilized this type of reactivity to prepare alkynes from acyl chlorides.[48]

Scheme 4.3. Mode of reactivity of tungsten alkylidynes with carbonyl species.

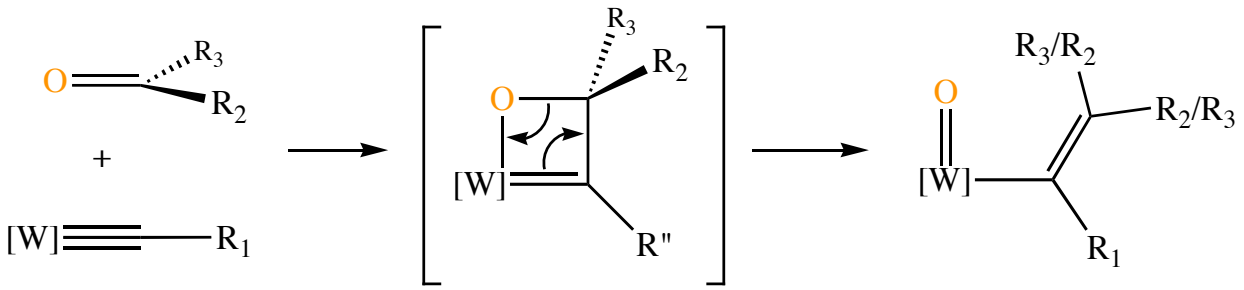

oxametallacyclobutene

Reactions of W(C-*t*-Bu)(CH_2-*t*-Bu)$(OAr)_2$ with selected carbonyl compounds were performed to determine the ability of the alkylidyne complex to effect the transformation shown in Scheme 4.3, and to examine the effect of the alkyl group on this type of reactivity. The various carbonyl compounds that were investigated are listed in Table 4.1 with comments concerning their observed reactivity. In all cases where the carbonyl was found to react, a color change to red was observed, consistent with the formation of a tungsten oxo species.[47] ^{1}H NMR spectra of the reaction mixtures indicated the formation of several isomeric products in each case. Many of these products displayed ^{1}H NMR resonances in the region of 2 – 3 ppm for the methylene protons of the neopentyl ligand.

As displayed in Scheme 4.2, several different isomers are possible in the resulting oxo-vinyl complexes. These may arise from both hindered rotation about the W-vinyl bond and *E*/*Z* disposition of R_1 and R_2 substituents on the alkene.[47] A notable trend observed from Table 4.1 is the diminished reactivity of the alkyl alkylidyne complex towards electron-deficient carbonyl compounds. No reaction was observed with benzoyl chloride after several days. Benzophenone and DMF were also found to react only sluggishly and gave unidentified products when heated.

Table 4.1. Results of reaction of selected carbonyl compounds with W(C-*t*-Bu)(CH_2-*t*-Bu)($OAr)_2$ in benzene-d_6 (mM concentration, 23 ºC).

Carbonyl compound	Number of isomers	Miscellaneous comments
Benzaldehyde	2	Instantaneous reaction
Acetone	3	Instantaneous reaction
Acetophenone	4	Requires several days to go to completion
Ethyl acetate	1	Very slow reaction
DMF	Unidentifiable	No reaction at room temperature; heating leads to decomposition
Benzophenone	Unidentifiable	No reaction at room temperature; heating leads to decomposition
Pivaldehyde	3	Reaction requires 2 days to go to completion
Benzoyl chloride	N/A	No reaction at room temperature
m-CF_3-Acetophenone	3	Requires several days to go to completion

Acetone and benzaldehyde reacted instantaneously, but the reaction with ethyl acetate required ~10 days to go to completion. Theses characteristics, while rendering the compound incapable of reactions similar to those reported by Grubbs, do suggest that as a metathesis catalyst, the tungsten complex may be functional group tolerant to some extent.

The tendency of W(C-*t*-Bu)(CH_2-*t*-Bu)($OAr)_2$ to form only one isomer in reactions with ethyl acetate prompted an attempt at isolating the tungsten oxo complex. Heating the reaction to encourage faster reactivity resulted in decomposition as judged by NMR spectroscopy.

However, when W(C-*t*-Bu)(CH_2-*t*-Bu)($OAr)_2$ was allowed to react at room temperature in neat ethyl acetate for 18 hours, the oxo complex shown in equation 4.4 could be isolated in very low yield (15%).

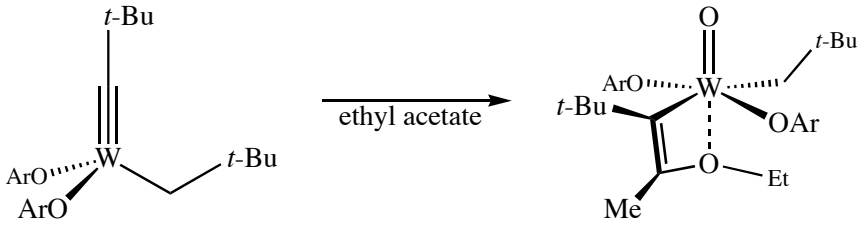

(4.4)

The oxo-vinyl species, W(O)[C(*t*-Bu)C(Me)(OEt)](CH_2-*t*-Bu)($OAr)_2$, crystallizes from concentrated pentane solutions as deep red cubes after several days at –25 ºC. The low yield is most likely due to decomposition of the oxo species during isolation, because reactions performed *in situ* demonstrate clean conversion by ^{1}H NMR. Prior to crystallization of the desired oxo-vinyl compound, colorless crystals are observed to precipitate from the mother liquor. The nature of this species is only speculative, but ^{1}H NMR spectra of the colorless crystals display resonances solely for the aryloxide ligand, suggesting a reduced tungsten-oxo complex. Such a species could arise from reductive elimination of the alkyl ligands, or through α-abstraction by the vinyl ligand and subsequent bimolecular coupling of alkylidenes.[49]

Despite the difficulties in preparing and handling W(O)[C(*t*-Bu)C(Me)(OEt)](CH_2-*t*-Bu)($OAr)_2$, small quantities can be obtained in pure form for spectroscopic analysis. The methylene protons appear as a singlet resonance at 2.42 ppm (J_{HW} = 8.4 Hz) in the benzene-d_6 ^{1}H NMR spectrum, indicating that the molecule contains a mirror plane of symmetry. The α and β carbon atoms of the vinyl ligand resonate at 184.4 (J_{CW} = 93 Hz) and 156.4 ppm, respectively. The regiochemistry of the double bond depicted in equation 4.4 is inferred from a strong cross peak between the *t*-Bu group and Me group of the vinyl ligand determined in a ^{1}H NOESY experiment (Figure 4.2). The geometry depicted in equation 4.4 is also favored because it would

allow possible coordination of the enol-ether oxygen atom. Such coordination may explain why only one isomer is observed in reactions with ethyl acetate.

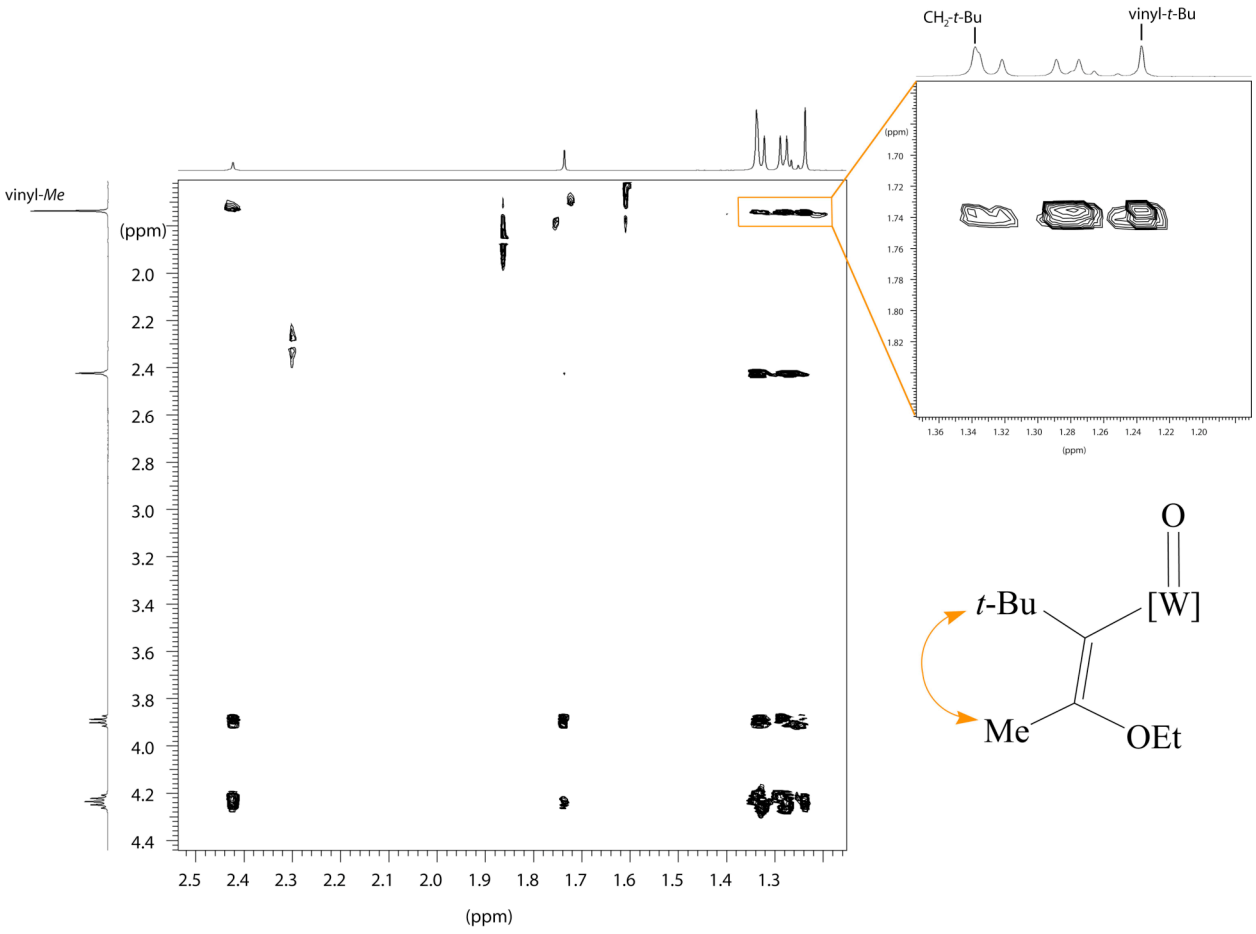

Figure 4.2. Selected region of the 500 MHz ^{1}H NOESY spectrum of W(O)[C(*t*-Bu)C(Me)(OEt)](CH$_2$-*t*-Bu)(OAr)$_2$ (mixing time = 200 ms).

An interesting secondary transformation appears to take place in reactions of W(C-*t*-Bu)(CH$_2$-*t*-Bu)(OAr)$_2$ with aldehydes. When the tungsten alkylidyne was exposed to one equivalent of benzaldehyde at room temperature, the color immediately changed to red. The ^{1}H NMR spectrum of the reaction mixture in benzene-d_6 indicated complete conversion of the alkylidyne complex to two new products in a 5:1 ratio. The minor product contains a peak at 8.20 ppm, which shows tungsten satellites (J_{HW} = 10.8 Hz). This species is consistent with the

expected oxo complex, possessing a *trans* arrangement about the vinyl ligand (equation 4.5). The methine groups of the aryloxide ligands appear as a septet, consistent with C_S symmetry

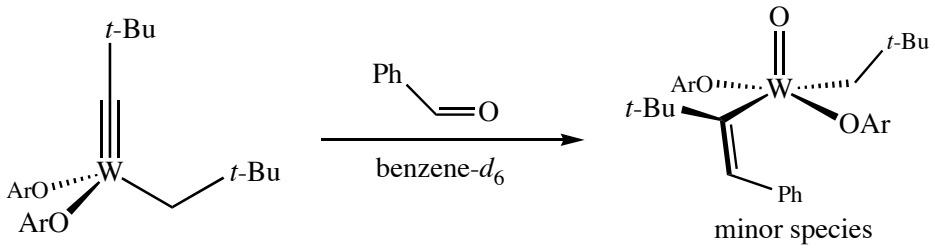

(4.5)

and a freely rotating aryl ring. The methylene protons of the alkyl ligand appear at 2.86 ppm and display similar coupling to ^{183}W as the compounds listed in Table 4.1.

Unlike the minor species discussed in the preceding paragraph, the major product of reaction with benzaldehyde does not display a resonance for the vinylic or methylene protons of the respective organic ligands. Neopentane is observable in the reaction mixture at 0.91 ppm, indicating loss of one neopentyl group. The ^{1}H NMR spectrum of the major species displays two sharp methine resonances consistent with the absence of mirror symmetry, but freely rotating aryl groups. A plausible proposal for the structure of the major species is the oxo-alkyne

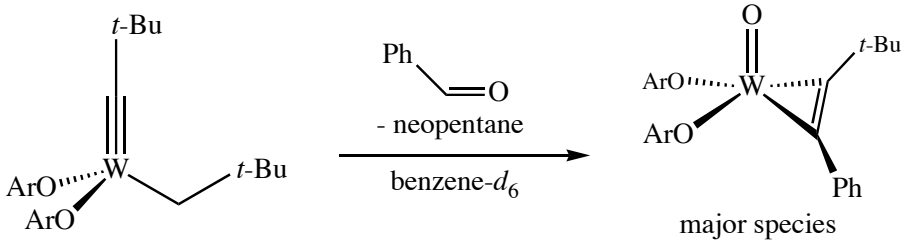

(4.6)

complex depicted in equation 4.6. A non-rotating alkyne ligand, disposed perpendicular to the oxo group is consistent with the observed spectroscopic features and simple molecular orbital arguments.[50] The oxo-alkyne complex may arise from formation of the *cis*-vinyl species analogous to the complex shown in equation 4.5. Proton transfer from the vinyl ligand to the neopentyl ligand generates neopentane and a reduced tungsten oxo species, which is immediately

trapped by the newly formed alkyne. The steric interactions in the *cis*-vinyl group may play a role in destabilizing the vinyl ligand, facilitating proton transfer. Reactions with pivaldehyde yielded similar results. The major species in this case possessed only one methine environment, consistent with a symmetrical di-*tert*-butylacetylene ligand (equation 4.7).

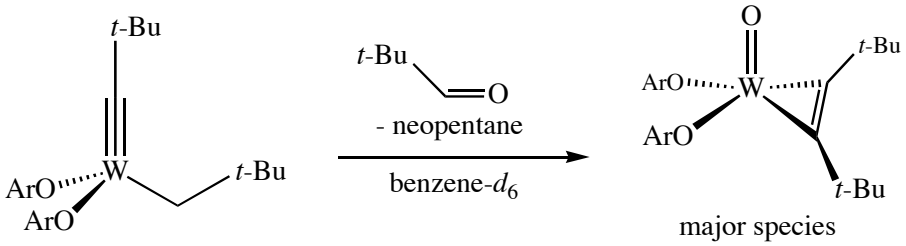

(4.7)

Attempts to isolate the oxo-alkyne species were unsuccessful. Preparative scale reactions resulted in colorless crystals with spectroscopic features akin to the reduced tungsten-oxo species described above. A small number of red crystals were isolated after prolonged cooling of a saturated pentane solution at –25 ºC, but spectroscopic analysis demonstrated the crystals to be predominantly the oxo-vinyl species shown in equation 4.5.

4.4 Alkylidyne complexes supported by amide ligands

Recent work in our laboratories concerning the preparation of *in situ* precursors to active olefin metathesis catalysts[51,52] led to us to examine the possibility of preparing an amide-based alkylidyne. Addition of two equivalents of $LiNPh_2 \cdot Et_2O$ to a diethyl ether solution of W(C-*t*-Bu)(CH_2-*t*-Bu)$(OAr)_2$ yielded W(C-*t*-Bu)(CH_2-*t*-Bu)$(NPh_2)_2$ as a pale yellow crystalline species in 70% isolated yield (equation 4.8). W(C-*t*-Bu)(CH_2-*t*-Bu)$(NPh_2)_2$ is related to recently

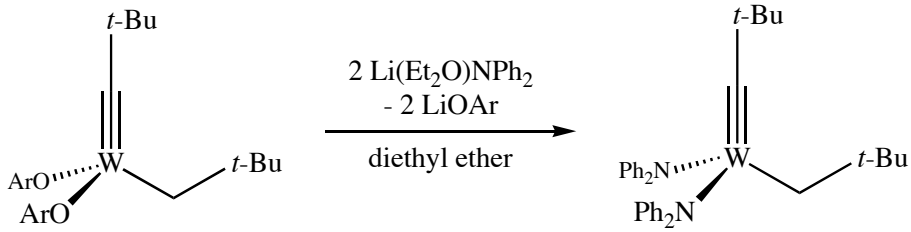

(4.8)

reported Mo(NAr)(CH-*t*-Bu)(NPh_2)$_2$,[51] which serves as a precursor to olefin metathesis catalysts of the type Mo(NAr)(CH-*t*-Bu)(OR)$_2$ upon addition of alcohols. The spectroscopic features of W(C-*t*-Bu)(CH_2-*t*-Bu)(NPh_2)$_2$ are very similar to those of the aryloxide species, with an upfield shift observed for the methylene protons of the neopentyl ligand (see Experimental section). Despite the reported lack of reactivity of amide based alkylidynes,[1] W(C-*t*-Bu)(CH_2-*t*-Bu)(NPh_2)$_2$ did react with 3-hexyne at high concentrations over prolonged time to afford the propylidyne species shown in equation 4.9. When the neopentylidyne was allowed to react in a 1:1 mixture of 3-hexyne to pentane over one week, the corresponding propylidyne could be isolated in low yield. Unfortunately, samples of the propylidyne contained ~10% of the neopentylidyne species as judged by ^{1}H NMR. The α carbon atom of the propylidyne resonates at 297.6 ppm in benzene-d_6 showing a coupling to ^{183}W of 273 Hz. The remainder of the spectroscopic features are consistent with the structure depicted in equation 4.9. Broadening of the aryl resonances of the diphenylamide ligands is apparent at 20 ºC and may be indicative of a monomer-dimer equilibrium. Broadened peaks were not observed with the bulkier neopentylidyne complex.

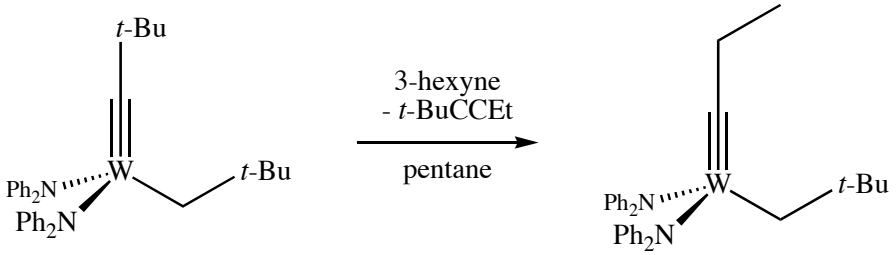

(4.9)

The protonolysis chemistry of W(C-*t*-Bu)(CH_2-*t*-Bu)(NPh_2)$_2$ was examined with several alcohols. Reaction of W(C-*t*-Bu)(CH_2-*t*-Bu)(NPh_2)$_2$ with two equivalents of 1-adamantanol

proceeded cleanly at room temperature to afford W(C-*t*-Bu)(CH_2-*t*-Bu)$(OAd)_2$ and two equivalents of diphenylamine as judged by ^{1}H NMR (equation 4.10). This transformation is not surprising in view of similar reactions involving molybdenum alkylidyne species that have been published in the last several years.[15,51,52]

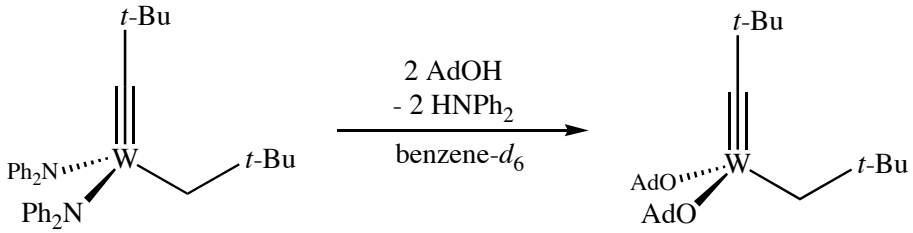

(4.10)

The metathetical reactivity of the adamantoxide species proved much more promising than that of the aryloxide compound. Addition of excess 3-hexyne to W(C-*t*-Bu)(CH_2-*t*-Bu)$(OAd)_2$, generated *in situ* from W(C-*t*-Bu)(CH_2-*t*-Bu)$(NPh_2)_2$, yielded only the propylidyne species, W(CEt)(CH_2-*t*-Bu)$(OAd)_2$, according to ^{1}H NMR after several minutes at 23 ºC. Additionally, there was no evidence for formation of tungstacyclobutadiene species, or poly-3-hexyne. W(C-*t*-Bu)(CH_2-*t*-Bu)$(OAd)_2$ was found to equilibrate 50 equivalents of 3-heptyne within 3 hours in pentane at 23 ºC with no evidence of polyalkyne formation. These results, along with the observation of the propylidyne species by NMR, are consistent with the resting state for alkyne metathesis in the adamantoxide derivative being an alkylidyne. Also significant is the observation that diphenylamine does not prevent metathesis by W(C-*t*-Bu)(CH_2-*t*-Bu)$(OAd)_2$. Such reactions bode well for the facile synthesis of a variety of mono or dialkoxide species in solution or on a silica surface.[53,54]

In contrast to protonolysis reactions with 1-adamantanol, reactions of W(C-*t*-Bu)(CH_2-*t*-Bu)$(NPh_2)_2$ with chelating phenols yielded alkylidene species as judged by NMR spectroscopy. For example, reaction of W(C-*t*-Bu)(CH_2-*t*-Bu)$(NPh_2)_2$ with one equivalent of binaphthol at 23 ºC in benzene-d_6 gave rise to a 1:1 to mixture of the starting material and an alkylidene species assigned as the tetraphenoxy neopentylidene shown in equation 4.11. Similar results were

observed for biphenol and the substituted bitetrol, 5,5′,6,6′,7,7′,8,8′-octahydro-1,1′-bi-2-naphthol (BenzBitet). Addition of *two* equivalents of chelating phenol resulted in complete conversion to

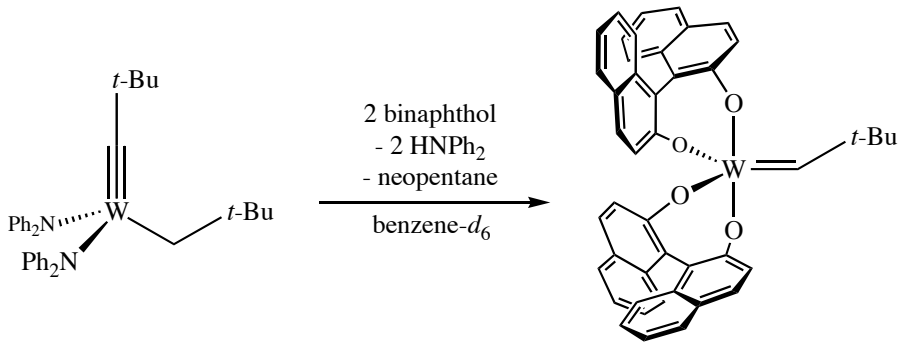

(4.11)

the alkylidene species. These observations suggest that subsequent protonation steps by chelating phenols in W(C-*t*-Bu)(CH_2-*t*-Bu)(NPh_2)$_2$ are more facile than initial protonation of the amide ligands. Whether the second equivalent of diol adds to the alkylidyne ligand or alkyl ligand could not be determined. Protonation experiments of W(C-*t*-Bu)(CH_2-*t*-Bu)(OAr)$_2$ with Brønsted acids led to species of the type W(CH-*t*-Bu)(X)$_2$(OAr)$_2$ (e.g. {$HNMe_2Ph$}{Cl}, X = Cl), similar to that shown in equation 4.11.

An alternative amide ligand examined in the course of reactions with W(C-*t*-Bu)(CH_2-*t*-Bu)(OAr)$_2$ was the lithium borylamide, {$Li(Et_2O)_2$}{$NHB(Mes)_2$}, reported by Power.[55] This ligand was targeted in hopes of preparing a borylimido alkylidene by tautomerization of a borylamido alkylidyne.[56] Reaction of one equivalent of the lithium amide with W(C-*t*-Bu)(CH_2-*t*-Bu)(OAr)$_2$ afforded W(C-*t*-Bu)(CH_2-*t*-Bu)(OAr)[$NHB(Mes)_2$] in 60% yield as a pale yellow crystalline solid after crystallization from pentane (equation 4.12).

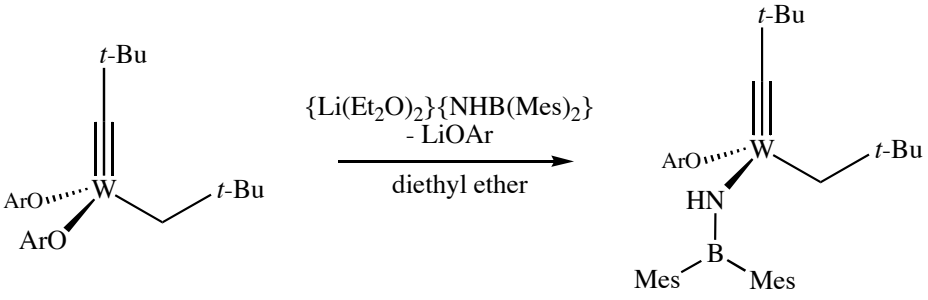

(4.12)

The borylamide species displays a broadened singlet resonance for the NH proton at 9.87 ppm in benzene-d_6. The alkylidyne carbon atom resonates at 299.6 ppm, and the diastereotopic methylene protons of the neopentyl ligand appear as a set of doublets at 1.20 and 0.79 ppm. One of the mesityl ligands displays hindered rotation at 20 ºC, while rotation about the N–B bond is locked as judged by the presence of distinct *para*-methyl group resonances for each of the mesityl rings. Variable temperature ^{1}H NMR spectra of the borylamide up to 70 ºC indicate a speeding up of rotational processes within the molecule (i.e. about N–B, and C–B bonds), but no major reactions appear to take place at elevated temperature. Thus far, all attempts to tautomerize the borylamide-alkylidyne to a borylimide-alkylidene have been unsuccessful. For example, reaction of the amido alkylidyne with bases such as $Ph_3P{=}CH_2$, and acid sources such as Et_3NHCl leads to unidentifiable decomposition products. These results are not surprising considering the observed stability of W(C-*t*-Bu)(NHAr)[OCMe$(CF_3)_2$]$_2$ towards tautomerization.[57]

4.5 Preparation and reactivity of W(N)(CH_2-*t*-Bu)(OAr)$_2$

As with alkynes, nitriles have previously been demonstrated to react with certain tungsten alkylidynes in a metathetical fashion.[58] The intermediate in this case is an α-azametallacyclobutadiene, and the metal containing product is a metal nitride (Scheme 4.4).

Scheme 4.4. Reaction of tungsten alkylidynes with nitriles.

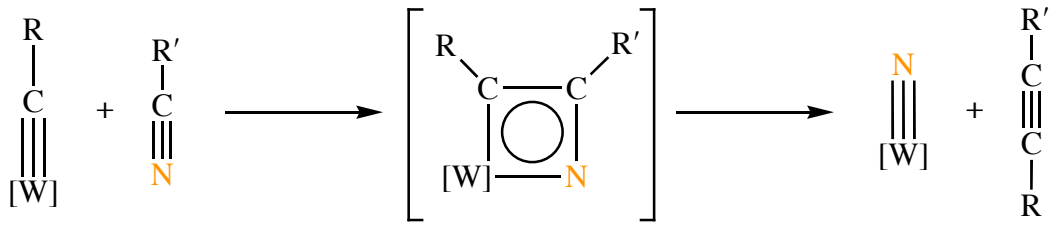

Although the azametallacycle intermediate has never been isolated or observed for a Group VI metal, recent work by Mindiola with a titanium nitride has produced a crystallographically characterized example.[59] Moreover, Johnson has recently reported the reverse of the reaction in Scheme 4.5 for selected molybdenum and tungsten nitrides.[60] As such, his work represents yet another facile route to alkyne metathesis catalysts, as molybdenum(VI) and tungsten(VI) nitrides may easily prepared from $TMSN_3$ and $MCl_4(solvent)_2$ (solvent = THF or 0.5 DME).[61] It should also be noted that degenerate exchange between nitriles and $W(N)(O\text{-}t\text{-}Bu)_3$ has also been studied by Chisholm using $CH_3C^{15}N$.[62,63] This reaction requires the intermediacy of an α,α-diazametallacyclobutadiene intermediate.

In order to expand the chemistry of $W(C\text{-}t\text{-}Bu)(CH_2\text{-}t\text{-}Bu)(OAr)_2$, the reaction with benzonitrile was examined. The alkylidyne complex reacts cleanly with benzonitrile in pentane to yield the nitride species in 80% isolated yield (equation 4.13). The reaction in equation 4.13 may also be performed with acetonitrile with similar results. The spectroscopic

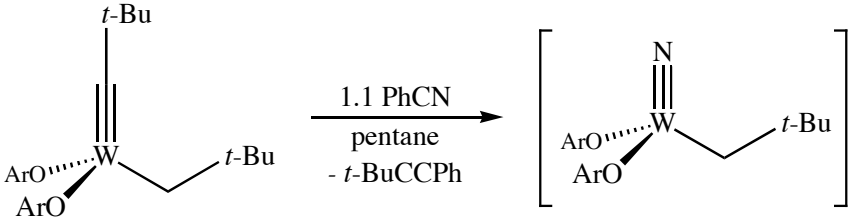

(4.13)

features of $W(N)(CH_2\text{-}t\text{-}Bu)(OAr)_2$ are consistent with the structure depicted in equation 4.13. The methylene protons resonate at 2.86 ppm (J_{HW} = 10.5 Hz) and the methylene carbon at 77.10 ppm (J_{CW} = 104 Hz) in benzene-d_6. Solid $W(N)(CH_2\text{-}t\text{-}Bu)(OAr)_2$ exists as dark red/black iridescent crystals. Upon dissolution, the compound gives rise to intensely dark red solutions. The color stems from a broad absorption centered at 468 nm in the visible spectrum (Figure 4.3, ε = 8070 $cm^{-1}\cdot M^{-1}$). Kinetics of formation of the nitride species from benzonitrile were examined by ^1H NMR in benzene-d_6. The reaction displayed a pseudo-first order rate constant (k_1) of 9.5 × 10^{-4} $M^{-1}s^{-1}$ at 18 ºC, consistent with rate limiting formation of the azametallacyclobutadiene.

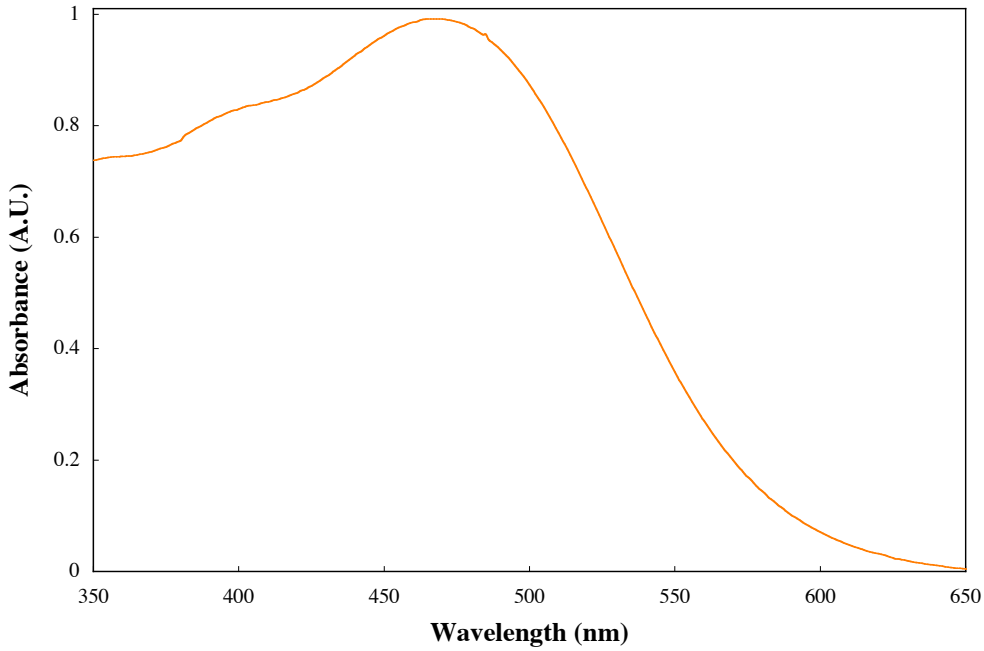

Figure 4.3. Electronic absorption spectrum of $[W(N)(CH_2\text{-}t\text{-}Bu)(OAr)_2]_2$ in pentane (1.22×10^{-4} M).

The nitride species was subjected to an X-ray diffraction study. Crystals suitable for diffraction were grown by cooling of a saturated pentane solution to –25 ºC. The solid state structure is shown in Figure 4.4. As evident from the figure, the nitride exists a dimer in the solid state with bridging W-N bonds. The W_2N_2 core is planar, with the bond to the bridging nitride and one aryloxide occupying the axial positions of a trigonal bipyramid. The core of the dimer is not rigorously symmetric, and displays alternating short and long bond lengths between tungsten and nitrogen (see caption to Figure 4.3). The shorter of the two W-N bond types occupies the equatorial position of the trigonal bipyramid. The structure of $[W(N)(CH_2\text{-}t\text{-}Bu)(OAr)_2]_2$ is similar to that reported for $[W(N)(OAr)_3]_2$, which was also found to be dimeric in the solid state.[64] The insolubility of $[W(N)(OAr)_3]_x$[58] in common organic solvents hampered full characterization, and no corroborating information of the structure of the nitride could be gathered in solution.

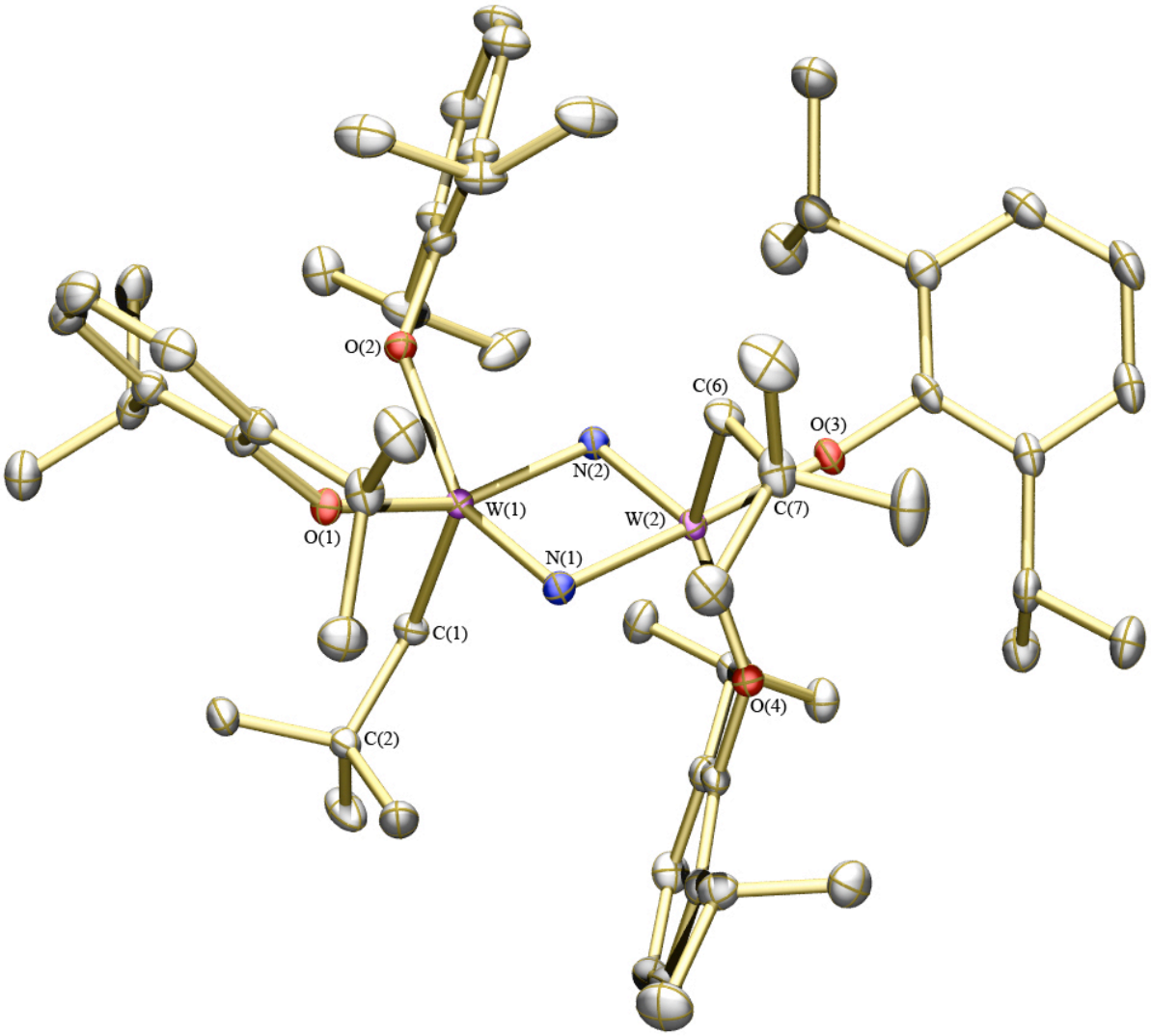

Figure 4.4. Thermal ellipsoid rendering (50%) of W(N)(CH_2-*t*-Bu)($OAr)_2$. Hydrogen atoms omitted for clarity. Selected bond distances (Å) and angles (º): W(1)–N(1) = 1.8185(17); W(1)–N(2) = 1.9606(18); W(2)–N(2) = 1.8054(18); W(2)–N(1) = 1.9454(18); W(1)–C(1) = 2.111(2); W(2)–C(6) = 2.180(2); W(1)–N(1)–W(2) = 95.20(8); W(1)–N(2)–W(2) = 95.10(8); N(1)–W(1)–N(2) = 84.46(8); N(1)–W(2)–N(2) = 85.25(8); W(1)–C(1)–C(2) = 123.58(15); W(2)–C(6)–C(7) = 123.93(16).

The structure of [W(N)(CH_2-*t*-Bu)($OAr)_2$]$_2$ in the solid state is not consistent with the spectroscopic features observed at 20 ºC in solution. Namely, the structure depicted in Figure 4.3 would be expected to show diastereotopic methylene resonances in the ^{1}H NMR spectrum

due to the absence of mirror symmetry. ^{1}H NMR spectra of the nitride down to –70 ºC are consistent with slowing down of fluxional/rotational processes on the NMR timescale as evidenced by broadening and decoalescence of several of the resonances in toluene-d_8. However, this observation does not offer any insight into the nature of the nitride species in solution (monomer vs. dimer), as fluxional processes within a dimeric species could account for the observed spectra at 20 ºC.

^{15}N NMR spectroscopy was employed in order to elucidate the multiplicity of W(N)(CH$_2$-*t*-Bu)(OAr)$_2$ in solution. The ^{15}N isotopomer was prepared by reaction of the alkylidyne with CH$_3$C^{15}N in toluene. The ^{1}H/^{13}C NMR features of W(^{15}N)(CH$_2$-*t*-Bu)(OAr)$_2$ in benzene-d_6 are essentially identical to that of the ^{14}N isotopomer (i.e. no ^{15}N-^{1}H or ^{15}N-^{13}C coupling could be observed). The ^{15}N{^{1}H} NMR spectrum of W(^{15}N)(CH$_2$-*t*-Bu)(OAr)$_2$ is shown in Figure 4.5.

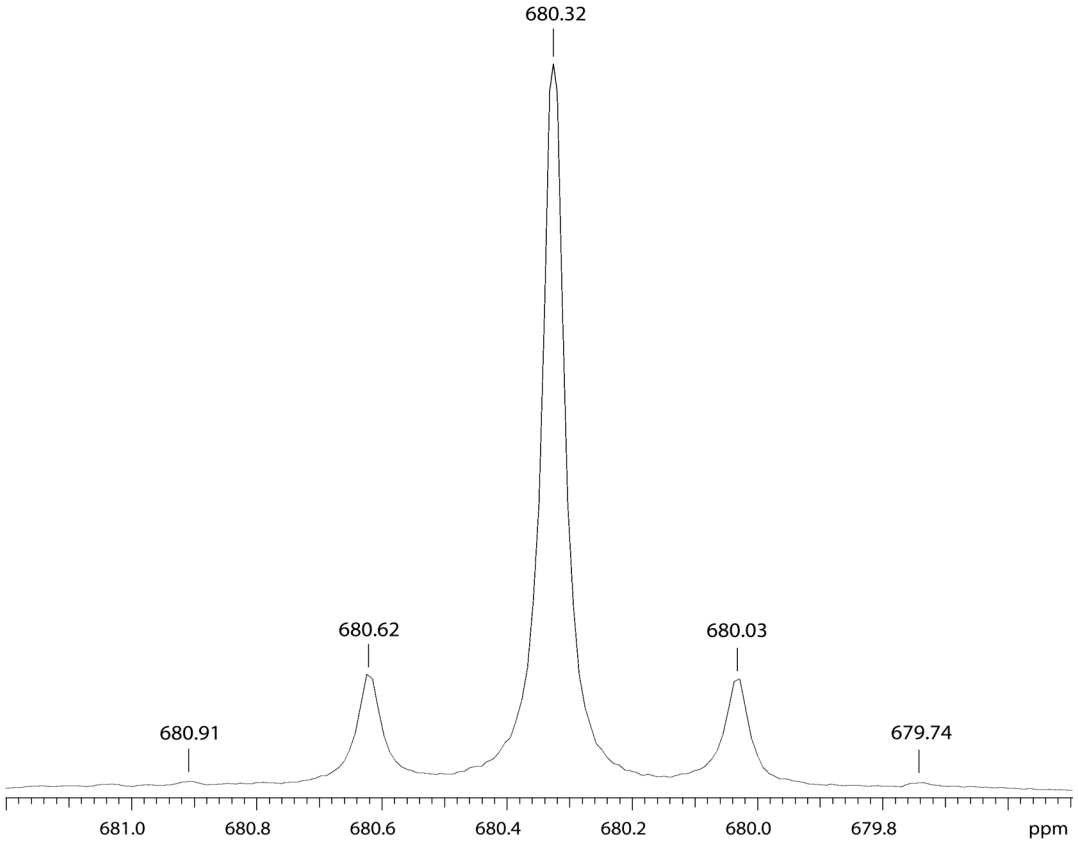

Figure 4.5. 50.7 MHz ^{15}N NMR spectrum of [W(^{15}N)(CH$_2$-*t*-Bu)(OAr)$_2$]$_2$.

A monomeric structure would be expected to show one set of ^{183}W satellites with an area of ~0.15 (~0.075 per satellite) with respect to the total peak areas. As evident from Figure 4.4, the nitride displays two sets of ^{183}W satellites with approximate areas of 0.26 and 0.02, a pattern that can only arise from ^{15}N coupling to two *equivalent* ^{183}W nuclei on the NMR timescale. This situation is depicted in Scheme 4.5. The observed J_{WN} value of 30.2 Hz is also consistent with a W−N bond order of less than three.[62] Therefore, the fact that the methylene protons of the alkyl ligand appear equivalent in solution must arise from a fluxional process at tungsten, such as pseudo-rotation.

Scheme 4.5. Schematic representation of the ^{183}W–^{15}N coupling in $[W(^{15}N)(CH_2\text{-}t\text{-}Bu)(OAr)_2]_2$.

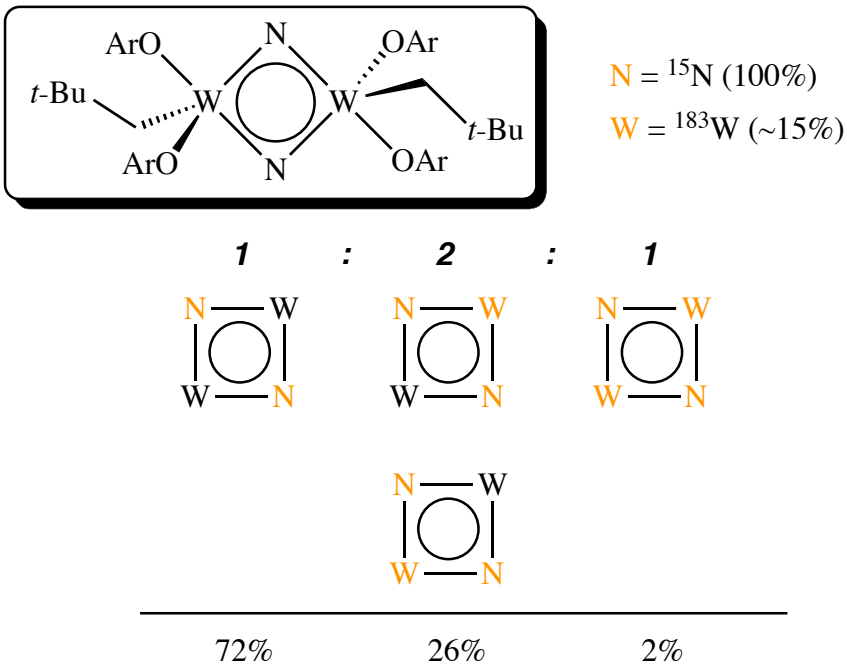

A region of the infrared spectrum of $W(N)(CH_2\text{-}t\text{-}Bu)(OAr)_2$ in pentane is shown in Figure 4.6. A dimeric structure possessing an inversion center such as that depicted in Scheme 4.5 is expected to show three IR active normal modes of the W_2N_2 core (A_u symmetry in C_i).

Two isotopically shifted peaks are observable, with the third (out of plane mode) likely being of too low energy to be observed in the range examined.

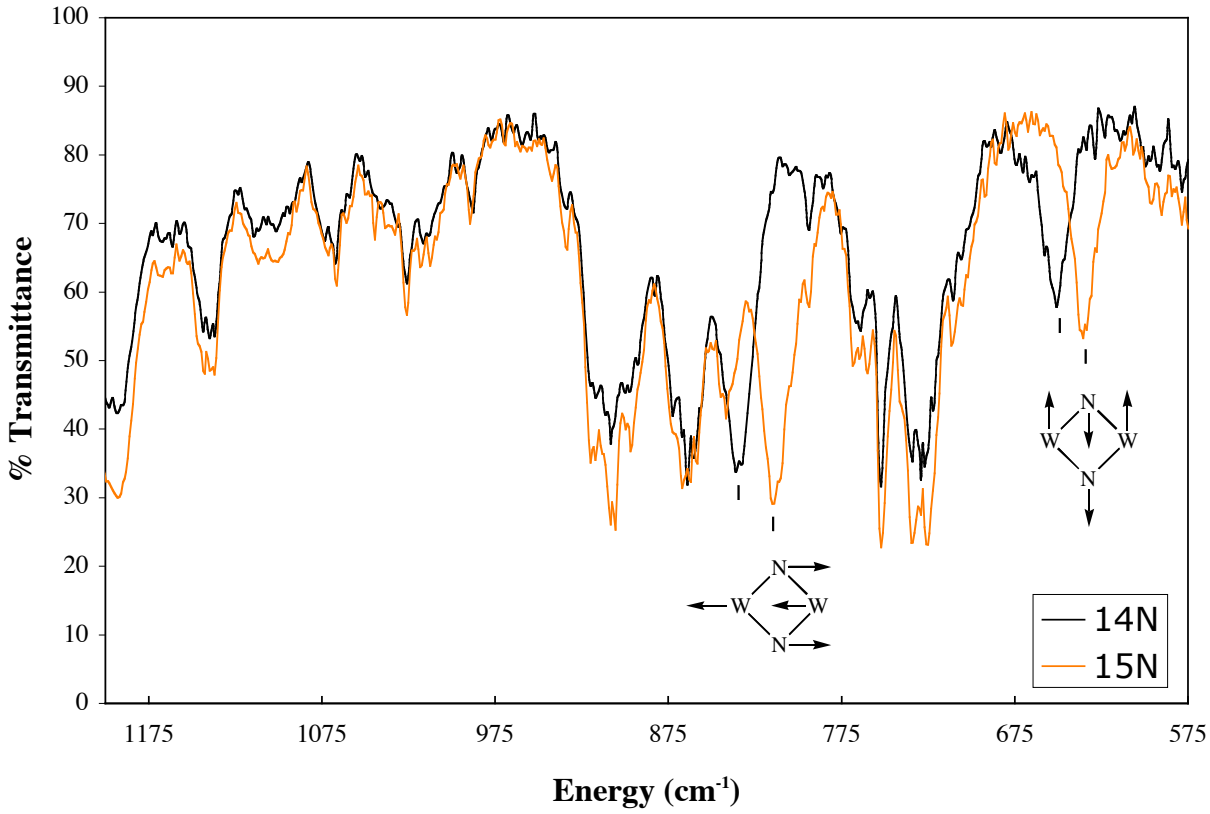

Figure 4.6. Region of the IR spectrum (KBr, pentane) of W(N)(CH_2-*t*-Bu)(OAr)$_2$ between 575 and 1200 cm^{-1}.

W(N)(CH_2-*t*-Bu)(OAr)$_2$ does not react with benzoyl chloride to form an oxo-chloride complex and regenerate benzonitrile in analogy to the reaction reported by Cummins with W(N)[N(*i*-Pr)(Ar^*)]$_3$ (Ar^* = 3,5-$Me_2C_6H_3$).[65] Nor does the nitride appear to react cleanly with one equivalent of acetone at room temperature. A color change is apparent, but no products could be identified by NMR. The nitride does react with trimethylsilyltriflate to afford the trimethylsilylimide complex shown in equation 4.14. W(NTMS)(CH_2-*t*-Bu)(OAr)$_2$(OTf) is a brilliant red crystalline solid that dissolves readily in pentane. Spectroscopic features of the complex are consistent with the structure depicted in equation 4.14. The methylene protons of

the alkyl ligand appear as a singlet resonance at 2.58 ppm (J_{HW} = 10.5 Hz) in benzene-d_6. The ^{15}N isotopomer was prepared in like fashion from W(^{15}N)(CH_2-*t*-Bu)$(OAr)_2$, and displayed a single resonance by ^{15}N NMR at 453.6 ppm, showing a 103 Hz coupling to one ^{183}W nucleus.

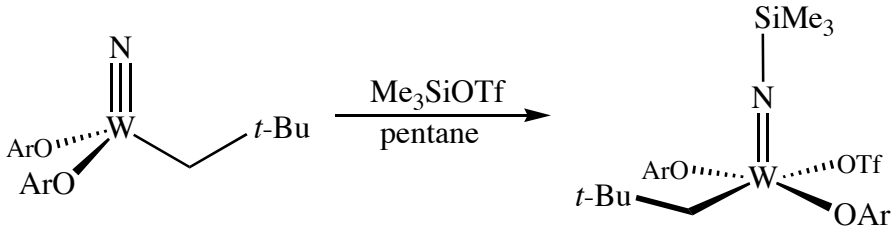

(4.14)

This larger coupling constant is consistent with a terminal imide structure in solution (compare 30.2 Hz for the bridging nitride). IR spectra of W($NSiMe_3$)(CH_2-*t*-Bu)$(OAr)_2$(OTf) in pentane show an isotopically shifted peak at 1146 cm^{-1} (^{14}N isotopomer). Assignment of this peak is not straightforward, as it may correspond to the ν_{WN} or ν_{NSi}, or a combination of the two. Previous work with transition metal imido complexes has highlighted the difficulty in assigning metal–nitrogen stretching modes.[66]

Confirmation of the structure of the trimethylsilylimide complex was afforded by an X-ray diffraction study of W($^{15}NSiMe_3$)(CH_2-*t*-Bu)$(OAr)_2$(OTf) (Figure 4.6). Due to a destructive phase change of the crystal near –60 ºC, diffraction data had to be collected at –55 ºC. As a result the triflate ligand was disordered, and the thermal motion of the atoms was greater than normal (thermal ellipsoids shown in Figure 4.6 at 30%). Metric data for the complex are listed in the caption. The structure clearly depicts square pyramidal geometry, with nearly identical bond angles about the equatorial plane. The W(1)–N(1) distance of 1.718(2) Å is significantly shorter than the corresponding W–N contacts in the nitride species. The W-O-C_{ipso} bonds of the diisopropylphenoxide ligands are quite obtuse (average = 166.9º) demonstrating the sterically congested nature of this five-coordinate compound.

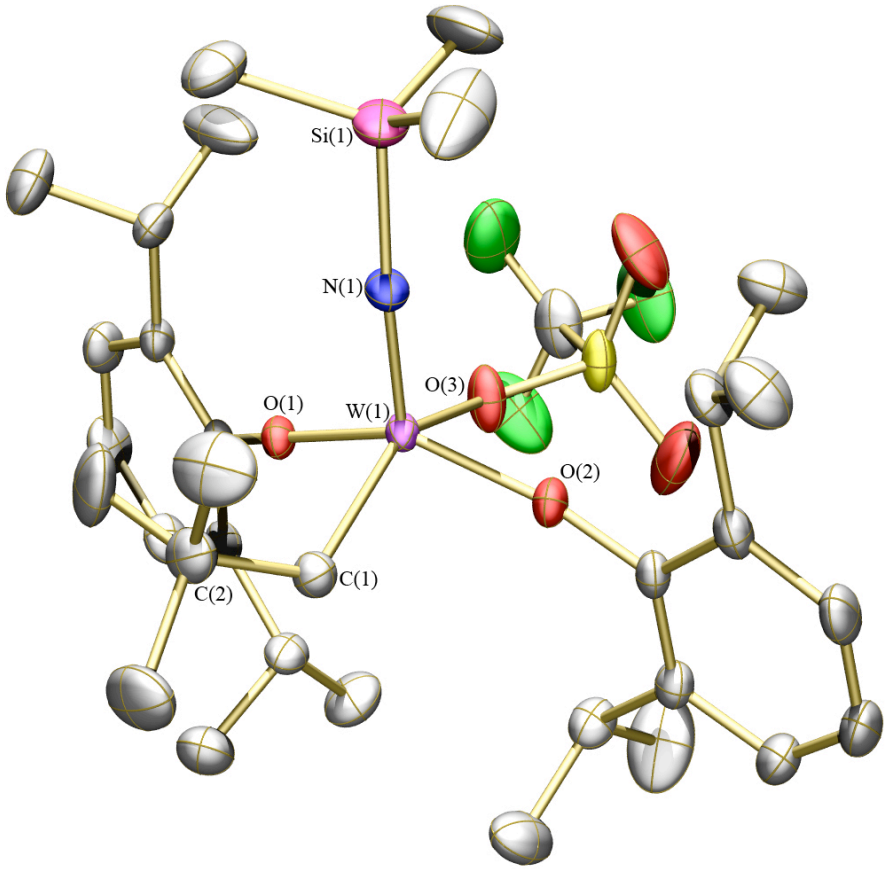

Figure 4.6. Thermal ellipsoid rendering (30%) of W(^{15}NSiMe$_3$)(CH$_2$-*t*-Bu)(OAr)$_2$(OTf). Hydrogen atoms and minor components of the disordered triflate ligand omitted for clarity. Selected bond distances (Å) and angles (°): W(1)–C(1) = 2.146(3); W(1)–N(1) = 1.718(2); W(1)–O(1,2) = 1.8427(17); W(1)–O(3) = 2.147(2); N(1)–Si(1) = 1.774(2); W(1)–N(1)–Si(1) = 170.25(16); W(1)–C(1)–C(2) = 126.1(2).

Substituting the triflate ligand with various groups such as neopentyl or 2,5-dimethylpyrrolide (N-2,5-Me$_2$C$_4$H$_2$) was attempted with the goal of preparing a species that would undergo α-abstraction to afford a trimethylsilylimido alkylidene. Reaction of W(NSiMe$_3$)(CH$_2$-*t*-Bu)(OAr)$_2$(OTf) with LiCH$_2$-*t*-Bu in toluene-d_8 afforded a brilliant purple solution. The ^{1}H NMR spectrum of the solution was consistent with formation of a species

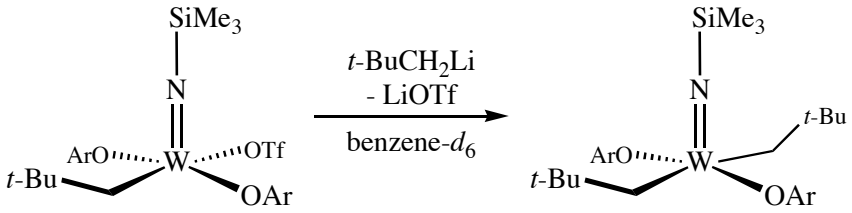

(4.15)

such as that shown in equation 4.15. The spectrum displays a lone resonance for the methylene protons, indicative of *trans* disposed neopentyl ligands. Similar results were obtained in reactions of $W(NSiMe_3)(CH_2\text{-}t\text{-}Bu)(OAr)_2(OTf)$ with LiN-2,5-$Me_2C_4H_2$ in diethyl ether. In neither case could solid material be isolated from any of these reactions. Both species were observed to form oils upon standing in pentane at -25 ºC for weeks. Furthermore, heating of the dialkyl species depicted in equation 4.15 in toluene-d_8 at 60 ºC for several days did not lead to clean α-abstraction and formation of a trimethylsilylimido alkylidene species as judged by ^{1}H NMR. The bulky nature of these species may slow fluxional processes, preventing the molecule from adopting the necessary conformation (i.e. *cis* neopentyl ligands) for α-abstraction to take place.

DISCUSSION

Alkylation of $W(OR)_3Cl_3$ complexes has been known for several decades to give W-C multiply bonded species.[67,68,] In some cases (e.g. R = Me), the products of alkylation can be isolated and characterized definitively.[8] Basset has reported that combinations of alkylating agents and $W(OAr)_3Cl_3$ afford mixtures capable of metathesizing olefins.[69] The nature of these catalytic mixtures was not determined conclusively, but their catalytic activity suggests that an alkylidene must be present. In light of this previous work, it is fortuitous that $W(C\text{-}t\text{-}Bu)(CH_2\text{-}t\text{-}Bu)(OAr)_2$ can be isolated in moderate yield given the number of different species that must be formed during the course of alkylation (alkyl, alkylidene, and alkylidyne). As mentioned

previously, the steric bulk of the 2,6-diisopropylphenoxide ligand is believed to be critical in allowing for isolation of the alkyl-alkylidyne species.

The presence of the alkyl ligand does not appear to affect the reactivity of W(C-*t*-Bu)(CH_2-*t*-Bu)($OAr)_2$ with alkynes. Previous work from several laboratories has demonstrated the ability of alkyl-alkylidyne species to participate in reversible proton transfer reactions giving *bis*-alkylidene species.[70,71,72] In no instance was evidence of an alkylidene species apparent in reactions of W(C-*t*-Bu)(CH_2-*t*-Bu)($OAr)_2$ with alkynes. Furthermore, W(C-*t*-Bu)(CH_2-*t*-Bu)($OAr)_2$ showed no reactivity with 1-hexene, which might be expected if a transient alkylidene was present.

The ability of W(C-*t*-Bu)(CH_2-*t*-Bu)($OAr)_2$ to metathesize alkynes complements recent work form this laboratory demonstrating the olefin metathesis activity of monoalkyl-monoalkoxide imido alkylidene species.[73] With several of these species, metathesis activity is comparable to that of traditional dialkoxide imido alkylidene compounds.[74] The role of the alkyl ligand in creating an asymmetric environment at the metal is still not understood completely, and continued work from this laboratory seeks to understand the catalytic potential of such mixed ligand species. In the present case however, the alkyl ligand does not appear to play a large role in directing the metathesis reactivity of W(C-*t*-Bu)(CH_2-*t*-Bu)($OAr)_2$. In contrast, the reactivity of the alkylidyne toward alkynes appears to be determined by the nature of the alkoxide ligand. With electron withdrawing ligands such as diisopropylphenoxide, intermediate metallacyclobutadienes are stabilized to a significant degree. Persistence of these intermediates leads to alkyne polymerization and poor catalytic turnover. When the aryloxides are replaced by adamantoxide, the catalytic performance of the alkyl alkylidyne improves markedly. These results are consistent with the higher reactivity of W(CR)(O-*t*-$Bu)_3$ versus W(CR)$(OAr)_3$.[1] As with many catalysts, the electronic balance of the ligands is finely balanced, as demonstrated by the very low reactivity of the more electron rich W(C-*t*-Bu)(CH_2-*t*-Bu)($NPh_2)_2$ species.

The reactivity of W(C-*t*-Bu)(CH_2-*t*-Bu)($OAr)_2$ toward carbonyl and nitrile species further demonstrates its similarity to W(C-*t*-Bu)$(OAr)_3$. Isolation and characterization of [W(N)(CH_2-*t*-

Bu)$(OAr)_2]_2$ demonstrated the dimeric nature of the complex in both solution and the solid state. The dimeric structure is analogous to that of $[W(N)(OAr)_3]_2$, though the poor solubility of [W(C-*t*-Bu)$(OAr)_3]_x$ prevented definitive characterization of this species in solution. Addition of the neopentyl ligand in the present case appears to render the nitride more soluble and perhaps hinders formation of larger oligomeric products. The dark color of the nitride is also interesting as several previously reported nitride species have been white or pale in color. The nature of the dark red color of $[W(N)(CH_2\text{-}t\text{-Bu})(OAr)_2]_2$ is only speculative, but $\pi \rightarrow \pi^*$ or $n \rightarrow \pi^*$ transitions within the W_2N_2 core are possibilities.

CONCLUSIONS

This chapter has demonstrated a facile synthesis of a metathetically active tungsten alkylidyne species. The alkylidyne serves as a precursor to several interesting organometallic species possessing the neopentyl ligand including other oxos, nitrides, and imides. The presence of the neopentyl ligand imparts crystallinity to several of the complexes described here, many of which could not be isolated in the related *tris*-diisopropylphenoxide system. It is concluded that the alkyl ligand does not deter catalytic alkyne metathesis activity, and that the reactivity of $W(C\text{-}t\text{-Bu})(CH_2\text{-}t\text{-Bu})(OAr)_2$ closely resembles the previously studied $W(C\text{-}t\text{-Bu})(OAr)_3$ catalyst.

EXPERIMENTAL

General comments. All manipulations were performed in oven-dried (200 ºC) glassware under an atmosphere of nitrogen on a dual-manifold Schlenk line or in a Vacuum Atmospheres glovebox. HPLC grade organic solvents were sparged with nitrogen and dried by passage through activated alumina, then stored over 4 Å Linde-type molecular sieves prior to use. Benzene-d_6 and toluene-d_8 was dried over sodium/benzophenone ketyl and vacuum-distilled prior to use. NMR spectra were recorded on Varian Mercury or Varian INOVA spectrometers

operating at 300 and 500 MHz (^{1}H), respectively. All spectra were recorded in benzene-d_6 at 20 ºC unless otherwise noted. Chemical shifts for ^{1}H and ^{13}C spectra were referenced to the residual ^{1}H/^{13}C resonances of the deuterated solvent (^{1}H: C_6D_6, δ 7.16; $C_6D_5CD_3$, δ 2.09; ^{13}C: C_6D_6, δ 128.39) and are reported as parts per million relative to tetramethylsilane. ^{19}F NMR chemical shifts were referenced externally to fluorobenzene (δ -113.15 ppm upfield of $CFCl_3$). ^{15}N NMR chemical shifts were reference externally to $CH_3C^{15}N$ (δ 247.6 ppm downfield of NH_3). UV-vis spectra were recorded in sealable quartz cuvettes (1 cm) on an Agilent diode array spectrometer. Infrared spectra were recorded in solution KBr cells on a Nicolet Avatar 360 FT-IR spectrometer. Elemental analyses were performed by H. Kolbe Microanalytics Laboratory, Mülheim an der Ruhr, Germany.

Materials. $\{Li(Et_2O)_2\}\{NHB(Mes)_2\}$ was prepared according to published procedures.[55] WCl_6 and Me_3SiOTf were purchased from Strem Chemicals and used as received. All alcohols, nitriles, and carbonyl species were purchased from commercial vendors, sublimed or distilled, and dried over 4 Å molecular sieves prior to use. Alkynes were purchased from commercial vendors and passed through activated alumina prior to use.

Crystallography. Mounting of crystals and refinement of X-ray diffraction data was performed by Dr. Peter Müller of the Department of Chemistry Diffraction Facility. Low temperature diffraction data were collected on a Siemens Platform three-circle diffractometer coupled to a Bruker-AXS Smart Apex CCD detector with graphite-monochromated Mo Kα radiation (λ = 0.71073 Å), performing φ- and ω-scans. All structures were solved by direct methods using SHELXS[75] and refined against F^2 on all data by full-matrix least squares with SHELXL-97[76]. All non-hydrogen atoms were refined anisotropically. All hydrogen atoms were included into the model at geometrically calculated positions and refined using a riding model. The isotropic displacement parameters of all hydrogen atoms were fixed to 1.2 times the U value of the atoms they are linked to (1.5 times for methyl groups).

***mer*-WCl_3(O-2,6-*i*-$Pr_2C_6H_3)_3$.** This compound has been reported previously[38] and was prepared by a slightly modified procedure. Briefly, a 500 mL Schlenk flask was charged with 13.158 g (33.2 mmol) of WCl_6, 18.4 mL (99.3 mmol) of 2,6-diisopropylphenol and 250 mL of toluene. The mixture was heated at 80ºC for 20 h during which time HCl was evolved through an oil bubbler connected to the flask. All volatiles were removed in vacuo at 50ºC and the residue was treated with pentane to afford 16.83 g (62%) of a dark red solid that was isolated by filtration and dried in vacuo. The spectroscopic features were identical to the previously published values and reappear here for convenience: ^{1}H NMR (300 MHz) δ 7.07 (d, 4, *m*-Ar), 6.93 (d, 2, *m*-Ar), 6.67 (t, 2, *p*-Ar), 6.62 (t, 1, *p*-Ar), 4.45 (sep, 4, C*H*Me_2), 3.91 (sep, 2, C*H*Me_2), 1.22 (d, 24, CH*Me*$_2$), 1.05 (d, 12, CH*Me*$_2$).

W(C-*t*-Bu)(CH_2-*t*-Bu)$(OAr)_2$. A flask was charged with 5.135 g (5.61 mmol) of *mer*-WCl_3(O-2,6-*i*-$Pr_2C_6H_3)_3$ and 75 mL of diethyl ether. The dark red mixture was chilled to –25 ºC, at which point 17.5 mL (26.3 mmol) of *t*-BuCH_2MgCl (1.5 M in ether) was added via syringe in one portion. The reaction was allowed to warm to room temperature and stir for 18 hours during which time it became brown and a precipitate formed. All volatiles were removed in vacuo and the residue was extracted into 80 mL of pentane. The extract was filtered through a plug of Celite and the solution volume was reduced to 10-15 mL in vacuo. The solution was set aside at –25 ºC for 24 hours yielding 1.932 g (44%) of yellow crystals that were isolated by filtration and dried in vacuo: ^{1}H NMR (300 MHz) δ 7.13 (d, 4, *m*-Ar), 6.99 (t, 2, *p*-Ar), 3.67 (sep, 4, C*H*Me_2), 3.02 (s, 2, C*H*$_2$-*t*-Bu, J_{HW} = 10.5 Hz), 1.35 (d, 12, CH*Me*$_2$), 1.32 (s, 9, *t*-Bu), 1.27 (d, 12, CH*Me*$_2$), 0.80 (s, 9, W≡C-*t*-Bu); ^{13}C NMR (125 MHz) δ 303.0 (W≡*C*, J_{CW} = 271 Hz), 162.1, 137.2, 128.7, 123.7, 74.6 (*C*H_2-*t*-Bu, J_{CW} = 124 Hz), 52.1 (W≡C*C*Me_3, J_{CW} = 42.2 Hz), 34.7, 32.3, 32.2, 27.5, 24.4, 23.8. Anal. Calcd for $C_{34}H_{40}N_2W$: C, 61.82; H, 6.10; N, 4.24. Found: C, 61.85; H, 5.98; N, 4.16.

Mixture of W[C(*t*-Bu)C(Et)C(Et)](CH_2-*t*-Bu)($OAr)_2$ and W[C_3Et_3](CH_2-*t*-Bu)($OAr)_2$. A flask was charged with 0.251 g (0.37 mmol) of W(C-*t*-Bu)(CH_2-*t*-Bu)($OAr)_2$ and 20 mL of pentane. To the stirring yellow solution was added 170 μL (1.5 mmol) of 3-hexyne via syringe in one portion. The solution immediately turned red and was allowed to stir at room temperature for 45 minutes. All volatiles were removed in vacuo and the resulting solid was dissolved in a minimal amount of pentane and stored at –25ºC for several days. Two different crystal types precipitated from the cold pentane solution, red urchins (asymmetric metallacycle) and orange needles (triethyl metallacycle). The crystals were washed with cold pentane and separated mechanically, though each compound still contained traces of the other. Mass: orange needles, 0.0543 g; red urchins, 0.1340 g; ^{1}H NMR (500 MHz, *red urchins*) δ 7.0 (v br, 6, Ar), 3.93 (br, 2, C*H*Me_2), 3.72 (m, 1, C*H*$_2CH_3$), 3.65 (m, 1, C*H*$_2CH_3$), 3.56 (m, 1, C*H*$_2CH_3$), 3.22 (m, 1, C*H*$_2CH_3$), 2.93 (br, 2, C*H*Me_2), 1.92 (t, 3, CH_2C*H*$_3$), 1.3 (br m, 24, CH*Me*$_2$), 1.16 (s, 9, *t*-Bu), 0.88 (s, 9, *t*-Bu), 0.83 (d, J_{HH} = 14.0 Hz, 1, C*H*$_2$-*t*-Bu,), 0.67 (t, 3, CH_2C*H*$_3$), 0.45 (d, J_{HH} = 14.0 Hz, 1, C*H*$_2$-*t*-Bu).

W[C_3Et_3](CH_2-t-Bu)(O-2,6-*i*-$Pr_2C_6H_3)_2$. A flask was charged with 0.1007 g (0.148 mmol) of W(C-*t*-Bu)(CH_2-*t*-Bu)($OAr)_2$ and 5 mL of pentane. To the solution was added 210 μL (1.85 mmol) of 3-hexyne via syringe. The solution immediately became red and was allowed to stir at 23 ºC for 18 hours. All volatiles were removed in vacuo and the residue extracted into 10 mL of pentane. The extract was filtered through Celite and the solution volume reduced to ~1 mL in vacuo. Storage of the pentane solution at –25 ºC for 24 hours gave 0.0702 g (65%) of orange needles: ^{1}H NMR (300 MHz) δ 7.11 (d, 4, *m*-Ar), 6.88 (t, 2, *p*-Ar), 3.65 (sep, 4, C*H*Me2), 3.45 (m, 2, α-C*H*$_2CH_3$), 3.22 (m, 2, α-C*H*$_2CH_3$), 3.04 (q, J = 7.7 Hz, 2, β-C*H*$_2CH_3$), 1.75 (t, J = 7.3 Hz, 6, α-CH_2C*H*$_3$), 1.31 (d, 24, CHMe2), 0.61 (t, J = 7.7 Hz, 3 β-CH_2C*H*$_3$), 0.57 (s, 2, C*H*$_2$-*t*-Bu, J_{HW} = 8.4 Hz), 0.51 (s, 9, *t*-Bu); ^{13}C NMR (125 MHz) δ 242.7 (α-*C*$_3Et_3$, J_{CW} = 122 Hz), 160.4, 146.8 (β-C_3Et_3, J_{CW} = 21 Hz), 137.3, 123.1, 120.8, 73.8 (*C*H_2-*t*-Bu, J_{CW} = 81 Hz), 36.1, 34.5,

31.4, 28.2, 25.0, 24.4, 15.1, 12.1. Anal. Calcd for $C_{38}H_{60}O_2W$: C, 62.29; H, 8.25. Found: C, 62.21; H, 8.20.

W[C_3Me_3](CH_2-*t*-Bu)(O-2,6-*i*-$Pr_2C_6H_3$)$_2$. This compound was prepared in identical fashion to the ethyl derivative starting from 0.2603 g (0.383 mmol) of W(C-*t*-Bu)(CH_2-*t*-Bu)(OAr)$_2$ and 300 μL of 2-butyne (3.8 mmol). The compound crystallized from pentane as 0.1453 g (55%) of fibrous red needles: ^{1}H NMR (300 MHz) δ 7.13 (d, 4, *m*-Ar), 6.92 (t, 2, *p*-Ar), 3.57 (sep, 4, C*H*Me$_2$), 2.91 (s, 6, α-Me), 2.19 (s, 3, β-Me), 1.34 (d, 24, CH*Me*$_2$), 0.85 (s, 2, C*H*$_2$-*t*-Bu, J_{HW} = 9.3 Hz), 0.49 (s, 9, *t*-Bu); ^{13}C NMR (125 MHz) δ 234.3 (α-*C*$_3$Me$_3$, J_{CW} = 124 Hz), 160.9, 147.8 (β-*C*$_3$Me$_3$, J_{CW} = 22 Hz), 137.5, 123.1, 120.9, 74.0 (*C*H$_2$-*t*-Bu, J_{CW} = 83 Hz), 36.2, 34.3, 28.1, 24.5, 22.7 (α-C$_3$*Me*$_3$, J_{CW} = 23 Hz), 15.9. Anal. Calcd for $C_{35}H_{54}O_2W$: C, 60.87; H, 7.88. Found: C, 60.98; H, 7.84.

W(O)[C(*t*-Bu)C(Me)OEt](CH_2-*t*-Bu)(O-2,6-*i*-$Pr_2C_6H_3$)$_2$. A vial was charged with 0.2656 g (0.391 mmol) of W(C-*t*-Bu)(CH_2-*t*-Bu)(OAr)$_2$ and 5 mL of ethyl acetate. The solution was stirred at room temperature for 18 hours during which time it turned from yellow to deep red. The volatiles were removed in vacuo and the residue dissolved in a minimal amount of pentane and stored at –25 ºC for several days. After precipitation of several crops of colorless crystals, the desired complex precipitated as 0.0421 g (16%) of red cubes: ^{1}H NMR (500 MHz) δ 7.11 (d, 4, *m*-Ar), 6.96 (t, 2, *p*-Ar), 4.23 (sep, 4, C*H*Me$_2$), 3.89 (q, J = 7.0 Hz, 2 OC*H*$_2$CH$_3$), 2.42 (s, 2 C*H*$_2$-*t*-Bu, J_{HW} = 8.4 Hz), 1.74 (s, 3, Me), 1.34 (s, 9, CH$_2$-*t*-Bu), 1.33 (d, 12, CH*Me*$_2$), 1.28 (d, 12, CH*Me*$_2$), 1.27 (t, J = 7.0 Hz, OCH$_2$C*H*$_3$), 1.24 (s, 9, vinylic *t*-Bu); ^{13}C NMR (125 MHz) δ 184.4 ([*C*(*t*-Bu)C(Me)OEt], J_{CW} = 93 Hz), 158.0, 156.4 ([C(*t*-Bu)*C*(Me)OEt]), 141.8, 124.8, 124.8, 86.5 (*C*H$_2$-*t*-Bu, J_{CW} = 87 Hz), 63.1, 35.5, 35.1, 34.3, 34.2, 26.0, 25.5, 25.4, 17.9, 17.7.

Mixture of W(O)[C(*t*-Bu)CH(Ph)](CH_2-*t*-Bu)(OAr)$_2$ and W(O)[C(*t*-Bu)C(Ph)](OAr)$_2$. A J-Young type NMR tube was charged with 10.5 mg (15.5 μmol) of W(C-*t*-Bu)(CH_2-*t*-Bu)(OAr)$_2$

and 0.7 mL of benzene-d_6. To the solution was added 2 μL (20 μmol) of benzaldehyde via microsyringe. The solution immediately became red upon mixing. The ^{1}H NMR spectrum was recorded immediately: (300 MHz) *selected peaks* δ 8.20 (s, 1, vinyl-C*H* of minor species, J_{HW} = 10.8 Hz), 7.53 (d, 2, *o*-Ph of minor species), 3.99 (sep, 4, C*H*Me$_2$ of minor species), 3.76 (sep, 2, C*H*Me$_2$ of major species), 3.57 (sep, 2, C*H*Me$_2$ of major species), 2.86 (s, 2, CH_2-*t*-Bu of minor species), 1.11 (s, 9, *t*-Bu of major species).

W(C-*t*-Bu)(CH$_2$-*t*-Bu)(NPh$_2$)$_2$. A flask was charged with 0.1511 g (0.222 mmol) of W(C-*t*-Bu)(CH$_2$-*t*-Bu)(OAr)$_2$ and 15 mL of diethyl ether. To the solution was added 0.1222 g (0.490 mmol) of LiNPh$_2$·Et$_2$O as a solid in one portion. The reaction became homogeneous within 2 minutes and was allowed to stir at room temperature for 2 hours. All volatiles were removed in vacuo and the residue extracted into pentane. The extract was filtered through Celite twice to remove any traces of insoluble LiOAr. The pentane solution was concentrated in vacuo to ~2 mL and set aside at –25 ºC for 3 hours. The compound precipitated as 0.1014 g (70%) of pale yellow crystals: ^{1}H NMR (300 MHz) δ 7.03 (m, 8, *o*-Ph), 6.93 (m, 8, *m*-Ph), 6.83 (m, 4, *p*-Ph), 2.05 (s, 2, CH_2-*t*-Bu, J_{HW} = 12.0 Hz), 1.44 (s, 9, *t*-Bu), 1.11 (s, 9, *t*-Bu); ^{13}C NMR (125 MHz) δ 307.6 (W≡*C*, J_{CW} = 266 Hz), 153.1 (br), 129.6, 125.7, 124.9, 81.3 (*C*H$_2$-*t*-Bu, J_{CW} = 117 Hz), 53.1 (W≡C*C*Me$_3$, J_{CW} = 43.6 Hz), 36.8, 35.8, 31.9. Anal. Calcd for $C_{34}H_{40}N_2W$: C, 61.82; H, 6.10; N, 4.24. Found: C, 61.85; H, 5.98; N, 4.16.

W(CCH$_2$CH$_3$)(CH$_2$-*t*-Bu)(NPh$_2$)$_2$. This species was obtained in very low yield by reaction of 0.1007 g of W(C-*t*-Bu)(CH$_2$-*t*-Bu)(NPh$_2$)$_2$ in a 1:1 mixture of 3-hexyne to pentane (by volume, 5 mL total) over 4 days. Crystallization of the mixture from pentane afforded 0.0168 g of the desired propylidyne which was observed to contain ~10% of the starting neopentylidyne by NMR: ^{1}H NMR (300 MHz) δ 7.03 (m, 8, *m*-Ph), 6.93 (t, 8, *o*-Ph), 6.84 (m, 4, *p*-Ph), 3.81 (q, *J* = 7.5 Hz, 2, CCH_2CH$_3$, J_{CW} = 7.5 Hz), 2.01 (s, 2, CH_2-*t*-Bu), 1.39 (s, 9, *t*-Bu), 0.92 (t, *J* = 7.5 Hz, 3, CCH$_2$CH_3); ^{13}C NMR (125 MHz) δ 297.6 (W≡*C*, J_{CW} = 273 Hz), 152 (v br, *ipso*-C), 129.7,

125.6, 124.8, 80.9 (CH$_2$-*t*-Bu, J_{CW} = 117 Hz), 42.4 (W≡CCH$_2$CH$_3$, J_{CW} = 46.8 Hz), 37.7, 35.5, 35.5, 15.0 (W≡CCH$_2$$CH_3$).

Observation of W(C-*t*-Bu)(CH$_2$-*t*-Bu)(O-1-adamantyl)$_2$ by ^{1}H NMR. To a solution of 10.2 mg (15 μmol) of W(C-*t*-Bu)(CH$_2$-*t*-Bu)(NPh$_2$)$_2$ in 0.6 mL of benzene-d_6, was added 5.0 mg (33 μmol) of 1-adamantanol. The color of the solution remained pale yellow. The ^{1}H NMR spectrum of the mixture was then recorded as soon as possible (~10 minutes). The spectrum displayed only HNPh$_2$, W(C-*t*-Bu)(CH$_2$-*t*-Bu)(O-1-adamantyl)$_2$, and a trace of 1-adamantanol: ^{1}H NMR (300 MHz) δ 7.12 (m, 8, *m*-Ph of HNPh$_2$), 6.85 (m, 12, *o*/*p*-Ph of HNPh$_2$), 4.9 (br s, 2, N*H* of HNPh$_2$), 2.50 (s, 2, CH_2-*t*-Bu, J_{HW} = 10.5 Hz), 2.0 (br m, 18, Ad-CH_2/C*H*), 1.5 (br m, 12, Ad-CH_2), 1.47 (s, 9, *t*-Bu), 1.29 (s, 9, *t*-Bu).

Observation of W(CH-*t*-Bu)(binaphth-1-yl-2,2′-diolate)$_2$ by ^{1}H NMR. A J-Young tube type NMR tube was charged with equimolar amounts of W(C-*t*-Bu)(CH$_2$-*t*-Bu)(NPh$_2$)$_2$ and *S*-binaphthol. To the tube was added 0.7 mL of benzene-d_6. A slight darkening of the solution was apparent upon dissolution of the solids: ^{1}H NMR (300 MHz) *selected peaks* δ 8.89 (s, 1, C*H*-*t*-Bu, J_{HW} = 14.1 Hz), 8.30 (d, 1, naph), 6.26 (d, 1, naph), 0.67 (s, 9, *t*-Bu).

W(C-*t*-Bu)(CH$_2$-*t*-Bu)(OAr)[NHB(Mes)$_2$]. A flask was charged with 0.2080 g (0.306 mmol) of W(C-*t*-Bu)(CH$_2$-*t*-Bu)(OAr)$_2$ and 20 mL of diethyl ether. The solution was chilled to –25 ºC, at which point 0.1168 g (0.338 mmol) of {Li(Et$_2$O)$_2$}{NHB(Mes)$_2$} was added as a solid in one portion. The mixture was allowed to stir at room temperature for 18 hours during which time the solution color changed from yellow to pale yellow. All volatiles were removed in vacuo and the residue extracted with pentane. The extract was filtered through a plug of Celite and concentrated in vacuo to ~2 mL. The solution was set aside at –25 ºC for several days during which time the desired compound crystallized as 0.1363 g (58%) of pale yellow shards: ^{1}H NMR (300 MHz) δ 9.87 (br s, 1, N*H*), 7.12 (d, 2, *m*-Ar), 6.97 (t, 1, *p*-Ar), 6.82 (br s, 2, *m*-Mes), 6.81

(s, 2, *m*-Mes), 3.39 (sep, 2, C*H*Me$_2$), 2.5 (v br, 6, *o*-Me), 2.44 (br s, 6, *o*-Me), 2.18 (s, 3, *p*-Me), 2.11 (s, 3, *p*-Me), 1.29 (s, 9, *t*-Bu), 1.26 (d, 6, CH*Me*$_2$), 1.24 (d, 6, CH*Me*$_2$), 1.19 (d, J_{HH} = 15.0 Hz, 1, C*H*$_2$), 1.03 (s, 9, *t*-Bu), 0.79 (d, J_{HH} = 15.0 Hz, 1, C*H*$_2$, J_{HW} = 14.3 Hz); ^{13}C NMR (343 K) δ 299.6 (W≡*C*), 163.1 (*ipso*-Ar), 142 (br, Mes), 140 (br, Mes), 137.3, 130.1 (*p*-Mes), 123.6, 123.2, 94.2 (*C*H$_2$-*t*-Bu, J_{CW} = 115 Hz), 52.1, 35.4, 35.0, 32.7, 27.4, 24.1, 23.8, 23.7, 21.4. Anal Calcd for $C_{40}H_{60}BNOW$: C, 62.75; H, 7.90; N, 1.83. Found: C, 62.74; H, 7.83; N, 1.78.

[W(N)(CH$_2$-*t*-Bu)(O-2,6-*i*-Pr$_2$C$_6$H$_3$)$_2$]$_2$. A flask was charged with 0.2494 g (0.368 mmol) of W(C-*t*-Bu)(CH$_2$-*t*-Bu)(OAr)$_2$ and 15 mL of pentane. To the yellow solution was added 45 μL (0.44 mmol) of benzonitrile. The solution was allowed to stir at room temperature for 2 days during which time it became dark red. All volatiles were removed in vacuo and the residue dissolved in 3 mL of pentane. The solution was set aside at –25 ºC for 24 hours yielding 0.1808 g (79%) of iridescent black crystals that were isolated by decantation of the mother liquor: ^{1}H NMR (300 MHz) δ 7.09 (d, 8, *m*-Ar), 6.95 (t, 4, *p*-Ar), 3.53 (sep, 8, C*H*Me$_2$), 2.86 (s, 4, CH$_2$, J_{HW} = 10.5 Hz), 1.24 (d, 24, CH*Me*$_2$), 1.20 (d, 24, CH*Me*$_2$), 1.12 (s, 18, *t*-Bu); ^{13}C NMR (125 MHz) δ 157.1, 140.0, 124.8, 124.3, 77.1 (*C*H$_2$-*t*-Bu, J_{CW} = 104 Hz), 36.4, 34.4, 28.1, 24.6. IR (KBr, pentane): 1326, 1252, 1193, 816, 752, 635. UV-vis (pentane): λ_{max} = 468 nm, ε = 8070 cm^{-1}M^{-1}. Anal. Calcd for $C_{29}H_{45}NO_2W$: C, 55.86; H, 7.27; N, 2.25. Found: C, 56.08; H, 7.36; N, 2.27.

[W(^{15}N)(CH$_2$-*t*-Bu)(O-2,6-*i*-Pr$_2$C$_6$H$_3$)$_2$]$_2$. Prepared in identical fashion from CH$_3$C^{15}N: ^{15}N NMR (50.7 MHz, toluene-d_8) δ 680.3 (J_{NW} = 30.2 Hz). IR (KBr, pentane): 816 (WN), 635 (WN).

W(NSiMe$_3$)(CH$_2$-*t*-Bu)(O-2,6-*i*-Pr$_2$C$_6$H$_3$)$_2$(OSO$_2$CF$_3$). A flask was charged with 0.106 g (0.169 mmol) of W(N)(CH$_2$-*t*-Bu)(OAr)$_2$ and 8 mL of pentane. To the stirring solution was added 35 μL (0.18 mmol) of Me$_3$SiOSO$_2$CF$_3$ via syringe. The solution was allowed to stir at room temperature for 45 hours during which time the color lightened from dark red to bright red. All volatiles were removed in vacuo and the residue dissolved in 2 mL of pentane. The solution was set aside at –25 ºC for 24 hours yielding 0.0983 g (80%) of bright red needles in two crops: ^{1}H

NMR (300 MHz) δ 7.06 (d, 4, *m*-Ar), 6.94 (t, 2, *p*-Ar), 3.65 (sep, 4, C*H*Me$_2$), 2.58 (s, C*H*$_2$, J_{HW} = 10.2 Hz), 1.36 (app t, 24, CH*Me*$_2$), 0.97 (s, 9, *t*-Bu), 0.39 (s, 9, Si*Me*$_3$); ^{13}C NMR (125 MHz) δ 159.0 (*ipso*-Ar), 140.4 (*o*-Ar), 127.1 (*p*-Ar), 124.5 (*m*-Ar), 120.8 (q, J_{CF} = 319 Hz, *C*F$_3$), 83.1 (*C*H$_2$, J_{CW} = 126 Hz), 36.3 (*C*Me$_3$), 33.8, 28.0, 25.1, 24.3, 2.0 (Si*Me*$_3$); ^{19}F NMR (282 MHz) δ –77.2 (OSO$_2$C*F*$_3$). IR (KBr, pentane): 1252, 1236, 1199, 1146, 1101, 969, 919, 906, 845, 635. Anal Calcd for $C_{33}H_{54}F_3NO_5SSiW$: C, 46.86; H, 6.44; N, 1.66. Found: C, 46.34; H, 6.40; N, 1.58.

W(^{15}NSiMe$_3$)(CH$_2$-*t*-Bu)(O-2,6-*i*-Pr$_2$C$_6$H$_3$)$_2$(OSO$_2$CF$_3$). Prepared in identical fashion from W(^{15}N)(CH$_2$-*t*-Bu)(OAr)$_2$: ^{15}N NMR (50.7 MHz) δ 453.6 (J_{NW} = 103 Hz). IR (KBr, pentane): 1120.

Observation of W(NSiMe$_3$)(CH$_2$-*t*-Bu)$_2$(O-2,6-*i*-Pr$_2$C$_6$H$_3$)$_2$ by ^{1}H NMR. A J-Young NMR tube was charged with equimolar amounts of W(NSiMe$_3$)(CH$_2$-*t*-Bu)(OAr)$_2$(OSO$_2$CF$_3$) and *t*-BuCH$_2$Li. The solids were dissolved in toluene-d_8 at which point the solution became deep purple: ^{1}H NMR (300 MHz) d 7.10 (m, 4, *m*-Ar), 6.92 (m, 2, *p*-Ar), 3.6 (v br, 4, C*H*Me$_2$), 1.80 (s, 4, C*H*$_2$-*t*-Bu), 1.32 (d, 24, CH*Me*$_2$), 1.11 (s, 18, *t*-Bu), 0.45 (s, 9, Si*Me*$_3$). UV-vis (pentane): λ_{max} = 352 nm, 512 nm.

General procedure for GC analysis of alkyne metathesis reactions. In a representative example, a 4.3 mM catalyst solution in pentane was treated with 150 μL of 3-heptyne (~50 equivalents). Aliquots (250 μL) of the solution were taken at specified intervals and diluted to 5.0 mL with pentane. The diluted solution was then passed through a small plug of silica gel and subjected to GC. The concentration of 3-heptyne to 4-octyne was then monitored over time.

Crystal data and structure refinement for **W(C-*t*-Bu)(CH_2-*t*-Bu)($OAr)_2$**.

Reciprocal net identification code	**06174**	
Empirical formula	$C_{34}H_{54}O_2W$	
Formula weight	678.62	
Temperature	100(2) K	
Wavelength	0.71073 Å	
Crystal system	Orthorhombic	
Space group	Pbca	
Unit cell dimensions	a = 11.5297(4) Å	α = 90º
	b = 19.4678(6) Å	β = 90º
	c = 29.0284(9) Å	γ = 90º
Volume	6515.7(4) $Å^3$	
Z	8	
Density (calculated)	1.384 g/cm^3	
Absorption coefficient	3.572 mm^{-1}	
F(000)	2784	
Crystal size	0.25 × 0.20 × 0.15 mm^3	
Theta range for data collection	2.09 to 29.57º.	
Index ranges	$-16 \le h \le 16$, $-27 \le k \le 27$, $-40 \le l \le 40$	
Reflections collected	108715	
Independent reflections	9132 [R(int) = 0.0381]	
Completeness to theta = 29.57º	100.0 %	
Absorption correction	Semi-empirical from equivalents	
Max. and min. transmission	0.6164 and 0.4688	
Refinement method	Full-matrix least-squares on F^2	
Data / restraints / parameters	9132 / 2 / 354	
Goodness-of-fit on F^2	1.048	
Final R indices [I>2sigma(I)]	R1 = 0.0222, wR2 = 0.0523	
R indices (all data)	R1 = 0.0290, wR2 = 0.0557	
Largest diff. peak and hole	1.682 and -0.469 $e \cdot Å^{-3}$	

Crystal data and structure refinement for **[W(N)(CH_2-*t*-Bu)(OAr)$_2$]$_2$**.

Reciprocal net ident. code	**07014**	
Empirical formula	$C_{58}H_{90}N_2O_4W_2$	
Formula weight	1247.02 g/mol	
Temperature	100(2) K	
Wavelength	0.71073 Å	
Crystal system	monoclinic	
Space group	P2(1)/n	
Unit cell dimensions	a = 14.022(3) Å	α = 90°
	b = 18.198(3) Å	β = 92.105(3)°
	c = 22.170(4) Å	γ = 90°
Volume	5653.4(18) Å^3	
Z	4	
Density (calculated)	1.465 g/cm^3	
Absorption coefficient	4.110 mm^{-1}	
F(000)	2528	
crystal size	0.15 × 0.15 × 0.10 mm^3	
Θ range for data collection	1.83 to 29.57°	
index ranges	$-19 \le h \le 19$, $-25 \le k \le 25$, $-30 \le l \le 30$	
Reflections collected	124692	
Independent reflections	15860 [R(int) = 0.0514]	
Completeness to Θ = 29.57°	100.0 %	
Absorption correction	semi-empirical from equivalents	
Max. and min. transmission	0.6840 and 0.5776	
Refinement method	full-matrix least-squares on F^2	
Data / restraints / parameters	15860 / 5 / 629	
Goodness-of-fit on F^2	1.032	
Final R indices [I>2σ(I)]	R1 = 0.0210, wR2 = 0.0465	
R indices (all data)	R1 = 0.0287, wR2 = 0.0497	
Largest diff. peak and hole	2.899 and -1.041 e·Å^{-3}	

Crystal data and structure refinement for **W(^{15}NSiMe$_3$)(CH$_2$-*t*-Bu)(OAr)$_2$(OTf)**.

Reciprocal net identification code	**07030**	
Empirical formula	$C_{33}H_{54}F_3NO_5SSiW$	
Formula weight	845.77 g/mol	
Temperature	218(2) K	
Wavelength	0.71073 Å	
Crystal system	Orthorhombic	
Space group	Pbca	
Unit cell dimensions	a = 18.9549(6) Å	α = 90°
	b = 19.1661(6) Å	β = 90°
	c = 21.8341(7) Å	γ = 90°
Volume	7932.1(4) Å^3	
Z	8	
Density (calculated)	1.416 g/cm^3	
Absorption coefficient	3.045 mm^{-1}	
F(000)	3440	
Crystal size	0.35 × 0.20 × 0.20 mm^3	
Θ range for data collection	1.78 to 29.13°	
Index ranges	$-25 \le h \le 25$, $-26 \le k \le 26$, $-29 \le l \le 29$	
Reflections collected	166109	
Independent reflections	10671 [R(int) = 0.0423]	
Completeness to Θ = 29.13°	100.0 %	
Absorption correction	Semi-empirical from equivalents	
Max. and min. transmission	0.5811 and 0.4154	
Refinement method	Full-matrix least-squares on F^2	
Data / restraints / parameters	10671 / 510 / 490	
Goodness-of-fit on F^2	1.069	
Final R indices [I>2σ(I)]	R1 = 0.0235, wR2 = 0.0528	
R indices (all data)	R1 = 0.0413, wR2 = 0.0630	
Largest diff. peak and hole	0.710 and -0.797 e·Å^{-3}	

REFERNCE

1. Schrock, R. R. in *Handbook of Metathesis*. Wiley-VCH: Weinheim, 2003; Vol. 1, p 173.
2. Schrock, R. R.; Freudenberger, J. H.; Listemann, M. L.; McCullough, L. G. *J. Mol. Catal.* **1985**, *28*, 1.
3. Fürstner, A.; Davies Paul, W. *Chem. Commun.* **2005**, 2307.
4. Schrock, R. R. *Chem. Rev.* **2002**, *102*, 145.
5. Wengrovius, J. H.; Sancho, J.; Schrock, R. R. *J. Am. Chem. Soc.* **1981**, *103*, 3932.
6. Clark, D. N.; Schrock, R. R. *J. Am. Chem. Soc.* **1978**, *100*, 6774.
7. Schrock, R. R.; Clark, D. N.; Sancho, J.; Wengrovius, J. H.; Rocklage, S. M.; Pedersen, S. F. *Organometallics* **1982**, *1*, 1645.
8. Schrock, R. R.; Sancho, J.; Pederson, S. F. *Inorg. Synth.* **1989**, *26*, 44.
9. Schrock, R. R.; Listemann, M. L.; Sturgeoff, L. G. *J. Am. Chem. Soc.* **1982**, *104*, 4291.
10. Listemann, M. L.; Schrock, R. R. *Organometallics* **1985**, *4*, 74.
11. Cotton, F. A.; Schwotzer, W.; Shamshoum, E. S. *Organometallics* **1984**, *3*, 1770.
12. Stevenson, M. A.; Hopkins, M. D. *Organometallics* **1997**, *16*, 3572.
13. McCullough, L. G.; Schrock, R. R.; Dewan, J. C.; Murdzek, J. C. *J. Am. Chem. Soc.* **1985**, *107*, 5987.
14. Weissman, H.; Plunkett, K. N.; Moore, J. S. *Angew. Chem. Int. Ed.* **2006**, *45*, 585.
15. Tsai, Y. C.; Diaconescu, P. L.; Cummins, C. C. *Organometallics* **2000**, *19*, 5260.
16. Fürstner, A.; Mathes, C.; Lehmann, C. W. *Chem. Eur. J.* **2001**, *7*, 5299.
17. Fürstner, A.; Mathes, C.; Lehmann, C. W. *J. Am. Chem. Soc.* **1999**, *121*, 9453.
18. Zhang, W.; Kraft, S.; Moore Jeffrey, S. *Chem. Commun.* **2003**, 832.
19. Zhang, W.; Kraft, S.; Moore Jeffrey, S. *J. Am. Chem. Soc.* **2004**, *126*, 329.
20. Cho, H. M.; Weissman, H.; Wilson, S. R.; Moore, J. S. *J. Am. Chem. Soc.* **2006**, *128*, 14742.
21. Schrock, R. R. *Acc. Chem. Res.* **1986**, *19*, 342.
22. Murdzek, J. S.; Schrock, R. R. in *Carbyne Complexes*, VCH: New York, 1988, pp 147.
23. *Handbook of Metathesis*, Grubbs, R. H., Ed. Wiley-VCH: Weinheim, **2003**; Vols. 1-3.
24. Schrock, R. R.; Hoveyda, A. H. *Angew. Chem. Int. Ed.* **2003**, *42*, 4592.
25. Fürstner, A.; Guth, O.; Rumbo, A.; Seidel, G. *J. Am. Chem. Soc.* **1999**, *121*, 11108.
26. Fürstner, A.; Stelzer, F.; Rumbo, A.; Krause, H. *Chemistry* **2002**, *8*, 1856.
27. Schrock, R. R.; Krouse, S. A.; Feldman, J. *Transition Met. Catal. Polym., [Proc. Int. Symp.], 2nd* **1988**, 688.
28. Krouse, S. A.; Schrock, R. R. *Macromolecules* **1989**, *22*, 2569.

29. Katz, T. J.; Hacker, S. M.; Kendrick, R. D.; Yannoni, C. S. *J. Am. Chem. Soc.* **1985**, *107*, 2182.
30. Woo, T.; Folga, E.; Ziegler, T. *Organometallics* **1993**, *12*, 1289.
31. Zhu, J.; Jia, G.; Lin, Z. *Organometallics* **2006**, *25*, 1812.
32. Fritch, J. R.; Vollhardt, K. P. C. *Angew. Chem.* **1979**, *91*, 439.
33. Churchill, M. R.; Ziller, J. W.; Freudenberger, J. H.; Schrock, R. R. *Organometallics* **1984**, *3*, 1554.
34. Freudenberger, J. H.; Schrock, R. R.; Churchill, M. R.; Rheingold, A. L.; Ziller, J. W. *Organometallics* **1984**, *3*, 1563.
35. Churchill, M. R.; Ziller, J. W.; McCullough, L.; Pedersen, S. F.; Schrock, R. R. *Organometallics* **1983**, *2*, 1046.
36. Pedersen, S. F.; Schrock, R. R.; Churchill, M. R.; Wasserman, H. J. *J. Am. Chem. Soc.* **1982**, *104*, 6808.
37. Tonzetich, Z. J.; Lam, Y. C.; Müller, P.; Schrock, R. R. *Organometallics* **2007**, *26*, 475.
38. Listemann, M. L.; Schrock, R. R.; Dewan, J. C.; Kolodziej, R. M. *Inorg. Chem.* **1988**, *27*, 264.
39 Quignard, F.; Leconte, M.; Basset, J. M.; Hsu, L. Y.; Alexander, J. J.; Shore, S. G. *Inorg. Chem.* **1987**, *26*, 4272.
40 Churchill, M. R.; Wasserman, H. J.; Turner, H. W.; Schrock, R. R. *J. Am. Chem. Soc.* **1982**, *104*, 1710.
41. Chisholm, M. H.; Eichhorn, B. W.; Folting, K.; Huffman, J. C. *Organometallics* **1989**, *8*, 49.
42. Andersen, R. A.; Wilkinson G., *J. Chem. Soc., Dalton Trans.* **1977**, 809.
43. Freudenberger, J. H.; Schrock, R. R. *Organometallics* **1986**, *5*, 1411.
44. Bray, A.; Mortreux, A.; Petit, F.; Petit, M.; Szymanska-Buzar, T. *J. Chem. Soc., Chem. Commun.* **1993**, 197.
45. Mortreux, A.; Petit, F.; Petit, M.; Szymanska-Buzar, T. *J. Mol. Catal. A* **1995**, *96*, 95.
46. Coutelier, O.; Mortreux, A. *Adv. Synth. Catal.* **2006**, *348*, 2038.
47. Freudenberger, J. H.; Schrock, R. R. *Organometallics* **1986**, *5*, 398.
48. Connell, B. T.; Kirkland, T. A.; Grubbs, R. H. *Organometallics* **2005**, *24*, 4684.
49 Lopez, L. P. H.; Schrock, R. R. *J. Am. Chem. Soc.* **2004**, *126*, 9526.
50. Crane, T. W.; White, P. S.; Templeton, J. L. *Organometallics* **1999**, *18*, 1897.
51. Sinha, A.; Schrock, R. R.; Müller, P.; Hoveyda, A. H. *Organometallics* **2006**, *25*, 4621.
52. Hock, A. S.; Schrock, R. R.; Hoveyda, A. H. *J. Am. Chem. Soc.* **2006**, *128*, 16373.
53. Copéret, C.; Chabanas, M.; Petroff Saint-Arroman, R.; Basset, J.-M. *Angew. Chem. Int. Ed.*

2003, *42*, 156.
54. Blanc, F.; Copéret, C.; Thivolle-Cazat, J.; Basset, J.-M.; Lesage, A.; Emsley, L.; Sinha, A.; Schrock. R. R. *Angew. Chem. Int. Ed.* **2006**, *45*, 1216.
55. Chen, H.; Bartlett, R. A.; Olmstead, M. M.; Power, P. P.; Shoner, S. C. *J. Am. Chem. Soc.* **1990**, *112*, 1048.
56 Murdzek, J. S.; Schrock, R. R. *Organometallics* **1987**, *6*, 1373.
57. Rocklage, S. M.; Schrock, R. R.; Churchill, M. R.; Wasserman, H. J. *Organometallics* **1982**, *1*, 1332.
58. Schrock, R. R.; Listemann, M. L.; Sturgeoff, L. G. *J. Am. Chem. Soc.* **1982**, *104*, 4291.
59. Bailey, B. C.; Fout, A. R.; Fan, H.; Tomaszewski, J.; Huffman, J. C.; Gary, J. B.; Johnson, M. J. A.; Mindiola, D. J. *J. Am. Chem. Soc.* **2007**, *129*, 2234.
60. Gdula, R. L.; Johnson, M. J. A. *J. Am. Chem. Soc.* **2006**, *128*, 9614.
61. Geyer, A. M.; Gdula, R. L.; Wiedner, E. S.; Johnson, M. J. A. *J. Am. Chem. Soc.* **2007**, *129*, 3800.
62. Chisholm, M. H.; Delbridge, E. E.; Kidwell, A. R.; Quinlan, K. B. *Chem. Commun.* **2003**, 126.
63. Gdula, R. L.; Johnson, M. J. A.; Ockwig, N. W. *Inorg. Chem.* **2005**, *44*, 9140.
64. Pollagi, T. P.; Manna, J.; Geib, S. J.; Hopkins, M. D. *Inorg. Chim. Acta* **1996**, *243*, 177.
65. Clough, C. R.; Greco, J. B.; Figueroa, J. S.; Diaconescu, P. L.; Davis, W. M.; Cummins, C. C. *J. Am. Chem. Soc.* **2004**, *126*, 7742.
66. Osborne, J. H.; Trogler, W. C. *Inorg. Chem.* **1985**, *24*, 3098.
67. Quignard, F.; Leconte, M.; Basset, J. M. *J. Mol. Catal.* **1985**, *28*, 27.
68. Quignard, F.; Leconte, M.; Basset, J. M.; Hsu, L. Y.; Alexander, J. J.; Shore, S. G. *Inorg. Chem.* **1987**, *26*, 4272.
69. Quignard, F.; Leconte, M.; Basset, J. M. *J. Mol. Catal.* **1986**, *36*, 13.
70. Churchill, M. R.; Youngs, W. J. *J. Chem. Soc., Chem. Commun.* **1978**, 1048.
71. LaPointe, A. M.; Schrock, R. R. *Organometallics* **1995**, *14*, 1875.
72. Chen, T.; Zhang, X.-H.; Wang, C.; Chen, S.; Wu, Z.; Li, L.; Sorasaenee, K. R.; Diminnie, J. B.; Pan, H.; Guzei, I. A.; Rheingold, A. L.; Wu, Y.-D.; Xue, Z.-L. *Organometallics* **2005**, *24*, 1214.
73. Sinha, A.; Schrock, R. R. *Organometallics* **2004**, *23*, 1643.
74. Sinha, A.; Lopez, L. P. H.; Schrock, R. R.; Hock, A. S.; Mueller, P. *Organometallics* **2006**, *25*, 1412.
75. Sheldrick, G. M. Acta Cryst. 1990, A46, 467.
76. Sheldrick, G. M (1997). SHELXL 97, University of Göttingen, Germany.

APPENDIX A

Reactions of Alkylidene Phosphoranes with Molybdenum Imido Alkylidene Catalysts: Synthesis and Reactivity of an Anionic Imido Alkylidyne

A portion of this appendix has appeared in print:

Tonzetich, Z. J.; Schrock, R. R.; Müller, P. "Reaction of Phosphoranes with Mo(N-2,6-*i*-$Pr_2C_6H_3$)($CHCMe_3$)[$OCMe(CF_3)_2]_2$: Synthesis and Reactivity of an Anionic Imido Alkylidyne Complex" *Organometallics* **2006**, *25*, 4301-4306.

INTRODUCTION

Olefin metathesis catalysts of the type Mo(NR)(CHR′)(OR′′)$_2$,[1] and variations that contain chiral diolates,[2] are known to decompose either via bimolecular decomposition of alkylidenes or via rearrangement of some intermediate metallacyclobutane complex. The metal is "reduced" in the process by two electrons to a d^2 species of some type (e.g., a bimetallic species that contains a M=M bond[3]). It would be highly desirable to discover a way of regenerating the catalyst through the use of an alkylidene source such as a phosphorus or sulfur ylide. The first demonstration of a reaction of this type was transfer of an alkylidene from an alkylidene phosphorane to a Ta(III) species to generate a Ta(V) *bis*-cyclopentadienyl complex.[4] Alkylidenes also have been transferred from phosphorus to W(IV) species to yield W(VI) alkylidene complexes.[5,6] However, in no case was the resulting alkylidene species a known metathesis catalyst. Therefore we decided to turn to an exploration of potential reactions between the prototypical metathesis catalyst, Mo(NAr)(CH-*t*-Bu)(O-*t*-Bu$_{F6}$)$_2$ (Ar = 2,6-*i*-Pr$_2$C$_6$H$_3$; *t*-Bu$_{F6}$ = C(CF$_3$)$_2$Me) and phosphorus ylides, reasoning that if a Mo(NAr)(CHR′)(O-*t*-Bu$_{F6}$)$_2$ species were to be regenerated from some "Mo(NAr)(O-*t*-Bu$_{F6}$)$_2$" species in a reaction involving an alkylidene phosphorane, then the resulting alkylidene ideally would have to react relatively slowly with that phosphorane in order to avoid potentially destructive secondary reactions. The susceptibility for alkylidene deprotonation and/or proton transfer in molybdenum imido alkylidene compounds is an ever-present concern in the synthesis and development of new olefin metathesis catalysts.[7] Nearly all reported molybdenum catalysts contain primary alkylidenes (M=CHR′), and with certain compounds, the hydrogen atom is believed to engage in an agostic interaction with the electron deficient metal center.[8,9] This interaction, paired with the highly basic nature of the alkylidene carbon activates the C−H bond creating the potential for unwanted reactivity. Proton transfer between alkylidene carbon and imide nitrogen is facilitated by Lewis bases, and has already been documented for specific imido groups.[7,10] In these instances, the

desired imido alkylidene compounds could only be isolated in low yield, or not at all. Such difficulties have led to the preparation of in situ generated catalysts in recent years.[11,12]

This appendix details reactions between Mo(NAr)(CHR)(O-*t*-Bu_{F6})$_2$ and several alkylidene phosphoranes. In some instances these reactions were found to involve proton transfer from the alkylidene on molybdenum generating an anionic imido alkylidyne. Characterization of the alkylidyne and its reactivity with selected electrophiles is discussed.

RESULTS

Addition of one equivalent of $Ph_3P{=}CH_2$ to Mo(NAr)(CHCMe$_2$R)(O-*t*-Bu_{F6})$_2$ (R = Me or Ph) in benzene-d_6 resulted in an immediate color change from yellow to deep orange. The ^{1}H NMR spectrum of the product showed it to be a single compound that has no alkylidene H_α resonance. The ^{1}H and ^{13}C NMR features are consistent with the product being an anionic alkylidyne complex (R = Me *or* Ph; equation A.1). The product can be isolated readily in high yield. ^{1}H NMR spectra reveal broad resonances for the isopropyl methyl groups of the arylimido ligand, consistent with hindered rotation about the N-C_{ipso} bond. For {Ph_3PMe}{Mo(NAr)(C-*t*-Bu)(O-*t*-Bu_{F6})$_2$}, coalescence of the methyl resonances of the isopropyl groups occurs near

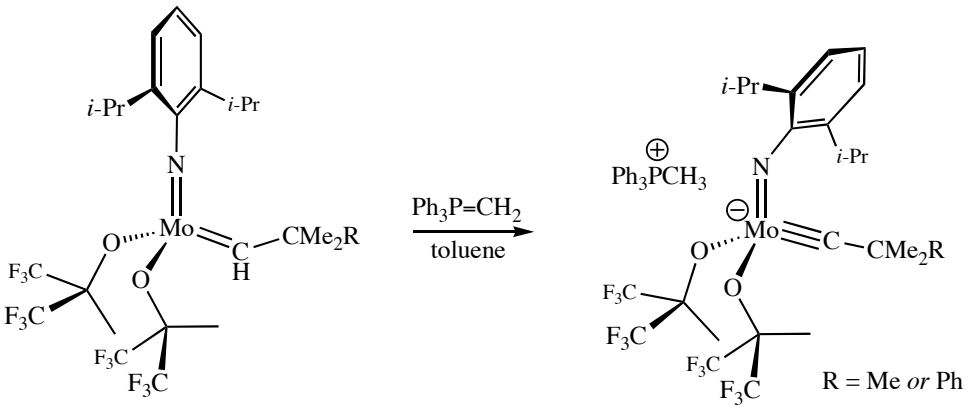

(A.1)

40 ºC in benzene-d_6. Spectra in tetrahydrofuran-d_8 show coalescence of the isopropyl methyl groups at 20 ºC. Therefore ion pairing is likely responsible for a slightly more hindered rotation in benzene. A ^{13}C NMR spectrum of the purified neopentylidyne displays a resonance at 300.7 ppm in benzene-d_6 that can be assigned to the alkylidyne carbon atom. No J_{CP} coupling was observed, consistent with the ionic formulation shown in equation A.1, while the ^{19}F NMR spectrum displays two resonances for the diastereotopic trifluoromethyl groups, as anticipated.

Slow cooling of a saturated toluene/pentane solution of {Ph_3PMe}{Mo(NAr)(C-*t*-Bu)(O-*t*-Bu_{F6})$_2$} afforded red spars suitable for X-ray diffraction. The solid-state structure contains two independent ion pairs in the asymmetric unit. A thermal ellipsoid rendering of one of the molecules is displayed in Figure A.1 and relevant crystallographic details are listed in the caption. The imido alkylidyne formulation is consistent with the large Mo(1)–C(1)–C(2) bond angle (168.2(2)º) and the bent Mo(1)–N(1)–C(21) angle (141.16(17)º; cf. 169 – 175º in typical four-coordinate alkylidenes of this type[1]). The anions in each molecule are virtually identical except for the Mo-N_{imido}-C_{ipso} bond angle, which is 141.16(17)º in the compound shown in Figure 1 and 158.66(17)º in the other (see Table A.1 for comparison of metric parameters). The reason for the large difference in bond angles might be ascribed to a closer approach of the phosphonium cation in the compound shown in Figure A.1 versus the latter (compare 3.566(3) Å versus 4.054(3) Å for the distance from the carbon atom of the methyl group of the phosphonium cation to the molybdenum center). Only one species is observed in solution and the low barrier to N_{imido}-C_{ipso} bond rotation in arene solvents suggests that the potential energy surface for flexing of the Mo-N_{imido}-C_{ipso} angle may be quite flat and sensitive to ion pairing. Therefore it is likely that crystal-packing effects are responsible for the observed differences in the solid state. Because of the presence of the triple bond to carbon and π bonding of the imido group to the metal, C_{ipso} of the aryl group must lie in the N-Mo-C plane. The aryl group points toward the alkylidyne ligand, away from the phosphonium cation, which is nestled into the NOO face of the tetrahedral central core.

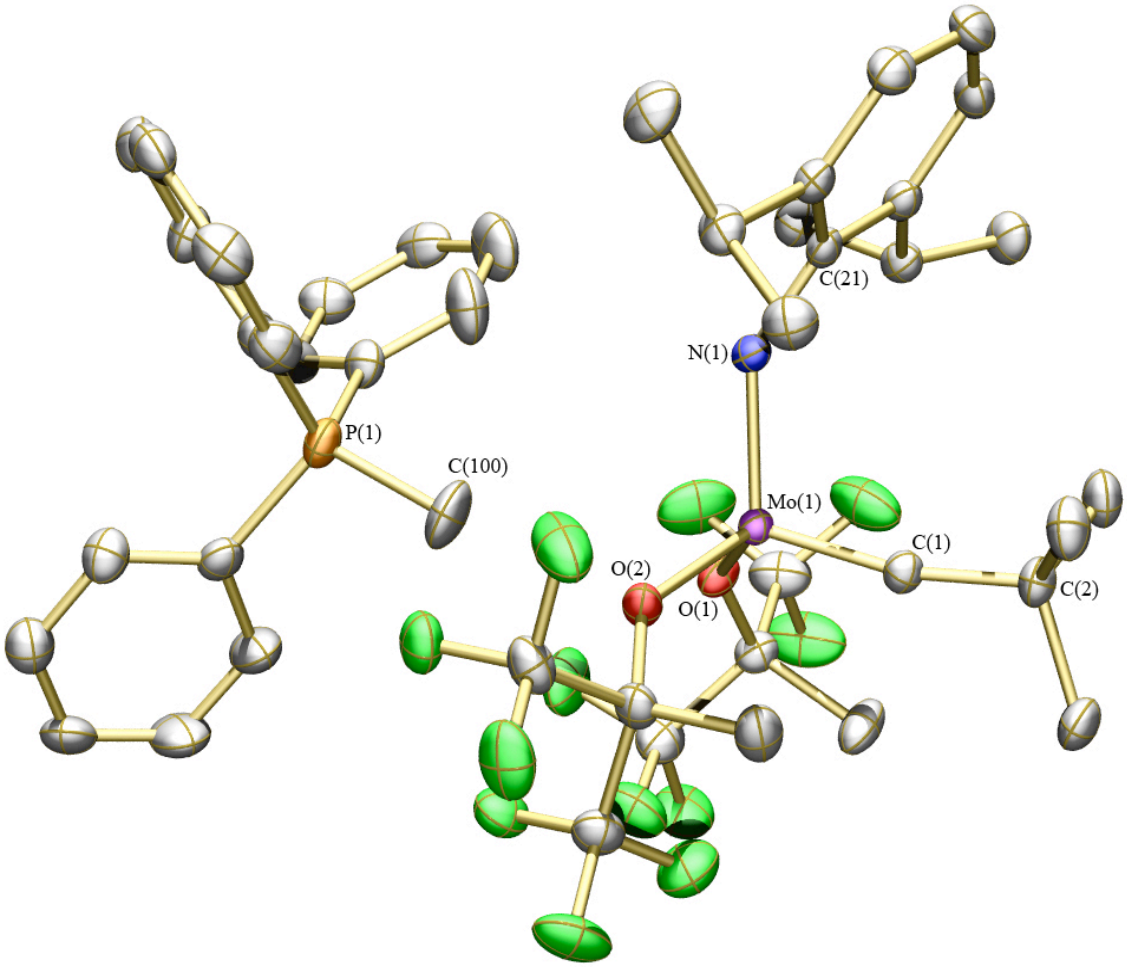

Figure A.1. Thermal ellipsoid rendering (50%) of one of the two independent molecules of $\{Ph_3PMe\}\{Mo(NAr)(C\text{-}t\text{-}Bu)(O\text{-}t\text{-}Bu_{F6})_2\}$ in the asymmetric unit. Hydrogen atoms removed for clarity. Selected bond distances (Å) and angles (°): Mo(1)–C(1) = 1.754(2); Mo(1)–N(1) = 1.813(2); Mo(1)–O(1) = 1.9838(18); Mo(1)–O(2) = 1.9763(18); C(100)–Mo(1) = 3.566(3); Mo(1)–C(1)–C(2) = 168.2(2); Mo(1)–N(1)–C(23) = 141.16(17); N(1)–Mo(1)–C(1) = 105.82(11).

$\{Ph_3PMe\}\{Mo(NAr)(C\text{-}t\text{-}Bu)(O\text{-}t\text{-}Bu_{F6})_2\}$ is isoelectronic with the known rhenium(VII) complex, $Re(NAr)(C\text{-}t\text{-}Bu)(O\text{-}t\text{-}Bu_{F6})_2$.[13] In the Re compound, the C_α resonance is found at 304.3 ppm (vs. 300.7 ppm in the Mo species above) and the isopropyl methyl groups appear as a single doublet resonance at room temperature, consistent with facile rotation of the aryl ring

about the N_{imido}-C_{ipso} bond on the NMR time scale. No structural study of Re(NAr)(C-*t*-Bu)(O-*t*-$Bu_{F6})_2$ was carried out.

Table A.1. Comparison of selected bond lengths (Å) and angles (º) for each of the independent molecules of {Ph_3PMe}{Mo(NAr)(C-*t*-Bu)(O-*t*-$Bu_{F6})_2$} in the unit cell (Mo(1) refers to the molecule in Figure A.1).

Bond metric	Mo1	Mo2
Mo – C(α)	1.754(2)	1.762(2)
Mo – N(imido)	1.813(2)	1.807(2)
Mo – O(avg)	1.9801(18)	1.9748(17)
Mo – C(cation)	3.566(3)	4.055(3)
N(imido) – Mo – C(α)	105.82(11)	108.89(10)
C(ipso) – N(imido) – Mo	141.16(17)	158.66(17)
Mo – C(α) – C(β)	168.2(2)	168.1(2)
N(imido) – Mo – O(avg)	109.55(9)	108.51(8)
C(α) – Mo – O(avg)	109.75(10)	109.74(10)

The benzylidene phosphorane, Ph_3P=CHPh, did not react with Mo(NAr)(CH-*t*-Bu)(O-*t*-$Bu_{F6})_2$ at concentrations of ~0.01 M in benzene-d_6, even upon heating to 40 ºC. Presumably for steric reasons this phosphorane can neither deprotonate the alkylidene readily, nor create adducts through addition to the metal, as described below.

The reaction of Mo(NAr)(CH-*t*-Bu)(O-*t*-$Bu_{F6})_2$ and Me_3P=CHPh in benzene-d_6 was followed by NMR and shown to give a mixture of two compounds initially (Scheme 1). The main component of the mixture is an alkylidene containing species with a neopentylidene H_α resonance at 11.65 ppm that is coupled weakly to phosphorus (J_{PH} = 1.5 Hz). Only one methyl resonance for the hexafluoro-*tert*-butyl group is observed, which suggests that the molecule possesses mirror symmetry. The imido aryl ring also shows free rotation as judged by the single doublet resonance for the methyl protons of the isopropyl groups. These spectral features are all consistent with an adduct in which the ylide is bound to the NOO face of the original tetrahedral

core. Base adducts of this type have been observed in several instances[14] and some have been structurally characterized.[15,16] Interestingly, the ylide coordinating to the Mo center is no longer a benzylidene but rather a methylidene, as judged by the doublet resonance at 2.48 ppm that integrates to two protons (PC*H*$_2$Ph). The minor component of the initial mixture shows no alkylidene resonance. The minor species also possesses mirror symmetry and the methyl protons of the isopropyl groups are broadened significantly. These features are consistent with an alkylidyne anion – phosphonium cation ion pair formed by deprotonation of the alkylidene by the ylide (Scheme A.1). The mechanism of formation of the methylene species is not known, although formation of {Me_3PCH_2Ph}{Mo(NAr)(C-*t*-Bu)(O-*t*-Bu_{F6})$_2$} followed by abstraction of a methyl proton in the phosphonium salt by the alkylidyne α carbon atom is one attractive possibility.

Scheme A.1. Observed reaction products upon addition of Me_3P=CHPh to Mo(NAr)(CH-*t*-Bu)(O-*t*-Bu_{F6})$_2$.

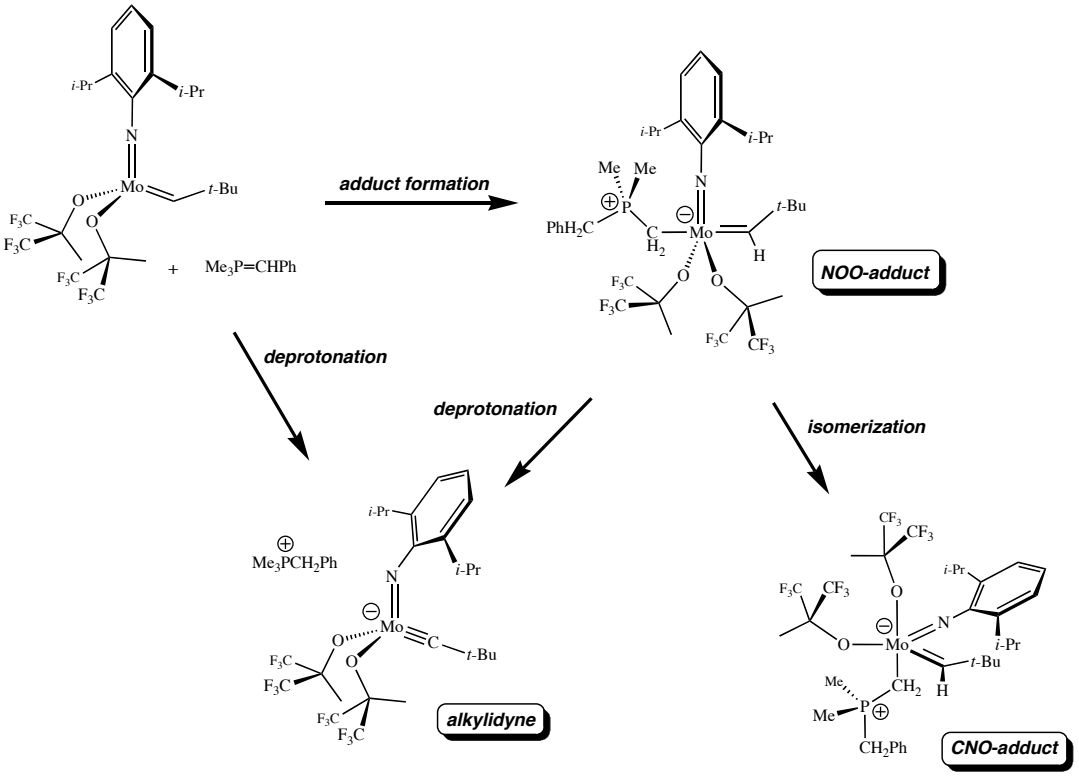

Upon standing at room temperature for several hours, the reaction evolves into a new mixture of products. The major component is now the alkylidyne anion (>70%) and the initial adduct is gone. The minor component is again an alkylidene containing species with the neopentylidene H_α resonance at 12.71 ppm (J_{PH} coupling could not be resolved). The spectrum is consistent with the lack of any symmetry element suggesting that the minor species is an adduct in which the ylide is bound to the CNO face of the original tetrahedral MoCNOO core. The spectrum shows a doublet resonance at 1.92 ppm with a relative integration of two demonstrating that the ylide is coordinating through a methylidene carbon as above. It remains a possibility that the NOO adduct is the initial product of reaction between the benzylidene ylide and that both the alkylidyne anion and the CNO adduct form from this initial complex (Scheme A.1). A variable temperature NMR study between 20 and 80 ºC revealed no exchange between the alkylidyne anion and the ylide (CNO) adduct. Preparative scale reactions in toluene yielded the same mixture of compounds even after recrystallization from toluene.

The reaction between $Me_3P{=}CH_2$ and Mo(NAr)(CH-*t*-Bu)(O-*t*-Bu_{F6})$_2$ produced a crystalline product for which proton and phosphorus NMR spectra suggest it to be a mixture of the NOO (10%) adduct, the CNO (26%) adduct, and the alkylidyne anion (64%).

The reactivity of {Ph_3PMe}{Mo(NAr)(C-*t*-Bu)(O-*t*-Bu_{F6})$_2$} has been explored briefly. Treatment of the imido alkylidyne with $[Me_3O]BF_4$ in methylene chloride generates the new amido alkylidyne species Mo(C-*t*-Bu)[N(Me)Ar](O-*t*-Bu_{F6})$_2$ (Scheme A.2). This new species is a pentane soluble, colorless solid, consistent with an alkylidyne amido *bis*-alkoxide complex formed by methylation at nitrogen.[7] The alkylidyne carbon resonance appears at 319.5 ppm in benzene-d_6 and the isopropyl methyl groups appear as well resolved doublets in the ^{1}H NMR spectrum, consistent with locked rotation about the N_{imido}-C_{ipso} bond. Treatment of the alkylidyne anion with $Me_3SiOSO_2CF_3$ yields the related species, Mo($CCMe_3$)[N($SiMe_3$)Ar](O-t-Bu_{F6})$_2$. This compound is also colorless and displays a resonance for C_α at 322.8 ppm (benzene-d_6). Both reactions appear to be quantitative by NMR, however isolated yields were only moderate due to the high solubility of the alkylidyne complexes in pentane.

The net result of protonation of {Ph_3PMe}{Mo(NAr)(C-*t*-Bu)(O-*t*-Bu_{F6})$_2$} with [$HNMe_2Ph$]Cl or [Et_3NH]Cl is formation of Mo(NAr)(CH-*t*-Bu)(O-*t*-Bu_{F6})$_2$, as judged by ^{1}H NMR. In the case of [$HNMe_2Ph$]Cl, the dimethylaniline byproduct does not coordinate to the metal and Mo(NAr)(CH-*t*-Bu)(O-*t*-Bu_{F6})$_2$ is formed cleanly (Scheme A.2). With [Et_3NH]Cl, the triethylamine appears to coordinate weakly to the metal giving rise to two observed alkylidene species. The reaction between {Ph_3PMe}{Mo(NAr)(C-*t*-Bu)(O-*t*-Bu_{F6})$_2$} and [$H(OEt_2)_2$]B[3,5-$(CF_3)_2C_6H_3$]$_4$ appeared to be instantaneous in benzene-d_6 as judged by immediate precipitation of [Ph_3PMe]B[3,5-$(CF_3)_2C_6H_3$]$_4$ as a brown oil. Spectra indicated that the major species formed was again Mo(NAr)(CH-*t*-Bu)(O-*t*-Bu_{F6})$_2$, though several resonances in the region of 8 – 9 ppm suggest that Mo(NHAr) species are present.

Reaction of {Ph_3PMe}{Mo(NAr)(C-*t*-Bu)(O-*t*-Bu_{F6})$_2$} with carbon dioxide was rapid upon warming the reaction mixture from 77 K to room temperature; the solution decolorized and a white precipitate formed. NMR examination of the precipitate in methylene chloride-d_2 showed it to be the κ^2-carbamate complex (Scheme A.2). The infrared spectrum in methylene chloride displays a strong peak at 1658 cm^{-1} consistent with the CO stretch of the carbamate ligand.[17] Heating the carbamate did not result in extrusion of aryl isocyanate, but rather decomposition to unidentifiable products.

Addition of several equivalents of 3-hexyne to {Ph_3PMe}{Mo(NAr)(C-*t*-Bu)(O-*t*-Bu_{F6})$_2$} led to no reaction at room temperature after several days. In contrast, Re(NAr)(C-*t*-Bu)(O-*t*-Bu_{F6})$_2$ has been reported to react with 3-hexyne to give metallacyclobutadiene species.[13] The more electron rich nature of the alkylidyne anion likely disfavors alkyne binding.

Scheme A.2. Reactions of the alkylidyne anion with electrophiles.

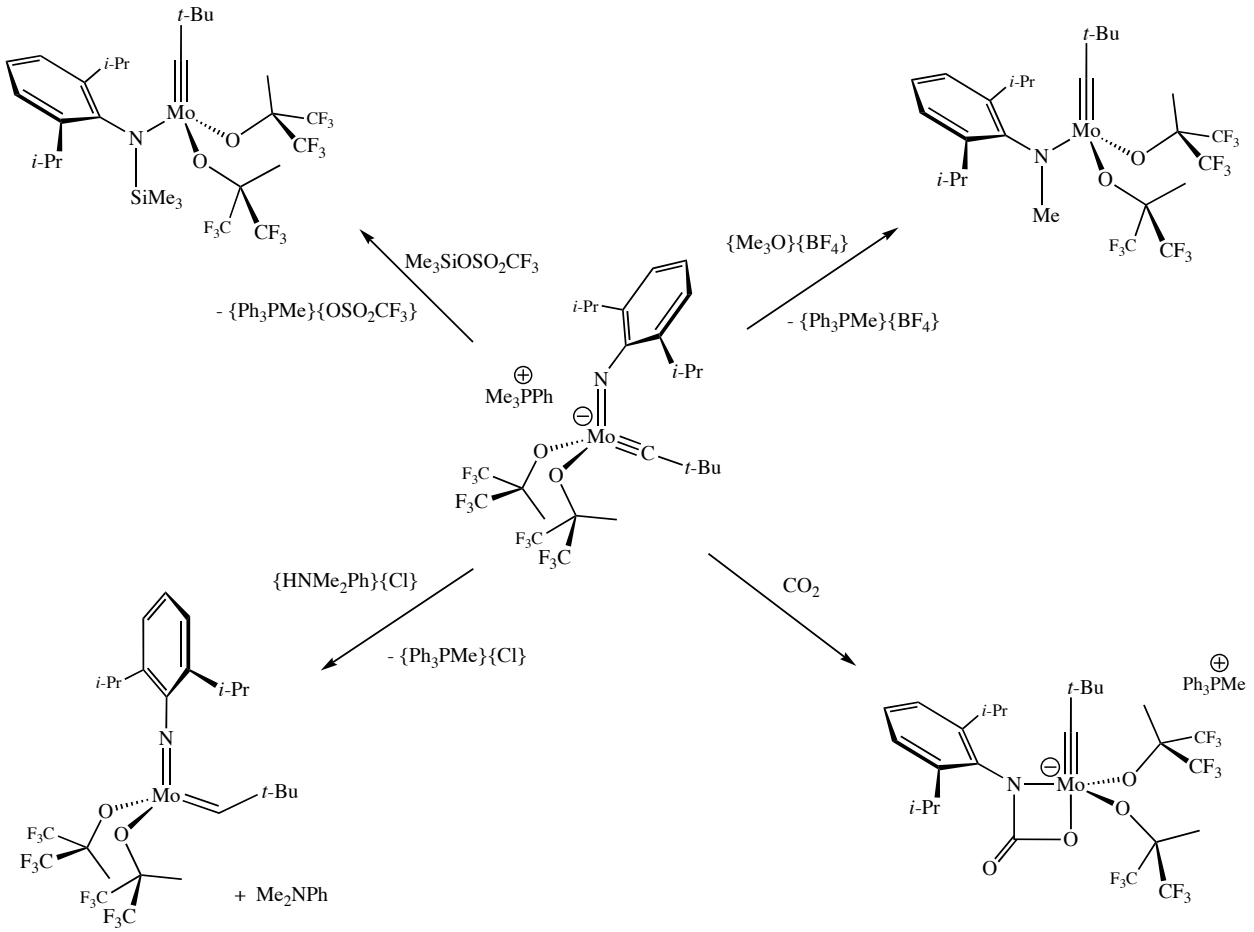

DISCUSSION

Deprotonation of a high oxidation state alkylidene was first demonstrated in a reaction between $Ta(CH\text{-}t\text{-}Bu)(CH_2\text{-}t\text{-}Bu)_3$ and LiBu.[18] Dehydrohalogenation of $W(NPh)(CH\text{-}t\text{-}Bu)(PEt_3)_2Cl_2$ with $Ph_3P{=}CH_2$ has been shown to lead to $W(NPh)(C\text{-}t\text{-}Bu)(PEt_3)_2Cl$.[19] Addition of HCl to this species regenerated $W(NPh)(CH\text{-}t\text{-}Bu)(PEt_3)_2Cl_2$. Moving a proton from an amido nitrogen to a neopentylidyne α carbon atom was the first general method of preparing imido

alkylidene complexes of tungsten,[20] while the reverse, deprotonation of a neopentylidene or neophylidene, has been a troublesome side reaction whenever alkoxides or diolates are added to Mo(NAr)(CHR)$(OTf)_2$(DME) (R = *t*-Bu or CMe_2Ph) species.[7] (This approach has been the standard method of preparing *bis*-alkoxide catalysts such as Mo(NAr)(CH-*t*-Bu)(O-*t*-$Bu_{F6})_2$.) Phosphorus ylides have been employed as bases in early experiments, e.g., $Me_3P{=}CH_2$ was employed as a base in order to cleanly deprotonate $[Cp_2TaMe_2]BF_4$ to yield $Cp_2TaMe(CH_2)$.[21] For all of these reasons, therefore, the deprotonation of the neopentylidene ligand in Mo(NAr)(CH-*t*-Bu)(O-*t*-$Bu_{F6})_2$ was not wholly unexpected. Nevertheless unambiguous examples are relatively rare and the example described here is first to our knowledge of a structurally characterized four coordinate high oxidation state imido alkylidyne species. These species represent isolable versions of intermediates thought to be present along the proton transfer pathway from Mo(NR)(CHR′)(OR′′)$_2$ to Mo(NHR)(CR′)(OR′′)$_2$.[7]

On the basis of the results described here, it would seem that regeneration of a metathetically active alkylidene complex through transfer of an alkylidene from an alkylidene phosphorane could be problematic. From this point of view, the fact that $Ph_3P{=}CHPh$ did *not* deprotonate Mo(NAr)(CH-*t*-Bu)(O-*t*-$Bu_{F6})_2$ is one of the more interesting results. However, whether $Ph_3P{=}CHPh$, or other sterically demanding phosphoranes could serve as a source of a benzylidene ligand in a reaction with some "Mo(NAr)(O-*t*-$Bu_{F6})_2$" species to yield Mo(NAr)(CHPh)(O-*t*-$Bu_{F6})_2$ remains unknown.

EXPERIMENTAL

General Comments. All manipulations were performed in oven dried (200ºC) glassware under an atmosphere of nitrogen in a Vacuum Atmospheres glove box. HPLC grade toluene, pentane, and methylene chloride were purified by passage through an alumina column and stored over 4 Å Linde-type molecular sieves prior to use. Benzene-d_6 was dried over sodium benzophenone ketyl and distilled prior to use. Methylene chloride-d_2 was dried over CaH_2, vacuum distilled and

stored over molecular sieves prior to use. NMR spectra were recorded on a Varian Mercury and Varian Inova spectrometers operating at 300 or 500 MHz (^{1}H), respectively. Spectra are referenced to the residual ^{1}H/^{13}C peaks of the solvent (^{1}H: C_6D_6, 7.16; CD_2Cl_2, 5.32; ^{13}C: C_6D_6, 128.39; CD_2Cl_2, 54.00) and are listed in ppm relative to tetramethylsilane. ^{19}F and ^{31}P NMR were referenced externally to fluorobenzene (δ –113.15 ppm upfield of $CFCl_3$) and 80% H_3PO_4 (δ 0.00 ppm), respectively. Combustion analyses were performed by H. Kolbe Mikroanalitisches Laboratorium, Mülheim an der Ruhr, Germany.

Materials. Mo(NAr)(CHCMe$_2$R)(O-*t*-Bu$_{F6}$)$_2$ (R = Me and Ph) were prepared according to published procedures.[22] $Me_3P{=}CHPh$, $Ph_3P{=}CHPh$, and $Me_3P{=}CH_2$ were prepared by addition of *n*-BuLi to a toluene suspension of the corresponding phosphonium halide salt, followed by filtration and crystallization from pentane or toluene ($Me_3P{=}CHPh$ and $Ph_3P{=}CHPh$) or distillation ($Me_3P{=}CH_2$). $Ph_3P{=}CH_2$ was prepared with $LiN(SiMe_3)_2$ in similar fashion and crystallized from toluene. $[Me_3O]BF_4$, $Me_3SiOSO_2CF_3$, and CO_2 were purchased from commercial vendors and used as received.

Crystallography. Low temperature diffraction data were collected on a Siemens Platform three-circle diffractometer coupled to a Bruker-AXS Smart Apex CCD detector with graphite-monochromated Mo Kα radiation (λ = 0.71073 Å), performing θ- and ω-scans. The structure was solved by direct methods using SHELXS[23] and refined against F^2 on all data by full-matrix least squares with SHELXL-97.[24] All non-hydrogen atoms, were refined anisotropically. All hydrogen atoms were included into the model at geometrically calculated positions and refined using a riding model. Two disordered $CMe(CF_3)_2$ groups in one of the two crystallographically independent molecules were refined with the help of similarity restraints on 1-2 and 1-3 distances and displacement parameters as well as rigid bond restraints for anisotropic displacement parameters. Similar ADP restraints were also applied to all atoms of the two $[Ph_3PMe]^+$ ions.

{Ph_3PMe}{Mo(NAr)(C-*t*-Bu)(O-*t*-Bu_{F6})$_2$}. A round bottom flask was charged with 1.035 g (1.47 mmol) of Mo(NAr)(CH-*t*-Bu)(O-*t*-Bu_{F6})$_2$ and 25 mL of toluene. To the stirring yellow solution was added 0.410 g (1.48 mmol) of $Ph_3P{=}CH_2$ as a solid in one portion, at which point the reaction solution became orange-red. The mixture was stirred for 90 minutes at room temperature and the volatiles removed in vacuo. The residue was dissolved in toluene and pentane was added until the solution became turbid. The suspension was set aside at –25 ºC for 18 hours during which time 1.093 g (76%) of formed orange microcrystals. Crystals suitable for X-ray diffraction were grown by slow cooling of a saturated toluene/pentane solution: NMR (C_6D_6) ^{1}H (500 MHz) δ 7.33 (d, 2, *m*-Ar), 7.02 (m, 10, aryl), 6.89 (m, 6, aryl), 3.79 (sep, 2, C*H*Me$_2$), 3.10 (d, J_{PH} = 12.6 Hz, 3, P*Me*$_3$), 2.07 (s, 6, OC*Me*), 1.8 – 1.0 (v br, 12, CH*Me*$_2$), 1.29 (s, 9, *t*-Bu); ^{13}C (125 MHz) δ 300.7 (MoC_α), 163.7, 138.0, 135.1 (d, J_{CP} = 3.0 Hz), 133.2 (d, J_{CP} = 10.8 Hz), 130.7 (d, J_{CP} = 12.3 Hz), 126.3 (q, J_{CF} = 288 Hz), 125.9 (q, J_{CF} = 289 Hz, *C*F$_3$), 122.4, 120.3, 119.5 (d, J_{CP} = 89.2 Hz), 80.1 (sep, C_{quat}-R_{F6}), 52.6, 32.3, 28.3, 24.2 (br, CH*Me*$_2$), 21.8, 9.9 (d, J_{CP} = 56.9 Hz); ^{31}P (121 MHz) δ 22.3; ^{19}F (282 MHz) δ –77.5 (q), –78.1 (q). Anal. Calcd for $C_{44}H_{50}F_{12}MoNO_2P$: C, 53.94; H, 5.14; N, 1.43. Found: C, 54.08; H, 5.17; N, 1.36.

{Ph_3PMe}{Mo(NAr)(CMe_2Ph)(O-*t*-Bu_{F6})$_2$}. A J-Young type NMR tube was charged with 38.5 mg (50.3 μmol) of Mo(NAr)(CHCMe_2Ph)(O-*t*-Bu_{F6})$_2$ and 14.2 mg (51.4 μmol) of $Ph_3P{=}CH_2$. Approximately 0.7 mL of benzene-d_6 was added to the solids producing an orange solution. ^{1}H NMR observation of the mixture indicated that the desired complex was present in ~90% along with a minor species that was not identified completely but appeared to be a phosphorane adduct of the alkylidene. All volatiles were removed in vacuo and the residue dissolved in a minimal amount of 3:1 pentane/toluene. The solution was set aside at –25 ºC for several days during which time the complex precipitated as 33.2 mg (63%) of orange needles: NMR (C_6D_6) ^{1}H (300 MHz) δ 7.74 (d, 2, *m*-Ar), 7.37 (d, 2, *o*-CMe_2*Ph*), 7.23 (t, 2, *m*-CMe_2*Ph*), 7.13 (t, 1, *p*-CMe_2*Ph*), 6.99 (m, 10, aryl), 6.87 (m, 6, aryl), 3.80 (sep, 2, C*H*Me$_2$), 3.08 (d, J_{HP} = 12.6 Hz, 3, P*Me*$_3$), 1.80 (s, 6, *Me*-R_{F6}), 1.72 (s, 6, C*Me*$_2$Ph), 1.56 (v br, 6, CH*Me*$_2$), 1.09 (v br, 6,

CH*Me*$_2$); ^{31}P (121 MHz) δ 21.7; ^{19}F (282 MHz) δ –77.6 (q), –78.1 (q). Anal. Calcd for $C_{49}H_{52}F_{12}MoNO_2P$: C, 56.59; H, 5.03; N, 1.34. Found: C, 56.36; H, 5.12; N, 1.29.

Mo(C-*t*-Bu)[N(Me)Ar](O-*t*-Bu$_{F6}$)$_2$. A flask was charged with 0.147 g (0.15 mmol) of {Ph_3PMe}{Mo(NAr)(C-*t*-Bu)[O-t-BuF6]$_2$} and 8 mL of methylene chloride. The solution was cooled to –25 ºC at which point 0.029 g (0.20 mmol) of $[Me_3O]BF_4$ was added as a solid. The mixture was stirred at room temperature for 45 minutes during which time the solution became pale yellow. All volatiles were removed in vacuo and the residue extracted with pentane. The pentane extract was filtered through Celite and the solution volume reduced to ~1 mL in vacuo. Slow cooling of the pentane solution at –25 ºC afforded 0.067 g (65%) of pale yellow to colorless crystals: NMR (C_6D_6) ^{1}H (500 MHz) δ 7.03 (m, 3, Ar), 3.28 (s, 3, N*Me*), 3.02 (sep, 2, C*H*Me$_2$), 1.69 (s, 6, *Me*-R$_{F6}$), 1.26 (d, 6, CH*Me*$_2$), 1.03 (d, 6, CH*Me*$_2$), 0.66 (s, 9, *t*-Bu); ^{13}C (125 MHz) δ 319.5 (Mo*C*$_\alpha$), 157.6, 142.1, 127.9, 124.6 (q, J_{CF} = 286 Hz, *C*F$_3$), 124.4, 124.2 (q, J_{CF} = 287 Hz, *C*F$_3$), 81.6 (sep, J_{CF} = 29.4 Hz, C_{quat}-R$_{F6}$), 55.0, 45.3 (N*Me*), 23.0, 28.1, 26.7, 23.8, 20.8; ^{19}F (470 MHz) δ –78.3 (q), –79.0 (q). Anal. Calcd for $C_{26}H_{35}F_{12}MoNO_2$: C, 43.52; H, 4.92; N, 1.95. Found: C, 43.64; H, 5.05; N, 1.87.

Mo(C-*t*-Bu)[N(SiMe$_3$)Ar](O-*t*-Bu$_{F6}$)$_2$. A flask was charged with 0.174 g (0.178 mmol) of {Ph_3PMe}{Mo(NAr)(C-*t*-Bu)(O-*t*-Bu$_{F6}$)$_2$} and 8 mL of toluene and chilled to –25 ºC. To the cold solution was added 40 μL (0.20 mmol) of $Me_3SiOSO_2CF_3$ at which point the solution became pale yellow and cloudy. The reaction was stirred at room temperature for 15 minutes and all volatiles were removed in vacuo. The residue was extracted into pentane and filtered through Celite. The solvent volume was reduced to ~1 mL in vacuo and set aside at –25 ºC. The product crystallized as 0.0503 g (39%) of pale yellow to colorless cubes in two crops: NMR (C_6D_6) ^{1}H (500 MHz) δ 7.06 (m, 3, Ar), 3.09 (sep, 2, C*H*Me$_2$), 1.71 (s, 6, *Me*-R$_{F6}$), 1.32 (d, 6, CH*Me*$_2$), 1.13 (d, 6, CH*Me*$_2$), 0.65 (s, 9, *t*-Bu), 0.23 (s, 9, *Me*$_3$Si); ^{13}C (125 MHz) δ 322.8 (Mo*C*$_\alpha$), 156.8, 140.9, 126.5, 124.5, 124.5 (q, J_{CF} = 287 Hz, *C*F$_3$), 124.1 (q, J_{CF} = 287 Hz, *C*F$_3$),

82.2 (sep, J_{CF} = 29.7 Hz, C_{quat}-R_{F6}), 56.1, 30.4, 28.3, 25.8, 25.7, 20.4, 1.0 (SiMe_3); ^{19}F (470 MHz) δ –77.1 (q), –78.5 (q). Anal. Calcd for $C_{28}H_{41}F_{12}MoNO_2Si$: C, 43.36; H, 5.33; N, 1.81. Found: C, 43.28; H, 5.30; N, 1.77.

{Ph_3PMe}{Mo(C-*t*-Bu)[κ^2-OC(O)NAr](O-*t*-Bu_{F6})$_2$}. A round bottom flask was charged with 0.185 g (0.189 mmol) of {Ph_3PMe}{Mo(NAr)(C-*t*-Bu)(O-*t*-Bu_{F6})$_2$} and 10 mL of toluene. To the flask was connected a needle valve. The solution was degassed by two consecutive freeze-pump-thaw cycles. The degassed solution was then exposed to 1 atm of CO_2 for 10 minutes while stirring and warming from the melting point of the solvent to room temperature. The flask was sealed and allowed to stir for an additional 20 minutes at room temperature during which time the solution turned from orange to pale yellow with formation of a white precipitate. All volatiles were removed in vacuo and the residue triturated in a 10:1 mixture of pentane to toluene causing formation of a white solid. The solid was collected by filtration yielding 0.177 g (91%) of a white powder: NMR (CD_2Cl_2) ^{1}H (300 MHz) δ 7.72 (m, 15, aryl), 7.14 (m, 3, Ar), 3.08 (sep, 2, C*H*Me_2), 3.00 (d, J_{PH} = 13.2 Hz, 3, PMe_3), 1.88 (s, 6, *Me*-R_{F6}), 1.21 (d, 6, CHMe_2), 1.03 (d, 6, CHMe_2), 0.70 (s, 9, *t*-Bu); ^{13}C (125 MHz) δ 309.3 (MoC_α), 165.5 (*C*=O), 151.7, 143.8, 135.3 (d, J_{CP} = 2.3 Hz), 133.9 (d, J_{CP} = 10.7 Hz), 130.7 (d, J_{CP} = 13.0 Hz), 126.2, 124.6 (q, J_{CF} = 288 Hz), 124.4 (q, J_{CF} = 287 Hz), 123.0, 120.1 (d, J_{CP} = 88.3 Hz), 81.2 (sep, J_{CF} = 28.4 Hz), 51.1, 29.8, 28.8, 25.2, 22.7, 20.2, 9.3 (J_{CP} = 57.5 Hz); ^{31}P (121 MHz) δ 22.6; ^{19}F (470 MHz) δ –78.3 (q), –78.6 (q); IR (KBr, CH_2Cl_2) 1658 cm^{-1} (νCO). Anal. Calcd for $C_{45}H_{50}F_{12}MoNO_4P$: C, 52.79; H, 4.92; N, 1.37. Found: C, 52.64; H, 5.08; N, 1.34.

Reaction of Mo(NAr)(CH-*t*-Bu)(O-*t*-Bu$_{F6}$)$_2$ with Me$_3$P=CHPh. A J-Young type NMR tube was charged with equimolar amounts of Mo(NAr)(CH-*t*-Bu)(O-*t*-Bu$_{F6}$)$_2$ and Me$_3$P=CHPh. The solids were dissolved in 0.7 mL of benzene-d_6 producing an orange solution. Shown below are the resulting 300 MHz ^{1}H NMR spectra taken after 15 minutes and 10 hours.

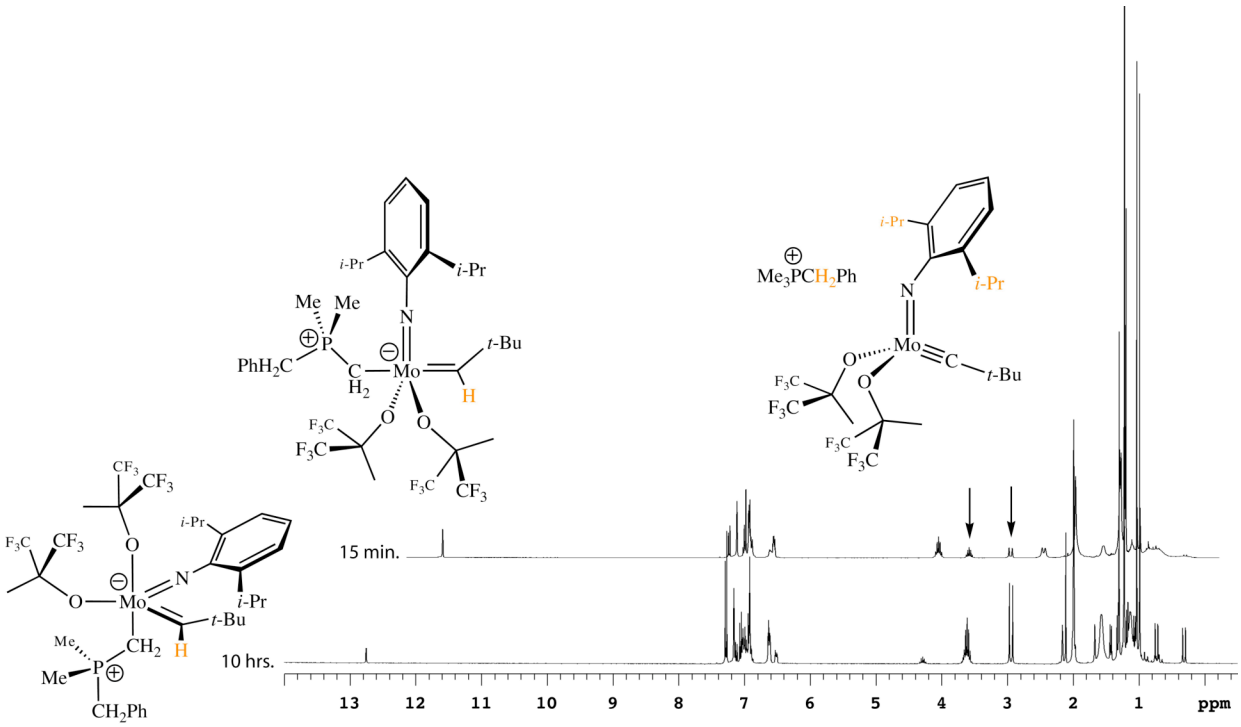

Crystallographic data and refinement parameters for **{Ph_3PMe}{Mo(NAr)(C-*t*-Bu)(O-*t*-Bu_{F6})$_2$}**.

Reciprocal net identification code	**06013**	
Empirical formula	$C_{44}H_{50}F_{12}MoNO_2P$	
Formula weight	979.76 g/mol	
Temperature	100(2) K	
Wavelength	0.71073 Å	
Crystal system	Monoclinic	
Space group	$P2_1/c$	
Unit cell dimensions	a = 25.3522(10) Å	α = 90°
	b = 17.7046(7) Å	β = 97.2830(10)°
	c = 20.2127(8) Å	γ = 90°
Volume	8999.3(6) Å^3	
Z	8	
Density (calculated)	1.446 g/cm^3	
Absorption coefficient	0.413 mm^{-1}	
F(000)	4016	
Crystal size	0.30 × 0.25 × 0.10 mm^3	
Θ range for data collection	1.67 to 29.57°	
Index ranges	$-34 \le h \le 35$, $-24 \le k \le 24$, $-28 \le l \le 27$	
Reflections collected	198822	
Independent reflections	25247 [R(int) = 0.0558]	
Completeness to Θ = 29.57°	100 %	
Absorption correction	Semi-empirical from equivalents	
Max. and min. transmission	0.9598 and 0.8860	
Refinement method	Full-matrix least-squares on F^2	
Data / restraints / parameters	25247 / 2270 / 1299	
Goodness-of-fit on F^2	1.031	
Final R indices [I>2σ(I)]	R1 = 0.0374, wR2 = 0.0841	
R indices (all data)	R1 = 0.0549, wR2 = 0.0928	
Largest diff. peak and hole	0.844 and -0.502 e·Å^{-3}	

REFERENCES

1. Schrock, R. R. *Chem. Rev*. **2002**, *102*, 145.

2. Schrock, R. R.; Hoveyda, A. H. *Angew. Chem. Int. Ed*. **2003**, *42*, 4592.

3. Lopez, L. P. H.; Schrock, R. R.; Müller, P. *Organometallics* **2006***, 25*, 1978.

4. Sharp, P. R.; Schrock, R. R. *J. Organometal. Chem.* **1979**, *171*, 43.

5. Johnson, L. K.; Virgil, S. C.; Grubbs, R. H.; Ziller, J. W., *J. Am. Chem. Soc.* **1990**, *112*, 5384.

6. Johnson, L. K.; Frey, M.; Ulibarri, T. A.; Virgil, S. C.; Grubbs, R. H.; Ziller, J. W., *J. Am. Chem. Soc*. **1993**, *115*, 8167.

7. Schrock, R. R.; Jamieson, J. Y.; Araujo, J. P.; Bonitatebus, P. J.; Sinha, A.; Lopez, L. P. H., *J. Organomet. Chem.* **2003**, *684*, 56.

8. Fox, H. H.; Schofield, M. H.; Schrock, R. R., *Organometallics* **1994**, *13*, 2804.

9. Solans-Monfort, X.; Eisenstein, O., *Polyhedron* **2006**, *25*, 339.

10. Sinha, A. *Ph.D. Thesis* **2006**.

11. Sinha, A.; Schrock, R. R.; Müller, P.; Hoveyda, A. H., *Organometallics* **2006**, *25*, 4621.

12. Hock, A. S.; Schrock, R. R.; Hoveyda, A. H., *J. Am. Chem. Soc.* **2006**, *128*, 16373.

13. Schrock, R. R.; Weinstock, I. A.; Horton, A. D.; Liu, A. H.; Schofield, M. H., *J. Am. Chem. Soc*. **1988**, *110*, 2686.

14. Schrock, R. R.; Crowe, W. E.; Bazan, G. C.; DiMare, M.; O'Regan, M. B.; Schofield, M. H. *Organometallics* **1991**, *10,* 1832.

15. Schrock, R. R.; Gabert, A. J.; Singh, R.; Hock, A. S. *Organometallics* **2005**, *24*, 5058.

16 Adamchuk, J.; Schrock, R. R.; Tonzetich, Z. J.; Müller, P. *Organometallics* **2006**, *25*, 2364.

17. Glueck, D. S.; Wu, J.; Hollander, F. J.; Bergman, R. G., *J. Am. Chem. Soc.* **1991**, *113*, 2041.

18. Guggenberger, L. J.; Schrock, R. R. *J. Am. Chem. Soc.*, **1975**, *97*, 2935.

19. Rocklage, S. M.; Schrock, R. R.; Churchill, M. R.; Wasserman, H. J. *Organometallics* **1982**, *1*, 1332.

20. Schaverien, C. J.; Dewan, J. C.; Schrock, R. R. *J. Am. Chem. Soc.* **1986**, *108*, 2771.

21. Schrock, R. R.; Sharp, P. R. *J. Am. Chem. Soc.* **1978***, 100,* 2389.

22. Oskam, J. H.; Fox, H. H.; Yap, K. B.; McConville, D. H.; O'Dell, R.; Lichtenstein, B. J.; Schrock, R. R., *J. Organomet. Chem.* **1993**, 459, 185.

23. Sheldrick, G. M. Acta Cryst. A **1990**, 46, 467.

24. Sheldrick, G. M. SHELXL 97 **1997**, Universität Göttingen, Göttingen, Germany.

CURRICULUM VITAE

Zachary John Tonzetich

Department of Chemistry
MIT Rm. 6-421
Cambridge, MA 02139
Home: 617.628.3353
Work: 617.253.5047
tonzetch@mit.edu

Education

2002 – 2007 **Massachusetts Institute of Technology**, Cambridge, MA

Ph.D. in Inorganic Chemistry 2007. Thesis advisor: Professor Richard R. Schrock. Dissertation entitled "Early Transition Metal Alkyl, Alkylidene, and Alkylidyne Chemistry".

1998 – 2002 **University of Rochester**, Rochester, NY

BS *summa cum laude* in Chemistry (3.98 GPA). Thesis advisor: Professor Richard Eisenberg. Senior thesis entitled "Synthesis and Photophysical Study of Luminescent Tantalum(V) and Iridium(I) Complexes".

Research Interests

Synthetic inorganic and organometallic chemistry with an emphasis on novel reactivity, catalysis, structure and bonding; spectroscopy; kinetics and reaction mechanisms.

Research Experience

2002 – 2007 **Massachusetts Institute of Technology**, Cambridge, MA

Thesis research conducted under Professor Richard R. Schrock on the organometallic chemistry of Group(IV) alkyls and Group(VI) alkylidene and alkylidyne complexes including:

- Synthesis of new catalytic compounds for olefin polymerization, olefin metathesis, alkyne metathesis, and alkyne metathesis polymerization.
- Development of new asymmetric amide based zirconium and hafnium catalysts for olefin polymerization.
- Exploration of fundamental organometallic chemistry of molybdenum and tungsten alkylidene and alkylidyne complexes including cationic and anionic complexes.

2001 – 2002 **University of Rochester**, Rochester, NY

Conducted undergraduate research under Professor Richard Eisenberg on the synthesis and photophysical charaterization of luminescent dithiolate complexes of iridium(I) and cyclopentadienyl complexes of tantalum(V).

Summer 2001 **Massachusetts Institute of Technology**, Cambridge, MA

Worked under Professor Richard R. Schrock on the development and characterization of diamido-pyridine complexes of tantalum(V) as models for activated versions of olefin polymerization catalysts.

Summer 1999 **Bucknell University**, Lewisburg, PA

Worked under Professor Charles Root on the synthesis and characterization of copper and nickel complexes bearing heterocyclic ligands.

Teaching Experience

2004 - 2007 **Graduate Course in Organometallic Chemistry Assistant Grader**
Massachusetts Institute of Technology, Cambridge, MA
- Assisted in preparing and grading problem sets and examinations.

2003 – 2006 **Lecturer for Advanced Laboratory**
Massachusetts Institute of Technology, Cambridge, MA
- Prepared lecture material and notes for undergraduate laboratory experiment on synthetic inorganic chemistry.

2002 **Advanced Laboratory Teaching Assistant**
Massachusetts Institute of Technology, Cambridge, MA
- Graded laboratory evaluations and oversaw biweekly lab sessions.

2001 – 2002 **General Chemistry Teaching Assistant**
University of Rochester, Rochester, NY
- Graded exams and other course material. Supervised and developed lecture material for weekly recitations.

2000 – 2001 **Honors Organic Chemistry Workshop Leader**
University of Rochester, Rochester, NY
- Supervised and led discussions in weekly workshop sessions.

2000 **General Chemistry Laboratory Teaching Assistant**
University of Rochester, Rochester, NY
- Supervised weekly laboratory sessions and graded reports.

Fellowships

2002 – 2005 National Science Foundation Predoctoral Fellow

2005 – 2006 Alan Davison Fellow

Awards

2005	Morse Travel Grant
2003	MIT Department of Chemistry Award for excellence in teaching by a graduate student
2002	John McCreary Memorial Prize for outstanding accomplishments as a senior chemistry major; Carl Whiteman Teaching Award for distinguished achievement as an undergraduate teaching assistant
2001	Merck Scholar Award for outstanding accomplishments as junior chemistry major
2000	Merck Index Award for Organic Chemistry

Publications

Tonzetich, Z. J.; Jiang, A. J.; Schrock, R. R.; Müller, P. "Molybdenum imido alkylidene complexes that contain a β-diketiminate ligand" *Organometallics* **2007**, submitted.

Blanc, F.; Thivolle-Cazat, J.; Basset, J.-M.; Coperet, C.; Hock, A. S.; Tonzetich, Z. J.; Sinha, A.; Schrock, R. R. "Highly active, stable, and selective well-defined silica supported Mo imido olefin metathesis catalysts *J. Am. Chem. Soc.* **2007**, *129*, 1044.

Tonzetich, Z. J.; Lam, Y. C.; Müller, P.; Schrock, R. R. "Facile synthesis of a tungsten alkylidyne catalyst for alkyne metathesis" *Organometallics* **2007**, *26*, 475.

Czekelius, C. C.; Hafer, J.; Tonzetich, Z. J.; Schrock, R. R.; Christensen, R. L.; Muller, P. "Synthesis of oligoenes that contain up to 15 double bonds from 1,6-heptadiynes" *J. Am. Chem. Soc.* **2006**, *128*, 16664.

Tonzetich, Z. J.; Jiang, A. J.; Schrock, R. R.; Müller, P. "Cationic imido alkylidene complexes of molybdenum supported by β-diketonate and β-diketiminate ligands" *Organometallics* **2006**, *25*, 4725.

Tonzetich, Z. J.; Schrock, R. R.; Müller, P. "Reaction of phosphoranes with Mo(N-2,6-*i*-$Pr_2C_6H_3$)($CHCMe_3$)[$OCMe(CF_3)_2$]$_2$: Synthesis and reactivity of an anionic imido alkylidyne complex" *Organometallics* **2006**, *25*, 4301-4306.

Adamchuk, J.; Schrock, R. R.; Tonzetich, Z. J.; Müller, P. "Initiators of the type Mo(NAr)(CHR′)(OR″)$_2$ for the controlled polymerization of diethyldipropargylmalonate" *Organometallics* **2006**, *25*, 2364-2373.

Tonzetich, Z. J.; Schrock, R. R. "Potential group IV olefin polymerization catalysts that contain a diamido ligand substituted with hexaisopropylterphenyl groups" *Polyhedron* **2006**, *25*, 469-476.

Tonzetich, Z. J.; Schrock, R. R.; Hock, A. S.; Müller, P. "Synthesis, characterization, and activation of zirconium and hafnium dialkyl complexes that contain a C_2-symmetric diaminobinaphthyl dipyridine ligand" *Organometallics* **2005**, *24*, 3335-3342.

Tonzetich, Z. J.; Lu, C. C.; Schrock, R. R.; Hock, A. S.; Bonitatebus, P. J., Jr. "Synthesis, characterization, and polymerization behavior of zirconium and hafnium complexes that contain asymmetric diamido-N-donor ligands" *Organometallics* **2004**, *23*, 4362-4372.

Tonzetich, Z. J.; Eisenberg, R. "Luminescent η^5-pentamethylcyclopentadienyl tantalum(V) complexes: Synthesis, characterization, and emission spectroscopy" *Inorg. Chim. Acta* **2003**, *345*, 340-344.

Presentations

"Living Polymerization of 1,6-Heptadiynes by Molybdenum Imido Alkylidene Compounds: New Mechanistic Insights and Avenues in Catalyst Design" Oral Presentation, *231st National Meeting of the ACS*, Atlanta, Spring 2006.

"Synthesis and Reactivity of New Cationic Molybdenum Alkylidene Complexes" Poster Presentation, *Bruker AXS Symposium*, MIT, January 2006.

"Synthesis, Characterization, and Activation of Zirconium and Hafnium Complexes Containing a C_2-Symmetric Diamido-Dipyridine Ligand" Poster Presentation, *229th National Meeting of the ACS*, San Diego, Spring 2005.

"Luminescent Cp*Ta(V) Complexes: Synthesis, Characterization, and Emission Spectroscopy" Poster presentation, *223rd National Meeting of the ACS,* Orlando, Spring 2002.

"Towards the Development of Luminescent Platinum Group Complexes" Poster presentation, *221st National Meeting of the ACS*, San Diego, Spring 2001.

"Student Perspectives on Learning Organic Chemistry in the Next Century" Member of panel discussion, *221st National Meeting of the ACS*, San Diego, Spring 2001.

Affiliations

Member of Phi Beta Kappa and Golden Key national honor societies.
Member of the American Chemical Society.

ACKNOWLEDGMENTS

It is my privilege to thank the many people whose efforts have made my time as a graduate student at MIT exceedingly productive and enjoyable. First and foremost I would like to acknowledge Professor Richard Schrock. I thank Dick for accepting me into his group during the Summer of 2001 when I was still an undergraduate student at the University of Rochester. My first experience with Dick and the Schrock group was so positive that it left me with little doubt about where I would be pursuing my graduate studies. Since joining the group as a graduate student, I have matured as a scientist under Dick's tutelage and gained a greater appreciation for inorganic chemistry. He has given me the opportunity to pursue my ideas within a supportive and encouraging environment. Dick has always made time to discuss projects with me and offer his tremendous insight when I came to an impasse. I am honored to be counted among his fine students.

I would also like to acknowledge the inorganic faculty at MIT. My interactions with the entire faculty have always been positive, and I have had the pleasure of learning from them all. I would especially like to thank Professor Christopher Cummins for serving as my thesis chair, and for his constant willingness to discuss my chemistry. I also thank my undergraduate advisor Professor Richard Eisenberg. Rich took me under his wing when I was a young student and has continued to help me throughout my studies.

The support I received from the faculty at MIT was met equally from those members of my incoming class, and from the past and present members of the Schrock group. The Schrock group has an excellent mix of students and personalities, and I have enjoyed getting to know everyone throughout my years here. Though the fellow students and postdocs who I have had the pleasure of working with are too numerous to mention all by name, I would like to thank two of them especially--Andrea Gabert and Tatiana Pilyugina. Both Andrea and Tanya were members of my incoming class of graduate students and also members of the Schrock group. They have been great friends and fantastic colleagues.

The members of the group with whom I have had the most interaction are my fellow labmates in 6-421. Dmitry Yandulov, Peter Tsang, Walter Weare, Rojendra Singh, Xuliang Dai, Corina Scriban, YanChoi Lam and Margaret Flook have all worked side by side with me during my time in the Schrock group. I thank them for making my time in lab very enjoyable. Roje in particular has been a great friend and an excellent scientific colleague. I wish him the best, as I know he will be very successful in the future.

I would like to thank Adam Hock, Dr. Peter Müller, Connie Lu, Jennifer Adamchuk, Annie Jiang, and YanChoi Lam for contributing in part to the work presented in my thesis. Each of them has been terrific to work with. For help with editing I thank Keith Wampler and Roje for reading through several chapters.

Lastly, I would like to acknowledge my family. Since I was young, my mother, father, and brother have given me all the love and support I needed to succeed in anything I chose. My dad is and will always be my greatest role model. My wisest decision since coming to graduate school has been marrying my wife Naomi. She is my greatest ally, and her love and support continue to bolster me in all my endeavors. She also did a fine job editing several of the chapters in this thesis.

To everyone again, I thank you. Peace!